MOLECULAR CHARACTERIZATION OF FEBRILE SEIZURES AND TEMPORAL LOBE EPILEPSY

- towards unraveling epileptogenesis and febrile seizure susceptibility -

Koen Lucien Irma van Gassen

ISBN: 978-90-393-4887-1

The research described in this thesis was mainly conducted at the Rudolf Magnus Institute of Neuroscience, Departement of Neuroscience and Pharmacology of the University Medical Center Utrecht and was financially supported by the National Epilepsy Foundation of the Netherlands and by the EPOCH Foundation (Focal Epilepsies of Childhood).

Printing of this thesis was financially supported by the National Epilepsy Foundation of the Netherlands, EPOCH, Sanofi-Aventis and UCB.

MOLECULAR CHARACTERIZATION OF FEBRILE SEIZURES AND TEMPORAL LOBE EPILEPSY

- towards unraveling epileptogenesis and febrile seizure susceptibility -

Moleculaire karakterisatie van febriele convulsies
en temporaal kwab epilepsie

- richting het ontrafelen van epileptogenese en febriele convulsie gevoeligheid -

(met een samenvatting in het Nederlands)

Proefschrift

ter verkrijging van de graad van doctor aan de Universiteit Utrecht
op gezag van de rector magnificus, prof. dr. J.C. Stoof, ingevolge het
besluit van het college voor promoties in het openbaar te verdedigen

op donderdag 4 september 2008 des middags te 14:30 uur

door

Koen Lucien Irma van Gassen

geboren op 23 februari 1978 te Sint-Niklaas, België

Promotoren:	Prof. dr. J.P.H. Burbach Prof. dr. D. Lindhout
Co-promotor:	Dr. P.N.E. de Graan

CONTENTS

CHAPTER 1

General Introduction

EPILEPSY

Clinical aspects of epilepsy

Epilepsy is a common chronic neurological disorder that is characterized by recurrent seizures and affects about 1% of the population worldwide [1,2]. Seizures are transient signs and/or symptoms due to abnormal, excessive or synchronous neuronal activity in the brain. In the majority of patients, seizures can be controlled with medication, although in specific cases surgery may be considered when drug-treatment fails. Epilepsy should not be considered a single disorder, but rather as a group of syndromes with divergent symptoms, wide etiological heterogeneity and involving episodic abnormal electrical activity in the brain, that may be secondary to pathological processes such as brain trauma, infection, neoplasm's or congenital disorders.

Epileptic seizures are most commonly defined and grouped according to a scheme proposed by the International League Against Epilepsy (ILAE) [3] in which seizures are dived into partial and generalized seizures. Partial seizures only involve a localized part of the brain, whereas generalized seizures involve the whole of both hemispheres. Partial seizures may be further subdivided into simple and complex seizures. This refers to the effect of such a seizure on consciousness; simple seizures cause no interruption to consciousness, whereas complex seizures interrupt consciousness to varying degrees.

Approximately 50% of all forms of epilepsy arise in the absence of neurological deficits or brain lesions and have no known or suspected external cause. They are classified as idiopathic epilepsies and many of these epilepsies have been shown to be of genetic origin. Acquired or symptomatic epilepsies are epilepsy syndromes of known origin due to pre- and post-natal acquired factors, such as brain infection, brain injury, neoplasm's or stroke. Although it remains convenient to divide cases into idiopathic and symptomatic, more and more data suggests that in many epilepsy cases there is an interaction between genes and environmental factors. These epilepsies have been named multifactorial epilepsies.

The genetics of epilepsy

Genetic factors play a role in many epilepsy syndromes. A small proportion of epilepsy syndromes are inherited as single-gene disorders. The genes found thus far mostly encode ion channels (summarized in table 1). These epilepsies have therefore also been called channelopathies. In most remaining cases, the etiology is complex, arising from the contribution of multiple genetic and non-genetic factors. The role of genetic factors in multifactorial epilepsies has been shown by twin studies. In monozygotic twins (MZ) a consistently higher concordance rate for epilepsy can be found compared to dizygotic twins (DZ) [4,5]. Among twin pairs concordant for idiopathic generalized epilepsy, MZ twins are also more concordant for epilepsy subphenotype than DZ twin pairs, suggesting that indeed genetic factors play a role not only in the occurrence of epilepsy but also in its phenotypic presentation [5].

The hypothesis that genes and environment interact in epilepsy was first proposed by W. Lennox [6]. He suggested that for most epilepsies, a mixture of genetic and acquired factors were important. Clinical studies in families with idiopathic epilepsy often show a large phenotypic diversity and incomplete penetrance. This shows that besides the epilepsy causing gene, other factors or modifier genes determine the phenotype. The effect of modifier genes in epilepsy has also been shown in animal models [7,8].

The role of genetic factors in predominantly acquired epilepsies has also been investigated [6]. It was found that 1.8% of relatives of patients with acquired brain injuries and epilepsy had epilepsy, while 0.5% of relatives

of control subjects had epilepsy. For patients without brain injuries, 3.6% of relatives were affected. These data suggest that the genetic predisposition for epilepsy is greatest in idiopathic epilepsy, but also higher than control in acquired epilepsies.

Temporal lobe epilepsy

Temporal lobe epilepsy (TLE) is considered the most common partial epilepsy type and is often medically intractable. Surgery may be considered when drug-treatment fails. Patients with TLE experience recurring episodes of spontaneous neuronal activity originating from the temporal lobe. TLE is considered to be a multifactorial disease, implying the involvement of multiple susceptibility genes and complex gene-environment interactions [4,9,10].

TLE can be divided in two main categories, mesial TLE (MTLE) and lateral TLE (LTLE). MTLE arises in the hippocampus, parahippocampal gyrus and amygdala (mesial/limbic structures) while LTLE arises in the neocortex of the temporal lobe of the brain. MTLE can further be divided in a group with hippocampal sclerosis (HS) and a group without HS (nonHS). MTLE patients with associated HS pathology often suffered from early life seizures, like febrile seizures (FS) [11]. Brain infections like meningitis and encephalitis are also common. NonHS MTLE is often associated with specific lesions, such as vascular malformations, neoplasm and dysplasias.

HS is characterized by neuronal cell loss, astrogliosis, granule cell dispersion and mossy fiber sprouting. The extent of this pathology varies between patients and is graded by the system devised by Wyler [46]. The neuronal cell loss is not uniformly distributed in the hippocampus, but mainly confined to the pyramidal cornu amonis (CA) 1, CA3 and CA4 neurons. Pyramidal CA2 neurons and granule cells are largely spared. Granule cell dispersion is characterized by dispersed granule cells which form a wider than normal granule cell layer [47]. The mechanism of granule cell dispersion is not completely understood but recent data suggests that displacement of mature neurons rather than altered neurogenesis underlies this dispersion [48]. Mossy fiber sprouting is characterized by reorganization of the mossy fibers. Mossy fibers that normally innervate hilar neurons send collaterals to the inner third of the molecular layer of the dentate gyrus [49]. Such fibers are thought to form recurrent excitatory circuits and contribute to synchronous firing and epileptiform activity. Whether HS is the cause or consequence of seizures is still a matter of controversy. Presumably HS can be both a cause and an effect of seizures [50,51]. Although human hippocampal resection tissue is available for research and many molecular changes have been described in the HS and nonHS hippocampus, little progress has been made in explaining epileptogenesis in human MTLE.

Molecular genetics has shown that TLE can be caused by single gene mutations. The *LGI1* gene, for example, has been shown to be responsible for autosomal dominant LTLE [38] and *SCN1B* for TLE which most often was associated with FS [21]. Besides these genes, several TLE linkage regions have been identified and association studies have identified several susceptibility genes. The *IL1B-511T* variant for example has been shown to be associated with FS and MTLE with HS. Although not replicated in all cases, a recent meta-analysis study has confirmed this association [52]. Table 2 lists positive association studies for TLE and FS and table 3 lists genomic linkage regions for familial TLE and FS.

FEBRILE SEIZURES

Clinical aspects of febrile seizures

Febrile seizures (FS) are relatively benign generalized convulsions induced by fever [3]. FS prevalence varies from 3-14% between

Gene	Description	Region	Epilepsy Type	References
Ion channels				
CHRNA4	Neuronal acetylcholine receptor protein, alpha-4 subunit	20q13.3	ADNFLE1	[12]
CHRNB2	Neuronal acetylcholine receptor protein, beta-2 subunit	1q21	ADNFLE3	[13]
KCNMA1	Calcium activated potassium channel large conductance subfamily M, alpha member 1	10q22.3	GEPD	[14]
KCNQ2	Voltage-gated potassium channel subfamily KQT, member 2	20q13.3	BFNC1	[15]
KCNQ3	Voltage-gated potassium channel subfamily KQT, member 3	8q24	BFNC2	[16]
SCN1A	Voltage-gated sodium channel type 1, alpha subunit	2q24	FEB3, GEFS+2, SMEI	[17-19]
SCN1B	Voltage-gated sodium channel type 1, beta subunit	19q13.1	GEFS+1, TLE, FS	[20,21]
SCN2A	Voltage-gated sodium channel type 2, alpha subunit	2q24	GEFS+, BFNIS	[22,23]
GABRA1	Gamma-aminobutyric-acid receptor, alpha-1 subunit	5q34	JME, CAE	[24,25]
GABRD	Gamma-aminobutyric-acid A receptor, delta subunit	1p36.3	*IGE, JME, GEFS+5*	[26]
GABRG2	Gamma-aminobutyric-acid receptor, gamma-2 subunit	5q34	GEFS+3, SMEI, CAE, FEB8	[27-30]
CACNB4	Voltage-gated L-type calcium channel, beta-4 subunit	2q22	JME+GTCS, IGE+GTCS	[31]
CACNA1A	Voltage-gated P/Q-type, alpha-1A subunit	19p13	IGE	[32]
CACNA1H	Voltage-gated calcium channel T-type, alpha-1H subunit	16p13.3	*CAE, JME, FS, TLE*	[33,34]
CLCN2	Chloride channel protein 2	3q26-qter	CAE, EGMA	[35]
Non-ion channels				
JRK	Jerky homolog	8q24	CAE, JME	[36]
Gpr98	Very large G-protein coupled receptor 1	5q14	FEB4	[37]
LGI1	Leucine-rich glioma-inactivated protein 1	10q24	ADPEAF, ADLTLE	[38]
EFHC1	EF-hand domain (C-terminal) containing 1	6p12-p11	JME	[39]
CRH	Corticotrophin-releasing hormone	8q13	ADNFLE	[40]
CSTB	Cystatin B	21q22.3	EPM1	[41]
CLN8	Ceroid Lipofuscinosis, Neuronal, 8	8pter-p22	EPMR	[42]
EPM2A	Laforin	6q24	EPM2	[43]
NHLRC1	Malin	6p22.3	EPM2	[44]
ALDH7A1	Aldehyde dehydrogenase 7 family, member A1	5q31	PDE	[45]

Table 1. Idiopathic epilepsy genes. Genes associated with *italic* printed epilepsy types are susceptibility genes. ADNFLE: autosomal dominant nocturnal frontal lobe epilepsy; GEPD: generalized epileptic seizures and paroxysmal nonkinesigenic dyskinesia; BFNIS: benign familial neonatal infantile seizures; FEB: familial febrile seizures; GEFS+: generalized epilepsy with febrile seizures +; SMEI: severe myoclonic epilepsy in infancy; TLE: temporal lobe epilepsy; FS: febrile seizures; JME: juvenile myoclonic epilepsy; IGE: idiopathic generalized epilepsy; CAE: childhood absence epilepsy; GTCS: generalized tonic-clonic seizures; EGMA: epilepsy with grand mal seizures on awakening; ADPEAF: autosomal dominant partial epilepsy with auditory features; ADLTLE: autosomal dominant lateral temporal lobe epilepsy; EPM1: myoclonic epilepsy of Unverricht and Lundborg; EPMR: progressive epilepsy with mental retardation; EPM2: myoclonic epilepsy of Lafora; PDE: pyridoxine-dependent epilepsy.

Gene	Description	Chromosomal Region	Positive association	Negative association
TLE associations				
IL1B	Interleukin 1 beta	2q14	[52-54]	[55-60]
PDYN	Prodynorphin	20pter-p12.2	[61,62]	[60,63,64]
BDNF	Brain-derived neurotrophic factor	11p13	[65]	[66]
GABBR1	Gamma-aminobutyric-acid B receptor, R1 subunit	6p21.3	[67,68]	[60,69-73]
PRNP	Prion protein	20pter-p12	[74,75]	[60]
SLC6A4	Serotonin transporter	17q11.1-q12	[76]	
SCN1B	Voltage-gated sodium channel type 1, beta subunit	19q13.1	[21]	
FS associations				
GABRG2	Gamma-aminobutyric-acid receptor, gamma-2 subunit	5q34	[77,78]	[60]
CHRNA4	Neuronal acetylcholine receptor protein, alpha-4 subunit	20q13.3	[79]	[60,80]
CSNK1G2	Casein kinase I gamma 2 isoform	19p13.3	[81]	
IMPA2	Myo-inositol monophosphatase 2	18p11.2	[82]	
IL1B	Interleukin 1 beta	2q14	[54,83]	[52,60,84]

Table 2. Genes associated with TLE and/or FS. Only genes with positive associations are shown. Genes with a positive replication are shown in bold face.

different populations worldwide [85,86]. In Europe and the United States, 2-4% of children up to the age of 5 years will suffer from at least one FS [85]. Of these affected children 30-40% develop recurrent FS [11]. FS can be divided in two categories, simple and complex FS. Simple FS are characterized by seizures lasting less than 15 minutes, no recurrence in the next 24 hours, and involvement of the entire body (classically a generalized tonic-clonic seizure). Complex FS are characterized by long duration (>15 minutes), recurrence, or focus on one part of the body. Retrospective studies showed a relationship between complex FS and TLE with HS. As many as 30-50% of patients with TLE had a history of prolonged FS during childhood [11], but it is still unclear if FS themselves contribute to the development of TLE, or whether a prenatal lesion, brain insult or a genetic predisposition exits, which is causal to both FS and TLE [87,88].

The genetics of febrile seizures

Epidemiological studies have shown that the etiology of FS is influenced by genetic susceptibility [103], and FS twin studies suggested a heritability of up to 70% [104]. These studies show that there is a strong genetic component to FS. Linkage analysis in familial pure FS disorders have resulted in several genetic loci, and genes (table 1 and 3). In contrast, an autosomal dominant generalized epilepsy disorder with associated FS (GEFS+) has provided more information about the genes involved in familial FS syndromes [105]. Known causative genes are the voltage-gated sodium channel α-subunit genes *SCN1A* and *SCN2A*, an associated β-subunit *SCN1B*, and a GABAA receptor γ-subunit gene, *GABRG2*. Although several genes, associations and loci for FS have been described (see table 1, 2 and 3), still little is known about genes influencing the susceptibility to non-familial FS seen in sporadic patients [106].

Febrile seizure animal models

Although it is possible to use adult human tissue from MTLE patients who experienced FS (resection tissue) to investigate pathology, physiology and gene expression, it is nearly

impossible to determine causal relationships between FS during childhood and alterations in the MTLE tissue resected often twenty or more years after FS. To investigate if childhood FS cause alterations in the brain that may lead to epilepsy several rat models for complex FS have been developed. In a number of these models, high fever is induced in young rats (10-days-old) using an infrared lamp or hot air, which results in tonic-clonic convulsions originating from the hippocampus. These convulsions can be sustained for a prolonged period of time [107-109].

Using this animal model, several structural, molecular and functional FS-induced changes have been described [reviewed by 110] and recently it was shown that prolonged experimental FS may lead to MTLE in a significant proportion of rats [111]. Structurally, hippocampal neurons were injured but not killed [112], minimal mossy fiber sprouting was present [113,114] and the MRI T2 signal in hippocampus and other limbic structures was increased after prolonged experimental FS [115]. Molecular changes included increased seizure threshold temperature in *Il1r1* deficient mice [116], altered HCN-channel expression [117], increased CB1 expression [118] and a transient increased FOS expression in the hippocampus [119] after prolonged experimental FS. Functionally, prolonged FS resulted in an increased *Ih*-current [120], increased GABAergic neurotransmission [121] and increased seizure susceptibility later in life [122].

Mechanistically, it was also shown that blocking CB1 signaling could inhibit the increased seizure susceptibility [123]. Recently, using an alternative hyperthermia seizure induction paradigm, it was shown that experimental FS can be caused by a respiratory alkalosis (hyperventilation) [109]. FS could be blocked by increasing ambient CO_2, which also prevented alterations in the *Ih*-current and CB1 levels. Although, these results suggest an interesting mechanism for triggering hyperthermia-induced seizures it is still unknown whether alkalosis is instrumental in the original FS model [107,108] and human FS.

Locus	Description	Chromosomal region	Gene	References
Temporal lobe epilepsy				
ETL1	Autosomal dominant lateral temporal lobe epilepsy	10q24	*LGI1*	[38]
ETL2	Familial temporal lobe epilepsy	12q22-q23.3		[89-91]
ETL3	Familial mesial temporal lobe epilepsy	4q13.2-q21.3		[92]
ETL4	Autosomal dominant occipitotemporal lobe epilepsy and migraine with visual aura	9q21-q22		[93]
Febrile seizures				
FEB1	Familial febrile convulsions	8q13-21		[94]
FEB2	Familial febrile convulsions	19p13.3		[95,96]
FEB3	Familial febrile convulsions	2q23-24	*SCN1A*	[17,97]
FEB4	Familial febrile convulsions	5q14-15	*GPR98*	[37,98]
FEB5	Familial febrile convulsions	6q22-24		[99]
FEB6	Familial febrile convulsions	18p11.2	*IMPA2*	[82,100]
FEB7	Familial febrile convulsions	21q22		[101]
FEB8	Familial febrile convulsions	5q31.1-q33.1	*GABRG2*	[30,102]
FEB9	Familial febrile convulsions	3p24.2-p23		[100]

Table 3. Genetic loci and genes associated with temporal lobe epilepsy and/or febrile seizures.

ANIMAL MODELS FOR EPILEPSY

General aspects of animal models for epilepsy

Besides the FS epilepsy model described in the previous section, many general and more specific epilepsy animal models have been developed to study the different aspects of epilepsy. These models help to determine causal relationships between alterations in human epilepsy tissue and epilepsy. Like in the human classification, animal models can be divided in two main categories: models investigating the genetic components, and models investigating acquired factors of epilepsy and epileptogenesis.

Genetic epilepsy models

Like in the human situation, single gene mutations which cause epilepsy can occur spontaneously in laboratory animals. A good example is the Frings mouse, which is prone to audiogenic seizures. A mutation in the *Gpr98* (also called *Mass1* or *VLGR1*) was identified [124] and led the way to identification of this gene in familial FS (FEB4 locus) in man [37]. Besides mono-genetic epileptic animal strains, animal strains like the GEARS rat and the EL mouse exist in which seizures are inherited as a multifactorial trait [125,126]. For EL mice several loci (El1-6) have been described which contribute to seizures in these mice [126]. Besides these spontaneously occurring variations, gene mutations can also be introduced in the laboratory. These approaches have been explored to explain gene variants in human epilepsy [7], but can also be used to identify new epilepsy causing mutations.

Another genetic approach is the identification of seizure susceptibility genes in non-epileptic mouse strains. Although most mouse strains do not develop spontaneous seizures, many widely used mouse strains differ significantly in seizure susceptibility induced by electrical stimulation [127] and chemoconvulsants [128]. Using this approach several quantitative trait loci (QTL) have been found, but identification of the underlying genes has proven difficult so far.

Acquired epilepsy models

Acquired epilepsy models have provided much information about the process of epileptogenesis. Most animal models use status epilepticus (SE) to induce the process of epileptogenesis. SE can be triggered by electrical or chemical stimulation [reviewed by 129,130]. Electrical stimulation is technically complex but most neuropathological changes reminiscent of human MTLE and spontaneous recurrent seizures develop after SE. Chemical stimulation can be achieved by applying chemoconvulsants like kainate or pilocarpine locally or systemically. These chemicals induce SE which can last for hours if untreated. After a latent period a high percentage of animals develop spontaneous recurrent seizures originating from the hippocampus with neuronal damage that resembles that of human MTLE. The kindling model is perhaps the most studied model of epileptogenesis. Kindling of epilepsy is achieved by repeated subconvulsive high frequency electrical stimulation of limbic structures in the amygdale, hippocampus or entorhinal cortex. Effects on neuropathology and spontaneous recurrent seizures depend on the site of stimulation and on the kindling procedures used [130].

Although these models show neuropathological changes that resemble the changes in human MTLE, the initiation of epileptogenesis does not resemble the situation in human MTLE. Most importantly, SE is not a major acquired factor contributing to epileptogenesis in human MTLE. Moreover, SE and kindling models are usually employed in adult animals, while acquired factors in MTLE usually occur in childhood. Finally, only a small percentage of people will develop epilepsy

after any of these acquired factors, while in the animal models most animals will develop epilepsy. These profound limitations raise the question to what extent these models are clinically relevant and whether they resemble the initial stages of epileptogenesis. Possibly they rather represent models of epileptogenesis in an already epileptic state, resembling the progressive nature of epilepsy.

Other epilepsy animal models, like the already described FS model, investigate human MTLE in a more physiological fashion. Epileptogenesis in these models is induced by brain damage (fluid percussion or hypoxia) or chemoconvulsant in a developmental period resembling childhood in humans. The models lack the high epilepsy rate found in the adult models, but do show several of the characteristics reminiscent of human MTLE [131,132]. In the next section several aspects of epileptogenesis will be discussed.

EPILEPTOGENESIS

General aspects of epileptogenesis

The term epileptogenesis refers to the complex process by which a normal brain transforms into an epileptic one. Processes leading to an epileptic brain are multifold, and involve genetic, environmental and combined factors. For MTLE the general idea is that a genetic predisposition and/or a pre- or postnatal lesions like FS, brain infection, neoplasm, brain trauma or stroke serves as starting point for epileptogenesis. Limbic structures like the hippocampus have been shown to be involved and understanding the cellular and molecular mechanisms of epileptogenesis may help to identify new therapeutic approaches to prevent or cure, rather then to treat, epilepsy.

Glutamate receptors and epileptogenesis

Ionotropic glutamate receptors mediate the vast majority of excitatory neurotransmission in the central nervous system (CNS) and are therefore of special interest in epilepsy. Ionotropic glutamate receptors can be divided into three major classes: α-amino-3-hydroxy-5-methyl-4-isoxazole propionate (AMPA)-, N-methyl D-aspartate (NMDA)-, and 2-carboxy-3-carboxymethyl-4-isopropenylpyrrolidine (kainate) type receptors. In respect to epileptogenesis, the NMDA and AMPA receptor and their signal transduction pathways are the most studied. NMDA receptors have mainly been shown to be involved in epileptogenesis in the SE models, while AMPA receptors have been shown to be involved in the juvenile models [reviewed by 133].

The importance of NMDA receptors has been shown in kindling and SE models of epilepsy by their effect on the promotion of epileptogenesis. Antagonists of the NMDA receptors have been shown to inhibit epileptogenesis in the kindling models and to prevent late-onset spontaneous, recurrent seizures in the pilocarpin model [134-136]. Moreover, gene-targeted mice lacking the large carboxy-terminal domain of the *Nr2a* subunit of the NMDA receptor showed impaired epileptogenesis similar to that induced by NMDA receptor antagonists [137]. Studies investigating the molecular signaling responses which result from the activation of NMDA receptors show that the most likely mechanisms for NMDA receptor-mediated epileptogenesis are decreased synaptic inhibition, enhanced synaptic excitation and structural pro-epileptogenic reorganization (mossy fiber sprouting) [reviewed by 133]. The crucial role of Ca^{2+} in the NMDA receptor induced plasticity changes suggests that the flux of Ca^{2+} through the NMDA receptor initiates the cascades that culminate in epileptogenesis.

In contrast to NMDA receptors, AMPA receptors have been shown to be key players in epileptogenesis in neonatal hypoxia models. In these models, hypoxic seizures are induced in animals of 10-12 days old, which result in increased seizure susceptibility to seizures later in life. The develop-

mental stage at which hypoxic seizures are induced coincides with peak expression of Ca^{2+}-permeable AMPA receptors. Treatment with the AMPA receptor antagonist NBQX right after neonatal seizures prevented enhanced sensitivity to seizure-induced cell death and slightly reversed (nonsignificant) the increased seizure susceptibility later in life. Molecular mechanisms include activation of calcineurin and subsequent endocytosis of GABAA receptors and decreased synaptic inhibition. Like the case with NMDA receptors in the adult brain, the flux of Ca^{2+} through the Ca^{2+}-permeable AMPA receptor is most likely the signal that initiates the cascades that culminate in neonatal induced epileptogenesis [reviewed by 133].

Calcium-calmodulin kinase 2 and epileptogenesis

Increased intracellular Ca^{2+} is one of the key steps in initiating neuronal signal transduction pathways [138], which includes the activation of Calcium-calmodulin kinase 2 (CAMK2). CAMK2 is abundantly expressed in the brain as a major constituent of the postsynaptic density (PSD) and is involved in long-term potentiation and neurotransmitter release [139]. The enzyme is an oligomeric protein composed of distinct but related subunits, alpha, beta, gamma, and delta, each encoded by a separate gene. CAMK2A assembles into hetero-oligomeric complexes with other CAMK2 subunits. After NMDA/AMPA receptor activation and Ca^{2+} influx, CAMK2 is activated and translocated from the cytosol to excitatory synapses [139].

Camk2a knockout mice develop limbic epilepsy and anti-sense oligonucleotide mediated reduction of CAMK2A levels in hippocampal cultures showed spontaneous epileptic discharges [140,141]. These studies suggest that reduced expression of CAMK2A is sufficient to induce limbic epilepsy. The significance of CAMK2 is even more substantiated by identification of reduced CAMK2 level/activity/phosphorylation in several models of acquired epilepsy. Reduced CAMK2 level/activity/phosphorylation was shown after pilocarpine induced seizures [142-144], after kainic acid induced seizures [145,146] after kindling seizures [147,148], after electroconvulsive seizures [149] and after repeated audiogenic seizures [150]. Altered CAMK2 expression has also been found in human epileptic tissue [151-153].

The evidence of reduced CAMK2 activity during epileptogenesis, supported by genetic and pharmacological data, suggests that reduced CAMK2 activity is sufficient to induce changes that render the brain epileptic. Its translocation from synapse to cytosol could further reduce its effectiveness [146]. In addition, reductions of CAMK2 content could structurally influence the PSD [154].

Immunity and epileptogenesis

In recent years more and more studies have suggested a link between epileptogenesis and the immune system. Certain types of epilepsy are thought to be caused by chronic inflammation by auto-antibodies or increased numbers of cytokines [reviewed by 155]. Supporting, a polymorphism in the cytokine *IL1B* has been shown to be associated with FS, MTLE and hippocampal sclerosis [52,53]. Moreover, in response to SE, stroke, trauma or infection, all acquired factors associated with TLE, the immune system can be activated. This can result in the recruitment of proinflammatory chemokines and cytokines, prostaglandin synthesis, complement activation and other inflammatory responses [144,156]. This first recruitment can be beneficial to the patient, but it is hypothesized that chronic high levels of these immune processes can induce excessive brain damage, cellular changes and epilepsy.

Of particular interest are the chemokines. First characterized in the immune system, chemokines act through G-protein-coupled receptors and utilize several transduction

pathways including inhibition of adenylate cyclase, activation of phospholipase C (PLC) and release of intracellular Ca^{2+} [157]. Recently, it was shown that chemokines and their receptors are widely expressed in microglia, astrocytes and neurons of the CNS [reviewed by 158]. Chemokine expression in the CNS is generally low, but elevated levels are produced in response to brain injury and disease and result in activation and chemoattraction of immune cells such as monocytes, which infiltrate the CNS [159,160]. Besides these chemoattractive properties chemokines can also have direct effects on neurons and astrocytes [158]. The effects include release of intracellular Ca^{2+}, altered neuronal excitability and effects on neuronal survival [158,161,162].
Chemokine expression has been identified directly after seizures but also during epileptogenesis when no seizures were present [156]. These results suggest an important role of chemokines in epileptogenesis. Effects of chemokines on neurons are probably mediated by release of intracellular Ca^{2+}, which in itself can activate several transduction pathways. Already described in detail in the previous section, increased intracellular Ca^{2+} can activate CAMK2A, which on the long run could be responsible for epileptogenesis and alterations of the PSD [reviewed by 133,154].

AIM AND OUTLINE OF THIS THESIS

The previous sections describe the current knowledge about the relationship between FS, MTLE and epileptogenesis. Despite our knowledge in this area, many of the molecular factors and cellular processes from which epilepsy originates have remained unknown. Due to novel high-throughput technology arisen from genome sequences, in particular expression microarrays, it is now possible to approach epilepsy in other ways. The overall aim of this thesis is to identify key genes, proteins and processes involved in MTLE, FS and epileptogenesis.

In **chapter 2** we have investigated human differential gene expression between hippocampus tissue of autopsy control and HS and nonHS MTLE patients in a three-way microarray analysis. The specific aim of this study was to identify relevant processes involved in the chronic pathogenesis of MTLE and HS.

In **chapter 2** we identified differential expression of a relatively new voltage gated sodium channel (Na_v) subunit (Navβ3 or *SCN3B*) in nonHS MTLE patients. Mutations in several other Na_v subunits have been shown to cause generalized epilepsy, FS and TLE, signifying the role of Na_v subunits in human epilepsy. **Chapter 3** describes a detailed analysis of Navβ3 expression. Protein distribution was investigated in autopsy controls and in HS and nonHS MTLE patients.

Immunity and defense was one of the processes found to be up-regulated in MTLE patients (**chapter 2**). Of particular interest were the chemokines *CCL3* and *-4*, which were approximately 20 times up-regulated. **Chapter 4** describes a detailed analysis of CCL3 and -4 expression in the normal and the epileptic human hippocampus. Neuronal effects induced by pathological concentrations of CCL3 were investigated using fura-2 based Ca^{2+} imaging in a rat hippocampal neuron culture system.

FS have been shown to be involved in MTLE and to investigate the relationship between FS and MTLE several rat animal models have been developed. Although these models have provided much data on the physiological effects of prolonged FS, molecular and genetic data are sparse. To allow for more detailed molecular analysis and genetic studies we developed two FS models in mice

(**chapter 5**). Prolonged FS were induced in 10-day-old mice and long-term functional FS effects, which have been described in the rat model, were validated in our mouse model. The model was slightly modified to investigate FS susceptibility. To investigate whether FS susceptibility in the mouse is influenced by common genetic variation we tested 7 genetically distinct mouse strains for FS susceptibility.

In **chapter 6** we have used the prolonged FS model to investigate differential gene expression longitudinally after FS. Aim of this study was to identify critical and functional mediator genes involved in epileptogenesis after FS.

Chapter 7 elaborates on the genetics of FS susceptibility in mice and describes the identification of QTLs that influence FS susceptibility in mice. QTLs were identified per chromosome by using a mouse chromosome substitution panel.

Preliminary data showed that newly diagnosed children with acquired epilepsies have approximately 50% less mRNA for glutamine synthetase (GS or *Glul*) in their white blood cells. Reduced hippocampal expression of GS has also been shown in human MTLE patients. GS is a key enzyme in glutamatergic neurotransmission and could influence seizure susceptibility. In **chapter 8** we have used the FS model to investigate whether mice with only half the normal GS expression (haploinsufficient *Glul* mice) are more susceptible to FS than normal GS expressing mice.

In **chapter 9**, results presented in this thesis are summarizes and discussed in the context of MTLE, FS and epileptogenesis.

CHAPTER 2

Possible role of the innate immunity in temporal lobe epilepsy

Koen LI van Gassen[1], Marina de Wit[1], Marian JA Groot Koerkamp[2], Marije GA Rensen[1], Peter C van Rijen[1], Frank CP Holstege[2], Dick Lindhout[3] and Pierre NE de Graan[1]

[1]Rudolf Magnus Institute of Neuroscience, Department of Neuroscience and Pharmacology, University Medical Center Utrecht, Utrecht, The Netherlands
[2]Department of Physiological Chemistry, University Medical Center Utrecht, Utrecht, the Netherlands
[3]DBG-Department of Medical Genetics, University Medical Center Utrecht, Utrecht, the Netherlands

Epilepsia. 2008, 49:1055-65.

ABSTRACT

Temporal lobe epilepsy (TLE) is a multifactorial disease often involving the hippocampus. So far the etiology of the disease has remained elusive. In some pharmaco-resistant TLE patients the hippocampus is surgically resected as treatment. To investigate the involvement of the immune system in human TLE, we performed large scale gene expression profiling on this human hippocampal tissue. Microarray analysis was performed on hippocampal specimen from TLE patients with and without hippocampal sclerosis and from autopsy controls (*n* = 4 per group). We used a common reference pool design to perform an unbiased three-way comparison between the two patient groups and the autopsy controls. Differentially expressed genes were statistically analyzed for significant over-representation of gene ontology (GO) classes. Three-way analysis identified 618 differentially expressed genes. GO analysis identified immunity and defense genes as most affected in TLE. Particularly the chemokines CCL3 and CCL4 were highly (>10-fold) up-regulated. Other highly affected gene classes include neuropeptides, chaperonins (protein protection) and the ubiquitin/proteasome system (protein degradation). The strong up-regulation of CCL3 and CCL4 implicates these chemokines in the etiology and pathogenesis of TLE. These chemokines, which are mainly expressed by glia, may directly or indirectly affect neuronal excitability. Genes and gene clusters identified here may provide targets for developing new TLE therapies and candidates for genetic research.

INTRODUCTION

Epilepsies are amongst the most common neurological disorders and affect up to 1% of the population [2]. Temporal lobe epilepsy (TLE) is the most common partial epilepsy and is often medically intractable. Patients with TLE experience recurring episodes of spontaneous neuronal activity originating from the medial temporal lobe. TLE is considered to be a multifactorial disease, implying the involvement of multiple susceptibility genes and complex gene-environment interactions [1,9]. Environmental factors implicated in TLE include febrile seizures, head trauma, brain infection and tumors. The molecular mechanisms involved in the etiology and neuropathology of TLE remain poorly understood [163-165]. Insight in these mechanisms is essential for the development of new antiepileptic drugs that interfere with the progression of the disease.

Evidence from experimental and clinical studies implicates inflammatory reactions in TLE [144,155,166] and genetically, the IL1-beta-511T allele is associated with human TLE [60,167]. Microarray analysis of enthorinal cortex samples from TLE patients revealed only 16 significant differentially expressed genes, mainly implicated in the local immune and complement system [168]. The few microarray studies performed on human hippocampal TLE specimens [169-171], show only limited overlap in their sets of differentially expressed genes.

The hippocampus of pharmaco-resistant TLE patients is often surgically resected as part of the treatment. In about two-thirds of the operated TLE patients the hippocampus is subject to hippocampal sclerosis (HS); massive neuronal loss, gliosis/sclerosis, granule cell dispersion and mossy fiber sprouting [172]. The other one-third usually suffers from focal lesions in the temporal lobe, but has no apparent hippocampal damage (nonHS). The resection material offers the unique opportunity to study the etiology and neuropathology of TLE.

The aim of our study was to investigate the involvement of the brain immune system in the complex etiology of TLE. We therefore performed a genome-wide expression analysis on hippocampal specimens of TLE patients with and without sclerosis and on autopsy controls using oligonucleotide microarrays. The common reference pool design allowed us to perform a three-way statistical analysis between the expression profiles of the three groups to identify differentially expressed genes for TLE, but also for HS neuropathology. These significant gene lists were subsequently subjected to gene ontology analysis for an unbiased identification of relevant gene functions, biological processes and signal transduction pathways in TLE.

METHODS

Patient samples

Hippocampal tissue of pharmaco-resistant TLE patients was obtained after surgery in the University Medical Centre in Utrecht. Patients were selected for epilepsy surgery according to the criteria of the Dutch Epilepsy Surgery Program [173]. The excision was based on clinical evaluations, interictal and ictal EEG studies (video EEG monitoring), MRI, and intraoperative electrocorticography. Informed and written consent was obtained from the patients for all procedures as approved by the Institutional Review Board. The hippocampus was resected *en bloc* and cut into three slices perpendicular to its long axis. The middle slice was used for molecular analysis, the other slices for pathological analysis. Middle slices were immediately frozen on powdered dry ice and stored at -80°C until further use. To match patients across groups, patients were carefully selected based on their neuropathology, anamnesis, ethnic background, gender, age at surgery, age of epilepsy onset and use of medica-

tion. Exclusion criteria included dual pathology or cortical, hippocampal or venous malformations. Representative paraffin sections (7 µm) were stained with cresyl violet (Nissl stain) for neuropathological evaluation. Only tissue samples containing all the hippocampal subregions were used to isolate RNA. Hippocampal sclerosis was diagnosed and classified according to Wyler [46]. In the TLE group without hippocampal sclerosis (nonHS, Wyler grade 0; *n* = 4; 40 ± 5.5 years old) we included two patients with oligodendroglioma and two with preexisting head trauma. None of the focal lesions extended into the hippocampus proper. In the hippocampal sclerosis group (HS, Wyler grade 4; *n* = 4; 37 ± 3.4 years old) we included two patients who had febrile convulsions during childhood and two patients without any evidence for a precipitating injury. At the time of surgery, all TLE patients received anti-epileptic medication either as mono- or polytherapy. Relevant clinical data for the TLE patients included in this study are listed in table 1.

Autopsy control slices were cut from the middle portion of hippocampi obtained from the Netherlands Brainbank (NBB). The autopsy controls (*n* = 4; 52.5 ± 5.0 years old; 2 males; 2 females) had no history of brain-related disease and suffered sudden deaths without associated brain damage. Autopsy was rapidly performed by the NBB with a short post-mortem delay. At autopsy hippocampi were dissected, pH was checked to be between 6 and 7 (optimal for RNA stability), and frozen in liquid nitrogen and stored at -80°C at the NBB. Normal hippocampal morphology was checked by neuropathological examination. Ages are reported as mean ± standard deviation.

Isolation of RNA

Hippocampal cryo-sections were cut, collected and stored at -80°C. Total RNA was isolated, purified and checked for quality. The RNA quality of all the patient and autopsy control samples was comparable. Careful analysis of individual gene expression data did not reveal any effect of post-mortem delay or any overall mRNA breakdown. To allow a three-way comparison between the HS, the nonHS and the autopsy control group, a common total RNA reference pool was generated. Total RNA of 10 cortex and 10 hippocampal tissue samples from a separate population of TLE patients with various pathologies were mixed in equal quantities to guarantee optimum representation of gene expression in the common reference pool.

Patient nr.	Pathology	Disease	Medical history	Sex	Age at surgery	Age onset epilepsy	Duration of Epilepsy	Sample site	Medication at surgery
1	nonHS	MTLE	trauma	F	48	26	22	Left	O
2	nonHS	MTLE	trauma	M	37	18	19	Right	C, P
3	nonHS	MTLE	tumor	M	39	16	23	Right	C, V, Cl
4	nonHS	MTLE	tumor	M	36	17	19	Right	V, L
5	HS	MTLE	blanc history	F	36	11	25	Right	C, T, L
6	HS	MTLE	blanc history	F	32	14	18	Left	C, Cl
7	HS	MTLE	FS	M	38	9	29	Left	C, P, La
8	HS	MTLE	FS	M	40	10	30	Right	C, Ph

Table 1. Relevant clinical data on temporal lobe epilepsy (TLE) patients used in this study. Age at tissue collection (in years) was significantly higher in autopsy controls but did not different between patients with hippocampal sclerosis and without hippocampal sclerosis (HS and nonHS patients). Age of epilepsy onset (in years) was significantly lower in HS patients than in nonHS patients. Duration of epilepsy (in years) was not statistically different between HS and nonHS patients. Statistical analysis was performed using a Student's t-test. nonHS: without hippocampal sclerosis, HS: hippocampal sclerosis, MTLE: mesial temporal lobe epilepsy, FS: febrile seizures, O: Oxcarbazepine, C: Carbamazepine, P: phenytoin, V: Valproate, Cl: Clobazam, L: Levetiracetam, T: Topiramate, La: Lamotrigine, Ph: Phenobarbital.

Microarray analysis

Two-channel oligonucleotide microarray analysis was performed as described [174]. Briefly, cDNA from 2 µg total RNA was synthesized using a T7 oligo(dT)24VN primer (Ambion, Cambridgeshire, UK). The T7 Megascript kit (Ambion) was used for cRNA synthesis and its quality was analyzed. Cy3 or Cy5 fluorophores (GE Healthcare Europe, Diegem, BE) were coupled to 2000 ng patient and common reference pool cRNA. The degree of label incorporation was monitored and hybridizations were set up with 1500ng of Cy3 and 1500 ng of Cy5 labeled cRNA, always hybridizing a patient sample and the common reference pool on the same chip, including a dye-swap.

The human Array-Ready oligo set (version 2.0, Operon Biotechnologies, Cologne, DE) was printed on UltraGAPS slides (Corning, Schiphol-Rijk, NL). Slides were washed by hand and scanned. Scanned slides were quantified and the background-corrected with Imagene v5.6.1 (BioDiscovery, El Segundo, USA) and Loess normalized per print-tip [175]. To identify significant differentially expressed transcripts, ANOVA analysis was applied (R/MAANOVA version 0.98-3, http://www.r-project.org/). Sample groups were compared via the common reference pool. In a fixed effect analysis, sample, array and dye effects were modeled. *P*-values were determined by a permutation F2-test, in which residuals were shuffled 5000 times globally after family-wise error correction. *P*-values were not corrected for the three comparisons. Transcripts with $P < 0.05$ were considered significant. MIAME-compliant descriptions of protocols, experimental design, arrays, raw and normalized data have been deposited in

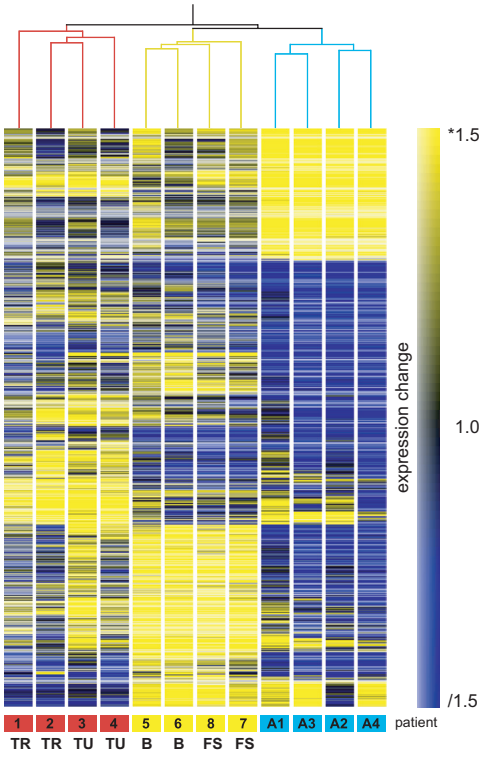

Figure 1. Patient clustering. An unbiased transcript list (expression above 300) was used to perform a condition tree clustering (standard correlation, Genespring v7.2) to order patients according to gene expression levels. Only significantly differentially expressed transcripts were plotted (colored according to patient versus common reference pool gene expression ratios), which were ordered by the gene tree clustering (standard correlation, Genespring v7.2). Patients are colored according to pathology (red: without hippocampal sclerosis/nonHS, yellow: with hippocampal sclerosis/HS, blue: autopsy controls) and medical histories are indicated (TR: trauma, TU: tumor, B: blanc medical history and FS: febrile seizures).

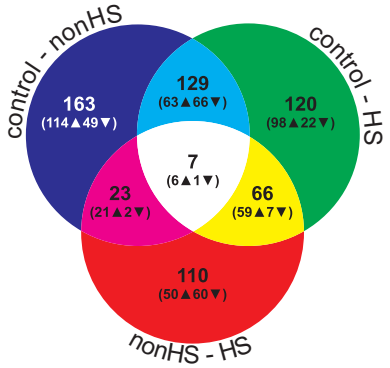

Figure 2. Venn diagram showing the distribution of significantly differentially expressed transcripts. The up- and down-expressed transcripts versus autopsy control are indicated. For the unique 110 transcripts of patients with hippocampal sclerosis (HS) compared to those without hippocampal sclerosis (nonHS), up and down was relative to nonHS expression.

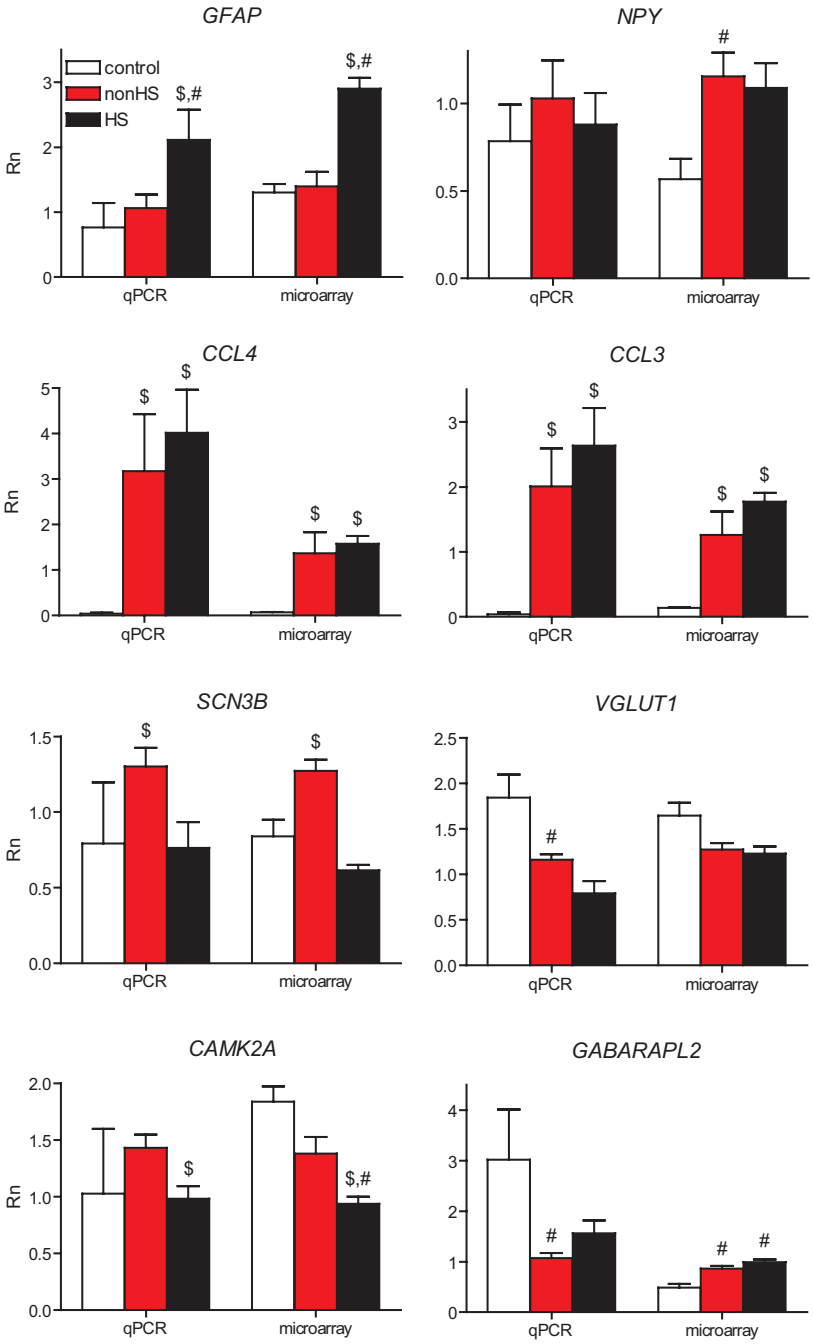

Figure 3. Microarray gene expression validation by qPCR analysis. Reference pool normalized microarray gene expression data and *PSMD2* normalized qPCR gene expression data (Rn) were plotted. #significantly differentially expressed between autopsy controls and patients with hippocampal sclerosis (HS) or without hippocampal sclerosis (nonHS) patients, $significantly differentially expressed between HS and nonHS patients. $P < 0.05$ was considered significant (microarray: R/MAANOVA, qPCR: 1-tailed Student's *t*-test). Plotted are means ± standard error of the mean.

the ArrayExpress public microarray database (www.ebi.ac.uk/arrayexpress/), all under the experiment accession number E-MEXP-744.

Quantitative RT-PCR

cDNA was synthesized from the RNA samples used for the microarray using oligo-dT primers. The qPCR reaction was performed using the LightCycler (Roche, Almere, NL) and the Fast Start DNA Master PLUS SYBRgreen I kit (Roche). Primer (Sigma Genosys, Cambridge, UK) specifications are listed in the supplementary table 1 (online; Epilepsia.com). Gene expression was calculated as normalized ratio and normalized to two reference genes. cDNA from the common reference pool was used for calibration. The reference genes (Proteasome 26S subunit, non-ATPase, 2 (*PSMD2*) and DEAD (Asp-Glu-Ala-Asp) box polypeptide 48 (*DDX48*)) were selected because of their housekeeping function and their microarray expression strength and stability. All samples were analyzed in duplicate and reported as mean ± standard error of the mean (SEM). Both reference genes gave similar results. To compare qPCR with microarray data, data were analyzed using one tailed Student's *t*-tests, with $P < 0.05$ considered significant.

Gene ontology (GO) analysis

For GO and pathway analysis, significant transcript lists (P<0.05) and a reference list comprising all the transcripts on the microarray were imported into the software tool Panther (www.pantherdb.org) [176]. Of the 17,898 transcripts with a RefSeq identifier 14,787 unique transcripts could be mapped to Panther and these were used to generate the reference gene list containing all the annotated genes in our microarray screen. 286 out of 322 transcripts for autopsy controls versus nonHS, 284 out of 322 transcripts for autopsy controls versus HS and 184 out of 206 transcripts for nonHS versus HS could be mapped against the Panther database. Of the transcripts with a RefSeq identifier assigned, all but one mapped to Panther. Panther's GO classes are greatly abbreviated and simplified to facilitate high-throughput analyses. Significant lists were statistically compared to the reference list for significant over-representation of genes within the gene ontology classes for molecular function, biological process and pathways. Only highly significant ($P < 0.01$) gene ontology classes containing more than one gene are shown. More in-depth analyses were performed with the software tool Webgestalt (bioinfo.vanderbilt.edu/webgestalt) [177], which is unsupervised and uses all the gene ontology classes from the gene ontology consortium [178].

RESULTS

Microarray gene expression analysis

To evaluate consistency in the expression patterns of patients within and between the three patient groups, dye-swaps were pooled and patient data was clustered (Genespring v7.2, Agilent, Amstelveen, NL) (figure 1). Unbiased cluster analysis of the expression profiles of all samples resulted in a clear clustering according to the neuropathology of the nonHS, HS and autopsy control groups (figure 1). No confounding factors were identified in the cluster diagram. This analysis validates the patient selection and shows that specific expression profiles can be found that are characteristic for the respective pathologies.

In order to identify genes that were differentially expressed between the nonHS group, the HS group and the autopsy controls we performed a MAANOVA analysis. In total 618 significantly differentially expressed transcripts were identified, distributed over the three comparisons (autopsy controls versus nonHS, autopsy controls versus HS and nonHS versus HS) (see figure 2). Comparing autopsy controls and nonHS revealed 322 differentially expressed transcripts (302 coding

for known Refseq genes), comparing autopsy controls and HS revealed 322 transcripts (300 known), and comparing nonHS and HS revealed 206 transcripts (190 known). We found that 136 out of the 322 differentially expressed genes (42%) were identical when we compared both the nonHS and the HS group with the autopsy controls. This indicates that, although the neuropathology in the two TLE groups is different, they share a large group of differentially expressed genes. However, clustering and statistical comparison of the nonHS and the HS groups also revealed some major differences between these patient groups (206 genes differentially expressed). Seven genes were differentially expressed in all three comparisons. Further analysis of these genes revealed that their expression was mildly affected in the nonHS group but strongly affected in the HS group (compared to autopsy controls). All significantly differentially expressed genes for the three comparisons are listed in supplementary table 2 (online; Epilepsia.com). Table 2 only shows the 25 most affected transcripts for each comparison.

Quantitative RT-PCR analysis

To independently validate our results we used qPCR to quantify mRNA levels. Eight genes were selected based upon differential expression and function. As shown in figure 3, the qPCR analysis for these eight genes replicates almost all the microarray data. From a total of 24 comparisons (8 genes x 3 comparisons), the results in 19 comparisons were replicated using qPCR (figure 3). To analyze the overall reliability of the microarray data in more detail, we plotted the microarray gene expression (versus the reference mRNA pool) for each individual patient against patient qPCR gene expression (versus the reference gene *PSMD2*) (figure 4). The correlation between microarray and qPCR values was significant ($r = 0.58$, $P < 0.0001$), and comparable to other validation studies [179].

Gene ontology (GO) analysis

To identify functionally relevant gene clusters we performed GO analysis using the web tool Panther. Although for exploratory research *P*-values of 0.05 are often used, we used a cutoff of 0.01 to select the most relevant functions, processes and pathways (table 3). The most striking overrepresentation of genes was found in the immunity and defense process and in chemokine function when comparing HS versus autopsy controls, in chaperonin function and the ubiquitin proteasome pathway when comparing nonHS versus autopsy controls and in neuronal activities and the ionotropic glutamate receptor pathway when comparing HS versus nonHS patients. Similar results were obtained when larger gene lists with less strict statistical tests were applied.

DISCUSSION

We have used large-scale expression profiling to identify genes that are differentially expressed between specimens from hippocampi surgically removed from TLE patients (with and without hippocampal sclerosis) and from autopsy controls. The study was performed using a common reference pool design, which enabled the unbiased three-way analysis of differential gene expression between the three experimental groups. Throughout the study we placed emphasis on patient selection, reliability and reproducibility control. We validated our selection of patients and autopsy controls by cluster analysis of the gene expression profiles of each individual patient and the microarray expression profiles were verified by qPCR analysis. The qPCR validation has recently been replicated in an independent patient population [van Gassen & de Graan, unpublished]. We have carefully selected autopsy control patients with a short post-mortem de-

Array feature	RefSeq	Gene symbol	Fold change	*P*-value	Average signal	Gene description
HS versus control						
6174	NM_002984	*CCL4*	▲ 21.94	0	2355	Small inducible cytokine A4
5774	NM_017634	*KCTD9*	▲ 14.82	0	1767	Potassium channel tetramerisation domain containing protein 9
5869	NM_002983	*CCL3*	▲ 12.15	0	1393	Small inducible cytokine A3
18169	NM_002982	*CCL2*	▲ 3.98	0	1011	Small inducible cytokine A2
3547	NM_005252	*FOS*	▲ 3.73	0	744	Proto-oncogene protein c-fos
6264	NM_004105	*EFEMP1*	▲ 3.63	0	2524	EGF-containing fibulin-like extracellular matrix protein 1
3166	NM_024411	*PDYN*	▲ 3.60	0	984	Beta-neoendorphin-dynorphin
18868	NM_004028	*AQP4*	▲ 3.53	0	2012	Aquaporin-4
17914	NM_002166	*ID2*	▲ 3.30	0	1087	DNA-binding protein inhibitor ID-2
5946	NM_000165	*GJA1*	▲ 3.18	0	6680	Gap junction alpha-1 protein
11766	NM_003118	*SPARC*	▲ 3.09	0	5246	Osteonectin
12600	NM_000576	*IL1B*	▲ 2.99	0	490	Interleukin-1 beta
4076	NM_024843	*CYBRD1*	▲ 2.65	0	930	cytochrome b reductase 1
5960	NM_001387	*DPYSL3*	▲ 2.57	0	1244	Dihydropyrimidinase-related protein 3
8268	NM_002414	*CD99*	▲ 2.54	0	4863	T-cell surface glycoprotein E2
14614	NM_000371	*TTR*	▼ 3.58	0	549	Transthyretin
18365		*RP11-436K8.1*	▼ 2.82	0	4618	novel transcript
19051	NM_032121	*NP_115497.3*	▼ 2.80	0	18147	implantation-associated protein
5334	NM_003097	*SNRPN*	▼ 2.74	0	18376	Small nuclear ribonucleoprotein associated protein N
19112	NM_153831	*PTK2*	▼ 2.72	0	9643	Focal adhesion kinase 1
9356	NM_020746	*MAVS_HUMAN*	▼ 2.69	0	11471	Mitochondrial antiviral signaling protein
6624	NM_032781	*PTPN5*	▼ 2.69	0	3293	Tyrosine-protein phosphatase non-receptor type 5
15923	NM_003518	*HIST1H2BG*	▼ 2.64	0	17984	Histone H2B.a/g/h/k/l
17035	NM_018038	*NP_060508.1*	▼ 2.61	0	6738	
14174	XM_292012	*PABPC1*	▼ 2.57	0	1217	Polyadenylate-binding protein 1

Table 2 continues

Array feature	RefSeq	Gene symbol	Fold change	*P*-value	Average signal	Gene description
nonHS versus control						
6174	NM_002984	*CCL4*	▲ 24.47	0	3412	Small inducible cytokine A4
5774	NM_017634	*KCTD9*	▲ 10.76	0	1379	Potassium channel tetramerisation domain containing protein 9
5869	NM_002983	*CCL3*	▲ 9.84	0	1250	Small inducible cytokine A3
3166	NM_024411	*PDYN*	▲ 4.51	0	1165	Beta-neoendorphin-dynorphin
18169	NM_002982	*CCL2*	▲ 3.33	0	912	Small inducible cytokine A2
244	NM_001888	*CRYM*	▲ 2.69	0	1840	Mu-crystallin homolog
17914	NM_002166	*ID2*	▲ 2.67	0	950	DNA-binding protein inhibitor ID-2
8005	NM_006379	*SEMA3C*	▲ 2.63	0	564	Semaphorin-3C precursor
18868	NM_004028	*AQP4*	▲ 2.52	0	1724	Aquaporin-4
12600	NM_000576	*IL1B*	▲ 2.50	0	446	Interleukin-1 beta
14614	NM_000371	*TTR*	▼ 3.67	0	544	Transthyretin
5334	NM_003097	*SNRPN*	▼ 3.28	0	16917	Small nuclear ribonucleoprotein associated protein N
19112	NM_153831	*PTK2*	▼ 3.24	0	8928	Focal adhesion kinase 1
19051	NM_032121	*NP_115497.3*	▼ 3.15	0	16984	implantation-associated protein
9475	NM_000405	*GM2A*	▼ 3.14	0	3937	Ganglioside GM2 activator
15923	NM_003518	*HIST1H2BG*	▼ 3.06	0	17403	Histone H2B.a/g/h/k/l
17035	NM_018038	*NP_060508.1*	▼ 3.05	0	6213	
18365		*RP11-436K8.1*	▼ 2.94	0	4435	novel transcript
13687		*ENSG00000196620*	▼ 2.77	0.0026	503	
15345		*ENSESTG00000025210*	▼ 2.71	0	5038	
7333	NM_014653	*NP_055468.2*	▼ 2.66	0	1372	
9356	NM_020746	*MAVS_HUMAN*	▼ 2.55	0	10510	Mitochondrial antiviral signaling protein
9274		*Q8WYW1_HUMAN*	▼ 2.51	0	33769	
15764	NM_016170	*TLX2*	▼ 2.51	0	19380	T-cell leukemia homeobox protein 2
1763	NM_004863	*SPTLC2*	▼ 2.50	0	34798	Serine palmitoyltransferase 2

Table 2 continued and continues

Array feature	RefSeq	Gene symbol	Fold change	*P*-value	Average signal	Gene description
HS versus nonHS						
6264	NM_004105	*EFEMP1*	▲ 2.88	0	2484	EGF-containing fibulin-like extracellular matrix protein 1
3545	NM_014017	*LM1P_HUMAN*	▲ 2.31	0	5272	Late endosomal/lysosomal Mp1 interacting protein
12106	NM_001129	*AEBP1*	▲ 2.31	0	1792	adipocyte enhancer binding protein 1
5634			▲ 2.23	0	2759	genomic:12-12399834-12399902
6333	NM_002167	*ID3*	▲ 2.03	0	1642	DNA-binding protein inhibitor ID-3
11766	NM_003118	*SPARC*	▲ 1.95	0	5639	Osteonectin
378	NM_002055	*GFAP*	▲ 1.92	0	29541	Glial fibrillary acidic protein
1565	NM_007177	*DRR1_HUMAN*	▲ 1.92	0	2537	Down-regulated in renal cell carcinoma 1
20442	NM_006425	*NP_006416.3*	▲ 1.90	0	10445	step II splicing factor SLU7
8353	NM_006472	*TXNIP*	▲ 1.87	0	1474	thioredoxin interacting protein
7027	NM_006272	*S100B*	▲ 1.87	0	7921	S-100 calcium-binding protein beta subunit
4076	NM_024843	*CYBRD1*	▲ 1.84	0	971	cytochrome b reductase 1
7867	NM_206821	*MYBPC1*	▲ 1.80	0	1096	Myosin-binding protein C, slow-type
876	NM_006621	*AHCYL1*	▲ 1.80	0	2224	Putative adenosylhomocysteinase 2
15988	NM_000524	*HTR1A*	▲ 1.79	0	3361	5-hydroxytryptamine 1A receptor
5946	NM_000165	*GJA1*	▲ 1.79	0	6994	Gap junction alpha-1 protein
15537	NM_023927	*GRAMD3*	▲ 1.76	0	618	GRAM domain-containing protein 3
10724	NM_000749	*CHRNB3*	▲ 1.71	0	4561	Neuronal acetylcholine receptor protein, beta-3 subunit
632	NM_000867	*HTR2B*	▼ 2.72	0	303	5-hydroxytryptamine 2B receptor
939	NM_018400	*SCN3B*	▼ 2.03	0	2839	Sodium channel beta-3 subunit
1205	NM_001031701	*NP_057659.1*	▼ 2.00	0	968	
4497	NM_015193	*ARC*	▼ 1.89	0	1074	activity-regulated cytoskeleton-associated protein
6726	NM_012329	*MMD*	▼ 1.88	0	2739	Monocyte to macrophage differentiation protein
11338	NM_003633	*ENC1*	▼ 1.84	0	2364	Ectoderm-neural cortex 1 protein
2947	NM_001682	*ATP2B1*	▼ 1.78	0	1759	Plasma membrane calcium-transporting ATPase 1

Table 2 continued. Significant differentially expressed gene list of the 25 genes with the highest fold change. Average signals were calculated from all patient expression values in each comparison. Genes were sorted based upon direction of change (indicated by up and down arrowheads) and fold change. A *P*-value of 0 represents $P < 0.0001$.

lay and checked mRNA quality to monitor mRNA degradation and we used GO analysis (based on comparison of large gene clusters rather than individual genes) to minimize potential confounding factors. However, due to the inherent problems of human TLE studies using autopsy samples [for discussion see 180], we cannot exclude that some of the observed differences between autopsy controls and TLE patients are due to anti-epileptic drug treatment, age difference or postmortem sample collection.

To identify gene clusters involved in specific biological processes, molecular functions and pathways, we performed an unbiased analysis of over-representation in the three significant genes lists (online; Epilepsia.com). Based on mRNA expression, genes involved in the biological process of immunity and defense were highly over-represented in the comparison between HS TLE patients and autopsy controls. The most affected functional gene classes were chemokines and neuropeptides. These two gene classes were also highly affected when comparing nonHS with autopsy controls, but not when comparing the HS and nonHS groups. These data provide strong support for the hypothesis that the brain immune system is important in TLE irrespective of the type of pathology. Our

Biological Process	**A-HS**	**A-nonHS**	**NonHS-HS**
Immunity and defense [981]	**0.000382 [35]**	0.189 [23]	0.337 [14]
Protein complex assembly [59]	0.319 [0]	**0.00109 [6]**	0.521 [1]
Protein folding [126]	0.229 [4]	**0.00334 [8]**	0.208 [3]
Cell structure [456]	0.478 [8]	0.514 [9]	**0.000646 [15]**
Cell structure and motility [818]	0.518 [16]	0.31 [18]	**0.0014 [21]**
Neuronal activities [470]	0.575 [9]	0.416 [10]	**0.00632 [13]**
Receptor protein tyrosine kinase signaling pathway [175]	0.252 [5]	0.248 [5]	**0.0067 [7]**
Cation transport [383]	0.388 [6]	0.205 [10]	**0.00897 [11]**
Ion transport [492]	0.387 [8]	0.0951 [14]	**0.00907 [13]**
Molecular Function	**A-HS**	**A-nonHS**	**NonHS-HS**
Neuropeptide [21]	**0.000808 [4]**	**0.000787 [4]**	0.77 [0]
Chemokine [38]	**0.00671 [4]**	**0.00655 [4]**	0.623 [0]
Chaperonin [16]	0.734 [0]	**0.0000172 [5]**	0.819 [0]
Hydrogen transporter [37]	0.488 [0]	**0.0000937 [6]**	0.0782 [2]
Synthase and synthetase [188]	0.121 [1]	**0.00119 [11]**	0.208 [4]
Other proteases [28]	0.418 [1]	**0.00224 [4]**	0.294 [1]
Transporter [495]	0.103 [14]	**0.0079 [18]**	0.166 [9]
Cytoskeletal protein [562]	0.203 [14]	0.127 [15]	**0.000257 [18]**
Actin binding cytoskeletal protein [283]	0.185 [8]	0.303 [7]	**0.00311 [10]**
Select calcium binding protein [210]	0.116 [7]	0.622 [4]	**0.00512 [8]**
Vesicle coat protein [29]	0.0193 [3]	0.427 [1]	**0.00592 [3]**
Voltage-gated sodium channel [11]	0.808 [0]	0.809 [0]	**0.00852 [2]**
Ion channel [283]	0.359 [4]	0.539 [5]	**0.00951 [9]**
Pathway	**A-HS**	**A-nonHS**	**NonHS-HS**
Ubiquitin proteasome pathway [65]	0.284 [0]	**0.0000453 [8]**	0.555 [1]
Huntington disease [129]	0.545 [2]	0.0398 [6]	**0.00127 [7]**
Ionotropic glutamate receptor pathway [51]	0.018 [4]	0.625 [1]	**0.004 [4]**

Table 3. Statistical analysis of gene ontology (GO) classifications. GO classes with $P < 0.01$ in one of the three comparisons are shown. Between [ ] is presented the total number of genes annotated per class in the reference gene list (most left) and in the gene lists of the three comparisons. A: autopsy control, HS: hippocampal sclerosis, nonHS: without hippocampal sclerosis. Bold indicates $P < 0.01$.

data are in line with a recent meta-analysis of microarray datasets from animal studies implicating immune system related genes in all phases of epileptogenesis [156].

Further analysis of the genes involved in immunity and defense revealed that five genes in the comparison of autopsy controls versus HS, and four genes in the autopsy controls versus nonHS, were highly over-represented in the GO subclass of viral genome replication genes. All these genes were up-regulated, three of them (*CCL2*, *-3* and *-4*) were present in both comparisons. *CCL3* and *CCL4* showed the highest up-regulation (10 to 20-fold) of all the genes identified. In the brain CCL3 and CCL4 are expressed predominantly by microglia and astrocytes [158]. Microglia and neurons may respond to chemokines, but the precise biological function of these chemokines in brain needs further investigation. Data from animal studies indicate that up-regulation of *CCL2*, *-3* and *-4* also occurs in the early stages of epileptogenesis [144,156]. Thus, up-regulation of these chemokines in the human TLE hippocampus may not only contribute to the neuropathology, but also to epileptogenesis. Early up-regulation of chemokines, for instance after viral infection, may be a common pathway linking the various predisposing factors in the etiology of TLE, such as trauma, febrile seizures, meningitis, encephalitis and tumors. Indeed, recent studies indicate that the role of viral infections in the etiology of TLE might be underestimated [181-183]. Neuropeptide genes are also over-represented in both TLE groups, for example, secretogranin II (*SCG2*). Secretoneurin, the active peptide derived from SCG2, exerts chemotaxis on monocytes and endothelial cells, processes closely related to chemokine function [184]. Several of these, including SCG2, play a role in the innate immunity and may also be involved in the etiology of TLE [185]. Highly over-represented processes in our comparison of nonHS and HS patients included cell structure, neuronal activities, and ion transport, and included the ionotropic glutamate receptor pathway. These expression changes probably reflect the neuropathological characteristics of the sclerotic hippocampus.

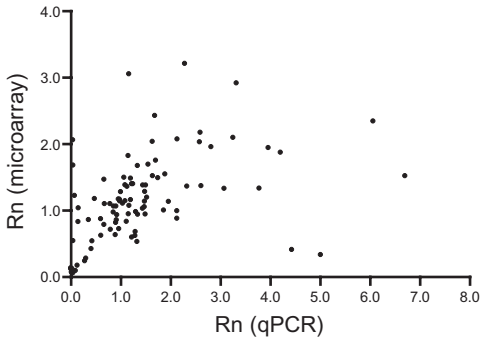

Figure 4. Correlation between microarray data and qPCR gene expression. Per patient microarray gene expression versus the reference mRNA pool (Rn) was plotted against patient qPCR gene expression versus the reference gene *PSMD2* (Rn). Spearman's $r = 0.58$.

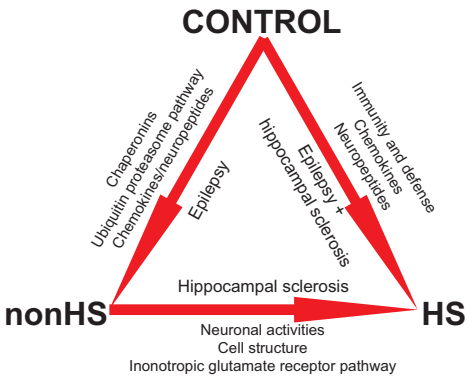

Figure 5. Summary diagram showing highly significant gene classes identified comparing nonHS, HS and autopsy controls with statistical GO analysis (based on table 3).

Pathway analysis of the comparison between the nonHS group and autopsy controls identified the ubiquitin/proteasome pathway to be highly up-regulated (about 50%). Biological process and molecular function analysis showed an up-regulation (about 50%) of protein folding/complex assembly and chaperonins. Molecular function analysis also identified hydrogen transporters as highly

over-represented. Three out of six of these hydrogen transporter genes are subunits of the vacuolar-type H(+)-ATPase, an enzyme important in protein sorting and receptor-mediated endocytosis. Disregulation of protein stability and degradation has been implicated in several neurodegenerative diseases including Parkinson's and Alzheimer disease [186]. The up-regulation of the ubiquitin and chaperonin pathways in nonHS hippocampi is not found in HS hippocampi. Whether this up-regulation contributes to the protection of neurons at risk or is related to specific nonHS pathology remains to be determined. Interestingly it has been shown that over-expression of chaperones can protect against neurodegeneration after chemically induced seizures [187].

Our data provides a concise overview of processes affected in TLE (summarized in figure 5) and might serve as starting point to investigate processes involved in human epileptogenesis and neuropathology in TLE. Moreover, the dataset provides a powerful tool to validate existing and future animal models. We found that chemokines genes were highly up-regulated in chronic TLE. As this up-regulation has also been shown in the early stages of epileptogenesis in animal models, it may not merely be a response to prolonged seizures, but may contribute to epileptogenesis. In any case blocking the effects of chemokines might prove beneficial for TLE patients. In fact, immunotherapy in particular epilepsy syndromes has been successful for many years [155]. We propose that specific antagonists for the major receptor for CCL3 and CCL4, like those under investigation for HIV/AIDS therapy [188], could be used to block most of the actions of CCL3 and 4 and could protect patients from progressive neuronal damage and repetitive seizures. This hypothesis is presently under investigation.

ACKNOWLEDGMENTS

This study was sponsored by the National Epilepsy Foundation of the Netherlands, grant number 03-12. We thank the Members of the Dutch Collaborative Epilepsy Surgery Program for their cooperation, the Netherlands Brainbank and Dr. Rivka Ravid for providing autopsy control material and Jackie Senior-Rogers for editorial support.

CHAPTER 3

Hippocampal Navβ3 expression in patients with temporal lobe epilepsy: An acquired channelopathy?

Koen L.I. van Gassen[1], Marina de Wit[1], Marian van Kempen[2], W. Saskia van der Hel[1], Peter C. van Rijen[3], Antony P. Jackson[4], Dick Lindhout[2], Pierre N.E. de Graan[1]

Rudolf Magnus Institute of Neuroscience, [1]Department of Neuroscience and Pharmacology, [3]Department of Neurosurgery, University Medical Center Utrecht, Utrecht, The Netherlands
[2]DBG-Department of Medical Genetics, University Medical Center Utrecht, Utrecht, The Netherlands
[4]Department of Biochemistry, University of Cambridge, Cambridge, UK

Revision under review

ABSTRACT

Voltage-dependent sodium channels consist of a pore-forming alpha-subunit and regulatory beta-subunits. Alterations in these channels have been implicated in temporal lobe epilepsy (TLE) and several genetic epilepsy syndromes. Recently we identified $Na_v\beta3$ as a TLE regulated gene. Here we performed a detailed analysis of the hippocampal expression of $Na_v\beta3$ in TLE patients with (HS) and without hippocampal sclerosis (nonHS), and compared expression with autopsy controls (AC). Immunoblot analysis showed that $Na_v\beta3$ levels were dramatically reduced in the hippocampus, but not in the cortex of nonHS patients when compared to HS patients. This was confirmed by immunohistochemistry showing reduced $Na_v\beta3$ expression in all principal neurons of the hippocampus proper. Sequence analysis revealed no $Na_v\beta3$ mutations. The functional consequences of the reduced $Na_v\beta3$ expression in nonHS patients are unknown. Altered $Na_v\beta3$ expression might influence micro-circuitry in the hippocampus, affecting excitability and contributing to epileptogenesis in nonHS patients.

INTRODUCTION

Voltage-dependent sodium channels (Na_v) are essential for generation and propagation of action potentials in neurons and have been implicated in epilepsy [189]. Na_v consist of a complex of pore-forming alpha-subunits and linked beta-subunits which are auxiliary components modulating channel function. Beta-subunits may also function as cell-adhesion molecules through extracellular Ig-like domains and have been implicated in targeting Na_v-complexes [reviewed by 190].

To date, 9 α-subunits and 4 β-subunits have been identified. Three of these genes (*SCN1A*, *-2A* and *-1B*) are linked to familial epilepsies [189]. Following experimental seizures in animals and in human chronic epilepsy, changes in the expression of Na_vα1.2, -1.3, -1.5, -1.6, Na_vβ1 and -2 have been reported [180,191-194]. In a microarray study we recently identified Na_vβ3 as one of the regulated genes in the hippocampus of TLE patients [195]. To investigate the role of Na_vβ3 in human TLE we studied Na_vβ3 expression in the hippocampus of AC, HS and nonHS patients.

MATERIAL AND METHODS

Patient samples

Hippocampal tissue of intractable TLE patients with complex partial seizures was obtained after surgery [196]. Informed and written consent was obtained from the patients for all procedures as approved by the Institutional Review Board. Hippocampal tissue from AC (obtained from the Netherlands Brain Bank) and HS and nonHS patients was rapidly frozen (immunoblotting) or fixed and paraffin-embedded (immunohistochemistry) [196]. Relevant clinical patient data are listed in table 1.

Immunoblotting

Tissue homogenates were blotted as described [196]. Blots were incubated with affinity-purified rabbit anti-Na_vβ3 (raised against peptide RPEGGKDFLIYE; Biogenes GmbH, Berlin, Germany) (1:2000 in Tris-buffered saline + 0.1% Tween and 10% normal human serum (NHS)) [197] and processed as described [196]. Controls without anti-Na_vβ3 did not reveal staining. Films were quantified by optical density (OD) measurement with ImageJ (v1.38) and normalized to a reference sample run on all blots.

Immunohistochemistry

Immunostaining was performed on hippocampal sections as previously reported [196]. Anti-Na_vβ3 (diluted 1:400 in phosphate-buffered saline + 2% NHS and 0.05% bovine serum albumin) was applied overnight at room temperature. Serial dilutions (10-50x excess) of immunizing peptide incubated with anti-Na_vβ3, progressively reduced staining showing specificity of the primary antibody. Controls without anti-Na_vβ3 did not reveal staining.

Splice-variant analysis of the Navβ3 gene *SCN3B*

Two *SCN3B* splice-variants have been described. Variant 1 (GI:93587339) and variant 2 (GI:93587331). Variant 1 retains intron-1 in its 5'-UTR, possibly affecting translation. Therefore, splice-variant ratio analysis was performed by qPCR on the same patient material as previously described [195]. One primer-pair was designed to recognize both *SCN3B* splice-variants and one primer-pair was designed to only recognize the intron-1-retention variant (table 2). Expression ratios between total *SCN3B* transcript and intron-1-retention variant transcript were calculated for nonHS and HS patients.

Genotyping of *SCN3B*

DNA of HS and nonHS patients was isolated from frozen cortex tissue. Primer sets used to amplify and sequence the coding regions in-

Patient	Epileptic focus	Sex (M/F)	Age (y)	Age at onset (y)	Neuropathological diagnosis	Used for	Medication
HS							
1	left	F	56	19	MTS W4	WB1	La, O, P
2	right	F	12	9	MTS W4	WB1,CX	La, O
3	right	F	39	14	MTS W4	WB1,CX	C, La
4	right	F	20	8	MTS W4	WB1,CX	La, T
5	left	F	19	1,5	MTS W4	WB1,CX	C, La
6	right	M	55	1,5	MTS W4	WB1	C, La, V
7	left	F	34	6	MTS W4	WB2	C
8	left	M	19	13	MTS W4	WB2	O
9	right	M	30	25	MTS W4	WB2	L
10	right	F	27	10	MTS W4	WB2	L, O
11	right	F	32	1	MTS W4	WB2	La
12	right	F	39	30	MTS W4	WB2,IHC	La, T
13	right	F	38	12	MTS W4	IHC	L
14	left	F	39	30	MTS W4	IHC	C, G
15	right	F	44	9	MTS W4	IHC	La, P
16	right	M	27	0,5	MTS W4	IHC	C, D, G, La
17	right	M	1	0	MTS W4	IHC	-
NonHS							
18	right	M	41	33	Vascular malformation	IHC	C, L
19	right	F	17	2,5	Ganglioglioma	WB1,CX	O, La
20	left	M	43	38	Pilocytair astrocytoma	WB1,CX	C
21	right	F	42	14	DNET	WB1,CX	O
22	right	F	23	12	Posttraumatic epilepsy	WB1,CX	O, La
23	left	M	16	12	Ganglioglioma	WB1,CX	O, La
24	right	M	24	20	Gangliocytoma	WB1,CX	C
25	left	M	31	26	Ganglioglioma	WB2	C, Cl, La
26	left	M	46	17	Normal	WB2	C, T
27	left	M	24	21	Dysgenesis	WB2	C, La, L
28	right	M	48	17	Posttraumatic epilepsy	WB2,IHC	C, L, V
29	right	F	33	22	Normal	WB2,IHC	C, Cl
30	right	M	40	25	Astrocytoma	IHC	C, La
31	left	F	24	10	Ganglioglioma	IHC	O
32	right	M	17	6	Cortical microdysgenesis	IHC	Cl, P, O, T
Autopsy control				**PMD (h)**			
33	-	F	67	14,5	Normal hippocampus	WB2	-
34	-	F	47	4	Normal hippocampus	WB2	-
35	-	M	51	7,7	Normal hippocampus	WB2,IHC	-
36	-	F	53	7,5	Normal hippocampus	WB2,IHC	-
37	-	F	61	6,2	Normal hippocampus	IHC	-
38	-	F	59	6,3	Normal hippocampus	WB2	-
39	-	M	53	14,5	Normal hippocampus	WB2,IHC	-
40	-	F	55	30	Normal hippocampus	WB2	-
41	-	M	54	12	Normal hippocampus	WB1	-
42	-	M	74	27	Normal hippocampus	WB1	-
43	-	M	66	11,5	Normal hippocampus	WB1	-
44	-	F	32	16	Normal hippocampus	WB1	-
45	-	F	74	22	Normal hippocampus	WB1	-
46	-	F	63	17	Normal hippocampus	WB1	-
47	-	M	55	22	Normal hippocampus	IHC	-

Table 1. Relevant clinical data on temporal lobe epilepsy (TLE) patients and autopsy controls used in this study. Age at tissue collection was significantly (ANOVA) higher in autopsy controls (57.6 ± 10.8 years) but did not differ between patients with hippocampal sclerosis (HS; 31.2 ± 14.4 years) and without hippocampal sclerosis (nonHS; 31.3 ± 11.3 years). Age of epilepsy onset was statistically different between HS (11.1 ± 9.8 years) and nonHS (18.4 ± 9.6 years) patients ($P = 0.05$), but duration of epilepsy (delta age at onset and age) was not statistically different between HS (20.0 ± 14.4 years) and nonHS (12.9 ± 9.4 years) patients ($P = 0.11$). Reported are means ± standard deviation. Statistical analysis was performed using a Student's *t*-test unless otherwise stated. MTS: mesial temporal sclerosis, W4: Wyler 4 [46], PMD: post mortem delay, M: male, F: female, WB: western blot, CX: cortex, qPCR: quantitative PCR, IHC: immunohistochemistry, O: Oxcarbazepine, C: Carbamazepine, P: Phenytoin, V: Valproate, Cl: Clobazam, L: Levetiracetam, T: Topiramate, La: Lamotrigine, Ph: Phenobarbital, G: Gabapentine, D: Diazepam.

cluding intron-exon boundaries of the *SCN3B* gene are provided as supplemental material. Direct sequencing was performed on the ABI 3100 automated sequencer (PE Applied Biosystems, Foster City, CA, USA) using standard procedures. Sequences were analyzed with Mutation Explorer v3.01 (SoftGenetics, LLC., State College, PA, USA).

Statistical analysis

Data were analyzed with SPSS v12.01 for significant group differences using one-way ANOVA combined with a post-hoc LSD test, unless otherwise stated. $P < 0.05$ was considered significant.

RESULTS

$Na_v\beta3$ quantification in hippocampal homogenates

Representative $Na_v\beta3$ immunoblots of AC, nonHS and HS patients are shown in figure 1a (WB1 group see table 1). As expected [197], a single immunoreactive band (apparent M_r=50 kDa) was detected in TLE patients. In AC additional bands (apparent M_r=42-48 kDa) were found, with varying intensities. As these bands are most likely breakdown products, $Na_v\beta3$ content was measured as the sum of all bands. Preadsorption of the antiserum with the immunizing peptide abolished staining (figure 1). Hippocampal $Na_v\beta3$ content was lowest in nonHS patients (figure 1) compared to HS patients ($P < 0.03$) and AC. We verified these results in an independent patient group (WB2 group, see table 1)($P < 0.02$). When data of both groups (WB1+WB2) was pooled, significance increased ($P = 0.0008$) and $Na_v\beta3$ expression in HS patients was significantly higher ($P < 0.05$) than in AC. No difference was found in $Na_v\beta3$ content between cortex homogenates of nonHS and HS patients ($P = 0.76$, figure 1).

Navβ3 immunohistochemistry

To analyze $Na_v\beta3$ distribution we performed

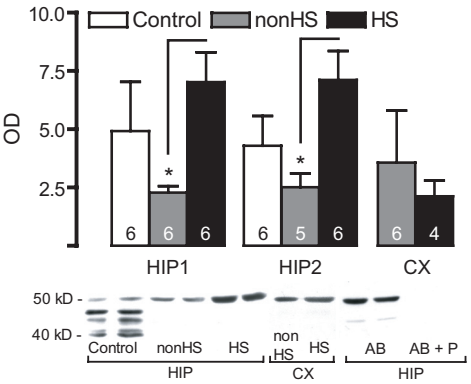

Figure 1. Quantification of $Na_v\beta3$ contents in the hippocampus of two control, nonHS and HS patient groups. Below the figure, typical immunoblot examples showing hippocampal band patterns of control, nonHS and HS patients. Also shown are typical cortical band patterns of a nonHS and HS patient. Preadsorption of the $Na_v\beta3$ antibody with immunizing peptide blocks all immunoreactivity. Quantification of optical densities (OD) shows a significant reduction of protein immunoreactivity in the hippocampus (HIP) of nonHS patients (in both independent HIP1 and HIP2 groups). No reduction was present in cortex (CX) samples from the same patients. Numbers of patients used are indicated in the bars. Data are expressed as means ± standard error of the mean. *$P < 0.05$. nonHS: without hippocampal sclerosis, HS: with hippocampal sclerosis, AB: antibody, P: peptide.

immunohistochemistry (IHC group see table 1). In ACs immunoreactivity (IR) was present in principle neurons in cornu amonis (CA) subregions, particularly CA2. In fiber tracks intense punctuate IR was present. CA neurons showed polarized IR in the soma. In contrast, in nonHS patients $Na_v\beta3$ IR was very low. Only faint IR was present in principle neurons and fiber tracks. In HS patients IR in the remaining principle neurons was comparable to AC. In CA1, intensive scattered IR was present, reminiscent of astrocytes and/or microglia.

Splice-variant analysis

For *SCN3B*, two splice-variants have been described so far. Although coding for the same protein, translation could be affected. To investigate alterations in splice-variant expression ratio between HS and nonHS patients, ratios between expression of the intron-1-retention variant and expression of the

Gene	Accession	forward primer	reverse primer	product length (bp)	start position (bp)	end position (bp)
Sequence PCR						
SCN3B exon 2	NT_033899.7	TGGCTGAAGG CTGTTTTCTT	AGTTCGTCCC AAAGGGTTTC	657	27086349	27087005
SCN3B exon 3	NT_033899.7	GAGAAGGAGC CAGTGTTTGC	CAGGGGAAGG ATTTCAGTCA	518	27078603	27079120
SCN3B exon 4	NT_033899.7	TCACTCGTGG AAAACTGCTG	TGTCCTTCCC TGTCTTTGCT	514	27075489	27076002
SCN3B exon 5	NT_033899.7	ATGAAGAGGG TGGAGGATGA	TCCACTGCTC GGCTACTTCT	482	27071204	27071685
SCN3B exon 6	NT_033899.7	AGAGGCAGGT GGATGTATGG	TCCTTCCCCA TCTTGTGTTC	621	27066779	27067399
qPCR						
SCN3B variant 1	NM_018400.3	AGTTCGTCCC AAAGGGTTTC	GCCTCCACCT CCTCTCTCTT	266	708	973
SCN3B variant 1+2	NM_018400.3	CCTGGGCATT AGGACTGAAA	GTGTAAACTG GGCAGCACCT	176	2241	2416

Table 2. Sequence and qPCR primer specifications

sum of both variants were calculated for both patient groups. No difference in splice-variant ratio was identified (HS: 0.21 ± 0.01; nonHS: 0.19 ± 0.03; Students *t*-test $P = 0.64$).

Mutation analysis

To exclude a mutational origin of the changes in expression level, the *SCN3B* gene was genotyped in 13 HS and 7 nonHS patients. No coding mutations were identified. Identification of heterozygote base pairs in all patients made larger sized deletions unlikely.

DISCUSSION

The present study demonstrates that expression of $Na_v\beta3$ in the hippocampus of human TLE patients is extensively down-regulated in nonHS TLE patients. Known splice-variations possibly influencing translation and coding mutations interfering with anti-body binding were excluded by qPCR and genotyping respectively. We cannot exclude that the observed differences between AC and TLE patients are due to anti-epileptic drug treatment, age difference or postmortem sample collection. However, these factors cannot be the cause of the differences observed between the two TLE patient groups.

Quantification showed a significant down-regulation of $Na_v\beta3$ in nonHS patients compared to HS patients and AC. It is highly unlikely that the $Na_v\beta3$ down-regulation in nonHS patients was due to protein breakdown, because tissues from nonHS and HS patients were collected and treated according to the same protocol, and in contrast to the AC,

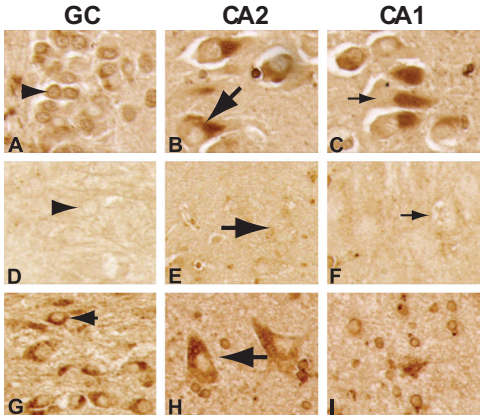

Figure 2. Immunostaining of hippocampal sections showing typical examples of the distribution of $Na_v\beta3$ immunoreactivity in a non-epileptic control (**A, B** and **C**), an epileptic non-sclerotic (nonHS; **D, E** and **F**) and an epileptic sclerotic (HS; **G, H** and **I**) hippocampus. Shown are dentate gyrus granule cells (**A, D** and **G**), CA2 pyramidal neurons (**B, E** and **H**) and CA1 pyramidal neurons (**C, F** and **I**). Arrowheads denote dentate gyrus granule cells (GC), large arrows denote CA2 pyramidal neurons, small arrows denote CA1 pyramidal neurons. Width of each figure section is 100 µm.

showed no signs of protein breakdown on the blots (figure 1). Moreover, we show that $Na_v\beta3$ down-regulation occurs specifically in the hippocampus and not in the cortex. $Na_v\beta3$ expression in HS patients was slightly higher when compared to AC. This may in part be caused by breakdown of the $Na_v\beta3$ protein in the AC. In view of the extensive neuronal death in HS hippocampi, we would have expected a reduction in $Na_v\beta3$ expression. Apparently, the loss of neuronal $Na_v\beta3$ expression is compensated by $Na_v\beta3$ expression in other cells (see below).

Immunohistochemistry (figure 2) confirmed the extensive down-regulation of $Na_v\beta3$ expression throughout the hippocampus of nonHS patients which was shown by immunoblotting. Although much lower, the $Na_v\beta3$ expression pattern resembled that of AC hippocampi. Neuronal IR in HS patients was comparable to AC. In areas with neuronal loss, extensive IR was present, presumably in microglia and/or astrocytes, a finding which has also been described for the $Na_v\beta1$ variant [192] and can account for the relative high expression found by immunoblotting.

The fact that $Na_v\beta3$ down-regulation was only present in the hippocampus of nonHS patients and not in the cortex of these patients suggests hippocampal specific expression regulation. *SCN3B* mRNA up-regulation in nonHS patients [195] was also restricted to the hippocampus [unpublished]. The mismatch between mRNA [195] and protein expression, suggests that $Na_v\beta3$ protein down-regulation in nonHS patients is translationally or post-translationally regulated. Post-translational regulation would be in line with up-regulation of ubiquitination and proteasomal degradation processes found specifically in nonHS patients [195]. Alternatively, reduced $Na_v\beta3$ expression could be due to cleavage by beta-site amyloid precursor protein-cleaving enzyme (BACE1) and gamma-secretase [198].

Although the functional consequences of the reduced hippocampal expression of $Na_v\beta3$ in nonHS patients are unknown, the importance of the hippocampus in the generation of seizures and epilepsy suggest a causal relationship between $Na_v\beta3$ down-regulation and epilepsy. Na_v-subunit composition determines the activation/inactivation kinetics of the channel [190], therefore reduced expression of $Na_v\beta3$ is likely to affect Na_v-activation/inactivation and excitability. $Na_v\beta$-subunits are also important for targeting Na_v-subunits to their normal locations. Regulation of $Na_v\beta3$ expression could play a role in dysgenesis and other developmental pathologies often associated with nonHS TLE (see table 1). Investigating the electrophysiological and targeting effects of reduced expression of $Na_v\beta3$ will be necessary to determine the functional role of this reduction and could help to understand the process of epileptogenesis in nonHS patients.

ACKNOWLEDGMENTS

This study was sponsored by the Epilepsy Fund of The Netherlands (grant 03-12). We thank the Members of the Dutch Collaborative Epilepsy Surgery Program for their cooperation and the Netherlands Brain Bank for providing autopsy control material.

CHAPTER 4

The chemokine CCL3 modulates neuronal activity and calcium dynamics in cultured hippocampal neurons by increasing NMDA receptor levels

Koen L.I. van Gassen[1], Marijn Kuijpers[1,2], Pierre N.E. de Graan[1], Donna Gruol[2]

[1]Rudolf Magnus Institute of Neuroscience, Department of Neuroscience and Pharmacology, University Medical Center Utrecht, Utrecht, The Netherlands
[2]Molecular and Integrative Neurosciences Department, The Scripps Research Institute, La Jolla, CA, USA

Manuscript in preparation

ABSTRACT

CCL3 and -4 chemokine expression has been identified in the brain short- but also long-term after seizures and has also been identified in human temporal lobe epilepsy (TLE). Chemokine receptor activation results in release of intracellular Ca^{2+} and activation of several transduction pathways and has been shown to modulate neuronal activity. Knowledge about the consequences of activation of CCL3 receptors in the hippocampus is limited, therefore we investigated the effects of chronic CCL3-treatment on Ca^{2+} dynamics in cultured hippocampal neurons. Immunohistochemical studies showed high expression of the chemokines CCL3 and -4 in the TLE hippocampus, but not in the hippocampus of autopsy controls. The effect of exogenous application of CCL3 on hippocampal neurons was studied in a hippocampal culture preparation. CCL3 was tested at high concentrations to simulate pathological states. Chronic CCL3 treatment increased average Ca^{2+} levels and the number and mean peak amplitude of Ca^{2+} oscillations. CCL3 treatment also increased NMDA receptor subunit expression (NR1 and NR2A/B). No direct toxic effect of CCL3 exposure was detected based on morphology and neurotoxicity analysis. These results suggest important roles for CCL3 in modulating neuronal functioning in epilepsy and other neuronal pathologies. Blocking the effects of these chemokines could be beneficial for TLE patients and is currently under investigation.

INTRODUCTION

Chemokines, a class of small proteins involved in inflammatory and chemoattractive processes [199], were initially characterized in the immune system, where they were shown to act through G-protein coupled receptors and several transduction pathways, including inhibition of adenylate cyclase and activation of phospholipase C (PLC) [157]. Recent studies show that chemokines and their receptors are also expressed in the central nervous system (CNS), including in the hippocampus, thalamus, cortex and cerebellum [200] where they function as components of the innate immune system. Microglia and astrocytes of the CNS are prominent sources of chemokines, but also neurons can produce chemokines [reviewed by 201]. In the CNS chemokines not only act as mediators during an immune response, but they can also influence neuronal development [202], neuronal death [161,203] and modulate neuronal activity [204]. Chemokine expression in the central nervous system (CNS) is generally low, but elevated levels are produced in response to brain injury and disease, and result in activation and chemoattraction of immune cells such as monocytes, which infiltrate the CNS [159,160]. Increased chemokine expression can be harmful to neurons, either through direct toxic effects (calcium release) or by activating cytotoxic microglia [203].

A number of studies show that elevated levels of CCL3 and/or -4, members of the chemokine family, are produced in the CNS during conditions associated with neuroinflammation [205-207]. Recently, we and others showed that the chemokines CCL3 and -4 and other components of the innate immune system were highly up-regulated in the hippocampus of temporal lobe epilepsy (TLE) patients [195,208]. Increased levels of CCL3 and CCL4 were also found during epileptogenesis in animal models for TLE [144,156]. Their up-regulation in all stages of epileptogenesis [reviewed by 156] suggest that they play a pivotal role in epileptogenesis.

To explore this possibility, we investigated CCL3 and CCL4 protein distribution in the hippocampus of human TLE patients using immunohistochemical techniques and characterized the cells expressing these chemokines. Subsequently, we determined if CCL3 could affect the functional properties of hippocampal neurons using a culture model system and an exposure paradigm involving chronic treatment.

MATERIAL AND METHODS

Patient samples

Hippocampal tissue of pharmaco-resistant TLE patients with complex partial seizures and of autopsy control patients was obtained as previously described [195]. Informed and written consent was obtained from the patients for all procedures as approved by the Institutional Review Board. Patients were carefully selected based on their neuropathology, anamnesis, ethnic background, gender, age at surgery, age of epilepsy onset and use of medication. Hippocampal sclerosis was diagnosed and classified according to Wyler (W0-4) [46]. Only W0 patients (no hippocampal sclerosis, nonHS) and W4 (extensive hippocampal sclerosis, HS) were used. At the time of surgery, all TLE patients received anti-epileptic medication either as mono- or polytherapy. Relevant clinical data for the TLE patients included in this study are listed in table 1. Average ages are reported as mean ± standard deviation (SD).

Antibodies

The following primary antibodies were used for immunostaining of sections and immunoblotting; a goat polyclonal antibody raised against human CCL3 (1:200, Santa Cruz Biotechnology, Santa Cruz, CA, USA), human CCL4 (1:200, Santa Cruz Biotechnology)

and rat NR1 subunit of the NMDA receptor (NMDA-R1, 1:1000, Santa Cruz Biotechnology); a mouse monoclonal antibody raised against human HLA-DR (1:80, M0746; Dako, Haverlee, BE) and rat beta-actin (1:10000, Sigma, St. Louis, MO, USA) and a rabbit polyclonal antibody raised against the rat NR2A/B subunit of the NMDA receptor (NMDA-R2A/B, 1:500, Chemicon International, Temecula, CA, USA). Secondary antibodies used for western blotting were a goat anti-rabbit, goat anti-mouse or rabbit anti-goat (1:10000, Southern Biotech, Birmingham, AL, USA). Rabbit anti-goat (1:200, Dako) and goat anti-mouse(1:400, Dako) secondary antibodies were used for immunohistochemistry of the sections.

Immunohistochemistry

Immunostaining was performed on 7 µm thick coronal hippocampal paraffin sections as described previously [196]. Sections were deparaffinized with xylene, rehydrated in graded ethanol and washed in 0.01 M phosphate-buffered saline (PBS) (pH 7.4). To reduce endogenous peroxidase activity all sections were pretreated with 3% H_2O_2 in PBS for 30 minutes at room temperature. Sections were rinsed thoroughly in PBS after each (pre)incubation. To expose immunoreactive sites, sections to be labeled with the CCL4 antibody were incubated in 10mM SodiumCitrate (pH 6.0) for 20 minutes and microwaved in the same solution for 7 minutes at 750 Watt. No microwave pre-treatment was needed for labeling with the CCL3 antibody. Non-specific background staining was minimized by incubation with 10 mM Tris/HCl, 5 mM EDTA, 150 mM NaCl, 0.25% gelatine (v/v), 0.05% Tween 20 (w/v) (pH = 8.0) supplemented with 0.5% milk powder (ELK, Campina) for 1 h. Next, the sections were incubated with the respective primary antibody in PBS (CCL3 or CCL4) overnight at room temperature. Biotinylated secondary rabbit anti-goat antibody supplemented with 2% normal human serum and 0.05% BSA was applied for 30 minutes. Sections were incubated for 30 minutes with the Vectastain ABC-reagent (Vectastain Elite, Vector Laboratories, Burlingame, CA). Immunoreactivity was visualized with 3,3-diaminobenzidine (DAB: Sigma Chemical Company, St Louis, MO) as the chromogen. Before mounting in Entellan (Merck, Darmstadt, Germany), sections were dehydrated in alcohol and submerged in xylene. Experiments without primary antibodies showed no staining. For pre-adsorption controls the primary antibody was incubated overnight with a 10-50x excess of blocking peptide.

Cell cultures

Hippocampal cultures were prepared from embryonic day 21 rat (Sprague-Dawley, Charles River) hippocampus as previously described [209]. Under sterile condition hippocampi were dissected, minced and triturated without enzymatic treatment. The cell suspensions were plated on Matrigel (BD Biosciences, Bedford, MA, USA) coated tissue culture dishes for immunoblotting and toxicity assays, or on Matrigel and poly-lysine-D coated glass bottom culture dished (MatTek Corp, Ashland, MA, USA) for calcium imaging. Approximately two hippocampi were added to a culture dish used for Western blotting and one hippocampus was added for calcium imaging. At the second day in vitro (DIV), the anti-mitotic agent 5-fluorodeoxyuridine (20 µg/µl, three day treatment) was added to limit the number of non-neuronal cells. Antibiotics were not used. Unless otherwise stated all chemicals were obtained from Sigma (St Louis, MO, USA). Animal care and all experimental procedures were carried out in accordance with standards set forth by the Animal Care Committee of The Scripps Research Institute.

Chronic CCL3 treatment

Cultures from each dissection were divided into control and chronic CCL3 treatment

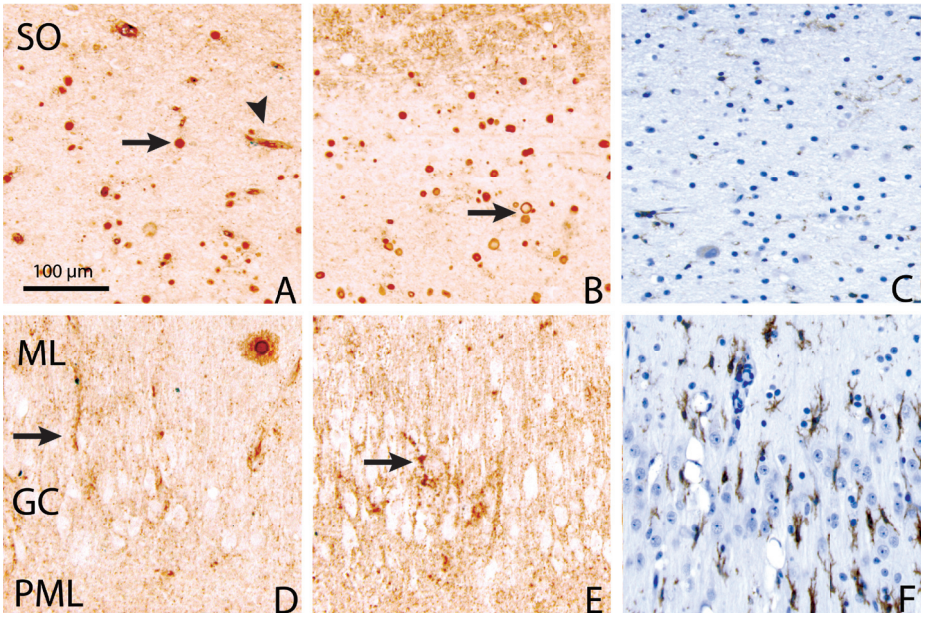

Figure 1. Representative photomicrographs of CCL3 (**A, D**), CCL4 (**B, E**) and HLA-DR (**C, F**) immunoreactivity in the hippocampal CA1 (**A-C**) and dentate gyrus (DG; **D-F**) area of a TLE patient with severe hippocampal sclerosis. Sections **C** and **F** were counterstained with hematoxylin. Arrows in **A** and **B** denote corpora amylacea. SO: stratum oriens, ML: molecular layer, GC: granule cells of the dentate gyrus, PML: polymorphic layer.

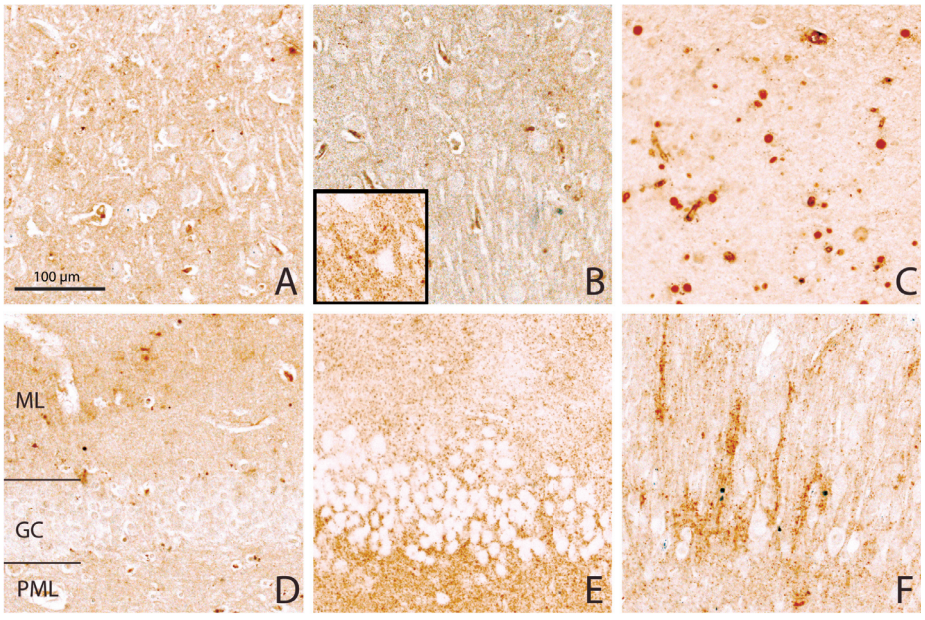

Figure 2. Representative photomicrographs of CCL3 immunoreactivity in the hippocampal CA1 (**A-C)** and dentate gyrus (**D-F**) areas of an autopsy control (**A, D**), a TLE patient without hippocampal sclerosis (nonHS; **B, C**) and a TLE patients with severe hippocampal sclerosis (HS; **D, F**). The insert in figure **B** shows strong neuropil staining in the CA3 area. ML: molecular layer, GC: granule cells of the dentate gyrus, PML: polymorphic layer.

groups. Recombinant rat CCL3 (BSA-free, Peprotech, Rocky Hill, NJ, USA) was reconstituted in 0.1% bovine serum albumin (BSA; fatty acid free) to a final concentration of 50 µM. At 9 DIV, CCL3 was added to the cultures during each media change. No CCL3 was added to the control cultures. In previous studies, CCL3 induced chemotaxis of lymphocytes under a concentration range of ~1-100 nM, with a maximum response at 10 nM [210]. Therefore, CCL3 was used in the final concentrations of 20, 50, 100 and 200 nM to model neuroinflammatory conditions under which CCL3 levels are elevated.

Neurotoxicity assays

Cell survival was assessed using the MTT assay (3-[4,5-dimethylthiazol-2-yl]-2,5-diphenyltetrazolium bromide) to measure mitochondrial activity [211] as described [212]. At 12 DIV, cell cultures (controls and treated with CCL3) were exposed to MTT (0.5 mg/ml). After 2h at 37°C, MTT was removed and isopropanol was added to dissolve the converted dye. After 1h at room temperature, absorbance of the dye was measured at 570 nm. Data for MTT was normalized to the values measured in the control cultures.

Immunoblotting

Hippocampal cell cultures (12 DIV) were scraped off culture plates as described before [209]. Samples (10 µg of protein) were separated by NuPAGE 4-12% Bis-Tris gels (Invitrogen, Carlsbad, CA, USA) and transferred onto Immobilon-P membranes (Millipore, Billerica, MA, USA). After washing, membranes were blocked with casein (Pierce Biotechnology, Rockford, IL, USA) in PBS or Tris-buffered saline (TBS) containing 0.1% Tween-20 and incubated at room temperature with primary antibody. After washing, membranes were incubated with horseradish peroxidase-conjugated secondary antibody, washed and visualized using the ECL system (Pierce Biotechnology, Rockford, IL, USA) and Kodak Biomax ML films (Kodak, Rochester, NY, USA). Working concentrations of the primary and secondary antibodies were selected to allow detection under linear conditions. Relative densitometry was performed using NIH Image software (http://rsb.info.nih.gov/nih-image). Membranes were stripped, washed and reprobed with beta-actin to normalize for variability in loading. Samples of CCL3-treated and control cultures (both in duplicate) were run on the same gel.

Calcium imaging

The effects of acute and chronic CCL3 treatment on intracellular Ca^{2+} levels were determined using standard microscopic fura-2 digital imaging techniques [213,214]. Briefly, at 12-16 DIV, hippocampal cultures were incubated for 30 min with the Ca^{2+} -sensitive fura-2/AM fluorescent dye as previously described [215]. Live fluorescence images of neurons in a microscopic field were acquired and data was collected at 0.8 second intervals. Calibration was performed using fura-2 salt solutions with known Ca^{2+} concentrations (Molecular probes calibration kit). Typical *R*max, *R*min, and *F*o/*F*s values were 0.40, 1.19 and 1.82, respectively. The low level of background fluorescence and adjustment of the black level of the SIT camera eliminated the need for background subtraction methods. All experiments were performed at room temperature. On each experimental day Ca^{2+} levels were recorded in control and CCL3-treated cultures from the same culture set. Neurons were identified by their size and morphology. To assess acute effects, 100 mM CCL3 in physiological saline was added to the cultures 10 minutes prior to data acquisition. To measure Ca^{2+} levels in resting neurons, 100 nM Tetrodotoxin (TTX, Calbiochem, San Diego, CA, USA) in Mg^{2+} -free physiological saline was used to block spontaneous synaptic activity in the cultures. To measure intracellular Ca^{2+} signals in response to a brief application of NMDA, NMDA

Patient	Epileptic focus	Sex (M/F)	Age (y)	Age at onset (y)	Neuropathological diagnosis	Medication
HS						
1	left	F	56	19	MTS W4	La, O, P
2	right	F	12	9	MTS W4	La, O
3	right	F	39	14	MTS W4	C, La
4	right	F	20	8	MTS W4	La, T
5	left	F	19	1,5	MTS W4	C, La
6	right	M	55	1,5	MTS W4	C, La, V
7	left	F	34	6	MTS W4	C
8	left	M	19	13	MTS W4	O
9	right	M	30	25	MTS W4	L
10	right	F	27	10	MTS W4	L, O
11	right	F	32	1	MTS W4	La
12	right	F	39	30	MTS W4	La, T
13	right	F	38	12	MTS W4	L
14	left	F	39	30	MTS W4	C, G
15	right	F	44	9	MTS W4	La, P
16	right	M	27	0,5	MTS W4	C, D, G, La
17	right	M	1	0	MTS W4	-
NonHS						
18	right	M	41	33	Vascular malformation	C, L
19	right	F	17	2,5	Ganglioglioma	O, La
20	left	M	43	38	Pilocytair astrocytoma	C
21	right	F	42	14	DNET	O
22	right	F	23	12	Posttraumatic epilepsy	O, La
23	left	M	16	12	Ganglioglioma	O, La
24	right	M	24	20	Gangliocytoma	C
25	left	M	31	26	Ganglioglioma	C, Cl, La
26	left	M	46	17	Normal	C, T
27	left	M	24	21	Dysgenesis	C, La, L
28	right	M	48	17	Posttraumatic epilepsy	C, L, V
29	right	F	33	22	Normal	C, Cl
30	right	M	40	25	Astrocytoma	C, La
31	left	F	24	10	Ganglioglioma	O
32	right	M	17	6	Cortical microdysgenesis	Cl, P, O, T
Autopsy control				**PMD (h)**		
33	-	F	67	14,5	Normal hippocampus	-
34	-	F	47	4	Normal hippocampus	-
35	-	M	51	7,7	Normal hippocampus	-
36	-	F	53	7,5	Normal hippocampus	-
37	-	F	61	6,2	Normal hippocampus	-
38	-	F	59	6,3	Normal hippocampus	-
39	-	M	53	14,5	Normal hippocampus	-
40	-	F	55	30	Normal hippocampus	-
41	-	M	54	12	Normal hippocampus	-
42	-	M	74	27	Normal hippocampus	-
43	-	M	66	11,5	Normal hippocampus	-
44	-	F	32	16	Normal hippocampus	-
45	-	F	74	22	Normal hippocampus	-
46	-	F	63	17	Normal hippocampus	-
47	-	M	55	22	Normal hippocampus	-

Table 1. Relevant clinical data on temporal lobe epilepsy (TLE) patients and autopsy controls used in this study. Age at tissue collection was significantly (ANOVA) higher in autopsy controls (57.6 ± 10.8 years) but did not differ between patients with hippocampal sclerosis (HS; 31.2 ± 14.4 years) and without hippocampal sclerosis (nonHS; 31.3 ± 11.3 years). Age of epilepsy onset was statistically different between HS (11.1 ± 9.8 years) and nonHS (18.4 ± 9.6 years) patients ($P = 0.05$), but duration of epilepsy (delta age at onset and age) was not statistically different between HS (20.0 ± 14.4 years) and nonHS (12.9 ± 9.4 years) patients ($P = 0.11$). Reported are means ± standard deviation. Statistical analysis was performed using a Student's *t*-test unless otherwise stated. MTS: mesial temporal sclerosis, W4: Wyler 4 [46], PMD: post mortem delay, M: male, F: female, WB: western blot, CX: cortex, qPCR: quantitative PCR, IHC: immunohistochemistry, O: Oxcarbazepine, C: Carbamazepine, P: Phenytoin, V: Valproate, Cl: Clobazam, L: Levetiracetam, T: Topiramate, La: Lamotrigine, Ph: Phenobarbital, G: Gabapentine, D: Diazepam.

(20 nM) was dissolved in Mg^{2+} -free physiological saline and acutely applied by a brief pressure (0.5 second) ejection from a glass micropipette. A dye (fast green) was included in the solution to monitor neuronal NMDA exposure. Axograph software (Axon Instruments, Foster City, CA) was used to measure average amplitudes during spontaneous Ca^{2+} oscillations. Ca^{2+} responses were quantified by the peak amplitude (peak minus baseline), time to peak (seconds after NMDA exposure) and duration of the peak (measured at half-maximum peak amplitude). Mean values for average Ca^{2+} level and peak amplitudes were calculated for the population of neurons studied under control conditions and data from all treatment groups were normalized to this value.

Statistical analysis

Statistical significance ($P \leq 0.05$) was determined using the one-group Student's *t*-test or unpaired Student's *t*-test. Data are reported as means ± standard error of the mean (SEM).

RESULTS

CCL3 and CCL4 immunoreactivity in the hippocampus of human TLE patients

In the hippocampus of TLE patients with severe hippocampal sclerosis (HS), high numbers of CCL3 and -4 immunoreactive (IR) corpora amylacea were detected in the CA1 area (arrows figure 1A, B and figure 2C), specifically in the part with massive neuronal death. In the hippocampus of nonHS patients and controls, corpora amylacea were present in lower numbers scattered throughout the hippocampus. Strong CCL3 IR was also detected in the capillaries and capillary endothelium of the hippocampus (figure 1A, arrowhead). Strong neuropil staining for CCL4, but not for CCL3, was observed in the stratum oriens (SO). Long CCL3 and -4 IR cells/processes were detected between the dispersed granule cells (GC) of the HS hippocampus (arrows figure 1D, E and figure 2F). In this area many similar HLA-DR IR cells (figure 1F) could be detected. Little HLA-DR staining was present in the CA1 area (figure 1C).

In nonHS patients, both CCL3 and CCL4 (CCL4 not shown) showed neuropil IR in the dentate gyrus, primarily in the polymorphic layer (PML) (figure 2E), molecular layer (ML) and around CA3 neurons (insert figure 2B). Neither of these patterns were observed in the control patients (figure 2A, D). When primary antibody was omitted, no staining was observed (results not shown). Pre-adsorption controls showed progressively lower IR with increasing peptide levels, showing specificity of the antibodies.

Characteristics of hippocampal cultures after chronic CCL3 exposure

Hippocampal cultures contained primarily astrocytes and neurons. Cultures were exposed to CCL3 (20, 50 and 200 nM) to simulate conditions during neuroinflammation. CCL3 treatment lasted for 3 days and was started at 6 DIV when the neurons and synaptic networks in culture were well-developed.

The morphological features of the cultures and of neurons and astrocytes were not noticeably affected by CCL3 treatment at any of the concentrations. Total protein content of cultures with and without CCL3 treatment

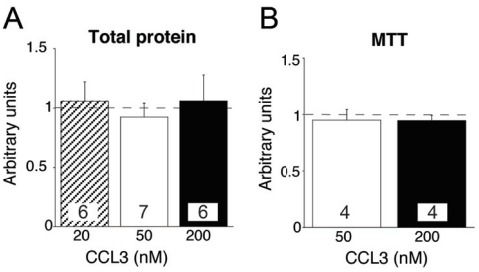

Figure 3. Culture characteristics after chronic CCL3 treatment. **A**. Total protein levels in control and CCL3-treated cultures. **B**. Toxicity (measured by MTT assay) for control and CCL3-treated cultures. Data represents mean values ± SEM. Dashed lines represent control levels. Numbers in boxes represent number of cultures used.

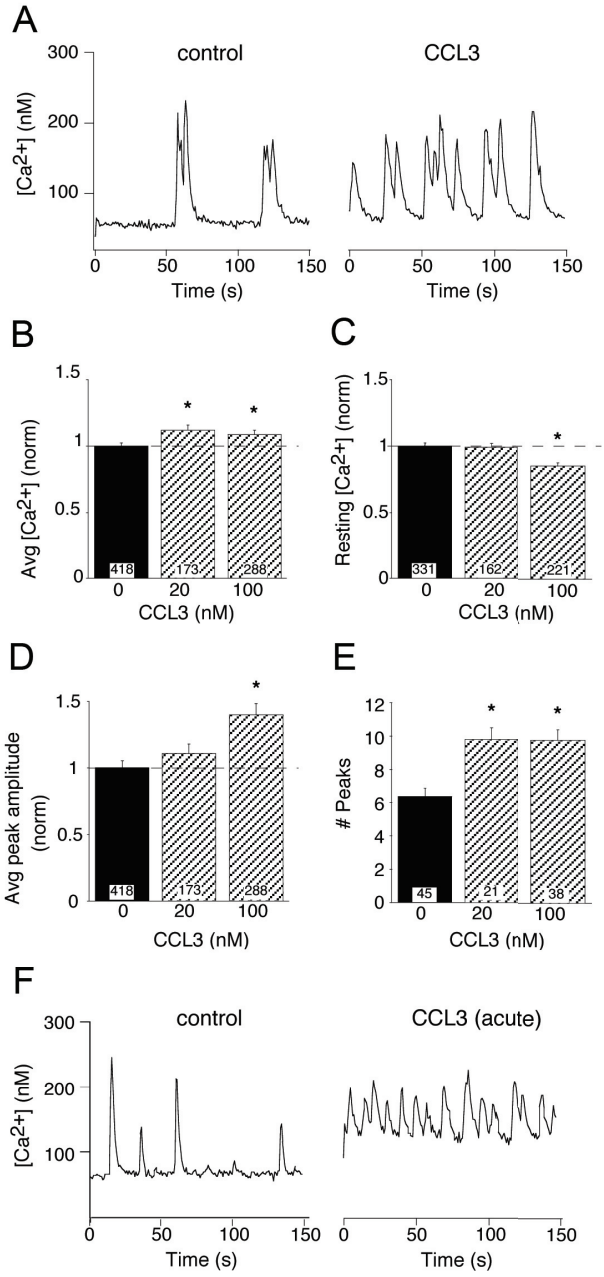

Figure 4. Chronic (A-E) and acute (F) CCL3 treatment alters Ca^{2+} signaling in hippocampal neurons **A**. Representative Ca^{2+} signal in a chronic CCL3-treated hippocampal neuron. **B**. Effect of chronic CCL3 treatment on average Ca^{2+} levels in spontaneously active neurons. **C**. Effect of chronic CCL3 treatment on resting (TTX-treated) hippocampal neurons. **D**. Average peak amplitude in response to chronic CCL3 treatment. **E**. Number of oscillations in response to chronic CCL3 treatment. **F**. Representative Ca^{2+} signal in acutely CCL3-treated hippocampal neuron. Data represents mean values ± SEM. Numbers in boxes are the number of neurons studied. Dashed lines represent control levels. * Statistical significant compared to control.

was identical (figure 3A), indicating that treatment had no overall effect on culture growth and viability. In addition, measurement of toxicity using the MTT assay showed that chronic CCL3 exposure did not alter cell survival (figure 3B).

Effects of chronic and acute CCL3 exposure on Ca^{2+} signals in neurons of hippocampal cultures

In cultured hippocampal neurons, spontaneous intracellular Ca^{2+} changes are observed and correlate with electrical events such as synaptic potentials and action potentials [216]. Spontaneous Ca^{2+} oscillations are often synchronized within one field of neurons and this activity has been shown to be produced by synaptic network activity [216]. Both NMDA receptors (NMDA-R) and L-type Ca^{2+} channels play prominent roles in generating these Ca^{2+} oscillations during synaptic network activity in hippocampal neurons [216,217].

Spontaneous Ca^{2+} oscillations were measured in individual neurons of control and chronically CCL3-treated (20 and 100 nM) cultures and were quantified by measurement of average Ca^{2+} levels, peak amplitudes (minus resting Ca^{2+} levels) and number of oscillations during a standardized recording period of 150 seconds (figure 4A).

The average Ca^{2+} level in control neurons was 97 ± 2 nM (n = 418). A small (10%) but significant increase in average Ca^{2+} level was observed in neurons in chronic CCL3-treated cultures compared with control cultures (figure 4B). Chronic treatment of cultures with 100 nM CCL3 increased the peak amplitude of the Ca^{2+} oscillations by about 40% (controls 24 ± 1 nM; n = 418), whereas treatment with 20 nM CCL3 had no effect (figure 4D). Chronic CCL3 treatment (20nM and 100 nM) also increased the number of Ca^{2+} oscillations (figures 4A, E). To determine whether acute application of CCL3 altered Ca^{2+} dynamics, 100 nM CCL3 was added to control cultures prior to measuring Ca^{2+} levels. Acute CCL3 treatment increased the average neuronal Ca^{2+} level by about 50% (controls: 82 ± 3 nM; n = 177) (figure 4F).

To determine if a CCL3-induced change in resting Ca^{2+} levels contributed to the increase in average Ca^{2+} levels observed in CCL3-treated neurons, resting Ca^{2+} levels were measured after applying TTX to the medium. The resting Ca^{2+} level in control neurons was 129 ± 3 nM (n = 331). Chronic treatment of cultures with 20 nM CCL3 did not affect the neuronal resting Ca^{2+} level, whereas treatment with 100 nM slightly decreased (15%) the resting Ca^{2+} level (figure 4C).

Effect of chronic CCL3 treatment on NMDA-evoked Ca^{2+} signals

Ca^{2+} influx through NMDA-R activation plays an important role in the generation of Ca^{2+} oscillations associated with synaptic network activity in hippocampal neurons [217]. To de-

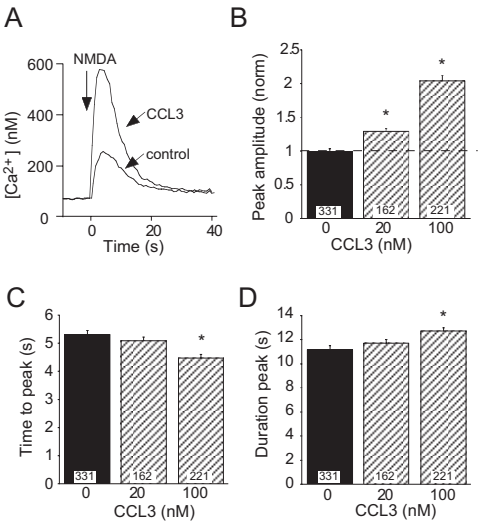

Figure 5. NMDA-evoked Ca^{2+} responses in cultured hippocampal neurons chronically treated with CCL3. **A**. Representative traces of an NMDA-evoked Ca^{2+} signal in a control and chronic CCL3-treated neuron. **B-D**. Effect of chronic CCL3 treatment on NMDA-induced peak amplitude (**B**), time to peak (**C**), and peak duration (**D**). Data represents mean values ± SEM. Numbers in boxes are the number of neurons studied. Dashed lines represent control levels. * Statistical significant compared to control.

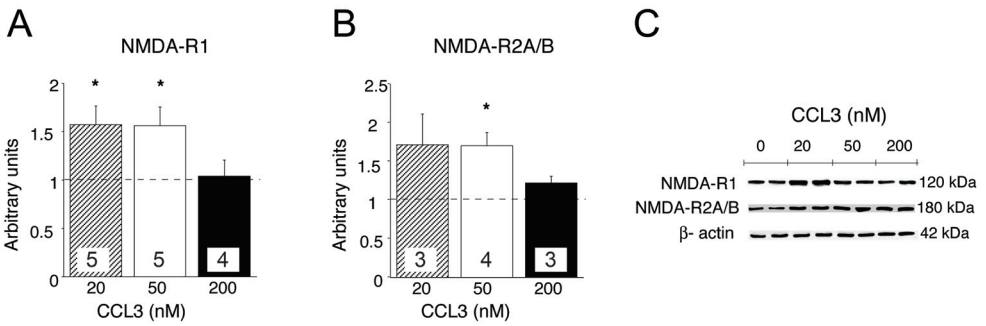

Figure 6. Immunoblot analysis of NR1 and NR2A/B NMDA-R subunits. **A-B**. NMDA-R subtype levels normalized to beta-actin levels in cultures chronically treated with different concentrations of CCL3. **C**. Representative immunoblots showing expression of beta-actin, NR1 and NR2A/B NMDA-R subunits. Data represents mean values ± SEM. Numbers in boxes are number of cultures used. Dashed lines represent control levels. * Statistical significant compared to control.

termine if the NMDA-R could play a role in the enhanced Ca^{2+} oscillations in the chronic CCL3 treated cultures, responses of hippocampal neurons to NMDA exposure in control and chronic CCL3 treated cultures were measured. Responses to NMDA were quantified by measurement of peak amplitude, time to peak and peak duration. Cells were exposed to NMDA (20 nM) by a brief pressure ejection from a micropipette. This resulted in a prominent neuronal Ca^{2+} response in both control and CCL3-treated cultures (figure 5A). The peak amplitude of the Ca^{2+} response to NMDA in control neurons was 246 ± 10 nM (*n* = 331). In cultures treated with 20 and 100 nM CCL3, NMDA exposure elicited a neuronal Ca^{2+} response with a significantly larger peak amplitude (30 and 200%, respectively) (figure 5B). In 100 nM CCL3-treated cultures, the NMDA induced Ca^{2+} response peaked significantly earlier (figure 5C) and peak duration was significantly increased (figure 5D) compared to controls.

Effect of chronic CCL3 exposure on NMDA-R subunit expression

The increased magnitude of the Ca^{2+} response produced by NMDA application in the CCL3-treated cultures could occur through a variety of mechanisms. One possible mechanism is through increased levels of NMDA-R in the cultures chronically treated with CCL3. To determine if the increase in Ca^{2+} signaling was indeed associated with changes in NMDA-R levels, the effect of CCL3 treatment on expression of NMDA-R subunits was examined by immunoblotting. Cultures were chronically treated with CCL3 (0, 20, 50 or 200 nM) and blots were probed with specific NR1 and NR2A/B antibodies to determine relative subunit protein levels (figure 6C). Chronic CCL3 treatment increased the level of NR1 (at 20 and 50 nM CCL3) and NR2A/B (at 50 nM CCL3) protein (figure 6A, B).

DISCUSSION

Our results show that the chemokines CCL3 and -4 are highly expressed in the dentate gyrus of TLE patients. Expression is mainly confined to IR cells in the dentate gyrus of HS patients and to neuropil staining of the PML, ML and CA3 in nonHS patients. Studies of neuronal effects of exposure to CCL3 using a culture preparation show that acute and chronic exposure of cultured rat hippocampal neurons to CCL3 causes increased Ca^{2+} levels and increased synaptic activity. Chronic CCL3 exposure also increased the level of protein for NMDA-R subunits and this effect was associated with a parallel increased magnitude of the Ca^{2+} response to NMDA. CCL3 did not influence neuronal morphology and survival.

CCL3 and -4 immunopositive cells in the hippocampus of TLE patients

CCL3 and -4 immunostaining in human control and epileptic hippocampus showed a marked distribution pattern. Little or no staining was present in controls and intense neuropil staining was found in the PML, ML and CA3 of nonHS patients (figure 2E). In HS patients high numbers of IR corpora amylacea were identified (especially in CA1) and strong IR was found in long cells/processes in between GC in the dentate gyrus.

The PML contains primarily interneurons and granule cell axons and contains a high level of chemokine IR in the absence of immune cells. Connection areas, like the ML and CA3 were also highly IR. The absence of immune cells suggests chemokine production by either astrocytes or neurons, possibly affecting calcium dynamics and excitability of surrounding neurons. In HS patients no neuropil staining was identified in the PML (figure 2D), but long processes between the dispersed GC layer were CCL3/4 IR (figure 1E, F and 2F). In this layer staining for HLA-DR revealed an almost identical staining pattern (figure 1H), suggesting that these CCL3/4 positive processes belong to activated microglia. Activated microglia are the major source of brain chemokines, including CCL3 and CCL4, and in various brain tissues these cells express CCL3 and -4 [201]. Activation of microglia is prominent in the hippocampus of HS patients [218] and the density of activated microglia appears to correlate with the duration and frequency of seizures [219,220]. In the CA1 area of HS patients large numbers of highly CCL3/CCL4 IR corpora amylacea were present. The CA1 area of HS patients is characterized by severe neuron loss/degeneration. Corpora amylacea develop in glial processes, are associated with neurodegeneration [221] and have been described in HS pathologies previously [222].The low levels of HLA-DR IR, a marker for activated glia, in the CA1 area of HS patients suggest that necrosis was complete.

Effect of CCL3 treatment on Ca^{2+} dynamics

The presence of high amounts of CCL3 and -4 suggest a role for these chemokines in seizures and TLE. Therefore, we investigated the effects of acute and chronic CCL3 treatment on Ca^{2+} dynamics and network properties in cultured hippocampal neurons.Chemokines, like CCL3, can activate signaling pathways through binding to G-protein coupled receptor, which induces release of Ca^{2+} from intracellular stores. CCL3-induced Ca^{2+} dynamics were examined using Fura-2 imaging techniques. An increase in average Ca^{2+} levels was observed in cultures acutely treated with CCL3 (figure 4F). These results are in agreement with results showing that acute CCL3 application evoked intracellular Ca^{2+} transients in cultured hippocampal neurons [204]. To mimic pathological states, such as epilepsy, CCL3 was chronically added to the cultures, resulting in an increase in average Ca^{2+} levels (figure 4A), This increase was not due to effects on resting Ca^{2+} levels (figure 4C). Chronic CCL3 exposure increased the number and mean peak amplitude of Ca^{2+} oscillations (figures 4A, D and E). Our results suggest that chronic CCL3 exposure mainly affects Ca^{2+} dynamics dependent on neuronal activity.

Effect of CCL3 treatment on neuronal Ca^{2+} dynamics induced by NMDA

Because NMDA-R activation plays an important role in the generation of Ca^{2+} oscillations, the effect of chronic CCL3 treatment on NMDA-evoked Ca^{2+} signals was assessed. Chronic CCL3 (20 and 100 nM) treatment increased Ca^{2+} responses to NMDA exposure (figure 5) and 100 nM CCL3 increased the peak Ca^{2+} response of NMDA by approximately 100% (figure 5B). These effects were associated with increased NMDA-R subunit expression. NR1 and NR2A/B subunits, the

principle NMDA-R subunits expressed in the hippocampus [223,224], were up-regulated (approximately 50%) after chronic exposure to 20-50 nM CCL3 (figure 6). The highest concentration of CCL3 (200 nM) did not affect NMDAR subunit levels, possibly due to concentration-dependent desensitization of the chemokine receptor. Although high levels of NMDA-Rs could cause excitotoxicity, no direct effects of chronic CCL3 exposure was detected based on morphology and neurotoxicity analysis (figure 3). Up-regulation of NMDA-Rs is highly relevant to epilepsy, because this may lead to increased excitatory neurotransmission and could contribute to the development of epileptic seizures and excitotoxicity [225-228]. Indeed, NMDAR activation has been implicated in epileptogenesis and in the development of epileptiform discharges [229-232]. Up-regulation of NMDARs has also been shown in animal models for TLE and in human TLE studies [225-227,233,234]. Moreover, blocking the NMDAR1 by auto-antibodies potently reduced seizures and seizure damage [235]. These results show that chronic CCL3 exposure can result in up-regulation of NMDA-Rs, which in their turn can contribute to the development of epilepsy.

CCL3 as therapeutic target

These data suggest important roles for CCL3 in modifying neuronal functioning in epilepsy and other neuronal pathologies associated with increased levels of CCL3. Although chemokine up-regulation in human TLE patients represents a chronic state with continuing seizures, chemokine up-regulation is not likely to be merely a response to seizures, as it was found to be up-regulated in all stages of epileptogenesis [156]. In hippocampal culture, chronic CCL3 exposure potently increased NMDAR subunit expression and responses. Particularly in the dentate gyrus area of TLE patients we identified high levels of CCL3 and -4. Continuing high levels of CCL3 could increase the expression levels of the NMDAR in hippocampal neurons, thus increasing their vulnerability to seizures, excitotoxicity and contributing to neuronal death.

Blocking the effects of chemokines might prove beneficial for TLE patients. Immunotherapy in particular epilepsy syndromes has been successful for many years [155]. As many diseases are associated with chemokines and chemokine receptors, several chemokine intervention approaches have been explored [236]. Some involve the use of antibodies that can bind to chemokines or their receptors and block their function. Others focus on the development of specific receptor antagonists. Approaches that block most of the actions of CCL3 and/or CCL4, and thus are expected to be most efficient in protecting patients from progressive neuronal damage and possibly repetitive seizures, are currently under investigation.

ACKNOWLEDGEMENTS

This study was sponsored by the Epilepsy fund of The Netherlands (grant 03-12) and by the Dr. Saal van Zwanenbergstichting. We thank Dr. J. van Horssen for neuropathological advise.

CHAPTER 5

Characterization of febrile seizures and febrile seizure susceptibility in mouse inbred strains

Koen L.I. van Gassen[1#], Ellen V.S. Hessel [1#], Geert M.J. Ramakers[1], Robbert G.E. Notenboom[1], Inge G. Wolterink-Donselaar[1], Jan H. Brakkee[1], Thea C. Godschalk[1], Xin Qiao[1], Berry M. Spruijt[2], Onno van Nieuwenhuizen[3], Pierre N.E. de Graan[1]

[1]Rudolf Magnus Institute of Neuroscience, Department of Neuroscience and Pharmacology, University Medical Center Utrecht, Utrecht, The Netherlands
[2]Ethology & Welfare, Department of Animals, Science and Society, Faculty of Veterinary Medicine, Utrecht University, Utrecht, The Netherlands
[3]Rudolf Magnus Institute of Neuroscience, Department of Child Neurology, University Medical Center Utrecht, Utrecht, The Netherlands

[#]These authors contributed equally to this work

Genes Brain Behav. 2008, 7:578-586.

ABSTRACT

Febrile seizures (FS) are the most prevalent seizures in children. Although FS are largely benign, complex FS increase the risk to develop temporal lobe epilepsy (TLE). Studies in rat models for FS have provided information about functional changes in the hippocampus after complex FS. However, our knowledge about the genes and pathways involved in the causes and consequences of FS is still limited. To enable molecular, genetic and knockout studies, we developed and characterized a FS model in mice and used it as a phenotypic screen to analyze FS susceptibility. Hyperthermia was induced by warm-air in 10-14 day-old mice and induced FS in all animals. Under the conditions used seizure-induced behavior in mice and rats was similar. In adulthood, treated mice showed increased hippocampal *Ih*-current and seizure susceptibility, characteristics also seen after FS in rats. Of the seven genetically diverse mouse strains screened for FS susceptibility, C57BL/6J mice were among the most susceptible, whereas A/J mice were among the most resistant. Strains genetically similar to C57BL/6J also showed a susceptible phenotype. Our phenotypic data suggest that complex genetics underlie FS susceptibility and show that the C57BL/6J strain is highly susceptible to FS. As this strain has been described as resistant to convulsants, our data indicate that susceptibility genes for FS and convulsants are distinct. Insight into the mechanisms underlying seizure susceptibility and FS may help to identify markers for the early diagnosis of children at risk for complex FS and TLE, and may provide new leads for treatment.

INTRODUCTION

Febrile seizures (FS) are considered to be relatively benign convulsions induced by fever [3]. Up to the age of 5 years, 2% to 4% of all West-European children will suffer from at least one FS [85]. Retrospective studies showed a relationship between complex FS and temporal lobe epilepsy (TLE) with mesial temporal sclerosis. Thirty to fifty percent of patients with TLE had a history of prolonged FS during childhood [11]. It is still unclear if FS themselves contribute to the development of TLE, or whether a prenatal lesion, brain insult or a genetic predisposition exits, which is causal to both FS and TLE [87,88].

Epidemiological studies showed that the etiology of FS is influenced by genetic susceptibility [103], and FS twin studies suggested a hereditability of up to 70% [104]. Monogenetic FS disorders have provided valuable information about the genes involved in familial febrile seizure syndromes [105]. However, little is known about genes influencing the susceptibility to non-familial FS seen in sporadic patients. Association studies have identified susceptibility genes, but have been difficult to reproduce [106].

The most frequently used FS animal model is the warm-air induced hyperthermia (HT) model in rats (postnatal day 10-11) which induces seizures originating from the hippocampus and amygdala [108]. This and other hyperthermia models [and the original paper by 107,109] have provided valuable information about the effects of FS on hippocampal development, network reorganization, plasticity and epileptogenesis [reviewed by 110]. Recently, it has been shown that these prolonged FS can result in mild spontaneous electro-clinical seizures in 35% of the adult rats [111].

Susceptibility to chemically- or electrically–induced seizes have been studied in genetic and phenotypic diverse mouse strains [128]. For example, C57BL/6J mice are relatively resistant to these seizures, compared to A/J mouse and several QTLs for these seizures have been identified [128,237-240]. Knockout and transgenic mice have also been used to study the role of specific genes, for instance IL-1 beta, in epilepsy and FS [116].

So far, no data are available on the complex genetics of febrile seizure susceptibility in mice or rats. Recently, recombinant inbred and consomic strains have been constructed from several commonly used mouse strains [241] to facilitate forward genetic strategies used to identify QTLs and genes in complex traits [242].

Here, we describe the characterization of a prolonged FS model in mice. This model can be used to study the long-term effects of prolonged FS and the genetic components in FS susceptibility. We have characterized the main features of this model and compared them with those of the rat model [108,110]. Subsequently, we developed a partially automated, high-throughput phenotypic screen to identify genes influencing susceptibility for FS and tested FS susceptibility in seven mouse inbred strains.

MATERIALS AND METHODS

Animals

Neonatal male Sprague Dawley rats (Hsd: SD) were obtained from Harlan Winkelmann GmbH (Borchen, Germany). Three litters were culled to ten male pups on the first postnatal day (P1) and supplied with a foster mother on P8. Rat pups were weaned on P21 and housed two per cage. Mice were bred from pairs of C57BL/6J, B6(Cg)-Tyr^{c-2J}/J, DBA/2J, AKR/J, C3H/HeJ, A/J and BALB/cByJ mice and raised by their mother, all obtained from Jackson Laboratories (ME, USA). Time of birth was recorded daily. At P0-P2 (P0 defined as day of birth), nests were reduced or culled to a maximum of six pups, usually consisting of both male and female pups. Mice pups were weaned on P21

and housed maximum four per cage. Animals were kept in a controlled 12 hour light-dark cycle with a temperature of 22 ± 1ºC and were given unrestricted access to food (2111 RMH-TM diet; Hope Farms, Woerden, The Netherlands) and water. All animals were housed in transparent Plexiglas cages with wood-chip bedding and tissue for nest building. All experiments conformed to institutional guidelines of the University Medical Center Utrecht.

Prolonged FS induction paradigm in mice

This paradigm was developed to study the long-term consequences of prolonged FS in mice. Body weight was determined in 8-10-day-old C57BL/6J mice (only males) and at least 30 minutes before the HT procedure; mice were injected subcutaneously with temperature sensitive transponders (IPTT-300, Plexx, Elst, The Netherlands). Core body temperature was quickly raised using a temperature regulated (automatic system) laminar stream of warm air (41-48ºC) directed vertically down into a Plexiglas cylindrical chamber of 46 cm height and 13 cm diameter. Air temperature was measured near the chamber wall at a height of approximately 2 cm. Air temperature was maintained (± 0.5ºC) by feedback electronics, which automatically adjusted heating levels several times per second in response to the air temperature. When a lower air temperature was required to prevent animal overheating, the system adapts within seconds. Overall noise production by the system was <30dB. Two chambers were used, one for control mice (core body temperature maintained at 35ºC) and one for HT (defined as core body temperature >39ºC) mice. To prevent skin burn and adverse effects on behavior, the temperature of the chamber floor (glass) was maintained at 35ºC and 39ºC, respectively, by heat exchange using an external thermostatic circulation water bath (Julabo, Seelbach, Germany). Chamber temperature was maintained at 32ºC for control mice and at 47ºC for HT mice. Mice were placed one by one on the floor of the preheated chambers and the experiment was started. Mouse core body temperature was measured every minute by wireless transponder readout (WRS-6006/6007, Plexx). Using temperature transponders, core body temperatures could be recorded from outside the chamber, thus avoiding interference with behavior. Moreover, this method allowed controlling core body temperatures more precisely during the HT period (figure 1). It also prevented the fluctuations in core body temperature observed after animals were removed for approximately 10 seconds from the chamber for rectal measurements. Moreover, HT could be induced with a lower air temperature (T2, figure 1). HT was typically reached within 2.5 minutes. After the core temperature of the HT mice had reached 42ºC, air temperature was

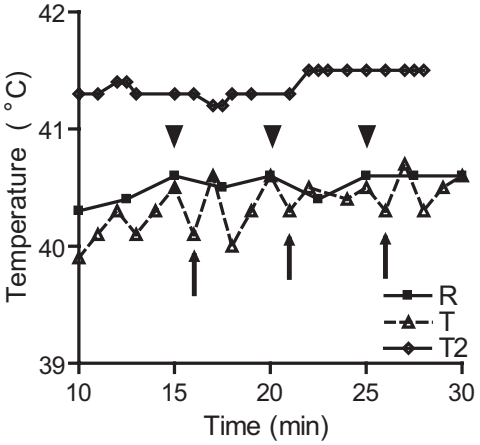

Figure 1. Typical example of mouse core body temperature measurements with transponders and a rectal probe. Rectal (R) and transponder (T) core temperature were measured in the same C57BL/6J mouse and gave similar results (arrowheads). However, handling of the animals during the rectal temperature measurement resulted in a temperature drop of approximately 0.5ºC (arrows). T2 represents a separate experiment in which the temperature was measured with a transponder without rectal measurements and without handling. When only transponders were used for measurements (to prevent temperature drops during rectal measurements), maximum core body temperature achieved was higher than with rectal measurements (T2).

	Mouse		Rat	
	Control (*n* = 8)	HT (*n* = 8)	Control (*n* = 8)	HT (n = 8)
Weight at P10 (g)	6.0 ± 0.3	6.2 ± 0.2	21.0 ± 1.1	20.8 ± 0.6
Animals with seizures (%)	0	100	0	100
Latency to clonic seizure (minutes)	NA	7.6 ± 0.9	NA	7.5 ± 2.1
Temperature at first clonic seizure (°C)	NA	41.3 ± 0.2	NA	41.7 ± 0.1
Tonic-clonic seizure latency (minutes)	NA	8.8 ± 0.9	NA	7.5 ± 2.1
Tonic-clonic seizure duration (minutes)	0	22.5 ± 1.6	0	22.5 ± 2.1
Average core temperature (°C)	34.9 ± 0.1	41.2 ± 0.1	36.0 ± 0.1	41.6 ± 0.1
Maximal core temperature (°C)	35.3 ± 0.2	41.9 ± 0.1	36.6 ± 0.1	42.2 ± 0.1

Table 1. Hyperthermia and seizure characteristics in C57BL/6J mice and Sprague Dawley rats. NA (not applicable). Data are expressed as means ± SEM.

adjusted to maintain a core body temperature between 41.5ºC and 42ºC. Time and temperature data was logged automatically on a computer (DASHost v1.0, Plexx**)** and were used to calculate seizure duration and temperature characteristics (table 1). HT was maintained for 30 minutes. Then, mice were partly submerged in water of room temperature to quickly normalize their core body temperature and were returned to their mother. Controls were treated as HT pups, except that the temperature of the animals was kept at 35ºC. Control pups were from the same litters as those exposed to HT. Behavioral analysis was performed as described for the phenotypic screen (see also table 2).

Prolonged FS induction paradigm in rats

Experimental prolonged FS were induced in 10-day-old rats as described [108,243]. Briefly, one rat pup was placed in a Plexiglas cylindrical chamber and exposed to heated air (41-53ºC). Core temperature was measured every 2.5 minutes using a rectal thermo probe. HT was typically reached within 5 minutes. To provoke prolonged HT, core body temperatures were maintained between 41-42ºC for 30 minutes. After 30 minutes of HT, the rat pups were cooled in a water bath at room temperature and returned to their mother. Controls were treated as HT rat pups, except that the temperature of the air was kept at 35ºC. Control pups were from the same litters as those exposed to HT. Behavioral analysis was performed as described for the phenotypic screen (see also table 2).

Pentylenetetrazol-induced seizures after prolonged FS in mice

At 8-12 weeks after the FS induction paradigm (P10), C57BL/6J mice were intravenously (tail vein) infused with the non-competitive GABAA-receptor antagonist pentylenetetrazol (PTZ; 0.04 mg/µl in phosphate-buffered saline) (Sigma, The Netherlands), using a 25x3/8 gauge needle with an infusion rate of 4 µl per 10 seconds. We used PTZ as convulsant because, unlike excitotoxins, it does not cause cell death, and is less likely to induce secondary epilepsies [244]. Also, PTZ does not have to be metabolized to be effective and has a rapid turnover. Then, mice were placed into a behavioral testing arena (30 cm diameter) and infusion was started after approximately 30 seconds and continued until a dose of 60 mg/kg body weight was reached [245]. Throughout the experiment (total duration 10 minutes), animals were monitored and behavioral parameters were scored and video taped. Latencies to the first occurrences of the following seizure endpoints were recorded: PTZ-stage 1 - twitch of limb; PTZ-stage 2 - repeated clonic seizures or abortive generalized seizure; PTZ-stage 3 - fully generalized seizure; PTZ-stage 4 - tonic-hind limb extension seizure (White, 1998). Video

tape analysis was used to obtain precise latencies and behavioral scores. To test the hypothesis for increased susceptibility to PTZ after FS, statistical analysis between control and HT was performed using a one-tailed Student's *t*-test, and reported as $t_{\text{degrees of freedom}}$=value, *P*-value. Data are expressed as mean ± SEM. *P*-values < 0.05 were considered significant.

Electrophysiological recordings from mouse and rat hippocampal slices after prolonged FS

Electrophysiological recordings on hippocampal slices were performed as previously described [243]. Briefly, at 6-7 weeks (C57BL/6J mice) after FS animals were decapitated. Brains were removed rapidly and immersed in ice-cold, $MgSO_4$-rich artificial cerebrospinal fluid and transverse slices (450 µm) were cut from the medial hippocampus. Intracellular recordings from hippocampal CA1 pyramidal neurons were obtained with sharp glass electrodes (resistance: 60~90 MΩ) filled with KAc (3M) and potentials were recorded using an Axoclamp-2B amplifier (Axon Instruments, Foster City, CA, USA) in bridge-mode. Resting membrane potentials (RMP) were determined when the membrane potential had stabilized. Only cells with stable bridge-balance and RMP were used for analysis. During recordings, the holding potential was manually clamped at -65 mV. The input resistance (R_{in}) was calculated using a small hyperpolarizing current injection (250 pA, 50 ms; [243]). Activation of *Ih* was measured by determining the amplitude of the voltage-sag during a hyperpolarizing current injection (0.1–0.8 nA, 250 ms; [243]). In all experiments bicuculline (free base; 10 µM; Sigma, St. Louis, USA) was present to prevent inhibitory postsynaptic potentials. Data were digitized at 10 kHz and subsequently analyzed using CED hardware and signal software v2.00 (CED Ltd., Cambridge, UK). To test the hypothesis for increased *Ih* activation after FS, statistical analysis between control and HT was performed using a Student's *t*-test and reported as $t_{\text{degrees of freedom}}$=value, *P*-value. Data are expressed as mean ± SEM. $P < 0.05$ was considered significant.

Phenotypic screen for FS susceptibility

To analyze FS susceptibility in mouse strains, we adapted the FS paradigm for high throughput analysis. We used 14-day-old instead of 10-day-old mice, because they are more autonomous, have increased survival and their behavioral repertoire is more elaborated and constant. Air temperature was automatically maintained at 50ºC throughout the phenotypic screen. This is higher than the temperature used in the prolonged FS induction paradigm, where an air temperature of 41-48ºC was used to keep the core body temperature at 41.5-42ºC. To prevent skin burn and adverse effects on behavior at this higher air temperature, the bottom plate temperature was maintained at 37ºC (2ºC lower than in the prolonged FS induction paradigm). The total time of the phenotypic screen was shortened to 15 minutes (about 30 minutes in the

Stage	Behavior	Description
Stage 0	Normal	Normal explorative behavior
Stage 1	Hyperactivity	Hyperactive behavior, jumping and rearing
Stage 2	Immobility	Sudden total immobility (duration 3-10 seconds)
	Ataxia	Unsteady, jerky gait
Stage 3	Circling	Running tight circles (approx. 2 circles / second)
	Shaking	Whole body shaking
	Clonic seizures	Contractions of hind- and forelimbs with reduced consciousness
Stage 4	Tonic-clonic convulsions	Continuous tonic-clonic convulsions with loss of consciousness

Table 2. Classification of mouse behavior during hyperthermia

prolonged FS induction paradigm).
At P10, weight was determined of C57BL/6J (n=10), B6(Cg)-Tyr^{c-2J}/J (n=8), DBA/2J (n=9), AKR/J (n=10), C3H/HeJ (n=8), A/J (n=12) and BALB/cByJ (n=9) mice and mice were injected subcutaneously with a temperature sensitive transponder (IPTT-300, Plexx) and returned to their mother within two minutes. At P14, weight was determined again and animals were placed in the heat chamber. Core body temperature was quickly raised as described before. Animal behavior was recorded by two cameras, one from the top and one from the side.
The observer recorded latencies to stage 2, 3 and 4 behavioral seizures (for descriptions of stages see table 2). As coat color might influence heat exchange during the experiment, we measured the core body temperature of C57BL/6J (black coat) and B6(Cg)-Tyr^{c-2J}/J (white coat) every 2.5 minutes during our screen (data not shown). Coat color had no effect on core body temperature during our screen. Because some strains did not show the particular phenotype within the duration of the screen, Cox proportional hazard regression was used for statistical analysis of observer latencies (Winawer *et al.*, 2007). To limit the number of statistical test, only statistics of all strains versus the C57BL/6J strain were calculated (table 3). One-way ANOVA (Dunnett post-hoc test) was used to compare P14 strain weights versus P14 C57BL/6J weights (table 3) and reported as $F_{\text{degrees of freedom}}$=value, *P*-value. To validate observer latencies, latency to complete arrest of the heat-induced hyperkinesias (immobility latency) and latency to circling behavior were detected and quantified using video tracking and behavioral analysis software Ethovision (version 3.2.16 Noldus BV, Wageningen, The Netherlands). Mice were detected by subtracting the background image from the live video. Animal arena position (two-dimensional coordinates), total animal area (average: 1175 pixels) and changes in animal area (measure for how much the animal moved between data points; approximately 150 pixels during normal behavior) were recorded 25 times per second. The changed area data (25 data points/second) was used to calculate the circling and immobility latency (Microsoft Excel Macro). Immobility was defined as the first immobility episode (changes in mouse surface area < 100 pixels/data sampling) of at least 4 seconds occurring at least 2 minutes after the start of the experiment (to exclude novelty induced behavior). Circling behavior was defined as a change in mouse surface area > 300 pixels/data sampling lasting for at least 0.4 seconds. Cumulative distance moved was calculated in 30 second bins.

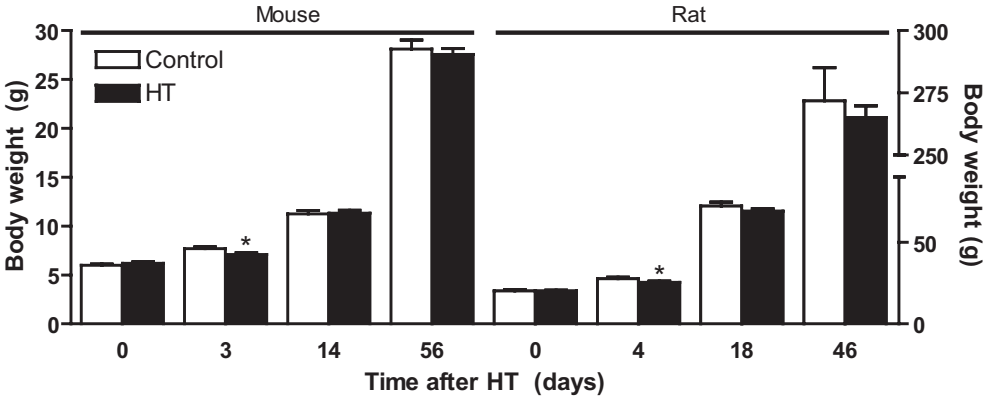

Figure 2. Time course of body weights after the FS paradigm in 10-day-old C57BL/6J mice and Sprague Dawley rats. At the first time point measured after hyperthermia (HT), weight of HT animals was reduced compared to controls. Data are expressed as means ± SEM. * $P < 0.05$.

RESULTS

Behavioral characterization and optimal parameters to study the long-term-effects of prolonged FS in mice

Postnatal days 8-14 correspond roughly to the stage of brain development at which human children are most susceptible to FS [246,247]. Eight-day-old C57BL/6J mice displayed HT-induced seizures, but behavioral characterization proved to be difficult as, at this age, mice showed little locomotion. Behavioral analysis was much more reliable and reproducible when FS were induced in 10-day-old mice.

HT induction criteria were optimized for mice so that seizure duration, average core body temperature and maximum core body temperature achieved during induction were similar to rats (table 1). Seizures were evoked in 100% of the animals, with an average total FS duration of 22.5 minutes. Mortality, in the HT paradigm was very low (< 5%) in C57BL/6J mice. Ten-day-old mice showed a behavioral repertoire (summarized in table 2) during HT similar to rats (Baram *et al*., 1997). Stage 4 duration was recorded and was used as a measure for FS induction quality (ideally 20-25 minutes). Mice with a stage 4 duration of <17.5 minutes were excluded from further analysis. Behavioral seizures stopped instantly when normal core body temperature was restored. The next day, HT animals were indistinguishable from their control littermates by visual inspection. Ten-day-old mice were chosen as optimum age for investigating the long-term effects of prolonged FS.

Effect of prolonged FS on body weight gain in mice and rats

As changes in body weight after FS might be a confounding factor for investigating long-term consequences, body weight gain was investigated in a separate group of animals (figure 2). Body weight was measured 3, 14 and 56 days after HT for mice and 4, 18 and 46 days after HT for rat. On day 3 and 4 after HT, respectively, HT mice (n = 11) and rats (n = 27) were significantly lighter (Student's t-test, mice: $t_{20} = 2.52$, $P = 0.02$; rat: $t_{5} = 2.02$, $P = 0.048$) than control mice (n = 11) and rats (n = 25). HT did not affect body weight at any of the other time points (mice: 14 days after HT, $t_{10} = 0.19$, $P = 0.86$; 56 days after HT, $t_{10} = 0.49$, $P = 0.63$) (rats: 18 days after HT, $t_{50} = 1.38$, $P = 0.17$; 46 days after HT, $t_{34} = 0.98$, $P = 0.33$).

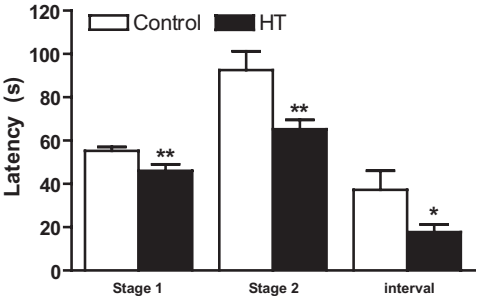

Figure 3. Susceptibility of adult control and hyperthermia (HT) C57BL/6J mice to pentylenetetrazol-induced seizures. Latencies until stage 1 and 2 seizures were significantly reduced in HT animals (n = 9) versus control animals (n = 10). The interval between stage 1 and 2 seizures was significantly shorter in HT animals. Data are expressed as means ± SEM. * $P < 0.05$, ** $P < 0.01$.

Effect of prolonged FS on sensitivity to pentylenetetrazol

To investigate whether prolonged FS in mice increase seizure susceptibility later in life, adult mice of 10-17 weeks old (control: 28.6 ± 0.6 g, n = 10; HT: 28.3 ± 0.8 g, n = 10), were tested with an increasing dose of PTZ. Animals received a cumulative dose of 60 mg/kg. Control animals usually displayed only short clonic seizures, after which they quickly recovered.

As expected, HT animals had a shorter latency to PTZ-stage 1 (HT: n =10; control: n = 10, $t_{18} = 2.59$, $P = 0.0092$) and to PTZ-stage 2 seizures (HT: n = 9; control: n = 10, $t_{17} = 2.69$, $P = 0.0078$) compared to control animals (figure 3). No control animals progressed into PTZ-stage 4, while one HT animal did. Due to large inter-animal variation, latencies to PTZ-

stage 3 seizures were not statistically different between control and HT animals (HT: n = 5, 184 ± 23 seconds; control: n = 6, 214 ± 19 seconds; t_9 = 1.03, P = 0.17). Additionally, the interval between PTZ-stage 1 and PTZ-stage 2 seizures was significantly shorter in HT compared to control animals (HT: n = 9; control: n = 10, t_{17} = 1.99, P = 0.031) (figure 3).

Electrophysiological recordings in mice after prolonged FS

To investigate electrophysiological properties of hippocampal neurons after prolonged FS in mice, sharp electrode current-clamp recordings were made from CA1 pyramidal neurons (13 control neurons; 8 HT neurons; 7 mice per group). The RMP of neurons from HT animals was significantly depolarized compared with control animals (figure 4C; t_{19} = 2.48, P = 0.023). In addition, as a measure for the *Ih*-current, the depolarizing sag during a hyperpolarizing current injection was increased in CA1 pyramidal cells from HT animals compared with controls (figure 4A). However, the input resistance (R_{in}) from HT animals was significantly reduced compared with control animals (control, 27.1 ± 2.1 MΩ, n = 13 neurons from 7 mice; HT, 19.5 ± 2.1 MΩ, n = 8 neurons from 7 mice; t_{19} = 2.38, P = 0.028). To quantify this effect despite the difference in R_{in}, we selected all experiments in which the hyperpolarizing current injection resulted in an initial voltage drop to -120 mV (selected range -118 to -124 mV: control mean -120.1 ± 2.4 mV; HT mean -120.3 ± 2.1 mV). On average, the current injection required to elicit an initial voltage drop to -120 mV was larger in HT animals compared with controls (control, 678 ± 31 pA, n = 13 neurons from 7 mice; HT, 781 ± 36 pA, n = 11 neurons from 7 mice; t_{22} = 2.19, P = 0.039). The voltage-sag following the hyperpolarization to -120 mV was significantly larger in HT animals compared with controls (figure 4B) (control, n = 13 neurons from 8 mice; HT, n = 11 neurons from 8 mice; t_{22} = 5.31, P = 0.000025). This increase in the depolarizing sag in HT animals was accompanied by an increase in rebound depolarization following the negative current injection. Actually, in some HT animals this rebound depolarization elicited action potentials (figure 4A, arrowhead). The *Ih*-current blocker ZD7288 (10 μM) completely inhibited both the voltage-sag and the rebound potential in control and HT animals (data not shown). Our mice findings are in agreement with previous published results in rat [120,243] and these electrophysiological data validate our mouse model.

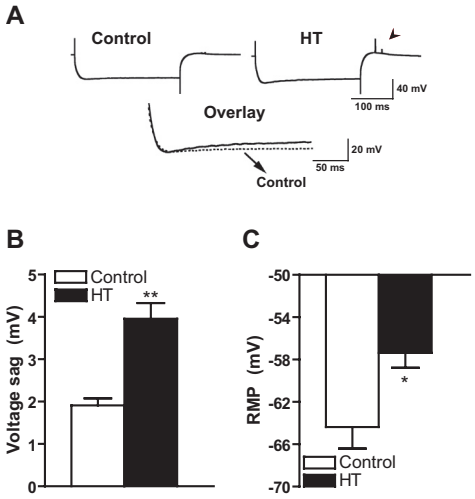

Figure 4. Voltage sag amplitude and resting membrane potential in CA1 pyramidal cells of hyperthermia (HT) and control mice. **A**. Top panels: typical examples of the voltage response of CA1 pyramidal cells to a hyperpolarizing current injection. The arrowhead indicates the occurrence of a rebound action potential. The example trace is an average of 5 individual traces, therefore the amplitude of the action potential is reduced. Bottom panels: overlay to illustrate the increased voltage-sag in HT (solid trace) compared to control (dotted trace) animals. **B**. The average amplitude of the voltage-sag elicited by an initial hyperpolarizing current to -120 mV is increased in HT compared to control mice. **C**. The average resting membrane potential is more depolarized in HT compared to control mice. Data are expressed as means ± SEM. * P < 0.05, ** P < 0.01.

Phenotypic screen for FS susceptibility

Subsequently, we analyzed FS susceptibility using our phenotypic screen in several

	B6(Cg)-Tyr^{c-2J}/J (4m, 4f)	C57BL/6J (6m, 4f)	BALB/cByJ (3m, 6f)	AKR/J (4m, 6f)	DBA/2J (6m, 3f)	A/J (7m, 5f)	C3H/HeJ (5m, 3f)
Immobility latency (seconds)	146.0 ± 13.4 HR = 1.61 *P* = 0.337	163.7 ± 8.8 NA NA	**191.7 ± 9.5 HR = 0.16 *P* = 0.012**	179.0 ± 14.0 HR = 0.59 *P* = 0.265	**237.2 ± 23.6 HR = 0.11 *P* = 0.000**	**271.8 ± 21.5 HR = 0.05 *P* = 0.000**	**245.7 ± 21.8 HR = 0.06 *P* = 0.000**
Circling latency (seconds)	352.3 ± 14.7 HR = 1.24 *P* = 0.660	350.3 ± 22.2 NA NA	**900 ± 0.0 HR = 0.02 P = 0.000**	**900 ± 0.0 HR = 0.01 P = 0.000**	384.5 ± 0.4 HR = 0.61 *P* = 0.332	**900 ± 0.0 HR = 0.01 P = 0.000**	**900 ± 0.0 HR = 0.01 P = 0.000**
Shaking latency (seconds)	**323.4 ± 20.5 HR = 12.43 *P* = 0.000**	499.0 ± 39.4 NA NA	502.2 ± 32.0 HR = 2.74 *P* = 0.134	487.4 ± 21.4 HR = 0.77 *P* = 0.577	**440.1 ± 27.6 HR = 2.74 *P* = 0.049**	**824.0 ± 39.4 HR = 0.11 *P* = 0.000**	625.1 ± 67.3 HR = 0.46 *P* = 0.168
Tonic-clonic convulsion latency (seconds)	**452.3 ± 20.5 HR = 5.54 *P* = 0.003**	599.0 ± 48.9 NA NA	604.9 ± 26.0 HR = 2.14 *P* = 0.284	**661.0 ± 51.1 HR = 0.30 *P* = 0.019**	**740.6 ± 76.5 HR = 0.21 *P* = 0.004**	**838.0 ± 33.1 HR = 0.16 *P* = 0.000**	**877.8 ± 18.2 HR = 0.14 *P* = 0.000**
Body weight (g)	6.8 ± 0.1 *P* = 0.199	7.2 ± 0.2 NA	**9.0 ± 0.1 *P* = 0.000**	7.0 ± 0.2 *P* = 0.265	7.2 ± 0.3 *P* = 0.993	7.9 ± 0.2 *P* = 0.233	**8.1 ± 0.2 *P* = 0.009**

Table 3. Phenotypic diversity of FS susceptibility in seven inbred mouse strains. Values of behavioral parameters represent average latencies (seconds) recorded during a 15-minute period of hyperthermia at P14. If a particular seizure behavior did not occur during this period, a latency value of 900 seconds was given. Strains in this table were ordered based on tonic-clonic convulsion latency. B6(Cg)-Tyr^{c-2J}/J was the most susceptible strain, whereas C3H/HeJ was the least susceptible strain for this parameter. Latencies, Cox proportional hazard ratios (HR) and significances for latencies of all strains versus the C57BL/6J strain are listed. Body weights of all strains versus the C57BL/6J strain are also listed. m (male), f (female), NA (not applicable). Data are expressed as means ± SEM. $P < 0.05$ was considered significant and indicated in bold font.

mouse strains. We placed 14-day-old male and female C57BL/6J, B6(Cg)-Tyr^{c-2J}/J, DBA/2J, AKR/J, C3H/HeJ, A/J and BALB/cByJ mice (see table 3) for 15 minutes in the HT chamber with an air temperature of 50ºC. The behavioral repertoire in this phenotypic screen is stereotyped and very well comparable to the behavior observed at P10 (table 2) and therefore also classified as such. Latencies until immobility (stage 2), circling (stage 3), whole body shaking (stage 3) and tonic-clonic convulsions (stage 4) were recorded by the observer as a measure for FS susceptibility. To visualize progression of the behavioral repertoire in C57BL/6J animals, average observer recorded latencies were indicated in the cumulative distance moved plot of C57BL/6J animals (figure 5).

Latencies until stage 2 and 3 in C57BL/6J mice were also automatically measured (Ethovision system) and were compared to data recorded by the observer (table 4). A highly significant correlation was present between automatically and observer recorded data (Pearson $r > 0.97$, $P < 0.0001$) and analysis with the Bland and Altman method for comparing two methods [248] also confirms that Ethovision detection and observation are equally reliable in detecting these phenotypes.

All strains showed the sudden immobility previously described in rats [116] and all strains

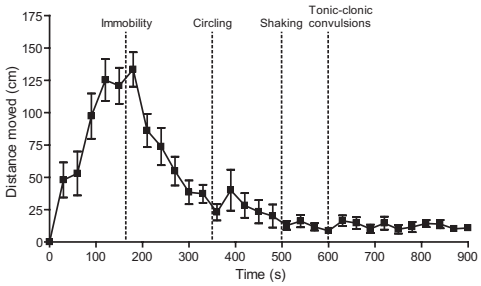

Figure 5. Cumulative distance moved of C57BL/6J mice during the febrile seizure phenotypic screen. Distance moved data of C57BL/6J mice ($n = 10$) averaged over 30 second time bins. The vertical dotted lines represent average observer recorded latencies of the C57BL/6J animals (taken from table 3). Data are expressed as means ± SEM.

Animal	Immobility latency (seconds)		Circling latency (seconds)	
#	O	E	O	E
1	187	177	334	342
2	140	145	368	369
3	180	169	386	410
4	144	135	432	438
5	135	126	435	435
6	142	141	395	410
7	141	143	267	263
8	191	181	361	364
9	187	182	313	328
10	188	181	306	301

Table 4. Inter observer-Ethovision reliability in detecting behavioral phenotypes. Latency values (in seconds) for immobility and circling behavior in 10 C57BL/6J mice during HT at P14 measured by an observer (O) and Ethovision (E). Both detection methods produce statistically highly comparable results.

developed tonic-clonic convulsions within our 15 minute screen, although in some strains not all individual animals developed these convulsions. In four strains (AKR/J, C3H/HeJ, A/J and BALB/cByJ) HT did not elicit the circling behavior, whereas it was clearly elicited in the other three strains. Table 3 summarizes the phenotypic diversity of FS susceptibility in the mouse strains examined as reflected by average latencies to a particular behavioral phenotype during the HT. As strategies and mechanisms for coping with an increase in body temperature could be different between strains, we analyzed whether body temperature gain during the phenotypic screen was different between strains. No inter-strain differences in body temperature gain could be identified. As there were significant inter-strain differences in body weight at P14 (ANOVA: $F_{6,59} = 15.71$, $P = 1.12E-10$, strain *P*-values are shown in table 3) and both genders were used, we treated body weight and gender as covariate in the Cox proportional hazard regression analysis (table 3). Weight and gender as covariates did not substantially influence statistical results.

DISCUSSION

As FS are one of the most common early precipitating lesions in the etiology of TLE, investigating the genetic predisposition and long-term effects of FS are of great importance. Several susceptibility genes have been identified in large human families [105], especially in the more severe FS phenotypes (for example GEFS+), but little is known about susceptibility in sporadic FS. Most data on the long-term effects of prolonged FS has been gathered using a rat HT model [108,110]. Since this rat model is not suitable for genetic studies, we developed a mouse FS model. Due to the limited size of 10-day-old mouse pups, several adaptations were needed. These include wireless body-temperature measurements using transponders (figure 1) to reduce body temperature variation and handling, and an automated air temperature control system to ensure precise core body temperature control. To test the validity of the prolonged FS model in the mouse species, we compared a number of key features with the rat model. Subsequently, we investigated FS susceptibility of several behaviorally and genetically distinct mouse strains.

The behavioral characteristics of the HT - induced FS in C57BL6/J mice were similar to those in Sprague Dawley rats (see table 2) [108]. All mice subjected to HT developed FS. Cooling the mice to normal core body temperature instantaneously terminated the behavioral seizures. Mice exposed to HT showed a short-lasting impairment in body weight gain (figure 2), as observed in rats [249]. This is probably due to a temporary reduction in food intake, but is unlikely to contribute to the long-term changes observed after prolonged FS.

Human studies have suggested that FS enhance excitability and increase the risk to develop unprovoked seizures later in life [11]. Our results show that prolonged FS in

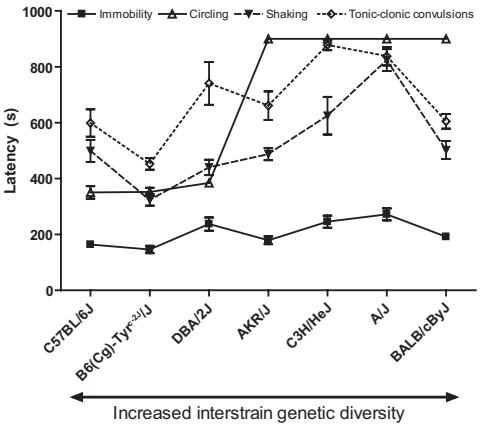

Figure 6. Phenotypic diversity of febrile seizure susceptibility in seven inbred mouse strains. Strains are listed on the x-axis, sorted by evolutionary distances based on a genetically determined family tree of mouse strains [252]. Latency values were taken from Table 3. B6(Cg)-Tyr^{c-2J}/J is the most susceptible strain and A/J the least susceptible. Data are expressed as means ± SEM.

mice enhance sensitivity to PTZ-induced seizures significantly (figure 3). The reduced interval between PTZ-stage 1 and PTZ-stage 2 seizures suggests impairments in inhibitory pathways after early-life seizures. The long-term reduction in seizure threshold is in agreement with data from the rat model [122] and suggests that prolonged FS induce long-lasting changes in the brain. Indeed, we found a depolarized RMP, increased depolarizing voltage-sag and increased rebound depolarization in CA1 pyramidal neurons of HT animals (figure 4). These mice data confirm earlier studies in rat [120] and rat data previously published by our lab [243]. These long-term electrophysiological alterations in the hippocampus are likely to contribute to the observed reduction in seizure threshold. Our data show that HT-induced changes in rat and mice are highly similar. Thus, the mice FS model can be used to study epileptogenesis after prolonged FS for instance in genetically modified animals.

We subsequently developed a phenotypic FS susceptibility screen in 14-day-old mice suitable for large scale testing of mice strains. This screening assay takes only 15 minutes per animal and is highly sensitive, because within this period, the mice pups show the complete HT-induced behavioral repertoire (see table 2 and 3) starting with immobility, circling and shaking. Heat-induced immobility is considered as the first sign of FS [116]. In C57BL/6J mice circling, occurring shortly after immobility, was a prominent phenotype, possibly caused by unilateral seizure activity. The direction of the circular movement alternated within the same mouse. Circling has occasionally been observed in humans as a distinctive phenotype in generalized and focal epilepsy [250]. In other animal models for epilepsy this circling phenotype has also been described [251].

To evaluate whether components of the HT-induced behavioral repertoire were influenced by common genotypes, strains were ordered based on evolutionary distances [252] (figure 6). Strikingly, the genetically most related strains C57BL/6J, B6(Cg)-Tyr^{c-2J}/J (C57BL/6J, but with white coat color) and DBA/2J, were the only strains showing the circling phenotype. Evaluating immobility, whole body shaking and tonic-clonic convulsions, the BALB/cByJ and C57BL/6J were the strains most susceptible for FS, while A/J and C3H/HeJ were most resistant. The differences in FS susceptibility could not be attributed to differences in body weight or temperature gain during the phenotypic screen. It is also very unlikely that developmental differences between these strains caused the observed differences in FS susceptibility. All mice tested at P14 had open eyes and pilot experiments with strains tested at P10 (C57BL/6J and A/J) showed a consistent difference in FS susceptibility. These results suggest complex genetic components for these traits. The average latencies for immobility and tonic-clonic convulsions were correlated (Pearson $r = 0.93$; $P < 0.01$) suggesting that immobility was indeed the first behavioral sign of FS.

Interestingly, the C57BL/6J strain was amongst the strains with the highest susceptibility to FS, while the A/J strain was one of the least susceptible strains (table 3 and figure 6). This is in contrast to our expectations, as A/J mice are much more susceptible to chemically- and electrically-induced seizures then C57BL/6J mice [128,253]. This could be partly due to the difference in the developmental stage at which the seizures were induced. In the chemically- and electrically-induced seizure models, seizures are induced in adult animals, while the FS are induced in 14-day-old pups. The striking difference in sensitivity to FS as compared to chemically- and electrically-induced seizures indicates that different mechanisms determine the sensitivity to these distinct seizures types. Therefore it is to be expected that FS susceptibility genes are distinct from those contributing to susceptibility to chemically- and electrically-induced seizures [128,237-240]. Possibly not only susceptibility genes, but also the molecular mechanism induced by FS may be distinct from those induced by chemically and electrically evoked seizures.

These observations warrant further experiments identifying loci and genes contributing to FS susceptibility (QTL analysis). QTL analysis classically involved large numbers of animals, but can be simplified by the use of recombinant inbred and consomic strains, which both have been constructed for the C57BL/6J and A/J strains [241]. We are in the process of screening these strains for FS susceptibility and have identified a number of strains carrying QTLs for EEG confirmed FS susceptibility [chapter 7]. The phenotypic screen for FS susceptibility is also highly suitable to test susceptibility in genetically modified mice and to test the effectiveness of anti-epileptic drugs.

ACKNOWLEDGEMENTS

This study was sponsored by the Epilepsy fund of The Netherlands (grant 03-12 and 06-09) and by the EPOCH Foundation (Focal Epilepsies of Childhood). We thank A. van der Linden for expert assistance during the PTZ experiments.

CHAPTER 6

Expression profiling after prolonged experimental febrile seizures reveals the involvement of neuronal remodeling and *Camk2a*

Koen L.I. van Gassen[1], Marina de Wit[1], Marian J.A. Groot Koerkamp[2], Onno van Nieuwenhuizen[3], Frank C.P. Holstege[2], Pierre N.E. de Graan[1]

[1]Rudolf Magnus Institute of Neuroscience, Department of Neuroscience and Pharmacology, University Medical Center Utrecht, Utrecht, The Netherlands
[2]Department of Physiological Chemistry, University Medical Center Utrecht, Utrecht, the Netherlands
[3]Rudolf Magnus Institute of Neuroscience, Department of Child Neurology, University Medical Center Utrecht, Utrecht, The Netherlands

Under review

ABSTRACT

Febrile seizures (FS), the most prevalent seizures in young children, increase seizure susceptibility and the risk to develop temporal lobe epilepsy (TLE) later in life. To investigate the relationship between FS and TLE and to identify critical and functional mediators involved in epileptogenic processes we performed gene expression profiling on the hippocampal of mice at different times after FS. Prolonged experimental FS were elicited in 10-day-old mice by warm-air induced hyperthermia. Hippocampal microarray analysis was performed at 1 hour, 3, 14 and 56 days after FS. Statistically differentially expressed genes were analyzed for over-representation of gene ontology (GO) classes. Transcriptional and stress responses were identified as most affected at 1 hour after FS, and active neuronal repair and remodeling was identified at 3 and 14 days after FS. At 56 days after FS, *Camk2a* was down-regulated. The GO classes immune system, angiogenesis and deregulation of the glutamate-glutamine cycle were identified throughout the process of epileptogenesis. These results show that FS induce an initial wave of transcriptional regulation in the hippocampus, inducing processes involved in neuronal repair and remodeling, immune reactions, angiogenesis and an altered glutamate-glutamine cycle. These processes probably lead to network reorganizations and eventually to down-regulation of *Camk2a*. *Camk2a* has been implicated in various forms of epilepsy and maybe an important mediator of epileptogenesis after FS and a potential target for intervention.

INTRODUCTION

Febrile seizures (FS) occur in 2-4% of Western-European children and are the most prevalent seizures in young children [85]. FS are characterized by convulsions induced by fever, without the evidence of an intracranial infection [3]. FS with complex features (recurrence or duration longer than 15 minutes) increase the risk for temporal lobe epilepsy (TLE) and can be recognized as precipitating event in 30-50% of TLE patients [11]. It is not clear whether FS themselves contribute to the development of TLE, or whether a prenatal lesion, brain insult or a genetic predisposition is causal to both FS and TLE [87,88].

Several TLE animal models have been used to investigate epileptogenesis induced in adult animals by status epilepticus (SE). In these adult models SE is induced by a chemoconvulsant or electrical stimulation and brains of these animals have been studied at various times after SE [reviewed by 133]. Molecular analysis indicates the involvement of glutamate receptors, neurotrophin receptors, Ca^{2+}-regulated enzymes, astrocytes and immunity-related processes in epileptogenesis in these models [133,144].

Although these adult TLE models show neuropathological characteristics that resemble human TLE, initiation of epileptogenesis in these models is not comparable to that in human TLE. In human TLE SE is not a major precipitating event initiating epileptogenesis and precipitating events usually occur in early childhood [reviewed by 132]. Therefore juvenile animal models for TLE have been developed. In some of these models brain damage (fluid percussion or hypoxia) is induced in a developmental period comparable with early childhood in humans. These models lack the high epilepsy induction rate, but do show several of the characteristics reminiscent of human TLE [132]. A recent meta-analysis of longitudinal regulated genes in these juvenile models indicated roles for cell death and survival, neuronal plasticity and immune response in epileptogenesis [156].

In other juvenile models prolonged FS are induced by elevation of the body temperature in pups, at a developmental age when FS occur in children [108,109,254]. These prolonged experimental FS reduce seizure threshold [122,254], have been associated with mechanisms underlying hyperventilation [109] and may result in mild spontaneous electro-clinical seizures in a small percentage of animals [111]. Besides these effects on excitability, several FS-induced specific molecular and functional changes have been described [reviewed by 110]. These changes include altered expression/function of hyperpolarization-activated cyclic-nucleotide-gated (HCN) channels [120,243,254,255] and the increased expression of interneuronal cannabinoid 1 receptors (CNR1) [109,118]. Although these data have provided insight into some of the processes affecting the intricate balance between inhibition/excitation in the hippocampus after prolonged FS, a detailed analysis of the short- and long-term molecular changes after FS is needed to understand the underlying mechanisms leading to plasticity changes, increased seizure susceptibility and epileptogenesis, possibly resulting in TLE.

To investigate the short- and long-term effects of prolonged FS, we induced prolonged experimental FS in highly FS susceptible C57BL/6J mice (10-day-old) by hyperthermia [254] and performed a genome-wide microarray and gene ontology analysis of hippocampal gene expression at one hour, three, 14 and 56 days after FS.

MATERIAL AND METHODS

Animals

Mice were bred from pairs of C57BL/6J mice (Jackson Laboratories, ME, USA) and raised by their mother. Time of birth was recorded daily. At P0-P2 (P0 defined as day of birth),

litters were reduced or culled to a maximum of six male pups. Pups were weaned on P21 and housed maximum four per cage. Animals were kept in a controlled 12h light-dark cycle with a temperature of 22 ± 1ºC and were given unrestricted access to food (2111 RMH-TM diet; Hope Farms, Woerden, The Netherlands) and water. Animals were housed in transparent Plexiglas cages with wood-chip bedding and tissue for nest building. All experiments conformed to institutional guidelines of the University Medical Center Utrecht.

Warm-air induced prolonged febrile seizures

Hyperthermia (HT) in mice was induced by quickly raising core body temperature with a temperature regulated laminar stream of warm air (41-48ºC) as previously described [254]. Briefly, body weight was determined in 10-day-old C57BL/6J male mice. At least 30 minutes before the HT procedure mice were injected subcutaneously with temperature sensitive transponders (IPTT-300, Plexx, Elst, The Netherlands). Two chambers were used, one for age-, weight- and litter-matched normothermic control mice (NT; core body temperature maintained at 35ºC) and one for HT (defined as core body temperature >39ºC) mice. Chamber temperature was maintained at 32ºC for NT mice and at 47ºC for HT mice. Mice were placed one by one on the floor of the preheated chambers and the experiment was started. Core body temperature was measured every minute by wireless transponder readout (WRS-6006/6007, Plexx). HT was typically reached within 2.5 minutes. After the core temperature of the HT mice had reached 42ºC, air temperature was adjusted to maintain a core body temperature between 41.5ºC and 42ºC. Time and temperature data was logged automatically on a computer (DASHost v1.0, Plexx). HT was maintained for 30 minutes. Then, mice were partly submerged in water of room temperature to quickly normalize core body temperature and were returned to their mother. NT mice were simultaneous treated as HT mice, except that the core body temperature of the animals was kept at 35ºC.

Hippocampal dissection and RNA isolation

At one hour, 3 days, 14 days and 56 days after HT animals were sacrificed by decapitation and brains were removed. Hippocampal tissue was dissected, collected and stored at -80°C. Total RNA was isolated, purified and checked for quality as described [195].

Microarray analysis

To investigate the causality between FS and TLE and to identify critical and functional mediator genes during epileptogenesis, acute, short- and long-term effects of prolonged FS on gene expression were investigated in whole hippocampal samples of C57BL/6J animals one hour (HT1h; n = 8), three days (HT3d; n = 6), 14 days (HT14d; n = 6) and 56 days (HT56d; n = 6) after HT. Two-channel oligonucleotide microarray analysis was performed as described [174,195]. Briefly, cDNA from 2 µg total RNA was synthesized using a T7 oligo(dT)24VN primer (Ambion, Cambridgeshire, UK). The T7 Megascript kit (Ambion) was used for cRNA synthesis and its quality was analyzed. Cy3 or Cy5 fluorophores (GE Healthcare Europe, Diegem, BE) were coupled to 2000 ng NT and HT cRNA. The degree of label incorporation was monitored and hybridizations were set up with 1500 ng of Cy3 and 1500 ng of Cy5 labeled cRNA, always hybridizing a NT and HT sample on the same chip, including a dye-swap (technical replicate). Just before hybridizing HT and NT sample were mixed and fragmented (AM8740, Austin, TX, USA).

The mouse Array-Ready oligo set (version 3, Operon Biotechnologies, Cologne, DE) was printed on UltraGAPS slides (Corning, Schiphol-Rijk, NL). Slides were washed by

Gene name	Refseq ID	Ratio	*P*-value	Description
HT1h up			**FW corrected**	
Cyr61	NM_010516	7.67	0.00000	cysteine rich protein 61
Slit2	NM_178804	5.50	0.00000	slit homolog 2 (Drosophila)
Jun	NM_010591	3.06	0.00000	Jun oncogene
Nr4a1	NM_010444	2.93	0.00000	nuclear receptor subfamily 4, group A, member 1
Fos	NM_010234	2.88	0.00000	FBJ osteosarcoma oncogene
Egr1	NM_007913	2.52	0.00000	early growth response 1
Hsp110	NM_013559	2.45	0.00000	heat shock protein 110
Hspb1	NM_013560	2.35	0.00000	heat shock protein 1
Dusp1	NM_013642	2.27	0.00000	dual specificity phosphatase 1
Dnajb1	NM_018808	2.19	0.00000	DnaJ (Hsp40) homolog, subfamily B, member 1
Atf3	NM_007498	2.06	0.00000	activating transcription factor 3
Ctgf	NM_010217	2.02	0.00000	connective tissue growth factor
Ube2q2	AK042515.1	2.01	0.00000	ubiquitin-conjugating enzyme E2Q (putative) 2
Gem	NM_010276	1.98	0.00000	GTP binding protein
Arc	NM_018790	1.92	0.00000	activity regulated cytoskeletal-associated protein
Wnt10b	NM_011718	1.87	0.00000	wingless related MMTV integration site 10b
Phlda1	NM_009344	1.73	0.00000	pleckstrin homology-like domain, family A, member 1
Pdcd2l	NM_026549	1.72	0.00000	programmed cell death 2-like
Mfsd11	NM_178620	1.65	0.00000	major facilitator superfamily domain containing 11
Ecd	NM_027475	1.63	0.00000	ecdysoneless homolog (Drosophila)
D4Wsu53e	NM_023665	1.62	0.00000	DNA segment, Chr 4, Wayne State University 53, expressed
Mrgpra3	XM_001003345	1.61	0.00000	MAS-related GPR, member A2
Gadd45g	NM_011817	1.61	0.00000	growth arrest and DNA-damage-inducible 45 gamma
Bag3	NM_013863	1.61	0.00000	Bcl2-associated athanogene 3
Btg2	NM_007570	1.59	0.00000	B-cell translocation gene 2, anti-proliferative
Edn1	NM_010104	1.58	0.00000	endothelin 1
Sfrs10	XR_002915	1.58	0.00000	splicing factor, arginine/serine-rich 10
Hspe1-rs1	XM_911363	1.57	0.00000	heat shock protein 1 (chaperonin 10), related sequence 1
Mt1	NM_013602	1.54	0.00000	metallothionein 1
Mfap1	XM_982954	1.52	0.00000	microfibrillar-associated protein 1
HT1h down			**FW corrected**	
3300001P08Rik	NM_026313	0.62	0.00000	RIKEN cDNA 3300001P08 gene
Ptgds	NM_008963	0.67	0.00000	prostaglandin D2 synthase (brain) (Ptgds), mRNA
Cldn5	NM_013805	0.68	0.00000	claudin 5
Tia1	NM_011585	0.70	0.00000	cytotoxic granule-associated RNA binding protein 1
Slc7a10	NM_017394	0.72	0.00000	solute carrier family 7, member 10
D4Wsu53e	NM_023665	0.73	0.00000	DNA segment, Chr 4, Wayne State University 53, expressed
Sox18	NM_009236	0.74	0.00000	SRY-box containing gene 18
Slc2a1	NM_011400	0.75	0.00000	solute carrier family 2, member 1
Lfng	NM_008494	0.76	0.00000	lunatic fringe gene homolog (Drosophila)
Gmpr	NM_025508	0.76	0.00000	guanosine monophosphate reductase
Gmpr	NM_025508	0.77	0.00000	guanosine monophosphate reductase
Hes5	NM_010419	0.79	0.00000	hairy and enhancer of split 5 (Drosophila)
Ramp2	NM_019444	0.80	0.00000	receptor (calcitonin) activity modifying protein 2
H1f0	NM_008197	0.80	0.00440	H1 histone family, member 0 (H1f0), mRNA
Sult1a1	NM_133670	0.80	0.00000	sulfotransferase family 1A, phenol-preferring, member 1
Gjb6	NM_001010937	0.80	0.00000	gap junction membrane channel protein beta 6
Bcl6	NM_009744	0.81	0.00000	B-cell leukemia/lymphoma 6
Pdgfra	NM_011058	0.81	0.00000	platelet derived growth factor receptor, alpha polypeptide
AB182283	XM_109794	0.81	0.00000	cDNA sequence AB182283
Snx14	NM_172926	0.81	0.00000	sorting nexin 14
Mfsd2	NM_029662	0.82	0.00000	major facilitator superfamily domain containing 2
Coro1a	NM_009898	0.82	0.00000	coronin, actin binding protein 1A
Rnase4	NM_021472	0.82	0.01360	ribonuclease, RNase A family 4
Pcdh20	NM_178685	0.82	0.00000	protocadherin 20
Dicer1	NM_148948	0.82	0.00000	Dicer1, Dcr-1 homolog (Drosophila)
BC022623	NM_177632	0.82	0.00000	cDNA sequence BC022623
Mylip	NM_153789	0.82	0.00000	myosin regulatory light chain interacting protein
Lrfn2	NM_027452	0.83	0.00000	leucine rich repeat and fibronectin type III domain containing 2
Tfrc	NM_011638	0.83	0.00000	transferrin receptor
Sfrs6	NM_026499	0.83	0.00000	splicing factor, arginine/serine-rich 6

Table 1 continues

Gene name	Refseq ID	Ratio	*P*-value	Description
HT3d up			**BH corrected**	
Nfix	NM_010906	1.33	0.04021	nuclear factor I/X
Elavl3	NM_010487	1.23	0.02799	ELAV-like 3 (Hu antigen C)
Dpysl3	NM_009468	1.17	0.00831	dihydropyrimidinase-like 3
Hmgb1	NM_010439	1.16	0.01127	high mobility group box 1
Tia1	NM_011585	1.15	0.03621	cytotoxic granule-associated RNA binding protein 1
Ptprd	NM_001014288	1.14	0.01531	protein tyrosine phosphatase, receptor type, D
Nrxn3	NM_172544	1.14	0.02612	neurexin III
S100a4	NM_011311	1.13	0.04453	S100 calcium binding protein A4
BC011426	NM_145490	1.13	0.00900	cDNA sequence BC011426
Tm7sf2	NM_028454	1.12	0.00949	transmembrane 7 superfamily member 2
Nrxn1	NM_020252	1.12	0.04571	neurexin I
Pabpn1	NM_019402	1.12	0.02649	poly(A) binding protein, nuclear 1
Mfge8	NM_008594	1.12	0.00905	milk fat globule-EGF factor 8 protein
Vcam1	NM_011693	1.12	0.04818	vascular cell adhesion molecule 1
Lbp	NM_008489	1.12	0.04571	lipopolysaccharide binding protein
Hod	NM_175606	1.11	0.02649	homeobox only domain
Tnc	NM_011607	1.11	0.04571	tenascin C
Fgfr1	NM_001079908	1.11	0.04571	fibroblast growth factor receptor 1
Mark2	NM_007928	1.10	0.04561	MAP/microtubule affinity-regulating kinase 2
Aqp4	NM_009700	1.10	0.02464	aquaporin 4
Hrasls3	NM_139269	1.10	0.04818	HRAS like suppressor 3
H2afx	NM_010436	1.10	0.02750	H2A histone family, member X
Atic	NM_026195	1.10	0.02338	AICAR transformylase/IMP cyclohydrolase
Rpl12	NM_009076	1.10	0.02750	ribosomal protein L12
Chl1	NM_007697	1.10	0.03993	cell adhesion molecule with homology to L1CAM
Mapre1	NM_007896	1.09	0.01531	microtubule-associated protein, RP/EB family, member 1
Tmem145	NM_183311	1.09	0.04818	transmembrane protein 145
Ltbp3	NM_008520	1.09	0.00900	latent transforming growth factor beta binding protein 3
Ddx20	NM_017397	1.09	0.04571	DEAD (Asp-Glu-Ala-Asp) box polypeptide 20
Ugp2	NM_139297	1.09	0.04021	UDP-glucose pyrophosphorylase 2
Fmnl1	NM_001077698	1.09	0.03334	formin-like 1
Pbxip1	NM_146131	1.09	0.04571	pre-B-cell leukemia transcription factor interacting protein 1
L2hgdh	NM_145443	1.08	0.02612	L-2-hydroxyglutarate dehydrogenase
Cav1	NM_007616	1.08	0.04571	caveolin, caveolae protein 1
Col6a1	NM_009933	1.08	0.04921	procollagen, type VI, alpha 1
HT3d down			**BH corrected**	
Hbb-b2	NM_008220	0.74	0.00074	hemoglobin, beta adult minor chain
Hba-a2	NM_008218	0.82	0.03069	hemoglobin alpha, adult chain 2
Mal	NM_010762	0.85	0.00108	myelin and lymphocyte protein, T-cell differentiation protein
Adrb3	NM_013462	0.87	0.03621	adrenergic receptor, beta 3
Htra1	NM_019564	0.88	0.01609	HtrA serine peptidase 1
Gjb6	NM_001010937	0.88	0.03621	gap junction membrane channel protein beta 6
Mobp	NM_001039364	0.88	0.01999	myelin-associated oligodendrocytic basic protein
Vsnl1	NM_012038	0.89	0.03998	visinin-like 1
9530077C05Rik	NM_026739	0.90	0.03664	RIKEN cDNA 9530077C05 gene
Cnp1	NM_009923	0.90	0.02820	cyclic nucleotide phosphodiesterase 1
Mag	NM_010758	0.90	0.03179	myelin-associated glycoprotein
Rasd1	NM_009026	0.90	0.04021	RAS, dexamethasone-induced 1
Lynx1	NM_011838	0.91	0.03010	Ly6/neurotoxin 1
Ly6c	NM_010738	0.91	0.04021	lymphocyte antigen 6 complex, locus A
4931407K02Rik	NM_029946	0.91	0.02649	RIKEN cDNA 4931407K02 gene
Gsn	NM_146120	0.91	0.04571	gelsolin
Ltb4r2	NM_020490	0.91	0.02464	leukotriene B4 receptor 2
Mfap4	NM_029568	0.92	0.02649	microfibrillar-associated protein 4
Itpka	NM_146125	0.92	0.04571	inositol 1,4,5-trisphosphate 3-kinase A
Shank3	NM_021423	0.92	0.04818	SH3/ankyrin domain gene 3
Ecm2	NM_001012324	0.92	0.03179	extracellular matrix protein 2, female organ and adipocyte specific
Psma1	NM_011965	0.92	0.04388	proteasome (prosome, macropain) subunit, alpha type 1
Pkhd1	NM_153179	0.92	0.04818	polycystic kidney and hepatic disease 1
Lgi4	NM_144556	0.92	0.04571	leucine-rich repeat LGI family, member 4
Mid1	NM_010797	0.92	0.04571	midline 1
Sh3bgrl3	NM_080559	0.92	0.03018	SH3 domain binding glutamic acid-rich protein-like 3
Ctcfl	XM_913620	0.93	0.04818	CCCTC-binding factor (zinc finger protein)-like
Olfr1298	NM_146886	0.93	0.04668	olfactory receptor 1298

Table 1 continued and continues

Gene name	Refseq ID	Ratio	*P*-value	Description
HT14d up			**BH corrected**	
Ncor1	NM_011308	1.27	0.04663	nuclear receptor co-repressor 1
Cnp1	NM_009923	1.26	0.01587	cyclic nucleotide phosphodiesterase 1
Cldn11	NM_008770	1.24	0.01367	claudin 11
Snx30	NM_172468	1.21	0.01446	sorting nexin family member 30
Efhc2	NM_028916	1.18	0.03173	EF-hand domain (C-terminal) containing 2
Wasl	NM_028459	1.15	0.01446	Wiskott-Aldrich syndrome-like (human)
Hspa8	NM_031165	1.15	0.01446	heat shock protein 8
Card11	NM_175362	1.15	0.01587	caspase recruitment domain family, member 11
HT14d down			**BH corrected**	
A630075K04	XM_974206	0.85	0.02904	RIKEN cDNA A630075K04 gene
Mgp	NM_008597	0.86	0.00460	matrix Gla protein
HT56d down			**FW corrected**	
Camk2a	NM_177407	0.90	0.0318	calcium/calmodulin-dependent protein kinase II alpha

Table 1 continued. Top 30 differentially expressed genes (up- and down-regulated) at HT1h and all differentially expressed Refseq genes at HT3d, HT14d and HT56d. FW: family wise, BH: Benjamin Hochberg. Ratios represent expression values of hyperthermic animals divided by expression values of normothermic animals.

hand and scanned. Scanned slides were quantified and the background-corrected with Imagene v5.6.1 (BioDiscovery, El Segundo, USA) and Loess normalized per print-tip [175]. To identify significant differentially expressed transcripts, ANOVA analysis was applied (R/MAANOVA version 0.98-3, http://www.r-project.org/). In a fixed effect analysis, sample, array and dye effects were modeled. *P*-values were determined by a permutation F2-test, in which residuals were shuffled 5000 times globally after Benjamin and Hochberg (BH) or family-wise (FW) error correction. $P < 0.05$ was considered significant.

Quantitative RT-PCR

cDNA was synthesized from the RNA samples used for the microarray using oligo-dT primers. The qPCR reaction was performed using the LightCycler (Roche, Almere, NL) and the Fast Start DNA Master PLUS SYBRgreen I kit (Roche). Primer (Sigma Genosys, Cambridge, UK) specifications are listed in supplementary table 1. Gene expression was calculated as normalized ratio and normalized to the housekeeping gene peptidylprolyl isomerase A (*Ppia*). All samples were analyzed in duplicate and reported as mean ± standard error of the mean (SEM). To compare qPCR with microarray data, data were analyzed using one-tailed Student's *t*-tests, with $P < 0.05$ considered significant.

Gene ontology (GO) analysis

For GO and pathway analysis, significant transcript lists ($P < 0.05$, minimal 15% change) and a reference list comprising all transcripts present on the microarray chip were imported into the software tool Panther (www.pantherdb.org) [176]. Of the 26,754 probes which could be mapped to a RefSeq identifier, a total of 18,103 unique transcripts could be mapped to Panther and these were used to generate the reference gene list containing all the annotated genes in our microarray screen. Up- and down-regulated genes lists were mapped against the Panther database. Panther's GO classes are greatly abbreviated and simplified to fa-

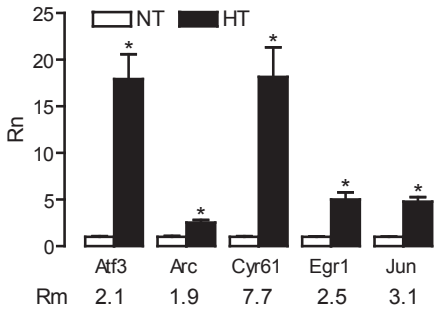

Figure 1. Microarray gene expression validation by qPCR analysis. Gene expression levels (Rn) in NT (normothermic) and HT (hyperthermic) animals. compared to microarray gene expression ratios (Rm) indicated below the figure. $P < 0.05$ was considered significant (Student's *t*-test). Indicated are means ± standard error of the mean.

	Refseq ID	Ratio	Description
Apoptosis			
Phlda1	NM_009344	1.73	Pleckstrin homology-like domain, family A, member 1
Mcl1	NM_008562	1.30	Myeloid cell leukemia sequence 1
Cell proliferation/differentiation			
Cyr61	NM_010516	7.67	Cysteine rich protein 61
Slit2	NM_178804	5.50	Slit homolog 2 (Drosophila)
Gadd45g	NM_011817	1.61	Growth arrest and DNA-damage-inducible 45 gamma
Btg2	NM_007570	1.59	B-cell translocation gene 2, anti-proliferative
Edn1	NM_010104	1.58	Endothelin 1
Myd116	NM_008654	1.33	Myeloid differentiation primary response gene 116
Gadd45b	NM_008655	1.31	Growth arrest and DNA-damage-inducible 45 beta
Cell structure			
Ank3	NM_170689	1.33	Ankyrin 3, epithelial
Cldn5	NM_013805	0.68	Claudin 5
Chaperone/Chaperonin			
Hsp110	NM_013559	2.45	Heat shock protein 110
Hspb1	NM_013560	2.35	Heat shock protein 1
Dnajb1	NM_018808	2.19	DnaJ (Hsp40) homolog, subfamily B, member 1
Bag3	NM_013863	1.61	Bcl2-associated athanogene 3
XM_911363	XM_911363	1.57	Similar to 10 kDa heat shock protein, mitochondrial
Hspd1	NM_010477	1.37	Heat shock protein 1 (chaperonin)
Dnaja4	NM_021422	1.36	DnaJ (Hsp40) homolog, subfamily A, member 4
EG623924	XM_974050	1.33	Predicted gene, EG623924
Development			
Arc	NM_018790	1.92	Activity regulated cytoskeletal-associated protein
Wnt10b	NM_011718	1.87	Wingless related MMTV integration site 10b
Fbxo5	NM_025995	1.33	F-box protein 5
Adm	NM_009627	1.32	Adrenomedullin
Adamts1	NM_009621	1.31	A disintegrin-like and metallopeptidase (reprolysin type) with thrombospondin type 1 motif, 1
Lfng	NM_008494	0.76	Lunatic fringe gene homolog (Drosophila)
Ptgds	NM_008963	0.67	Prostaglandin D2 synthase (brain)
G-protein mediated signaling			
Gem	NM_010276	1.98	GTP binding protein (gene overexpressed in skeletal muscle)
XM_001003345	XM_001003345	1.61	Similar to MAS-related GPR, member A2
mRNA splicing			
Rbm12b	NM_028226	1.41	RNA binding motif protein 12B
Tia1	NM_011585	0.70	Cytotoxic granule-associated RNA binding protein 1
3300001P08Rik	NM_026313	0.62	RIKEN cDNA 3300001P08 gene
mRNA transcription			
Jun	NM_010591	3.06	Jun oncogene
Nr4a1	NM_010444	2.93	Nuclear receptor subfamily 4, group A, member 1
Fos	NM_010234	2.88	FBJ osteosarcoma oncogene
Egr1	NM_007913	2.52	Early growth response 1
Atf3	NM_007498	2.06	Activating transcription factor 3
Pdcd2l	NM_026549	1.72	Programmed cell death 2-like
Ecd	NM_027475	1.63	Ecdysoneless homolog (Drosophila)
Hes1	NM_008235	1.44	Hairy and enhancer of split 1 (Drosophila)
Id1	NM_010495	1.41	Inhibitor of DNA binding 1
Klf10	NM_013692	1.41	Kruppel-like factor 10
Atf4	NM_009716	1.38	Activating transcription factor 4
Nab2	NM_008668	1.38	Ngfi-A binding protein 2
Klf6	NM_011803	1.31	Kruppel-like factor 6
Maff	NM_010755	1.30	V-maf musculoaponeurotic fibrosarcoma oncogene family, protein F (avian)
Sox18	NM_009236	0.74	SRY-box containing gene 18
Protein Phosphorylation			
Dusp1	NM_013642	2.27	Dual specificity phosphatase 1
Dusp6	NM_026268	1.38	Dual specificity phosphatase 6
Mast1	NM_019945	1.35	Microtubule associated serine/threonine kinase 1
Aurkb	NM_011496	1.35	Aurora kinase B
Ppp2r2a	NM_028032	1.31	Protein phosphatase 2 (formerly 2A), regulatory subunit B (PR 52), alpha isoform
Trib1	NM_144549	1.31	Tribbles homolog 1 (Drosophila)
Transporter			
Slc2a1	NM_011400	0.75	Solute carrier family 2 (facilitated glucose transporter), member 1
Slc7a10	NM_017394	0.72	Solute carrier family 7, member 10
Various			
Ctgf	NM_010217	2.02	Connective tissue growth factor
Amotl2	NM_019764	1.51	Angiomotin like 2
Has1	NM_008215	1.49	Hyaluronan synthase1
Serpine1	NM_008871	1.49	Serine (or cysteine) peptidase inhibitor, clade E, member 1
XM_992322	XM_992322	1.36	Similar to H-2 class I histocompatibility antigen, L-D alpha chain precursor
Pcdhb6	NM_053131	1.34	Protocadherin beta 6
Rnmtl1	NM_183263	1.33	RNA methyltransferase like 1
Gmpr	NM_025508	0.76	Guanosine monophosphate reductase
Unclassified			
D4Wsu53e	NM_023665	0.73-1.62	DNA segment, Chr 4, Wayne State University 53, expressed
Mfsd11	NM_178620	1.65	RIKEN cDNA 2600014M03 gene
Mt1	NM_013602	1.54	Metallothionein 1
EG382804	XM_982954	1.52	Predicted gene, EG382804
Yipf6	XM_985822	1.50	Yip1 domain family, member 6
Ccdc7	NM_029061	1.50	Coiled-coil domain containing 7
Lmbrd1	NM_026719	1.49	LMBR1 domain containing 1
LOC672809	XM_001001544	1.47	Hypothetical protein LOC672809
1200016B10Rik	NM_025819	1.42	RIKEN cDNA 1200016B10 gene
1700007K13Rik	NM_027040	1.35	RIKEN cDNA 1700007K13 gene

Table 2. Differentially expressed genes 1 hour after HT (expression change > 1.3), ordered based on gene ontology.

Biological Process	HT1h up	HT1h down	HT3d up	HT3d down
Stress response [175]	**0.0000000392 [14]**	0.485 [2]	0.275 [1]	0.776 [0]
Protein folding [128]	**0.0000000699 [12]**	0.303 [0]	0.791 [0]	0.831 [0]
mRNA transcription regulation [1069]	**0.00000068 [33]**	0.462 [9]	0.411 [1]	0.205 [0]
mRNA transcription [1424]	**0.0000985 [34]**	0.431 [12]	0.512 [2]	0.382 [1]
Cell proliferation and differentiation [761]	**0.000382 [21]**	0.278 [9]	0.161 [3]	0.0946 [3]
Nucleoside/nucleotide/nucleic acid metabolism [2526]	**0.000771 [48]**	0.0415 [32]	0.0334 [9]	0.275 [2]
Immunity and defense [1172]	**0.00197 [26]**	0.203 [14]	0.637 [2]	0.236 [3]
Protein phosphorylation [575]	**0.00437 [15]**	0.554 [5]	0.283 [2]	0.431 [0]
MAPKKK cascade [167]	**0.00438 [7]**	0.21 0]	0.736 [0]	0.786 [0]
Protein metabolism and modification [2458]	**0.00698 [43]**	0.521 [23]	0.155 [2]	0.294 [2]
Lipid, fatty acid and steroid metabolism [683]	0.0845 [4]	**0.00191 [15]**	0.356 [2]	0.367 [0]
Chromatin packaging and remodeling [163]	0.584 [2]	**0.00445 [6]**	0.258 [1]	0.79 [0]
Phospholipid metabolism [128]	0.214 [0]	**0.00724 [5]**	0.791 [0]	0.831 [0]
Cell adhesion-mediated signaling [312]	0.517 [4]	0.212 [1]	**0.0000197 [6]**	0.364 [1]
Cell communication [988]	0.211 [15]	0.314 [11]	**0.0000506 [9]**	0.051 [4]
Cell adhesion [497]	0.286 [4]	0.492 [5]	**0.000253 [6]**	0.516 [1]
Neurogenesis [533]	0.111 [10]	0.446 [4]	**0.00266 [5]**	0.541 [1]
Ectoderm development [605]	0.115 [11]	0.334 [4]	**0.00457 [5]**	0.587 [1]
Pre-mRNA processing [215]	0.26 [4]	0.323 [3]	**0.00704 [3]**	0.733 [0]
Blood circulation and gas exchange [79]	0.0707 [3]	0.479 [0]	0.865 [0]	**0.00579 [2]**
Molecular Function	**HT1h up**	**HT1h down**	**HT3d up**	**HT3d down**
Chaperone [142]	**0.00000000297 [14]**	0.266 [0]	0.771 [0]	0.815 [0]
Chaperonin [20]	**0.000112 [4]**	0.83 [0]	0.964 [0]	0.972 [0]
Other chaperones [79]	**0.000431 [6]**	0.479 [0]	0.865 [0]	0.892 [0]
Transcription factor [1524]	**0.000719 [33]**	0.344 [16]	0.465 [2]	0.343 [1]
Hsp 70 family chaperone [11]	**0.00796 [2]**	0.903 [0]	0.98 [0]	0.984 [0]
Histone [51]	0.542 [0]	**0.00141 [4]**	0.0891 [1]	0.929 [0]
Nuclease [153]	0.158 [0]	**0.00328 [6]**	0.755 [0]	0.802 [0]
Transferase [744]	0.115 [5]	**0.00424 [15]**	0.397 [2]	0.335 [0]
Glycosyltransferase [192]	0.328 [1]	**0.00957 [6]**	0.703 [0]	0.757 [0]
Cell adhesion molecule [320]	0.537 [4]	0.427 [2]	**0.000273 [5]**	0.372 [1]
Other receptor [207]	0.288 [1]	0.128 [4]	**0.00635 [3]**	0.741 [0]
CAM family adhesion molecule [71]	0.574 [1]	0.516 [0]	**0.00752 [2]**	0.0973 [1]
Extracellular matrix structural protein [73]	0.415 [0]	0.493 [1]	**0.00793 [2]**	0.0999 [1]
Myelin protein [12]	0.866 [0]	0.894 [0]	0.978 [0]	**0.000142 [2]**
Select calcium binding protein [235]	0.0584 [0]	0.111 [0]	0.0685 [2]	**0.00457 [3]**
Pathway	**HT1h up**	**HT1h down**	**HT3d up**	**HT3d down**
Circadian clock system [13]	**0.000558 [3]**	0.886 [0]	0.977 [0]	0.981 [0]
Apoptosis signaling pathway [120]	**0.000692 [7]**	0.693 [1]	0.803 [0]	0.841 [0]
Oxidative stress response [65]	**0.00123 [5]**	0.546 [0]	0.888 [0]	0.911 [0]

Table 3. Statistical analysis of gene ontology (GO) classifications. GO classes with $P < 0.01$ are shown. Numbers in parenthesis represent total number of genes annotated per class in the reference gene list (most left) and in the gene lists. Bold indicates $P < 0.01$. HT1h: 1 hour after hyperthermia (HT), HT3d: 3 days after HT.

cilitate high-throughput analyses. Significant lists were statistically compared to the reference list for significant over-representation of genes within the GO classes for molecular function, biological process and pathways. Only highly significant ($P < 0.01$) GO classes are shown. Significant GO classes with only one regulated gene were excluded. More in-depth analyses were performed with the software tool Webgestalt (bioinfo.vanderbilt.edu/webgestalt) [177], which is unsupervised and uses all the GO classes from the GO consortium [178]. To identify overrepresented transcription factor-binding sites within the

promoters of genes in our significant gene lists, the web tool GATHER (gather.genome.duke.edu) was used [256].

RESULTS

Hippocampal mRNA expression 1 hour after prolonged febrile seizures

To investigate acute mRNA expression changes induced by prolonged FS, hippocampal mRNA content of HT mice was compared with NT mice (HT1h group) by microarray hybridization. 1952 statistically significant differentially expressed probes were identified (BH error correction). Because of the large number of significant probes, we applied a more stringent error correction method (FW error correction). After FW error correction 660 statistically significant differentially expressed probes were identified. Of these 660, 461 probes were up-regulated and 199 probes were down-regulated in HT mice. Filtering by fold-change (at least 15% change), resulted in 259 (231 coding for known Refseq genes, 220 unique) up-regulated probes and 192 (184 coding, 172 unique) down-regulated probes. Several highly up-regulate genes belong to the immediate early genes (for example *Cyr61*, *Jun*, *Fos*, *Egr1* and *Nr4a1*) and to heat-shock proteins (*Hsp110*, *Hspb1* and *Dnajb1*). Top 10 down-regulated genes include *Slc2a1*, *Sox18*, *Cldn5* and *Ptgds*. Table 1 lists the top 30 up- and down-regulated genes. Table 2 lists and orders the genes (expression changes > 1.30x) based on gene ontology. All significant genes are listed in supplementary table 2.

To independently validate the HT1h microarray results, we used qPCR to quantify mRNA levels of several genes in the HT and NT animals. *Jun*, *Cyr61*, *Atf3*, *Egr1* and *Arc* were selected for validation (figure 1). Verifying microarray results, these five genes were up-regulated in HT animals compared to NT animals.

Short- and long-term mRNA expression changes in the hippocampus after prolonged FS

To investigate the short- and long-term mRNA expression changes induced by prolonged FS, hippocampal HT3d, HT14d and HT56d tissue was used for microarray analysis. At these time-points statistical analysis (with stringent FW error correction) revealed that the genes *Hbb-b2*, *Mal* and *Mobp* were down-regulated at HT3d. *Mgp* was down-regulated and *Cldn11* was up-regulated at HT14d. *Camk2a* was down-regulated at HT56d. Less stringent error correction (BH correction) showed that at HT3d, 91 probes (35 up- and 28 down-regulated unique Refseq genes) were differentially expressed, at HT14d 12 probes (8 up- and 2 down-regulated Refseq genes) and at HT56d one down-regulated probe (*Camk2a*). Table 1 lists all unique Refseq genes regulated at these time-points. Among the down-regulated genes at HT3d several myelin associated genes were identified (*Mobp*, *Cnp1*, *Mag*, and *Lgi4*). The up-regulated genes included *Hmgb1*, *Nrxn1* and *Nrxn3*. Instead of down-regulated, several myelin associated genes were up-regulated at HT14d (*Cldn11* and *Cnp1*).

Gene ontology (GO) analysis of acutely regulated genes

To identify functionally relevant gene clusters acutely regulated after prolonged FS we performed GO analysis using the web tool Panther. This analysis groups differentially expressed genes according to molecular function, biological processes and pathways. Significant gene lists (HT1h) were uploaded and mapped against the Panther database. 217 unique transcripts out of 231 up-regulated probes and 168 unique transcripts out of 184 down-regulated probes could be mapped against the Panther database. Gene lists were statistically compared to the reference gene list to identify significant overrepresentation of genes within the gene ontology

classes for molecular functions and biological processes (table 3). Although for exploratory research *P*-values < 0.05 are often used, we used a cutoff of 0.01 to select the most relevant functions and processes. The most striking over-representation of up-regulated genes was found in stress response, protein folding, mRNA transcription regulation, cell proliferation/differentiation and chaperone/chaperonin classes. Immunity/defense and MAPKKK cascade genes were also over-represented. In the down-regulated genes, nuclear processes were overrepresented (chromatin packaging and remodeling, histones and nucleases).

More detailed analysis (Webgestalt) of up-regulated genes showed overrepresentation of heat response (5 genes, *P* = 0.0000028), glial cell differentiation (3 genes, *P* = 0.0035), angiogenesis (9 genes, *P* = 0.000017), MAPK phosphatase activity (3 genes, *P* = 0.000079) and nuclear genes (72 genes, *P* = 0.000000011). Detailed analysis of down-regulated genes showed over-representation of electrochemical potential-driven transporter activity (6 genes, *P* = 0.0072) and iron ion transporter activity (2 genes, *P* = 0.00028).

Gene ontology (GO) analysis of short and long-term regulated genes

Significant gene lists were uploaded and mapped against the Panther database. For HT3d 33 unique up-regulated transcripts and 26 unique down-regulated transcripts and for HT14d 8 up-regulated transcripts and 2 down-regulated transcripts could be mapped against the Panther database. At 56 days after HT only *Camk2a* was regulated and therefore this time-point was not investigated using Panther. Gene lists were statistically compared to the reference list as described before. At 3 days after HT genes involved in cell adhesion (6 genes, *P* = 0.0000197) and communication (9 genes, *P* = 0.0000506)

Annotation	% genome	% genelist	# genes	Bayes factor	*P*-value
V$E2F1_Q3_01	27	50	82	16	6.59E-06
V$E2F1_Q6: E2F-1	51	74	121	15	6.59E-06
V$E2F_Q3_01	34	56	92	14	6.59E-06
V$CREB_02: cAMP-responsive element binding protein	10	26	42	12	6.59E-06
V$E2F1_Q6_01	35	55	90	11	6.59E-06
V$CREBATF_Q6	29	46	75	8	6.59E-06
V$EGR3_01: early growth response gene 3 product	1	7	11	8	6.59E-06
V$DEAF1_01	19	34	56	8	6.59E-06
V$E2F1DP1_01: E2F-1:DP-1 heterodimer	28	45	73	7	9.93E-06
V$E2F_Q4: E2F	34	51	83	7	1.65E-05
V$E2F_Q6: E2F	73	87	143	7	1.65E-05
V$ATF1_Q6	6	16	9	7	2.30E-05
V$ATF_B: ATF binding site	3	10	17	7	2.65E-05
V$ATF_01: activating transcription factor	10	21	35	6	3.30E-05
V$CREB_Q4: cAMP-response element binding protein	8	18	30	6	3.30E-05
V$EGR2_01: Egr-2	1	7	11	6	3.30E-05
V$E2F1_Q4: E2F-1	28	43	71	6	4.97E-05
V$ATF4_Q2: activating transcription factor 4	24	38	63	6	4.97E-05
V$CREB_Q4_01	29	44	72	6	5.95E-05

Table 4. Statistical analysis (http://gather.genome.duke.edu) of transcription binding sites within the promoters of the HT1h up-regulated significant gene list. All transcription binding motives with Bayes factor > 6 are listed.

were overrepresented in the up-regulated gene list. Neurogenesis genes (5 genes, *P* = 0.00266) were also overrepresented (table 3). Myelin genes (2 genes, *P* = 0.000142) and genes involved in blood circulation and gas exchange (2 genes, *P* = 0.00579) were overrepresented in the down-regulated gene list (table 3). No statistically significant overrepresented GO classes were present in the 14 days after HT gene lists.

Pathway analysis

To identify functionally relevant pathways we performed pathway analysis using the web tool Panther (table 3). At HT1h circadian clock system, apoptosis signaling and oxidative stress response genes were overrepresented in the acutely up-regulated genes. At HT3d, HT14d and HT56d no significant overrepresented pathways were present. HT1h pathways were also investigated using Webgestalt. MAPK signaling pathway (KEGG pathways; 12 genes *P* = 0.000028), oxidative stress induced gene expression via *Nrf2* (Biocarta pathways; 3 genes *P* = 0.00000038), regulation of MAP kinase pathways through dual specificity phosphatases (Biocarta; 3 genes *P* = 0.00011) and pertussis toxin-insensitive CCR5 signaling in macrophage (Biocarta; 2 genes *P* = 0.0099) were overrepresented in the up-regulated genes. The chondroitin sulfate biosynthesis pathway (KEGG; 3 genes *P* = 0.00048) was overrepresented in the down-regulated genes.

Transcription factor binding site analysis

To identify factors important in transcriptional regulation in the acute phase after HT, overrepresentation of transcription factor-binding sites within the promoters of the HT1h up-regulated significant gene lists were investigated. Of 220 unique probes with a Refseq identifier, 164 had a TRANSFAC annotation. Of these 164, 82 genes contained an *E2f* motive (Bayes factor 16.4, *P* = 6.6e-6) and 42 genes contained a *CREB* motive (Bayes factor 12.2, *P* = 6.6e-6). Other significant motives include *Egr2-3*, *Deaf*, *Atf1,-3* and *-4*. All transcription factor binding motives with Bayes factor > 6 are listed in table 4.

DISCUSSION

FS are one of the most common early precipitating lesions in the etiology of TLE. Thus, the elucidation of the acute, short- and long-term effects of FS is of great importance. We hypothesized that FS induce expression changes in a group of critical mediators, which in their turn induce changes in functional mediators ultimately leading to the functional changes observed and possibly TLE [reviewed by 110] (summarized in figure 2). Therefore, we investigated the acute, short- and long-term effects of FS on mRNA expression in a mouse model for FS. Hippocampal expression profiles of normothermic control mice were compared to those of animals that experienced prolonged FS at HT1h (critical mediators), HT3d, HT14d and HT56d (functional mediators).

Critical mediators after prolonged FS

Investigating the acute effects (HT1h) of prolonged experimental FS on hippocampal gene expression can provide insight in the initial processes leading to functional alterations. We identified 660 significant differentially expressed probes and have verified several of these effects by qPCR expression analysis (figure 1). As expected, we identified several up-regulated immediate early genes (IEG) and heat-shock proteins. Among the IEG was *Fos*, which was also found to be up-regulated in an earlier FS study [119]. Up-regulation of heat-shock proteins was expected in response to hyperthermia, [257], but interestingly, up-regulation of these genes was also shown in response to seizures and in human epilepsy [258,259]. We found that more than 30% (23 of 62; see table 5) of our HT1h differentially expressed genes

are identical to those identified acutely after nicotine-induced seizures [260]. Additionally, five out of six genes identified as seizure responsive genes after pentylenetetrazol-induced generalized seizures [261], were also identified in our study (*Fbxo33*, *Egr1*, *Nr4a1*, *Btg2* and *Sgk*). Thus, although it is difficult to distinguish between hyperthermia and seizure responsive genes, our results indicate that some of the acute expression changes, presumably at least those genes previously associated with seizures, may be considered as critical mediators in the early phases after FS.

To identify gene clusters involved in specific biological processes, molecular functions and pathways, we performed an unbiased analysis of over-representation in the significant up- and down-regulated transcript list ($P < 0.05$, minimal 15% change; supplementary table 1). Genes involved in the biological process of stress response and protein folding were highly over-represented in the up-regulated transcript list. Most of these genes are chaperones and are likely to be up-regulated in response to fever and seizures. Genes involved in mRNA transcription regulation, cell proliferation and differentiation, immunity and defense were also over-represented. Most of the genes involved in transcriptional regulation were also classified as immediate early genes and act as transcription factors. Therefore we analysed over-representation of transcription factor-binding sites within the promoters of up-regulated significant transcripts (table 4). Several over-represented binding motives showed regulation of the corresponding transcription factor family. For example, *Atf4* was up-regulated and 63 up-regulated genes contained the *Atf4* binding site in their promoter (V$ATF4_Q2), which was a significant over-representation. In the down-regulated transcript list most striking over-representation was present in the classes chromatin packaging/remodeling, histone and nucleases, implying more effects on transcriptional regulation. These results show that transcriptional programs can be identified from complex gene lists and that transcriptional regulation acutely after prolonged FS model shares properties with other seizure models [260,261].

Gene ontology analysis showed that the MAPK signaling pathway was over-represented in the acutely up-regulated genes. Activation of the MAPK signaling pathway is in agreement with the transcription factor binding site analysis (table 4). All major MAPK cascades were activated [reviewed by 262,263]: the ERK signaling cascade or classical MAPK cascade, which is involved in proliferation and differentiation (see table 3); the c-Jun N-terminal kinase (JNK) cascade, which is involved in proliferation, differentiation and inflammation; the p38 MAPK cascade, which is involved in differentiation and apoptosis; and finally the ERK5 cascade, which is involved in proliferation and differentiation. The combined activation of all MAPK cascades probably resulted from the parallel effects of seizure activity and heat-shock. Heat-shock studies in rats (50 minutes at 41-41.5°C) identified in the hippocampus only activation of the p38 MAPK cascade, while the ERK en JNK signaling cascades were down-regulated [264]. Our results show activation of all three signaling cascades, suggesting that the ERK en JNK signaling cascades were activated specifically in response to seizures. Kainate-induced seizures appear to activate only the JNK signaling cascade [265]. ERK2 has been implicated in human epilepsy [266] and has been shown to respond to glutamate levels. A recent study also showed that chronic ERK activation in-vivo caused phosphorylation of CREB (up-regulated in our study), increased transcription of *Efnb2* and augmented NMDA receptor 2B (NR2B) protein levels [267]. *Efnb2* over-expression resulted in increased NR2B

tyrosine phosphorylation, which was found to be essential for chronic ERK activation-induced epilepsy in vivo [267]. NR2B levels were also found to be up-regulated in TLE patients [268]. In our study *Efnb2* expression tended to be increased, but the increase was not significant after correction for multiple testing. *Mapk1* (ERK2) and possibly *Efnb2*, could be critical mediators shortly after FS, contributing to transforming the brain to a more seizure susceptible state.

Functional mediators after prolonged FS

Investigating short- and long-term molecular alterations after prolonged FS can provide insight in the genes contributing to the functional changes described in this model [reviewed by 110,195]. Therefore gene expression was investigated in HT3d, HT14d and HT56d groups and when relevant related to critical mediators (HT1h).

At HT3d cell adhesion/communication, extracellular matrix and neurogenesis genes were over-represented in up-regulated genes, while myelin (eg. *Cnp1* and *Lgi4*) and calcium binding proteins were over-represented in down-regulated genes. At HT14d no over-representation of GO classes was present, but several interesting genes were regulated (up-regulation of myelin genes *Cldn11*, *Cnp1* and actin remodeling gene *Wasl*). Regulation of adhesion/communication, extracellular matrix, neurogenesis, myelin and actin genes suggests active neuronal repair and remodeling in the post-FS hippocampus. Up-regulation of these genes (eg. *Tnc* and *Cnp1*) may indicate active mossy fiber sprouting at HT14d [133,269], which occurs in this model [113]. Several other genes involved in neuro-

Gene	Description	Febrile seizures (HT1h)	Nicotine seizures
Ak3l1	adenylate kinase 3 alpha-like 1	1.13	1.33
Atf3	activating transcription factor 3	2.06	2.17
Btg2	B-cell translocation gene 2, anti-proliferative	1.59	1.63
Cyr61	cysteine rich protein 61	7.67	2.27
Dusp1	dual specificity phosphatase 1	2.27	1.57
Dusp6	dual specificity phosphatase 6	1.38	1.57
Egr1	early growth response 1	2.25	1.47
Egr2	early growth response 2	1.17	2
Errfi1	ERBB receptor feedback inhibitor 1	1.2	1.61
Fos	FBJ osteosarcoma oncogene	2.88	3.34
Gem	GTP binding protein	1.98	2.18
Klf10	Kruppel-like factor 10	1.41	1.6
Klf4	Kruppel-like factor 4	1.23	1.85
Nedd9	neural precursor cell expressed, developmentally down-regulated gene 9	1.12	1.32
Nr4a1	nuclear receptor subfamily 4, group A, member 1	2.93	2.74
Pcf11	cleavage and polyadenylation factor subunit homolog	1.19	1.34
Per1	period homolog 1	1.21	1.73
Ppan	peter pan homolog	1.16	1.45
Rgs2	regulator of G-protein signaling 2	1.14	1.42
Sgk	serum/glucocorticoid regulated kinase	1.2	1.74
Sox18	SRY-box containing gene 18	0.74	0.66
Tiparp	TCDD-inducible poly(ADP-ribose) polymerase	1.16	1.64
Txnip	thioredoxin interacting protein	1.23	1.36

Table 5. Overlap between genes regulated at HT1h and after nicotine-induced seizures [260].

nal repair and remodeling showed a tendency to up-regulation at HT14d (*Gfap*, *Kif1b*, *Vsnl1*, *Qk*, *Mag*, *Jup*, *Spin1* and *Mbp*), although this was not significant after error-correction. The FS model used in our study does not induce massive neuronal cell death and gliosis [113], but our results shows modest actin and myelin remodeling. Moreover, *Gfap* tended to be up-regulated, but to a variable degree, and was not significant after error-correction. *Gfap* up-regulation suggests reactive astrogliosis [270] which is also present in other TLE animal models and in human TLE [271]. In our study we used one of the most FS sensitive strains (C57BL/6J) [254], However, this strain is rather resistant to chemically- and electrically-induced seizures, which are accompanied by pronounced neuronal death [272]. Investigating the long-term effects of FS in a mouse strain more prone to neurodegeneration may be more suitable to investigate FS-induced changes in actin and myelin remodeling.

At 56 days after HT *Camk2a* was significantly down-regulated. Although, this was the only regulated gene at this time-point the implications are profound. *Camk2* is abundantly expressed in the brain as a major constituent of the postsynaptic density and is involved in glutamate receptor trafficking during long-term potentiation (LTP) [273]. Reduced expression of *Camk2a* has been shown to induce limbic seizures in a dose-dependent way and several epilepsy/epileptogenesis models have also shown a down-regulation or reduced activity of this gene [reviewed by 133]. The evidence of reduced CAMK2 activity during epileptogenesis, supported by genetic and pharmacological studies, suggests that reduced CAMK2 activity is sufficient to induce changes that render the brain epileptic and suggests that *Camk2a* plays a pivotal role in epileptogenesis irrespectively of the epilepsy model used. Data from a recurrent FS model has also shown that repetitive FS impair LTP [274], while recent data from our group suggests enhanced LTP after prolonged FS (Notenboom, Ramakers and de Graan, in preparation). The precise role of reduced *Camk2a* expression after prolonged experimental FS needs to be further investigated.

Previous studies have shown that the CB1 receptor (*Cnr1*) was robustly up-regulated in the whole hippocampus 2-10 days after experimental FS [109,118]. We did not find an up-regulated for this receptor, indicating that this receptor is regulated at protein level in this model. Although we did observe electrophysiological changes consistent with *Hcn*-channel expression alterations [254], we did not observe expressional differences for subunits of this channel, which have been described in this model before [117]. Modest *Hcn*-channel subtype expression differences were observed in specific sub-regions of the hippocampus and thus may have escaped detection in whole hippocampal samples.

Processes both critically and functionally involved after prolonged FS

Gene ontology analysis showed that the immunity and defense class was over-represented in the up-regulated genes at HT1h. Immunity and defense genes (26 transcripts up-regulated) included the chemokines *Ccl2* and *-3* (both 1.2x up-regulated), which are important mediators of CCR5 signaling in macrophages [158]. Up-regulation of these chemokines was previously found in hippocampi of TLE patients [195], and in several animal models for epilepsy [144,reviewed by 156]. They are important mediators of the innate immunity in response to stress, injury or infection [158] but can also have direct effects on neurons [215]. *Ptgds*, the gene responsible for synthesis of brain PGD2 was robustly down-regulated at HT1h (ratio: 0.67). A recent study also showed that *Ptgds* among other components of the prostaglandin pathway, was acutely down-regulated after elec-

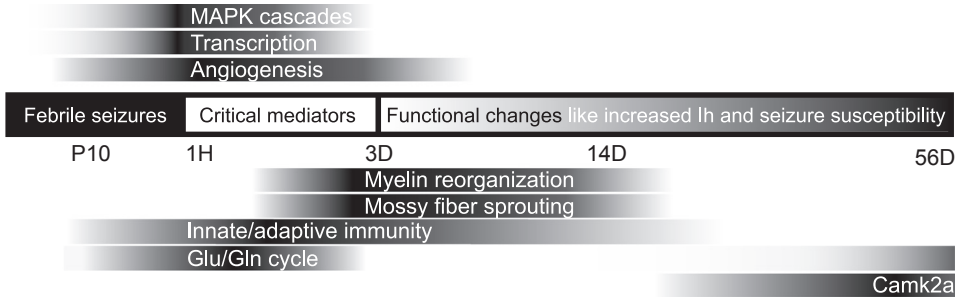

Figure 2. Time-line diagram showing summary of critical and functional mediators after prolonged experimental febrile seizures induced epileptogenesis. Bar blackness shows peak effect of processes. P10: postnatal-day-10; 1H: 1 hour after hyperthermia (HT); 3D: 3 days after HT; 14D: 14 days after HT; 56D: 56 days after HT; MAPK: Mitogen-activated protein kinases; Glu/Gln cycle: glutamate/glutamine cycle.

trically induced status epilepticus, while up-regulated in the latent and chronic phases [144]. In our study, *Ptgds* was the only affected gene in this pathway. Physiological concentrations of PGD2 were shown to potently rescue neurons in excitotoxicity paradigms [275,276], while conversely, in the context of an inflammatory stimulus enhances neuronal injury [277,278]. Additionally, PGD2 has been shown to have seizure-inhibiting properties [279]. A reduction in *Ptgds* will likely result in a reduction of PGD2 levels. In the FS model it is impossible to predict the effect of low levels of PGD2 as excitotoxicity and inflammation are both present. *Ptgds* provides a promising target for detailed analysis of acute and long-term effects of FS. *Hmgb1*, which was up-regulated at HT3d, acts as a potent proinflammatory cytokine, responds to elevated levels of tumor necrosis factor-alpha, interleukin-beta or lipopolysaccharide and is involved at the crossroads of the innate and adaptive immunity [reviewed by 280]. Moreover, *Card11*, a gene also involved in the innate and adaptive immune response was significantly up-regulated at HT14d [281]. The immune system has been implicated in both the acute and chronic phases of epilepsy [144,156] and in human TLE [195]. Our data show that immunity and defense genes are also regulated in the acute, short- and long-term phases after FS. They are likely to play both critical and functional mediator roles during epileptogenesis after FS.

Further in-depth analysis showed that several angiogenesis genes were up-regulated at HT1h (*Arts1*, *Ctgf*, *Cyr61*, *Id1*, *Serpine1* and *Tnfrsf12a*). *Cyr61*, which was highly up-regulated (7.7x), has been shown to promote angiogenesis [282], but has also been implicated in neuronal cell death in a JNK and *Srf* (also up-regulated)-dependent way [283]. A role of *Cyr61* and the other angiogenesis genes is also indicated by the up-regulation of *Hba-a2* and *Hbb-b2*, which probably represents an increased vascularization. In contrast, at HT3d, a down-regulation of the blood circulation and gas exchange GO process was identified (table 2; genes *Hba-a1*, *Hbb-b2* and *Adrb3*). Angiogenesis occurs in both animal models and human TLE [284]. Although the effects in the FS model are short-lasting, angiogenesis may play a role in hippocampal remodeling after FS.

The glutamate-glutamine cycle plays a key role in the regulation of glutamatergic transmission. Most extra-cellular glutamate is transported into glial cell by the glial glutamate transporter (*Slc1a2*), converted into non-toxic glutamine by the enzyme glutamine synthetase (*Glul*). Glutamine is then transported back to the neuron, where the enzyme

glutaminase (*Gls*) reconverts glutamine into glutamate. All three genes were regulated in the acute phase of our study (HT1h). *Glul* was down-regulated, while *Slc1a2* and *Gls* were up-regulated. Up-regulation of *Slc1a2* suggests an increased capacity to transport extra-cellular glutamate. Down-regulation of *Glul* would reduce conversion of this extra-cellular glutamate. In the chronic phase (HT56d) part of the HT animals showed a strong down-regulation of *Glul* (Average ratio: 0.80; *P*-value before correction: 0.000047; *P*-value after correction: 0.40). Reduced expression of *Glul* is likely to affect glutamate conversion and could lead to glutamate toxicity [285]. In parallel with reduced *Glul* expression [271,286], slow rates of glutamate-glutamine cycling have been identified in the human TLE hippocampus [287]. Additionally, a 50% reduction in *Glul* dramatically increase the susceptibility to FS [chapter 8]. The short- and long-term effects of deregulation of this cycle are difficult to predict from expression studies, but our data suggests that this cycle plays both critical and functional roles in epileptogenesis after FS.

Concluding remarks

This study provides the first concise overview of the molecular hippocampal changes induced by early life prolonged FS in mice. More than 600 genes, mainly involved in transcription and stress response were differentially expressed acutely (1 hour) after prolonged FS. Three days later, fever genes were differentially expressed; most of them are involved in neuronal repair and remodeling, a process that was still active 11 days later. Another 6 weeks later these processes had normalized, but *Camk2a*, one of the most consistently down-regulated genes in other epileptogenesis models, was down-regulated. Although subtle expression changes in specific cell populations could not be detected with our microarray approach [117], our results suggest that early life prolonged FS induce a process of local network reorganization, possibly including mossy fiber sprouting [113], that is not associated with large overall expressional changes in the hippocampus and occurs within a narrow time window. It is likely that these reorganizations contribute to the observed increase in seizure susceptibility [254] and eventually result in the observed reduction in expression of *Camk2a* and altered synaptic plasticity. The lack of regulation of immediate early genes and stress genes at HT56d suggest that no spontaneous seizures occurred after prolonged FS in mice and indicates that additional factors (a second hit), like trauma or a genetic susceptibility, may be necessary to develop spontaneous seizures and epilepsy after prolonged FS. Our data set provides a starting point to further explore the relationship between FS and TLE and to investigate potential targets for early diagnosis and treatment of FS.

ACKNOWLEDGEMENTS

This study was sponsored by the Epilepsy Fund of The Netherlands (grant 03-12) and by the EPOCH Foundation (Focal Epilepsies of Childhood). We thank Inge Wolterink-Donselaar and Gokhan Ertaylan for assistance during the animal experiments and analysis of microarray data.

Gene	GI accession	forward primer	reverse primer	product length (bp)	start position (bp)	end position (bp)	annealing temperature (°C)	elongation time (sec)	PCR efficiency
Arc	86604725	ATGTCTGGAAAGGGCATCAC	GCTGGCTTGTCTTCACCTTC	180	2177	2356	58	11	1.90
Atf3	31542153	GCAGCTTTGTCCTTGGCTAC	GGCTGTGGCTGTGGTTATCT	131	1560	1690	57	15	1.99
Cyr61	6753593	CTCAGTCAGAAGGCAGACCC	CAAACCCACTCTTCACAGCA	211	467	677	57	15	2.02
Egr1	76559936	TTCATCGTCTTCCTCTGCCT	AGGTCTCCCTGTTGTTGTGG	258	810	1067	57	15	2.01
Jun	6754401	CGACCAGAACGATGGACTTT	AGTTTGTAACCCCTCCCACC	102	2180	2281	57	15	2.07
Ppia	6679438	GGCTATAAGGGTTCCTCCTTTC	CTTGCCATCCAGCCATTC	238	180	417	57	15	1.98
Slit2	30794373	CAGTCATTCATGGCTCCCTC	TTCCCTCGGCAGTCTACAAT	87	1022	1108	57	15	2.01

Supplementary table 1. qPCR primer-pair characteristics

Gene					
0610037L13Rik	*Acat1*	*Bcl10*	*Coq10b*	*Egr1*	*Gtpbp4*
0910001A06Rik	*Adamts1*	*Bcl6*	*Coro1a*	*Egr2*	*Gusb*
1110007M04Rik	*Adcyap1*	*Bcor*	*Crat*	*Eif4e3*	*Gzmm*
1110012D08Rik	*Adm*	*Bcorl1*	*Crem*	*Endog*	*H2-Q2*
1110037F02Rik	*Agt*	*Bhlhb5*	*Crsp9*	*Epha2*	*H3f3b*
1110054O05Rik	*AI464131*	*Bmp2k*	*Cryab*	*Ercc8*	*Haghl*
1110059G10Rik	*Ak3l1*	*Bmpr2*	*Csn3*	*Errfi1*	*Haghl*
1190005F20Rik	*Amotl2*	*Bola1*	*Csnk2b*	*Esf1*	*Has1*
1190005P17Rik	*Ank*	*Brp16*	*Ctdsp1*	*Etaa1*	*Hba-a2*
1200003I07Rik	*Ank3*	*Brpf1*	*Ctgf*	*Exosc1*	*Hba-a2*
1200016B10Rik	*Ankrd16*	*Brpf1*	*Ctnna3*	*Exosc7*	*Hbb-b2*
1300018I05Rik	*Ankrd47*	*Btaf1*	*Ctsa*	*Ext2*	*Hbb-b2*
1700007K13Rik	*Ankrd49*	*Btg1*	*Cyfip1*	*F3*	*Hbp1*
1700012B15Rik	*Ap4e1*	*Btg2*	*Cyp2j13*	*Fbxl10*	*Heatr3*
1700102P08Rik	*Apex2*	*Btg3*	*Cyp51*	*Fbxl11*	*Herc4*
1810008A18Rik	*Apln*	*Bxdc2*	*Cyr61*	*Fbxo33*	*Herpud1*
1810026J23Rik	*Apoa1bp*	*C1d*	*Cys1*	*Fbxo5*	*Hes1*
1810032O08Rik	*Apold1*	*C1qa*	*D030013I16Rik*	*Fem1a*	*Hes5*
2010111I01Rik	*Arc*	*C1qdc2*	*D11Wsu99e*	*Fkbp4*	*Hexb*
2010111I01Rik	*Arhgap30*	*C1ql1*	*D230005D02Rik*	*Fkbpl*	*Hey1*
2010309E21Rik	*Arid5a*	*C330021A05Rik*	*D230025D16Rik*	*Flnb*	*Hiat1*
2310005P05Rik	*Arl4a*	*Cacybp*	*D230037D09Rik*	*Fmnl1*	*Hist1h2ao*
2310037I24Rik	*Armc7*	*Carm1*	*D330012F22Rik*	*Fnbp4*	*Hist1h2ao*
2310037I24Rik	*Arntl*	*Cbfa2t3h*	*D4Wsu132e*	*Fos*	*Hivep3*
2410015M20Rik	*Arts1*	*Cbx4*	*D4Wsu53e*	*Foxh1*	*Hmox1*
2510039O18Rik	*Atf3*	*Ccdc117*	*D4Wsu53e*	*Foxj1*	*Homez*
2510042P03Rik	*Atf4*	*Ccdc130*	*Dact1*	*Frmd6*	*Hsd17b7*
2600011E07Rik	*Atf4*	*Ccdc64*	*Ddit3*	*Fstl1*	*Hsp110*
2600014M03Rik	*Atp11b*	*Ccdc7*	*Ddx5*	*Fxr1h*	*Hsp90aa1*
2810026P18Rik	*Atp11b*	*Ccdc86*	*Dicer1*	*Fxyd5*	*Hspa5*
2810403A07Rik	*Atp8b1*	*Ccl12*	*Dio2*	*Fzd3*	*Hspa8*
2900024C23Rik	*Atr*	*Ccl2*	*Dmkn*	*Gab1*	*Hspa8*
3100002J23Rik	*AU021092*	*Ccl3*	*Dnaja1*	*Gadd45b*	*Hspa8*
3110001A13Rik	*Aurkb*	*Ccnl2*	*Dnaja1*	*Gadd45g*	*Hspb1*
3300001P08Rik	*Axud1*	*Ccnt2*	*Dnaja1*	*Galnact2*	*Hspd1*
4632415L05Rik	*B3galt2*	*Cd109*	*Dnaja4*	*Gem*	*Hspd1*
4732474A20Rik	*B630005N14Rik*	*Cdc34*	*Dnajb1*	*Gjb6*	*Hspd1*
4930548G07Rik	*Bag3*	*Cdr2*	*Dnajb4*	*Gls*	*Hspe1*
4932414K18Rik	*Baiap2*	*Chac1*	*Dnajc5*	*Gls*	*Hspe1*
4933413J09Rik	*Banp*	*Chmp4c*	*Dock4*	*Glul*	*Hspe1-ps2*
4933439C20Rik	*Bat5*	*Chordc1*	*Drd1a*	*Glyat*	*Hspe1-rs1*
6430527G18Rik	*Bbc3*	*Chrac1*	*Dusp1*	*Gm527*	*Htr3a*
6430527G18Rik	*BC008155*	*Chst12*	*Dusp16*	*Gmpr*	*Htra1*
6530403A03Rik	*BC011426*	*Cks2*	*Dusp6*	*Gmpr*	*Icam1*
8430408G22Rik	*BC017643*	*Cldn15*	*Dusp8*	*Gnl3*	*Id1*
9030607L17Rik	*BC022623*	*Cldn5*	*Ebpl*	*Gpr19*	*Idi1*
9530053A07Rik	*BC031781*	*Clk4*	*Ecd*	*Gpr34*	*Ier3*
9530077C05Rik	*BC035295*	*Cnn3*	*Edc3*	*Gsdm2*	*Ifrd1*
A930028L21Rik	*BC038167*	*Col7a1*	*Edn1*	*Gstm1*	*Il10ra*
AB182283	*BC048651*	*Coq10b*	*Egln3*	*Gtf2h1*	*Il10rb*

Supplementary table 2 continues

Gene					
Impact	*Mettl6*	*Osgepl1*	*Rab40c*	*Skil*	*Tmem147*
Insl3	*Mfap1*	*Osgin2*	*Rabggtb*	*Slc15a4*	*Tmem161b*
Ints6	*Mfsd2*	*Otx1*	*Ramp2*	*Slc1a2*	*Tmem168*
Irf1	*Mkks*	*P4ha1*	*Rars*	*Slc22a8*	*Tmem46*
Irf2bp2	*Mobk1b*	*P4ha1*	*Rasgef1b*	*Slc24a5*	*Tmem86a*
Ivns1abp	*Morf4l1*	*Pard3*	*Rasl11b*	*Slc25a16*	*Tnfrsf12a*
Josd3	*Mrgpra3*	*Parp1*	*Rassf1*	*Slc25a25*	*Tnik*
Jun	*Mrm1*	*Pbef1*	*Rbm12b*	*Slc2a1*	*Tns1*
Jund1	*Mrpl39*	*Pcdh20*	*Rbm15*	*Slc38a5*	*Tpmt*
Kcnn2	*Msx2*	*Pcdhb6*	*Rbm4*	*Slc40a1*	*Trfp*
Kctd15	*Mt1*	*Pcf11*	*Reln*	*Slc7a10*	*Trib1*
Kif14	*Mtfmt*	*Pdcd2l*	*Rg9mtd1*	*Slc7a5*	*Trim9*
Kif1b	*Mtmr4*	*Pdcd7*	*Rgs2*	*Slc7a6os*	*Trnt1*
Kif1b	*Myd116*	*Pde4b*	*Rhobtb3*	*Slco1b2*	*Trp53inp1*
Kif1b	*Mylip*	*Pde9a*	*Rit1*	*Slit2*	*Tsc22d2*
Klf10	*Nab2*	*Pdgfra*	*Rlf*	*Slitrk3*	*Tsc22d4*
Klf2	*Nasp*	*Pdha2*	*Rnase4*	*Smad7*	*Tubb2c*
Klf4	*Nck1*	*Pdlim5*	*Rnd3*	*Smarcd1*	*Tubb3*
Klf6	*Ndufa11*	*Peg12*	*Rnf19*	*Snag1*	*Tubgcp5*
Klhdc8b	*Nebl*	*Pelo*	*Rnf26*	*Snx14*	*Txn1*
Krt18	*Nedd9*	*Per1*	*Rnmtl1*	*Son*	*Txnip*
Lars2	*Negr1*	*Pfkfb3*	*Rnmtl1*	*Sox18*	*U99*
Leprot	*Nfkbiz*	*Pglyrp1*	*RP23-237I22.1*	*Sox7*	*Ubap1*
Lfng	*Ngdn*	*Phf13*	*Rps6kl1*	*Spata2*	*Ubap2l*
Lip1	*Nlrc3*	*Phf17*	*Rrs1*	*Spen*	*Ubc*
Lmbrd1	*NM_008197.3*	*Phf23*	*Rundc1*	*Srf*	*Ube2f*
LOC627894	*NM_008963.2*	*Phlda1*	*Rxfp4*	*Ssfa2*	*Ube2g2*
LOC638892	*NM_011141.1*	*Phyhd1*	*Safb2*	*St13*	*Ubxd7*
LOC666904	*NM_021427.2*	*Plscr3*	*SAP30_MOUSE*	*St6galnac5*	*Uchl4*
Lrfn2	*NM_025564.1*	*Pmvk*	*Sars*	*St7*	*Unc45a*
Lrrc4b	*NM_025980.2*	*Pnkd*	*Sat1*	*Stab1*	*Usp38*
Lrrc4b	*NM_030244.3*	*Pnn*	*Sc4mol*	*Stambpl1*	*Uspl1*
Lsm14b	*NM_178699.2*	*Polg*	*Scarf1*	*Stambpl1*	*Utp11l*
Lsm8	*Nol5a*	*Polr2b*	*Sdc4*	*Stip1*	*Utp14b*
Ly6c	*Nol5a*	*Ppan*	*Sdccag3*	*Stk17b*	*Vars2l*
Ly6c	*NR_002886.1*	*Ppapdc2*	*Sdhc*	*Stmn4*	*Vps37b*
Ly75	*Nr1d1*	*Ppid*	*Sec23ip*	*Sult1a1*	*Wdr20a*
Lypla1	*Nr4a1*	*Ppm1b*	*Sel1l2*	*Tanc2*	*Wnt10b*
Maff	*Nup37*	*Ppp1r10*	*Sema4f*	*Taok2*	*Wtap*
Mafk	*Nup54*	*Ppp1r15b*	*Serpine1*	*Tardbp*	*Xbp1*
Map4k2	*Nvl*	*Ppp2r2a*	*Sertad1*	*Tfrc*	*Xpa*
Mapk1	*Obfc2a*	*Ppp4r1*	*Setd8*	*Thrsp*	*Xpo1*
March3	*Odc1*	*pPtp4a3*	*Sfpq*	*Tia1*	*XR_001870.1*
Mast1	*Olfml3*	*Prkab1*	*Sfrs10*	*Tia1*	*XR_005049.1*
Mbnl1	*Olfr806*	*Prkcd*	*Sfrs6*	*Tial1*	*Xylt2*
Mbtps1	*Olfr862*	*Prpf38b*	*Sgk*	*Tiparp*	*Yeats4*
Mcl1	*Omg*	*Ptpn1*	*Sh2d3c*	*Tipin*	*Yipf6*
Mcl1	*Orc4l*	*Rab11b*	*Shbg*	*Tle3*	*Zbtb1*
Mctp2	*Ormdl3*	*Rab26*	*Siah1a*	*Tmc4*	*Zbtb11*
Mctp2	*Osbpl1a*	*Rab34*	*Siah2*	*Tmem11*	*Zbtb44*

Supplementary table 2 continued

CHAPTER 7

Phenotyping mouse chromosome substitution strains reveal multiple QTLs for febrile seizure susceptibility

Ellen V.S. Hessel[1#], Koen L.I. van Gassen[1#], Inge G. Wolterink[1], Peter J. Stienen[2], Cathy Fernandes[3], Jan H. Brakkee[1], Martien J. Kas[1] and Pierre N.E. de Graan[1]

[1]Rudolf Magnus Institute of Neuroscience, Department of Neuroscience and Pharmacology, University Medical Center Utrecht, Utrecht, The Netherlands
[2]Division Anesthesiology & Neurophysiology, Department of Clinical Sciences of Companion Animals, Faculty of Veterinary Medicine, Utrecht University, Utrecht, The Netherlands
[3]Department Psychological Medicine and Psychiatry, Institute of Psychiatry, King's College London, UK

[#]These authors contributed equally to this paper

Under review

ABSTRACT

Febrile seizures (FS) are the most common seizure type in children affecting 2-4% of the population and complex FS have been shown to be a risk factor for developing temporal lobe epilepsy (TLE). Although the mechanisms underlying FS are largely unknown, recent family, twin and animal studies indicate that genetics are important in FS susceptibility. Here we used a forward genetic strategy employing mouse chromosome substitution strains (CSS) to identify novel FS susceptibility genes. FS were induced by warm-air exposure at postnatal-day-14. Video EEG monitoring identified tonic-clonic convulsion (TCC) onset as reliable phenotypic parameter to determine FS susceptibility. TCC latencies were determined in both genders of the host (C57BL/6J, *n* = 66), the donor (A/J, *n* = 20) and CSS (*n* = 13-23/strain).
We verified that C57BL/6J mice were more susceptible to FS than A/J mice. Phenotypic screening identified five strains (CSS1, -2, -10, -13 and -X) carrying quantitative trait loci (QTLs) for FS susceptibility. CSS1, -10 and -13 were less susceptible (protective QTLs), whereas CSS2 and -X were more susceptible (susceptibility QTLs) than the C57BL/6J strain. Our data show that mouse FS susceptibility is determined by complex genetics, which is distinct from that for chemically-induced seizures. This data set provides the first evidence for common FS susceptibility QTLs in mice and serves as starting point to fine-map FS susceptibility QTLs and to identify FS susceptibility genes. The identification of FS susceptibility genes will increase our understanding of human FS and could possibly provide new therapeutic targets.

INTRODUCTION

Febrile seizures (FS) represent the most common seizure type during childhood. FS occur in 2-4% of the children in Europe and North-America [85] between the age of six months and five years. Of these affected children 30-40% develops recurrent FS [11]. These so-called complex FS increase the risk (10 times) of developing temporal lobe epilepsy (TLE) later in life [11]. It is not clear whether susceptibility to FS and TLE originates from a common (genetic) predisposition [87,88]. Several lines of evidence indicate that genetic factors contribute to increased FS susceptibility [103]. Twin studies showed a higher concordance rate in monozygotic (36%) than in dizygotic twins (12%) [104]. Human linkage studies identified nine familial FS loci: FEB1 (8q13-q21), FEB2 (19p), FEB3 (2q23-q24), FEB4 (5q14-q15), FEB5 (6q22-q24), FEB6 (18p11), FEB7 (21q22), FEB8 (5q31.1-q33.1) and FEB 9 (3p24.2-p23) [reviewed by 100-102,167]. Four FS genes were identified (FEB3: *SCN1A*; FEB4: *GPR98*; FEB6: *IMPA2*; FEB8: *GABRG2*) so far. In addition, mutations in several genes coding for voltage-gated sodium channel subunits (*SCN1A*, *SCN2A* and *SCN1B*) and a GABA(A) receptor subunit (*GABRG2*) were identified in families with generalized epilepsy with febrile seizure plus (GEFS+) [105]. Common forms of FS are considered to be genetically complex disorders, implying the involvement of multiple susceptibility genes. Although several positive FS gene associations have been reported, reproduction has proven difficult so far [106]. Therefore, new genetic strategies are required to identify genes involved in FS susceptibility.

Recently, a panel of mouse chromosome substitution strains (CSS) was developed derived from the C57BL/6J (host) and the A/J strain [241]. This panel has successfully been used to identify quantitative trait loci (QTLs) for complex traits such as anxiety [241,242] and pilocarpine-induced seizure susceptibility [288]. Chromosomes 10 and 18 were identified as pilocarpine-induced seizure susceptibility QTLs [288]. To study the mechanisms underlying FS, prolonged experimental FS have been induced by hyperthermia in rats [107-109]. Recently, we adapted the most frequently used rat FS model [108] to mouse and developed a semi-automated, high throughput phenotypic screen to analyze FS susceptibility in inbred mouse strains [254]. We showed that C57BL/6J mice are more susceptible to FS than A/J mice [254]. Here, we used this phenotypic screen to analyze FS susceptibility in the CSS panel based on C57BL/6J (host) and A/J (donor) strains.

MATERIALS AND METHODS

Animals

Breeding pairs for C57BL6/J, A/J and all 21 CSS (autosomal, X and Y) were obtained from The Jackson Laboratory (Bar Harbor, ME, USA). Colonies of each strain were bred in our animal house. Date of birth was recorded daily. On postnatal-day-1 (P1) litters were culled to 4-6 pups with a balanced male/female ratio. Animals were kept in a controlled 12 hour light-dark cycle with a temperature of 22 ± 1ºC and a humidity of 60%. Food and water access was *ad libitum* (2111 RMH-TM diet; Hope Farms, Woerden, The Netherlands). All animals were housed in Plexiglas cages (Macrolon type II) with wooden bedding and a paper tissue for nest building. All experiments were performed according to the institutional guidelines of the University Medical Center Utrecht. Pups were screened for FS susceptibility at P14 and sacrificed immediately after the experiments. For each gender, 33 C57BL/6J were screened across the whole screening period to control for any environmental or seasonal effects. Litters used were derived from multiple breeding pairs to exclude potential inter-litter effects. For each CSS and A/J strain both males and

females were screened. The whole CSS panel was screened within a period of 9 months. To avoid maternal effects, CSS4 pups were fostered by C57BL/6J mothers at P0.

Phenotypic screen for FS susceptibility

Experimental FS were induced in 14-day-old mice as described previously [254]. Briefly, at P10 a temperature sensitive transponder (IPTT-300, Plexx BV, Elst, The Netherlands) was rapidly injected subcutaneously (separation time from the mother < 2 minutes). At P14, body weight was determined and mice were placed in the pre-heated cylindrical chamber for 900 seconds and exposed to a warm air stream of 50ºC ± 0.5ºC. To prevent skin burn and adverse effects on behavior, the temperature of the chamber floor was maintained at 37ºC. Core body temperature was measured by wireless readout (WRS-6007, Plexx BV) of the temperature transponder and automatically recorded by software (DASHost v1.0, Plexx BV). All experiments were video monitored by two cameras, one positioned at the side and one at the top of the cylinder. Several successive behavioral stages can be recognized: Early heat-induced hyperkinesias (stage 1); A sudden complete arrest of the heat-induced hyperkinesias followed by ataxia (stage 2); Circling, shaking of the whole body and tonic motionless postures with occasional automatisms and clonuses (stage 3); Tonic-clonic convulsions (stage 4) [254]. Latencies for these behaviors were determined by an observer throughout the 900 second trial. If a particular seizure behavior did not occur during this period, a latency value of 900 seconds was given. All experiments were performed between 10:00-15:00 hour. Time of day, date, humidity, mother/litter, room temperature and body weight of each mouse was recorded for covariate analysis.

EEG recording

To select the most reliable phenotypic parameter for FS susceptibility, we studied the relationship between epileptic activity in the brain (Electroencephalography (EEG) spike wave discharges (SWD)) and hyperthermia-induced behavior. C57BL/6J mice (n = 7) carrying a temperature sensitive transponder, were equipped with epidural EEG electrodes on P14. Electrodes were positioned in the hippocampus and the motor cortex using a stereo tactic frame. Additional electrodes were placed in the bulbus olfactorius (reference) and in the cerebellum (ground). After surgery, the pups recovered (at least 30 minutes) under a heating lamp.

Subsequently, pups were placed inside the hyperthermia cylinder, where they could freely move and phenotypically screened as described above. Cortical and hippocampal signals were fed to separate, but identical amplifiers (Bio-electrioc amplifier AB 601-G, Nihon Kohden, Tokyo, Japan), amplified 1000 times, band-pass filtered between 1.59 and 100 Hz (using an additional 50 Hz notch-filter), and digitized online at 1000 Hz by dedicated software build in house in a Labview environment (Labview 7.2, National Instruments Netherlands B.V., Woerden, The Netherlands). EEG seizures were defined as high amplitude (> 2-fold increase over baseline EEG recorded prior to HT) and high frequency (8-12 Hz) SWD that lasted at least 5 seconds [111,289]. For each animal the latency to SWD was determined and cor-

	SWD HIP (n = 7)		SWD CX (n = 7)	
	r	*P*	*r*	*P*
Immobility (n = 7)	0.049	0.918	0.081	0.863
Shaking (n = 7)	0.831	**0.021**	0.841	**0.018**
TCC (n = 7)	0.934	**0.002**	0.918	**0.004**
SWD CX (n = 7)	0.972	**0.000**	-	-

Table 1. Correlation between latencies of hyperthermia-induced behaviors and occurrence of EEG spike wave discharges (SWD). *r* denotes the Pearson product-moment correlation. $P < 0.05$ was considered significant and indicated in bold font. n represents the number of observations. HIP: hippocampus; CX: cortex; TCC: tonic-clonic convulsions.

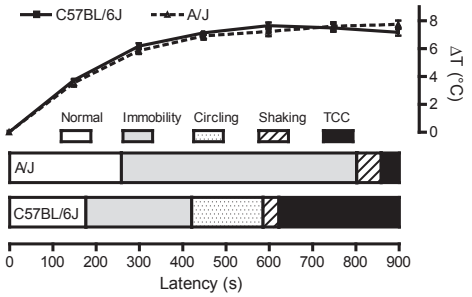

Figure 1. Graph represents the increase in mouse core body temperature from the start of the experiment (ΔT) as measured each 150 seconds during hyperthermia. Data are expressed as means ± standard error of the mean (SEM). No statistically significant differences were observed between the C57BL/6J and A/J strain (n = 10). Horizontal bars represent a schematic illustration of A/J and C57BL/6J behavior during hyperthermia. Data are expressed as stacked means. The latency for immobility in A/J was 258.18 ± 16.2 seconds and in C57BL/6J 176.2 ± 4.5 seconds (P < 0.001). A/J pups did not show any circling behavior, whereas the latency for circling in C57BL6/J was 420.5 ± 19.5 seconds. Shaking latency for the A/J pups was 801.7 ± 17.7 seconds and for the C57BL/6J 585.6 ± 12.9 seconds (P < 0.0001). The tonic-clonic convulsion (TTC) latency for C57BL/6J mice was 621.9 ± 14.1 seconds and for A/J mice 858.2 ± 17.7 seconds (P < 0.0001).

related to the latencies for the progressive hyperthermia-induced behaviors.

Statistical Analysis

The CSS panel data was analyzed by comparing CSS phenotypic latencies with C57BL/6J background strain phenotypic latencies using SPSS (v12.0.1, Chicago, IL, USA). To correct for multiple testing, phenotypic differences were only considered significant when P < 0.003 [290]. To improve statistical power, larger numbers of C57BL/6J mice (n = 66) were screened compared to each CSS (ideal ratio C57BL/6J: CSS= 4.5:1) [290]. Because hyperthermia did not induce seizure related behaviors in all animals, latencies were analysed by Cox-proportional hazard regression [288] to generate hazard ratios and P-values. The hazard ratio is the relative risk of an endpoint at any given time. In the Cox analysis, start body temperature, body weight and gender were considered covariates. Strain body weights were compared using one-way ANOVA (Dunnett post-hoc test). Pearson product-moment correlation (SPSS) was used for al correlative analyses.

RESULTS

FS susceptibility of the parental strains

A total of 66 C57BL6/J and 20 A/J mice were subjected to warm-air induced hyperthermia. No statistically significant strain differences (two-way ANOVA: F_1 = 0.35, P = 0.55) in fever induction (ΔT= core body temperature during the experiment minus start body temperature) at any time during the procedure were observed (figure 1). Latencies to immobility, circling, shaking and tonic-clonic convulsions were significantly longer in the A/J when compared to the C57BL/6J strain (figure 1). The latency for immobility was 258.2 ± 16.2 seconds in the A/J and 176.2 ± 4.5 seconds in the C57BL/6J strain (P < 0.001). A/J pups did not show circling behavior, whereas the latency for circling in C57BL6/J pups was 420.5 ± 19.5 seconds. Shaking latency was 801.7 ± 17.7 seconds for the A/J and 585.6 ± 12.9 seconds for the C57BL/6J pups (P < 0.0001). Tonic-clonic convulsion latency was 621.9 ± 14.1 seconds for C57BL/6J and 858.2 ± 17.7 seconds for A/J pups (P < 0.0001). Most A/J pups did not reach the FS seizure state with tonic-clonic convulsions within the 900 second test period. Coat color did not influence FS susceptibility [254]. No gender effects were found in either strain and at P14 the body weight of the A/J pups (7.58 ± 0.17 g) was similar to the body weight of C57BL/6J pups (7.38 ± 0.08 g, P = 0.343).

EEG recording

To determine the most reliable behavioral phenotype for FS susceptibility we performed behavioral video analyses in parallel with EEG monitoring. The SWD latencies in the cortex (CX) correlated with SWD latencies in the hippocampus (HIP) (r = 0.972, P =

Mouse strain	*n* (M:F)	P14 BW (g)	*P*-value BW	Tstart (°C)	ΔT (°C)	TCCL (seconds)	Cox HR	*P*-value TCCL
C57BL/6J	33:33	7.38 ± 0.08	NA	35.36 ± 0.09	8.37	621.87 ± 14.21	NA	NA
CSS1	6:3	7.08 ± 0.07	0.97	35.52 ± 0.09	8.24	859.40 ± 19.60	**0.21**	**0.0001**
CSS2	11:12	7.00 ± 0.12	0.21	35.93 ± 0.13	7.76	464.00 ± 16.07	**4.65**	**0.0001**
CSS3	8:7	7.44 ± 0.16	1.00	35.41 ± 0.19	8.51	607.12 ± 33.27	1.29	0.39
CSS4	7:4	7.64 ± 0.16	0.99	35.96 ± 0.12	8.12	683.67 ± 26.13	0.53	0.13
CSS5	9:9	7.25 ± 0.15	1.00	35.66 ± 0.18	7.85	617.27 ± 41.04	0.62	0.08
CSS6	9:9	7.05 ± 0.25	0.60	34.14 ± 0.67	9.49	528.83 ± 20.02	2.22	0.004
CSS7	8:9	6.99 ± 0.08	0.37	35.68 ± 0.23	8.11	531.14 ± 32.71	1.38	0.24
CSS8	9:6	7.23 ± 0.19	1.00	35.65 ± 0.18	8.50	649.08 ± 43.40	0.70	0.22
CSS9	8:9	8.10 ± 0.13	**0.0008**	35.82 ± 0.11	8.39	638.29 ± 28.28	0.58	0.89
CSS10	9:9	7.28 ± 0.15	1.00	35.93 ± 0.26	8.23	746.00 ± 43.61	**0.30**	**0.0001**
CSS11	9:9	7.01 ± 0.10	0.41	35.82 ± 0.10	8.25	628.77 ± 38.69	0.57	0.04
CSS12	9:9	6.74 ± 0.06	0.004	36.12 ± 0.18	7.61	583.33 ± 21.29	1.36	0.25
CSS13	9:9	7.92 ± 0.16	0.03	35.51 ± 0.13	8.79	813.90 ± 24.99	**0.27**	**0.0001**
CSS14	9:8	7.60 ± 0.10	0.98	± 35.64 ± 0.13	7.90	539.43 ± 26.60	1.84	0.03
CSS15	9:8	8.02 ± 0.21	0.01	36.05 ± 0.17	8.15	623.69 ± 25.33	0.97	0.91
CSS16	6:7	7.45 ± 0.26	1.00	35.84 ± 0.13	7.96	585.18 ± 49.75	0.72	0.28
CSS17	9:9	7.58 ± 0.13	0.99	35.74 ± 0.09	8.12	614.70 ± 36.74	0.72	0.23
CSS18	8:7	8.19 ± 0.16	**0.0002**	35.93 ± 0.14	7.48	588.28 ± 18.38	1.34	0.32
CSS19	9:9	7.72 ± 0.18	0.57	35.38 ± 0.20	8.74	733.17 ± 34.69	0.49	0.02
CSSX	9:9	6.78 ± 0.07	0.01	35.25 ± 0.12	8.42	477.08 ± 14.30	**4.59**	**0.0001**
CSSY	8:9	7.31 ± 0.08	1.00	35.25 ± 0.31	8.82	577.16 ± 20.52	1.42	0.21
A/J	11:9	7.58 ± 0.17	0.99	36.49 ± 0.11	7.10	858.18 ± 17.74	**0.20**	**0.0001**

Table 2. Febrile seizures susceptibility defined as tonic-clonic convulsion latency (TCCL) in the CSS panel. Data are expressed as means ± standard error of the mean (SEM). $P < 0.003$ was considered significant and indicated in bold font. *n*: number of animals; M: male; F: female; P10 BW: body weight at postnatal-day-10; P14 BW: body weight at postnatal-day-14; Tstart: body temperature at start of procedure; ΔT=Tstart – body temperature at TCCL; HR: hazard ratio; NA: not applicable.

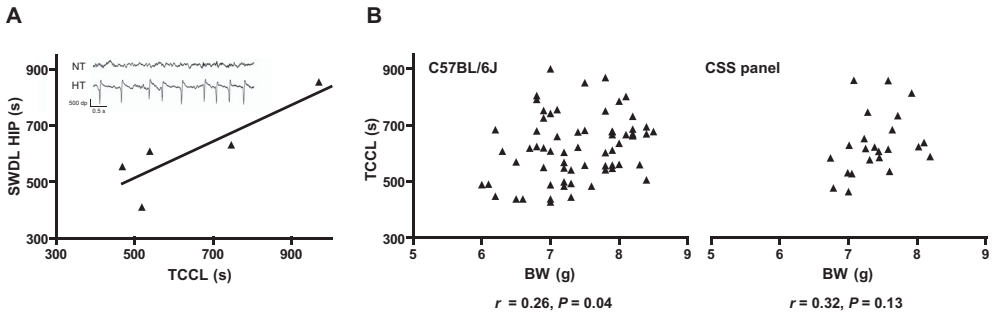

Figure 2. **A**. Correlation between tonic-clonic convulsion latencies (TCCL) and latencies for hyperthermia-induced spike wave discharges (SWD) (r = 0.918, P = 0.003). Insert shows example electroencephalography (EEG) traces of normothermia (NT) (4-8Hz) and hyperthermia (HT) induced activity (8-10Hz; SWD). **B**. Correlation between body weight (BW) and tonic-clonic convulsion latency (TCCL) in individual C57BL/6J animals (n = 66) and in the CSS panel (means per strain, including C57BL/6J and A/J). Correlation coefficients (r) and P-values are indicated below the figures.

0.000) (Table 1). SWD latencies did not correlate with immobility latency (CX: r = 0.081, P = 0.863; HIP: r = 0.049, P = 0.917) and latencies to circling behavior could not be correlated with SWD latency, because not all animals displayed this behavior (4 out of 7). Both CX and HIP SWD latencies correlated with tonic-clonic convulsion latency (CX: r = 0.918, P = 0.003; HIP: r = 0.934, P = 0.002) (figure 2A) and shaking latency (CX: r = 0.841, P = 0.018; HIP: r = 0.831, P = 0.021). Although tightly correlated, SWD discharges occurred approximately 150 seconds before behavioral tonic-clonic convulsions (figure 2A) suggesting focal onset and subsequent generalization. Shaking occurred shortly before tonic-clonic convulsions, but was difficult to detect and define, and therefore rather variable. Therefore, tonic-clonic convulsion latency (TCCL) is the most reliable and representative behavioral FS susceptibility parameter.

FS susceptibility of CSS panel

To identify chromosomes carrying genes contributing to FS susceptibility, TCCL was determined for male and female pups of all 21 CSS. To exclude environmental (season, humidity, room temperature and time of day) and animal covariates (start body temperature, body weight, gender and litter), these covariates were measured for all C57BL/6J animals. Environmental covariates and the litter covariate did not influence statistics and were excluded. The other animal covariates could not be excluded (for body weight example in the C57BL/6J strain see figure 2B), were measured for all strains and were included in the statistics as covariate. Because statistical analysis revealed no gender TCCL differences in any of the CSS, data for both genders were pooled. Five strains (CSS1, -2, -10, -13 and -X) were identified as significantly different from the host strain (C57BL/6J) (P < 0.003) (figure 3). For CSS1 (852.05 ± 19.87 seconds), -10 (746 ± 43.6 seconds) and -13 (813.9 ± 25 seconds) TCCL was significantly longer than for the C57BL/6J strain (621.9 ± 14.1 seconds). In fact, TCCL was close to that of the A/J strain (858.2 ± 17.7 seconds). CSS2 (464 ± 16.1 seconds) and -X (476.9 ± 14.7 seconds) showed a shorter TCCL than the C57BL/6J strain (621.9 ± 14.1 seconds). P14 body weight was also investigated and statistically analyzed by ANOVA ($F_{22,412}$ = 7.01, P < 0.001). CSS9 and -18 were identified as significantly heavier than the C57BL/6J strain (P < 0.003; figure 3). Table 2 summarizes all relevant data, P-values and Cox hazard ratios for the complete CSS panel compared to the C57BL/6J host strain. P-values for P14 body weight are also included.

DISCUSSION

FS represent one of the most common lesions in the etiology of TLE, but it is not clear whether susceptibility to FS and TLE share a common genetic background [87,88]. Little is known about susceptibility genes for sporadic FS, but in large families several rare susceptibility genes and QTLs have been identified [105]. To investigate genetic determinants for common FS susceptibility genes, we have developed a phenotypic screen for FS [254] that can be applied to any mouse genetic mapping strategy. Here we established by video/EEG monitoring that TCCL (tonic-clonic convulsion latency) shows a strong correlation with hippocampal spike wave discharges, and is the most reliable behavioral parameter to determine FS susceptibility. TCCL in A/J mice was considerably longer than in C57BL/6J, showing that the latter strain is much more susceptible to FS [see also 254]. We used the C57BL/6J x A/J CSS panel to sensitively identify chromosomes carrying QTLs for FS susceptibility without the interference of possible modifier genes on other chromosomes.

Chromosomes 1, 2, 10, 13 and X showed a TCCL distinct from C57BL/6J and thus carry one or more FS QTLs. We identified chromosomes carrying susceptibility QTLs as well as carrying protective QTLs. A/J genes on chromosomes 1, 10 and 13 decreased susceptibility to FS, whereas A/J genes on chromosomes 2 and X increased susceptibility to FS. Surprisingly, CSS2 and -X strains were more susceptible than the C57BL/6J strain. The identification of five chromosomes carrying at least 5 FS QTLs confirms the hypothesis that FS is a multigenetic syndrome [167,254], in which multiple genes contribute to the FS susceptibility and may interact to determine the ultimate phenotype. After the *P*-value cutoff was corrected for multiple testing ($P < 0.003$) the TCCL of CSS6 was not significantly shorter than C57BL/6J ($P < 0.004$). CSS6 should be considered as a strongly suggestive FS QTL. We propose to designate the FS QTLs on chromosome 1, 2, 6, 10, 13 and X with locus symbols FSS1-6 (Febrile Seizure Susceptibility 1-6). Detailed data were collected from pups of all CSS strains to allow for covariate analysis and to detect potential confounding factors. Maternal care, and subsequent body weight was identified as confounding factor in the CSS4. Therefore, CSS4 pups were fostered by C57BL/6J mothers. In the statistical TCCL

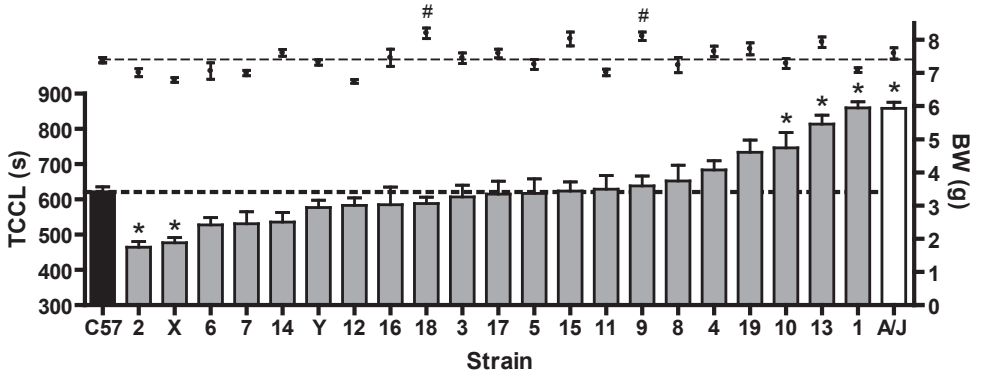

Figure 3. Tonic-clonic convulsion latency (TCCL; bars, left axis) and body weights (BW; dots, right axis) for the C57BL/6J (C57), A/J and each CSS (1-19, X, Y). Founder strains are graphed on the outsides of the graph and CSS were ordered by TCCL. CSS1, -2, -10, -13 and -X were identified as CSS that carry a FS susceptibility QTL. CSS9, and -18 were significantly heavier at P14 than C57BL/6J. Data are expressed as means ± standard error of the mean (SEM). $^{*\#}P < 0.003$ was considered significant. Mean TCCL and BW of the C57BL/6J strain are represented by bold and plain dashed lines respectively.

analysis, body weight, start body temperature and gender (not always a 1:1 gender distribution) were considered covariates. Other potential confounding factors (season, time of day, litter) were excluded by covariate analysis. It is unlikely that CSS strains differ in postnatal development, because all mice screened at P14 had open eyes and showed normal P14 exploratory behavior. Moreover, comparing behavioral data at P10 and P14 from A/J and C57BL/6J showed a constant phenotype [254], suggesting that developmental differences between strains did not influence FS susceptibility.

Several FS genes have been identified in human familial FS syndromes. These include genes coding for ion-channels like *SCN1A*, *SCN2A* and *SCN1B*, but also for non-ion channels like *GPR98* and *IL1B* (summarized in table 3). Several of these genes map to mouse syntenic regions identified in our screen. Although the mice used in our screen do not display spontaneous seizures and hardly develop epilepsy, it is possible that variations in genes previously identified in human FS also contribute to FS susceptibility in mice and in the general human population. Possibly, gene variations that only slightly affect gene function, could increase seizure susceptibility without causing unprovoked seizures and epilepsy.

Our data show that mouse chromosome 2 carries a strong FS QTL. Gene(s) on donor A/J strain chromosome 2 increase the FS susceptibility of the host C57BL/6J strain. Several of the FS genes identified by human linkage and association studies can be found on mouse chromosome 2 (*SCN1A*, *SCN2A*, *CHRNA4* and *IL1B*; table 3). The *Il1b* gene is a strong candidate, because the IL1β pathway has been implicated in the susceptibility to FS. Nul-mutants for the IL1β-receptor (*Il1r1*$^{-/-}$) showed delayed FS and high doses of IL1β induced convulsions in immature mice [116]. Chromosome X also carries a QTL, increasing FS susceptibility. Syntenic human region Xq22 was recently linked to epilepsy and mental retardation in females [291]. Although these patients did not show classic FS, they did have seizures associated with fever during childhood.

Chromosome 13, carrying a protective QTL for FS, harbors *Gpr98*, a gene implicated in a mouse model for audiogenic seizures. In the Frings mouse a spontaneous occurring mutation in the *Gpr98* (also called *Mass1* or *VLGR1*) was identified [124] and led the way to identification of this gene in human familial FS (FEB4 locus) [37]. Chromosomes 1 and 10 were also identified to carry protective QTLs. Part of the mouse syntenic region for the human FEB1 locus (8q13-21) resides on mouse chromosome 1 [94]. The causative gene in the FEB1 locus is unknown as yet. Possibly fine-mapping of the QTL on chromosome 1 may lead the way to identification of the FEB1 gene. Recently, we have identified *Glul* (involved in glutamatergic neurotransmission) as a FS susceptibility gene in a reverse genetics approach [chapter 8]. *Glul* is also located on chromosome 1 and could be a candidate for the QTL on chromosome 1.

Seizure susceptibility mapping studies in mice have been performed for almost 20 years now, but CSS have been used only once so far. Winawer and colleagues [288] screened seizure susceptibility in the CSS panel by using the chemoconvulsant pilocarpine. They identified chromosomes 10 and 18 as susceptibility QTLs. In this and other chemically-induced seizure models [128,292], the A/J strain was more susceptible to seizures when compared to the C57BL/6J strain. Studies using other chemically- or electrically-induced seizure models to compare the C57BL/6J strain to other strains (eg. DBA/2J), also showed that the C57BL/6J strain is relative resistant to seizures and seizure-induced cell death [128,237-240]. In contrast, the C57BL/6J strain is one of the most FS susceptible strains [this study and 254]. This difference in susceptibility to FS and electrically- or chemi-

cally-induced seizures indicates that distinct mechanisms are involved in these distinct seizure types. This is further corroborated by the fact that the only chromosome carrying a QTL for FS and pilocarpine-induced seizures (chromosome 10), carries a protective QTL for FS, but a susceptibility QTL for pilocarpine-induced seizures [288]. Another major difference between the two types of seizure studies is the age at seizure induction. FS are induced in 14-days-old pups, whereas the chemically-induced seizures are induced in adult mice. Regulation of excitability and neuronal network stability in the developing brain may differ considerably from the mature brain, as evident from the narrow developmental time-window in which FS occur in children. In this respect, *Csnk1g2* is an interesting candidate gene mapping to mouse chromosome 10. *CSNK1G2* has also been associated with human FS and has been implicated in development and synaptic transmission [81]. Moreover, the *Csnk1g2* gene is only 2 Mbp removed from the LOD-score peak marker for the epilepsy locus El3, which was identified in EL-mice [293] and the gene in C57BL/6J (the more FS susceptible one) carries a missense mutation (Trp>Arg;rs46447802), which is not present in A/J.

This study describes the first step in identifying FS susceptibility genes in a forward genetics approach. Five QTLs of A/J strain origin influencing FS susceptibility in the C57BL/6J strain were identified. Three chromosomes (1, 10 and 13) carry FS protective QTLs, and two chromosomes (2 and X) carry FS susceptibility QTLs. The identification of both decreasing and increasing FS susceptibility loci

Gene	Description	Human Region	Mouse Chr	Epilepsy Type	References
Linkage studies					
SCN1A	Voltage-gated sodium channel type 1, alpha subunit	2q24	2	FEB3, SMEI, GEFS+2	[17-19]
SCN1B	Voltage-gated sodium channel type 1, beta subunit	19q13.1	7	GEFS+1, FS	[20,21]
SCN2A	Voltage-gated sodium channel type 2, alpha subunit	2q24	2	GEFS+	[22]
GABRD	Gamma-aminobutyric-acid A receptor, delta subunit	1p36.3	4	GEFS+5	[26]
GABRG2	Gamma-aminobutyric-acid receptor, gamma-2 subunit	5q34	11	GEFS+3, SMEI, FEB8	[27,28,30]
CACNA1H	Voltage-gated calcium channel T-type, alpha-1H subunit	16p13.3	17	FS, TLE	[34]
Gpr98	Very large G-protein couples receptor 1	5q14	13	FEB4	[37]
Association studies					**Positive / Negative**
GABRG2	Gamma-aminobutyric-acid receptor, gamma-2 subunit	5q34	11	FS	[77,78] / [60]
CHRNA4	Neuronal acetylcholine receptor protein, alpha-4 subunit	20q13.3	2	FS	[79] / [60,80]
CSNK1G2	Casein kinase I gamma 2 isoform	19p13.3	10	FS	[81] /
IMPA2	Myo-inositol monophosphatase 2	18p11.2	18	FS	[82] /
IL1B	Interleukin 1 beta	2q14	2	FS	[54,83] / [52,60,84]

Table 3. Genes associated with FS epilepsy syndromes. Genes indicated in bold are located on one of the mouse chromosomes identified for FS susceptibility. Chr: chromosome; FEB: familial febrile seizures; SMEI: severe myoclonic epilepsy in infancy; GEFS+: generalized epilepsy with febrile seizures +; FS: febrile seizures.

shows the power of genetic mapping in the CSS panel. It is likely that in classic genetic mapping approaches these opposing effect loci would have hampered identification. Syntenic human-mouse regions and data from various other studies pinpoint *Gpr98*, *Scn1a*, *Scn2a*, *Chrna4*, *Il1b*, *Csnk1g2* and *Glul* as FS susceptibility gene candidates in mice. Fine-mapping QTLs (backcross of CSS x C57BL/6J followed by an F1-generation intercross) will be the next step toward identifying candidate genes contributing to the regulation of mouse FS susceptibility, and could lead the way to understanding the mechanisms involved in human FS.

ACKNOWLEDGEMENTS

This study was sponsored by the Epilepsy fund of The Netherlands (grant 06-09 and 03-12) and by the EPOCH Foundation (Focal Epilepsies of Childhood). We would like to thank Hugo Oppelaar for providing mouse breeding pairs.

CHAPTER 8

Haploinsufficiency of glutamine synthetase increases susceptibility to experimental febrile seizures

Koen L.I. van Gassen[1], W. Saskia van der Hel[1], Theo B.M. Hakvoort[2], Wout H. Lamers[2], Pierre N.E. de Graan[1]

[1]Rudolf Magnus Institute of Neuroscience, Department of Neuroscience and Pharmacology, University Medical Center Utrecht, Utrecht, The Netherlands
[2]AMC Liver Center, Academic Medical Center, University of Amsterdam, Amsterdam, The Netherlands.

Under review

ABSTRACT

Glutamine synthetase (GS) is a pivotal glial enzyme in the glutamate-glutamine cycle. GS is important in maintaining low extracellular glutamate concentrations and is down-regulated in the hippocampus of temporal lobe epilepsy patients with mesial-temporal sclerosis, an epilepsy syndrome which is frequently associated with early life febrile seizures (FS). Human congenital loss of GS activity has been shown to result in brain malformations, seizures and death within a few days after birth. Recently, we showed that GS knockout mice die during embryonic development and that haploinsufficient GS mice have no obvious abnormalities or behavioral seizures. In the present study we investigated whether reduced expression/activity of GS in haploinsufficient GS mice increased the susceptibility to experimentally induced FS. FS were elicited by warm-air induced hyperthermia in 14-day-old mice and resulted in seizures in most animals. FS susceptibility was measured as latencies to four behavioral FS characteristics. Our phenotypic data shows that haploinsufficient mice are more susceptible to experimentally induced FS ($P < 0.005$) than littermate controls. Haploinsufficient animals did not differ from controls in hippocampal amino-acid content, structure (Nissl and calbindin), glial properties (GFAP and vimentin) or expression of other components of the glutamate-glutamine cycle (EAAT2 and VGLUT1). Thus, we identified GS as a FS susceptibility gene. GS activity disrupting mutations have been described in the human population, but heterozygote mutations were not clearly associated with seizures or epilepsy. Our results indicate that individuals with reduced GS activity may have reduced FS seizure thresholds. Genetic association studies will be required to test this hypothesis.

INTRODUCTION

Glutamate, the major excitatory neurotransmitter, is released by neurons during synaptic activity and is toxic at sustained high levels [285]. Released glutamate is normally taken up by glial cells and converted into glutamine by glutamine synthetase (GS; EC 6.3.1.2). The nontoxic glutamine is then transported back into neurons, which can reconvert glutamine to glutamate.

The rate of this process, known as the glutamate-glutamine cycle, was found to be decreased in the hippocampus of temporal lobe epilepsy (TLE) patients with hippocampal sclerosis (HS) [287]. The reduced rate of this cycle could in part be explained by decreased expression and enzyme activity of GS in the hippocampus of TLE patients with HS [271,286]. However, other components of this cycle have also been implicated. For instance the glutamate-synthesizing enzyme, phosphate-activated glutaminase, was upregulated in remaining neurons of the hippocampus of TLE patients with HS [294] and altered sub-regional expression of the major glial glutamate transporter, excitatory amino acid transporter-2 (EAAT2), has also been reported [271,295,296]. A role for GS in epilepsy is also indicated by studies in genetically epilepsy-prone animal showing reduced GS brain expression [297,298], by a gene expression-phenotype correlation study showing a strong correlation between expression of GS and electroconvulsive threshold [299], and by the finding that pharmacological inhibition of GS activity induces seizures [300].

The glutamate-glutamine cycle has also been implicated in the generation of febrile seizures (FS) [301,302]. Up to 50% of the TLE patients with HS suffered from FS during childhood [11]. Although the relationship between FS and TLE is not clear, it seems that impairments in components of the glutamate-glutamine cycle may contribute to the development of FS and TLE with HS.

In this study we tested the hypothesis that a reduction in GS expression increases the susceptibility for FS. We used mice in which only one GS allele was inactivated. These mice have a 50% reduction in GS expression and no apparent phenotype. We recently showed that a complete knockdown of GS in mice results in early embryonic lethality [303]. FS susceptibility in haploinsufficient mice was tested in a model for experimental FS [254].

MATERIAL AND METHODS

Animals

Mice were kept in a controlled 12 hour light-dark cycle with a temperature of 22 ± 1ºC and were given unrestricted access to food (2111 RMH-TM diet; Hope Farms, Woerden, The Netherlands) and water. All mice were housed in transparent Plexiglas cages with wood-chip bedding and tissue for nest building. Time of birth was recorded daily. All experiments conformed to institutional guidelines of the University Medical Center Utrecht.

Generation of $GS^{+/+}$ and $GS^{+/LacZ}$ mice

The mouse GS gene (*Glul*) was disrupted by homologous recombination, replacing exon II-VII with a β-galactosidase (LacZ)/neomycin phosphotransferase (NEO) fusion gene [303]. Because complete GS knockout animals were embryonically lethal, $GS^{+/LacZ}$ mice (on the FVB background) were generated. $GS^{+/+}$ and $GS^{+/LacZ}$ mice were bred from FVB (female) and $GS^{+/LacZ}$ (male) mice. $GS^{+/LacZ}$ mice were indistinguishable from there $GS^{+/+}$ litter mates. Both sexes were used for the experiments and animals were genotyped as described [303]. Throughout the experiments the researcher was unaware of the genotype of the animals.

FS susceptibility screen

FS susceptibility was tested as previously de-

scribed [254]. In short, ten-day-old animals were injected subcutaneously with a temperature sensitive transponder (IPTT-300, Plexx) and returned to their mother within two minutes. Four days later, these animals were placed in the heat chamber. Core body temperature was quickly raised using heated air and animal behavior was recorded by an overhead camera. Several successive behavioral stages can be recognized: Early heat-induced hyperkinesias (stage 1); A sudden complete arrest of the heat-induced hyperkinesias followed by ataxia (stage 2); Circling, shaking of whole body and tonic motionless postures with occasional automatisms and clonuses (stage 3); Tonic-clonic convulsions (stage 4). Latencies until immobility (stage 2), circling (stage 3), whole body shaking (stage 3) and tonic-clonic convulsions (stage 4) were recorded by the observer as a measure for FS susceptibility. The experiment was terminated after the animals had reached stage 4 seizures or after a maximum of 25 minutes. For animals not reaching the subsequent behavioral stage, the maximal latency of 1500 seconds was scored.

Hippocampal homogenates

Mice (14-days-old) were decapitated and brains were quickly dissected, collected in ice-cold sterile physiological salt and placed on an ice-cold cutting surface. Brains were cut in left and right hemispheres and hippocampi were dissected *en bloc*. Left and right hippocampi were separately collected in pre-cooled vials, snap-frozen on dry-ice and stored at -80°C until further use.

GS enzyme activity

GS enzyme activity was measured as previously described [271]. Left hippocampi of 14-day-old $GS^{+/+}$ and $GS^{+/LacZ}$ mice (all from one litter), were homogenized in 10 volumes of lysis buffer (100 mM Tris–HCl, 1 mM EGTA, 1 mM EDTA, complete protease inhibitor (Roche). Protein content was determined with the BCA Protein Assay Kit (Pierce, Rockford, IL). GS enzyme activity was determined using a standard curve with predetermined amounts of glutamyl-τ-hydroxamate (GMH) and expressed as nmol/min.mg protein. Enzyme activity increased linear with time and protein concentration under the assay conditions used. One freeze-thaw cycle did not affect GS activity levels.

GS protein expression

GS protein expression was measured by immunoblotting [271] in the same hippocamapal homogenates as used for GS activity measurements. Proteins were separated by sodium dodecyl sulphate–polyacrylamide gel (12%) electrophoresis and transferred to a PVDF membrane (Amersham). Non-specific binding of immunoglobulins was blocked for one hour at room temperature in Tris-buffered saline with 0.1% Tween (TBS-T; pH=7.4) containing 5% nonfat dry milk. After washing with TBS-T, blots were incubated for 16 hours at 4°C with mouse monoclonal anti-GS (clone 6; BD Biosciences, Erembodegem, Belgium; diluted 1:1,000 in TBS-T). Next blots were washed in TBS-T and incubated with alkaline phosphatase-conjugated goat anti-mouse (diluted 1:5,000; Promega Corporation, Madison, WI) second layer antisera for one hour at room temperature. Finally, membranes were washed, developed with enhanced chemofluorescence substrate (Supersignal; Pierce) and exposed to ECL film (Pierce). Antibody specificity was checked by preadsorption of the antiserum with the immunizing peptide. Antiserum samples without peptide were run in parallel. Control experiments without the primary antibody did not reveal any staining (data not shown). Films were scanned on a flatbed scanner in transmission mode and quantified by optical density (OD) measurement with the software package Image J (v1.38).

Hippocampal amino-acid concentrations
20-50 mg of hippocampal tissue, collected from the right hemispheres of 14-day-old $GS^{+/+}$ and $GS^{+/LacZ}$ mice, was added to 250 μl sulphosalicylic acid solution (2.5%), containing 100 mg glass beads. Tissue was homogenized by vortexing for 30 seconds at 4°C, centrifuged, and supernatants were stored at -80°C. Supernatants were used for amino-acid analysis using a gradient reversed-phase HPLC system with precolumn derivatization with o-phtalaldehyde (Pierce) and 3-mercaptopropionic acid (Sigma), and fluorescence detection. An Omnisphere 3 C18 column (Varian, Middelburg, The Netherlands) was used for separation.

Immunohistochemistry
Brains of 14-day-old $GS^{+/+}$ (n = 4) and $GS^{+/LacZ}$ (n = 6) mice were removed and fixed overnight in 4% formaldehyde in phosphate buffered saline (PBS; pH 7.4). Coronal paraffin sections (7 μm) were cut and general histology was assessed by cresyl-violet (Nissl) staining. Immunostaining was performed with commercially available antibodies for rabbit-anti-calbindin (1:500; Chemicon Int. Inc. Temecula, CA, USA), mouse-anti-vimentin (1:400; DakoCytomation, Glostrup, Denmark), guinea pig-anti-excitatory amino acid transporter-2 (EAAT2) (1:1,000; Chemicon Int. Inc. Temecula, CA, USA), or rabbit antiserum for glial fibrillary acidic protein (GFAP) (1:12,800; Dako) and vesicular glutamate transporter-1 (VGLUT1) (1:16,000; Synaptic Systems, Göttingen, Germany) using the avidin-biotin detection system (Vectastain Elite ABC Kit; Vector Laboratories, Burlingame, CA) with 3,3'-diaminobenzidine tetrahydrochloride (DAB; Sigma Chemical Co., St. Louis, MO, USA) as chromogen [271]. Each slide contained three adjacent sections. Vimentin and GFAP, as well as calbindin, EAAT2, and VGLUT1 stainings were performed on the same slide. Optimal antibody concentrations were determined with serial dilutions on control mouse brain sections. All sections were subjected to microwave treatment (7 minutes 650W, 5 minutes 350W) for antigen retrieval. Sections were preincubated with 3% normal horse serum (vimentin), 3% fetal calf serum (GFAP) or 3% normal goat serum (calbindin, EAAT2, VGLUT1) to block non-specific binding of immunoglobulins. Biotinylated horse-anti-mouse (1:200) and horse-anti-goat (1:250) serum was obtained from Brunschwig Chemie (Amsterdam, The Netherlands), goat-anti-guinea pig (1:500) from Jackson Laboratories (Inc, Cambridgeshire, UK), and goat-anti-rabbit (1:250) from Dako. Control experiments without the primary antibodies did not reveal any staining (not shown).

Statistical analysis
For expression analysis we used the two-sided Students t-test. The Cox proportional hazard regression was used for statistical analysis in the phenotypic screen, because we measured latencies and not all the animals reached each seizure stage [254]. We

	$GS^{+/+}$ (n = 13)	$GS^{+/LacZ}$ (n = 10)		
	Mean	Mean	Cox HR	P-value
Immobility (seconds)	178 ± 13	199 ± 15	0.78	0.58
Shaking (seconds)	1076 ± 67	794 ± 48	3.80	0.005
Circling (seconds)	1168 ± 110	490 ± 65	9.46	<0.0001
Tonic-clonic convulsions (seconds)	1368 ± 53	999 ± 82	4.51	0.005
Body Weight (g)	7.1 ± 0.3	7.1 ± 0.3	NA	0.96

Table 1. Phenotypic characterization of FS susceptibility in $GS^{+/+}$ and $GS^{+/LacZ}$ mice. Values of behavioral parameters represent average latencies (seconds) recorded during a 25-minute period of hyperthermia at P14. If a particular seizure behavior did not occur during this period, a latency value of 1500 seconds was given. FS phenotype latencies, Cox proportional hazard ratios (HR) and significances for latencies are listed. Data are expressed as means ± SEM. $P < 0.05$ was considered significant. NA: not applicable.

generated *P*-values and Cox hazard ratios. $P < 0.05$ was considered significant. All data are expressed as means ± standard error of the mean (SEM).

RESULTS

Febrile seizure susceptibility in $GS^{+/+}$ and $GS^{+/LacZ}$ mice

To investigate effects of reduction of GS expression on FS susceptibility normal $GS^{+/+}$ (n = 13) and $GS^{+/LacZ}$ (n = 10) mice were subjected to hyperthermia. Latencies to immobility (stage 2), circling (stage 3), whole body shaking (stage 3) and tonic-clonic convulsions (stage 4) were measured. All mice showed immobility (stage 2). Circling was recorded in all $GS^{+/LacZ}$ mice, but only in seven out of 13 $GS^{+/+}$ mice. Whole body shaking was recorded in all mice, except for one $GS^{+/+}$ mouse. Nine out of ten $GS^{+/LacZ}$ mice showed tonic-clonic convulsions, compared to only seven out of 13 $GS^{+/+}$ mice. Average latencies are summarized in table 1 and figure 1. $GS^{+/LacZ}$ mice reached stage 3 and 4 seizures (shaking, circling and tonic-clonic convulsions) significantly earlier than $GS^{+/+}$ mice. Especially for circling the decreased latency was remarkable (2.4x earlier). Immobility latency was not different between $GS^{+/+}$ and $GS^{+/LacZ}$ mice (figure 1). None of the $GS^{+/+}$ or $GS^{+/LacZ}$ mice showed unprovoked seizure related behavior.

GS enzyme activity and protein expression

To verify the 50% knockdown of GS we measured enzyme activity and expression in hippocampal homogenates of 14-day-old $GS^{+/+}$ (n = 8) and $GS^{+/LacZ}$ (n = 4) mice (figure 2). $GS^{+/LacZ}$ mice showed a 50% decrease in both GS activity (51.8 ± 2.5%; $P < 0.00001$) and protein expression (45.5 ± 7.4%; $P < 0.0001$) compared to $GS^{+/+}$ mice.

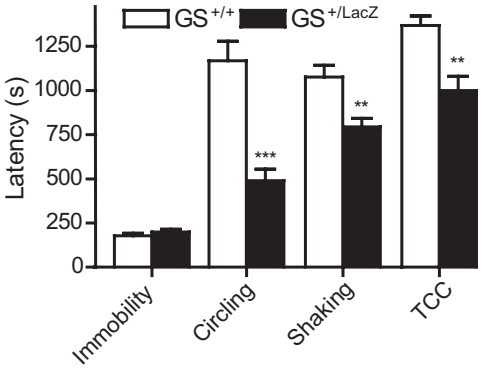

Figure 1. Phenotypic characterization of FS susceptibility in $GS^{+/+}$ and $GS^{+/LacZ}$ mice. Latency values including detailed statistics are also listed in table 1. $GS^{+/LacZ}$ animals were much more susceptible to the circling, shaking and tonic-clonic convulsion (TCC) FS phenotypes. Data are expressed as means ± SEM. $^{**}P < 0.01$, $^{***}P < 0.001$.

Hippocampal amino-acid composition of $GS^{+/+}$ and $GS^{+/LacZ}$ mice

To investigate possible alterations in amino-acid composition due to the reduced expression of GS, amino-acid concentrations were determined in the hippocampus of 14-day-old $GS^{+/+}$ (n = 8) and $GS^{+/LacZ}$ (n = 4) mice (table 2). In $GS^{+/LacZ}$ mice alanine levels appeared to be slightly increased, however, this was not significant. Levels of glutamate and glutamine were normal in $GS^{+/LacZ}$ mice.

Immunohistochemical analysis of hippocampi of $GS^{+/+}$ and $GS^{+/LacZ}$ mice

To investigated whether a 50% reduction of GS results in alterations of hippocampal structure, glial composition or expression of components of the glutamate-glutamine cycle, we analyzed Nissl, calbindin, GFAP, vimentin, EAAT2 and VGLUT1 staining on hippocampal sections of 14-day-old $GS^{+/LacZ}$ and $GS^{+/+}$ mice. Nissl (figure 3A, B) and calbindin (figure 3C, D) stains did not reveal structural abnormalities in the hippocampus of $GS^{+/LacZ}$ mice compared to $GS^{+/+}$ mice. Nissl staining showed normal neuronal cell layer structure and neuronal cell numbers. Calbindin staining revealed no changes in the granule cell layer and mossy fibers in the hilus and den-

Amino acid	$GS^{+/+}$ (n = 8) Mean	$GS^{+/LacZ}$ (n = 4) Mean	Uncorrected P-value	Bonferroni –corrected P-value
ALA	717 ± 22	814 ± 25	0.02	0.48
ARG	267 ± 21	229 ± 9	0.24	1.00
ASN	133 ± 26	103 ± 5	0.44	1.00
ASP	2145 ± 87	2124 ± 112	0.89	1.00
CIT	85 ± 18	74 ± 18	0.70	1.00
GLN	2861 ± 91	2710 ± 75	0.31	1.00
GLU	7618 ± 285	8450 ± 268	0.09	1.00
GLY	354 ± 34	354 ± 23	0.99	1.00
HIS	154 ± 10	152 ± 8	0.92	1.00
ILE	60 ± 18	33 ± 1	0.33	1.00
IS	1406 ± 32	1407 ± 27	0.98	1.00
LEU	129 ± 39	53 ± 17	0.22	1.00
LYS	873 ± 38	857 ± 52	0.80	1.00
MET	118 ± 21	103 ± 3	0.63	1.00
PHE	112 ± 16	82 ± 3	0.24	1.00
SER	1113 ± 39	1221 ± 50	0.13	1.00
TAU	14443 ± 395	14556 ± 987	0.90	1.00
THR	412 ± 31	380 ± 23	0.52	1.00
TYR	283 ± 23	258 ± 14	0.48	1.00
VAL	160 ± 22	123 ± 4	0.26	1.00

Table 2. Hippocampal amino acid composition in $GS^{+/+}$ and $GS^{+/LacZ}$ animals. No amino-acid differences were identified. Data are expressed as means ± standard error of the mean (SEM). P-values were corrected for multiple testing.

tate gyrus [304]. To investigate the effect of down-regulation of glial GS on glial cells and reactive glia, we analyzed distribution of the glial marker GFAP and of intermediate filament vimentin, as a marker for reactive gliosis [270]. GFAP immunostaining (figure 3E, F) showed no differences between animal groups. Vimentin immunostaining (figure 3G, H) was only detected in the wall of blood vessels of both animal groups, but no reactive glia were seen in response to reduced expression of GS. The distribution of hippocampal EAAT2 (figure 3I, J), the principal glial glutamate transporter, and VGLUT1 (figure 3K, L), the presynaptic vesicular glutamate transporter did not differ between the two animal groups, showing that other main glial and neuronal components of the glutamate-glutamine cycle are not affected by GS down-regulation.

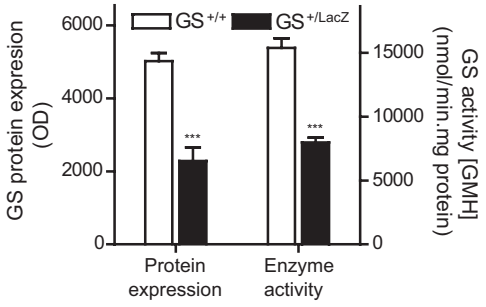

Figure 2. Hippocampal GS protein content and enzyme activity in $GS^{+/+}$ and $GS^{+/LacZ}$ mice. GS protein content and enzyme activity in $GS^{+/LacZ}$ mice were approximately 50% of that in $GS^{+/+}$ mice. Data are expressed as means ± SEM. ***P < 0.001. OD: optical density, GMH: glutamyl-τ-hydroxamate.

DISCUSSION

In this study we show that a partial knock-down of GS, a pivotal glial enzyme in the glutamate-glutamine cycle, increases the susceptibility to experimental prolonged FS. Disruption of one of the GS alleles resulted in a near perfect gene-dosage effect on GS protein expression and enzyme activity in the hippocampus, indicating there was no compensation of GS expression. Reduced expression of GS had no marked effect on hippocampal morphology, or on the expres-

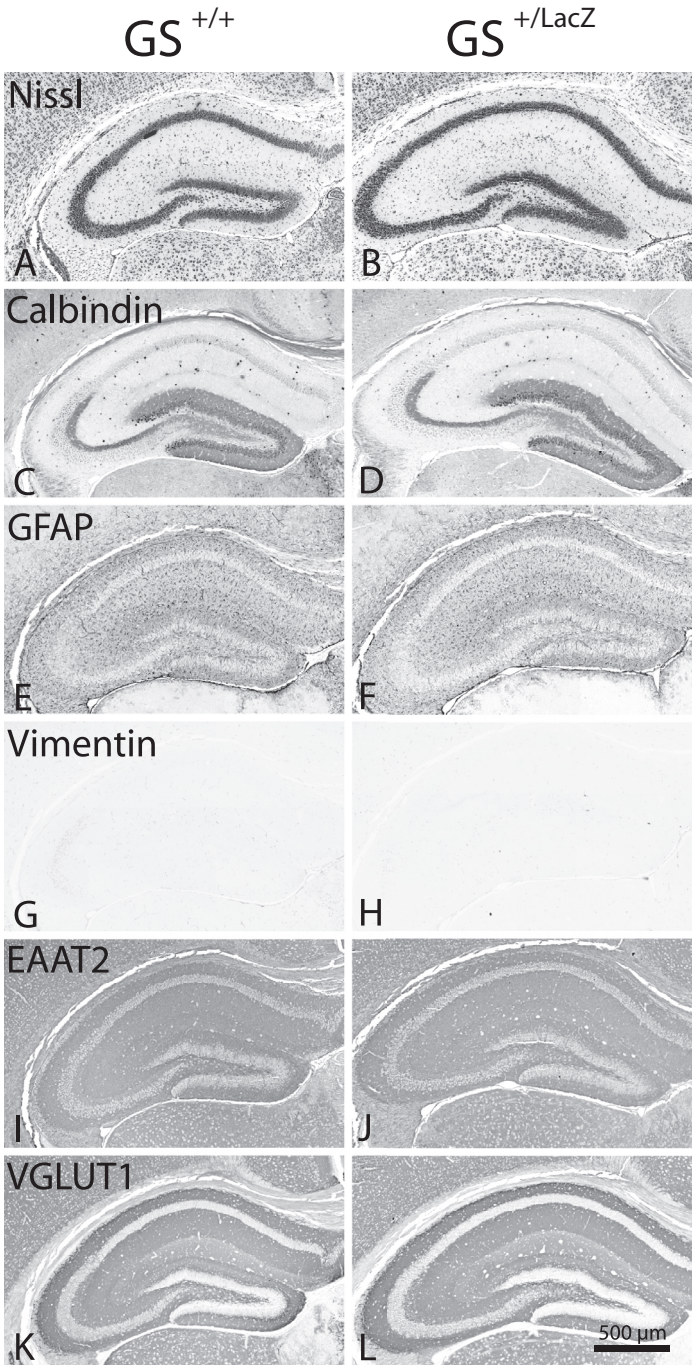

Figure 3. Hippocampal sections showing typical examples of Nissl (A, B), calbindin (C, D), GFAP (E, F), vimentin (G, H), EAAT2 (I, J), and VGLUT1 (K, L) immunostaining in $GS^{+/+}$ (A, C, E, G, I and K) and $GS^{+/LacZ}$ animals (B, D, F, H, J and L). None of these immunostainings showed a difference between $GS^{+/+}$ and $GS^{+/LacZ}$ mice.

sion of other components of the glutamate-glutamine cycle. Apparently, the reduction in GS activity does not induce compensatory mechanisms detectable by expression analysis. Reduced GS expression does not influence hippocampal amino-acid composition either. Although our data do not show general compensatory mechanisms, of course local synaptic changes are likely to occur in response to reduction GS levels, for instance in the regulation of glutamatergic and/or GABAergic transmission. Physiological experiments in hippocampal slices will be required to address this issue.

Phenotypic analysis revealed that mice with reduced GS expression are more susceptible to warm-air induced experimental FS (figure 1) than control littermates. These observations show that under baseline conditions a 50% reduction in GS expression does not result in spontaneous seizure activity, whereas under hyperthermia conditions seizures are more readily provoked. Possibly the reduction in GS enzyme capacity cannot cope with increased levels of extracellular glutamate induced by hyperthermia, thereby accelerating and aggravating seizures.

These results show the importance of GS and the glutamate-glutamine cycle in the control of FS. A recent gene expression-phenotype correlative study showed a strong correlation between GS expression and electroconvulsive threshold [299]. Moreover, the GS gene (*Glul*) is located in the QTL, SZS1, identified for electroconvulsive threshold [127]. Another key component of the glutamate-glutamine cycle, the principal glial glutamate transporter EAAT2, has also been implicated in seizure control. EAAT2 nul-mutants developed spontaneous seizures and showed exacerbation of brain injury [305]. A correlation between EAAT2 expression and electroconvulsive threshold was also identified [299], suggesting a more general impairment of the glutamate-glutamine cycle in susceptibility to electroconvulsive shock. Interestingly, the EAAT2 (*Slc1a2*) gene is located in one of the loci (EL2) responsible for epilepsy in the EL-mouse [126,306]. Thus, our data, showing a direct relationship between GS expression and febrile seizure susceptibility, are in line with several other studies implicating GS and other components of the glutamate-glutamine cycle in the control of other types of seizures. Additionally, alterations in GS as well as EAAT2 expression have been implicated in the pathology of TLE [271,286,296].

Recently, two unrelated consanguine human neonates with congenital loss of GS activity were identified [307]. These patients had extensive brain malformations, seizures and multiorgan failure and died within a few days after birth. Nonsynonymous mutations in the GS gene (*Glul*) were identified in highly conserved regions. Detailed analysis showed that in one patient only 12% GS activity was remained and that this was only achieved after robust up-regulation of mutant GS protein. Both parents, heterozygous for the mutation, also had reduced GS activity, but were unaffected. Although unaffected, these families have not been investigated in detail for epilepsy symptoms (no MRI, EEG). It is possible that *Glul* mutation carriers, especially in the light of our results, are more susceptible to seizures and possibly predispose to epilepsy. Currently, we are studying blood GS levels in epilepsy patients and controls to determine if GS expression and activity predisposes for epilepsy. Association studies will be required to investigate whether gene variation in GS and other components of the glutamate-glutamine cycle are associated with epilepsy and FS.

ACKNOWLEDGEMENTS

This study was sponsored by the Epilepsy Fund of The Netherlands (grant 03-12) and by the EPOCH Foundation (Focal Epilepsies of Childhood).

CHAPTER 9

Summary and General Discussion

INTRODUCTION

Epilepsy is a neurological disorder that is characterized by recurrent seizures and affects about 1% of the population worldwide [2]. Epilepsy can occur because of a genetic predisposition, because of acquired factors or because of a combination between the two (multifactorial). Temporal lobe epilepsy (TLE) is considered to be the most common partial epilepsy type with extensive etiological heterogeneity. Most cases probably can be classified as mulitfactorial. Although much progress has been made about the understanding of TLE, the molecular mechanisms involved in the etiology and neuropathology of TLE remain poorly understood [163,165]. Febrile seizures (FS) are the most common initial precipitating event in mesial TLE (MTLE), but it is unclear whether FS themselves contribute to the development of MTLE, or whether a prenatal lesion, brain insult or a genetic predisposition is causal to both FS and MTLE [87,88]. The overall aim of this thesis was to identify key genes, proteins and processes involved in MTLE, FS and epileptogenesis. This was investigated by detailed molecular characterization of MTLE in human epileptic tissue, by molecular characterization of prolonged experimental FS in mice and by identifying genetic determinants of FS susceptibility.

We demonstrate that the innate immune system plays an important role in human MTLE **(chapter 2)** and that an acquired $Na_v\beta3$ channelopathy had developed in a subset of human MTLE patients **(chapter 2-3)**. Chemokines were identified as highly regulated in human MTLE **(chapter 2)**, and therefore the effects of these chemokines on hippocampal neurons were investigated. We showed that the chemokine CCL3 can alter neuronal activity and calcium dynamics in cultured hippocampal neurons by increasing NMDA receptor levels **(chapter 4)**. To investigate the longitudinal effects of FS and to identify FS susceptibility genes we developed and validated two FS models in mice. We also showed that mouse FS susceptibility is influenced by a complex genetic background **(chapter 5)**. Longitudinal effects of FS in the hippocampus were investigated using microarrays, which showed us that prolonged FS acutely induce transcriptional and heat-shock responses, and on the more long-term induce network reorganizations and reduced expression of *Camk2a* **(chapter 6)**. FS susceptibility was investigated in more detail using a chromosome substitution mouse panel. We identified FS susceptibility loci on chromosomes 1, 2, 10, 13 and X **(chapter 7)**. Using mice haploinsufficient for glutamine synthetase (*Glul* or GS), we characterized *Glul* as a major FS susceptibility gene **(chapter 8)**. In the next sections results presented in this thesis are discussed in the context of MTLE, FS and epileptogenesis.

IMMUNITY IN MTLE, FS AND EPILEPTOGENESIS

Originally the brain was thought to be an immunity privileged site. Nowadays this view has considerably changed and it is clear that not only blood-derived immune cells can enter the brain during pathological states, but that the brain itself contains cells which can initiate immune responses (innate immunity) [308,309]. Besides the obvious functions of the immune system, brain immunity and in particular cytokines and chemokines, have been shown to be involved in neuronal signaling, neuron-glia interactions and neuronal development [158,310]. Certain types of epilepsy are thought to be caused by chronic inflammation by either auto-antibodies or increased expression of cytokines [155]. Moreover, a polymorphism in the cytokine *IL1B* has been shown to be associated with FS, MTLE and hippocampal sclerosis [52,53]. Studies in animal models have shown that the immune

system can be activated in response to SE, stroke, trauma or infection, all acquired factors associated with TLE. This can result in the recruitment of proinflammatory chemokines and cytokines, prostaglandin synthesis, complement activation and other inflammatory responses [144,156]. We showed that inflammatory responses also play a role in human MTLE **(chapter 2)** and in epileptogenesis after FS **(chapter 6)**. Especially the chemokines *CCL3* and *-4* were highly up-regulated in the hippocampus of TLE patients and we showed that *Ccl3* was also modestly up-regulated acutely after prolonged FS in mice. A meta-analysis of microarray studies in animals models for epileptogenesis also suggested an important role for chemokines in epilepsy and epileptogenesis [156]. To investigate whether CCL3 had direct effects on neurons, the effect of chronic pathological concentrations of CCL3 on neuronal activity and neuronal calcium dynamics were studied in a rat hippocampal neuronal culture system **(chapter 4)**. We showed that CCL3 potently modulates neuronal activity and calcium dynamics and that this was mostly mediated by increasing N-methyl D-aspartate (NMDA) receptor levels. These results suggest important roles for chemokines in MTLE and epileptogenesis and blocking the actions of chemokines could prove beneficial for MTLE patients.

ACQUIRED CHANNELOPATHY IN MTLE

Most monogenetic idiopathic epilepsies have been shown to be caused by mutations in ion channel genes (**chapter 1**) and were therefore named channelopathies. In multifactorial epilepsy disorders like MTLE both genetic and environmental factors are implicated and increasingly more data show the involvement of ion channel dysfunction in acquired epilepsies [reviewed by 1]. Probably, environmental factors like trauma and hypoxia can induce processes which lead to altered gene expression and post-transcriptional modifications of ion channels [1,132]. In **chapter 2** hippocampal gene expression was determined in patients with hippocampal sclerosis (HS), without HS and in autopsy controls and compared with each other in a three-way analysis. Besides genes involved in the immune response (see previous section) when comparing MTLE patients with controls, genes involved in neuronal activities and the ionotropic glutamate receptor pathway were identified when comparing MTLE patients with and without HS. Expression changes in this pathway were probably reminiscent of neuronal cell death in HS patients and are not likely to be causal for epilepsy in these patients. Of particular interest was *SCN3B*, which codes for one of the beta-subunits of the voltage-gated sodium channel (Na_v). Three other Na_v subunit genes (*SCN1A*, *SCN2A* and *SCN1B*) have been linked to familial epilepsies [189]. *SCN3B* expression was two-fold higher in nonHS patients than in HS patients and this increase could not be attributed to neuronal cell death. In contrast, when analyzing SCN3B protein expression ($Na_v\beta3$) in hippocampal homogenates we identified a 2- to 3-fold decrease in protein expression in nonHS MTLE patients compared to autopsy control and HS MTLE patients (**chapter 3**). We excluded the involvement of mutations in the coding regions of *SCN3B*. The mismatch between mRNA (**chapter 2**) and protein expression (**chapter 3**), suggests that $Na_v\beta3$ protein down-regulation in nonHS patients is translationally or post-translationally regulated. Post-translational regulation is in line with up-regulation of ubiquitination and proteasomal degradation processes found specifically in nonHS patients (**chapter 2**), which could degrade $Na_v\beta3$ protein. The functional consequences of reduced $Na_v\beta3$ expression remain to be elucidated, but these results suggest that acquired epilepsies like MTLE are partly caused by ion channel dysfunc-

tion. Figure 1 illustrates the role of Na_vs in idiopathic and symptomatic epilepsies [modified from 1]. *SCN1A*, *-2A* and *-1B* have been implicated in familial epilepsies and familial FS syndromes (SMEI, GEFS+) (see also **chapter 1**), and although we cannot exclude *SCN3B* mutations in familial epilepsies, coding mutations were not observed in MTLE patients (**chapter 3**) and therefore its down-regulation can be considered an acquired channelopathy.

FS SUSCEPTIBILITY AND FS-INDUCED EPILEPTOGENESIS

Complex FS are the most common initial precipitating factor in MTLE, but it is unclear whether FS themselves contribute to the development of MTLE (epileptogenesis), or whether a prenatal lesion, brain insult or a genetic predisposition is causal to both FS and MTLE [87,88]. To investigate whether FS by themselves can lead to epileptogenesis, adult seizure thresholds were investigated after mice were subjected to early life prolonged FS (**chapter 5**). We showed that early life prolonged FS reduced seizure thresholds in adult animals, which showed that FS can lead to epileptogenesis. To investigate the molecular determinants of epileptogenesis after FS, hippocampal gene expression was investigated longitudinally after mice were subjected to prolonged FS (**chapter 6**). In the acute phase after FS (1 hour) we identified mainly genes involved in transcription and stress responses. Most of these responses appeared seizure related and have been identified before in epilepsy [258-261,266]. Three days later, most differentially expressed genes were involved in neuronal repair and remodeling, a process that was still active 11 days later. These processes were probably reminiscent of mossy fiber sprouting which has previously been identified in this model [113,114] and in human MTLE patients [49]. Mossy fibers are thought to form recurrent excitatory circuits and may contribute to synchronous firing and epileptiform activity (discussed in **chapter 1**). Another 6 weeks later neuronal repair and remodeling processes had normalized, but *Camk2a* was down-regulated. CAMK2 is abundantly expressed in the brain as a major constituent of the postsynaptic density and is involved in glutamate receptor trafficking during long-term potentiation (LTP) [273]. Down-regulation of the *Camk2a* gene is one of the most consistently identified effects in epileptogenesis [reviewed by 133] and recently we also identified *CAMK2A* down-regulation in human MTLE patients (**chapter 2**). Moreover, reduced expression of CAMK2A has been shown to induce limbic seizures in a dose-dependant way [133]. The evidence of reduced CAMK2 activity during epileptogenesis, supported by genetic and pharmacological studies, suggests that reduced CAMK2 activity is sufficient to induce changes that render the brain epileptic and suggests that CAMK2A plays a pivotal role in epileptogenesis. Recent data from our group suggests enhanced LTP after prolonged FS [Notenboom, Ramakers and de Graan, unpublished], but the precise role of reduced *Camk2a* expression after prolonged FS needs to be further

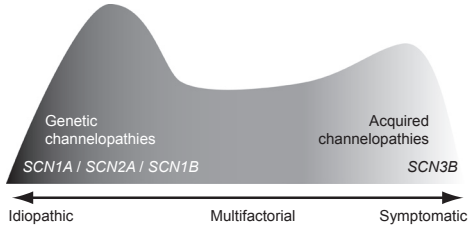

Figure 1. Voltage-gated sodium channel genes as example for ion channels in a central mechanism of idiopathic, multifactorial and symptomatic epilepsies [modified from 1]. The vertical axis indicates a general estimated frequency of epilepsy causes in the spectrum of idiopathic and symptomatic epilepsies (horizontal axis). Grey scaling indicates the influence of genetics. On the far left single-gene epilepsies can be found; the highest peak represents epilepsies with complex inheritance and multigenetic origin. In multifactorial epilepsies both genetic and acquired factors interact, but in pure symptomatic epilepsies the genetic influence is small (far right). Channel dysfunction can be relevant throughout the epilepsy spectrum.

investigated. These data strongly suggest that prolonged FS, although not leading to spontaneous seizure and epilepsy, are sufficient to induce a process of epileptogenesis in which CAMK2A plays a pivotal role.

To investigate whether a genetic predisposition exits which is causal to both FS and MTLE, we determined FS susceptibility in mouse inbred strains (**chapter 5**) and identified five significant and one suggestive FS quantitative trait loci (QTL) in chromosome substitution strains (CSS) **(chapter 7)**. We showed that FS susceptibility in mouse inbred strains is determined by a complex genetic background and that the C57BL/6J strain was relatively susceptible to FS while the A/J strain was relatively resistant (**chapter 5**). This is in contrast to what was found in chemically- and electrically-induced seizure susceptibility studies, which showed that the A/J strain was more susceptible to these seizures than the C57BL/6J strain [128,237]. Our data indicate that susceptibility genes for FS and convulsants are distinct. We subsequently identified chromosomes carrying QTLs which determine FS susceptibility in the C57BL/6J and A/J strains by using the CSS panel [241] **(chapter 7)**. A/J chromosomes 2 and X increased FS susceptibility, whereas A/J chromosomes 1, 10 and 13 decreased FS susceptibility. Chromosomes 1, 2, 10 and 13 contain candidate genes which have been implicated in human FS. Using haploinsufficient *Glul* knockout mice we identified *Glul* as a FS susceptibility gene on chromosome 1 (**chapter 8**). The evidence that distinct mechanisms are involved in FS and electrically- or chemically-induced seizures (**chapter 5**) is also illustrated by a chemoconvulsant seizure susceptibility study [288] and by data from **chapter 7**. Although these authors [288] also identified chromosome 10 as susceptibility QTL, their QTL increased seizure susceptibility, whereas our QTL decreased FS susceptibility. Probably, the underlying genes are different in the two models, or the gene involved has different effects on neuronal signaling in childhood when compared to adulthood (chemically-induced seizures are induced in adult animals). Fine-mapping and subsequent gene sequencing will be needed to identify the genes responsible for mouse FS susceptibility and could lead the way to understanding the mechanisms involved in human FS. These data suggest that FS themselves contribute to the development of MTLE and that susceptibility genes for MTLE are distinct from FS susceptibility genes.

THE INVOLVEMENT OF THE GLUTAMATE-GLUTAMINE CYCLE IN MTLE AND FS

The glutamate-glutamine cycle plays a key role in the regulation of glutamatergic transmission. Most extra-cellular glutamate is transported into glial cell by the glial glutamate transporter (*Slc1a2*; EAAT2), and converted into non-toxic glutamine by the enzyme glutamine synthetase (*Glul*; GS). Glutamine is then transported back to the neuron, where the enzyme glutaminase (*Gls*; PAG) reconverts glutamine into glutamate (figure 2). The rate of this cycle was found to be decreased in the hippocampus of TLE patients with HS [287]. The reduced rate of this cycle could in part be explained by decreased expression and enzyme activity of GS in the hippocampus of TLE patients with HS [271,286]. However, other components of this cycle have also been implicated. For instance PAG was up-regulated in neurons of the hippocampus of TLE patients with HS [294] and altered subregional expression of EAAT2 has also been reported [271,295,296]. In response (acute) to prolonged FS, *Glul* was down-regulated, while *Slc1a2* and *Gls* were up-regulated (**chapter 6**). Down-regulation of *Glul* would reduce conversion of glutamate to glutamine. In the chronic phase some animals showed a strong down-regulation of *Glul* after prolonged FS. Reduced expression of *Glul* is likely to af-

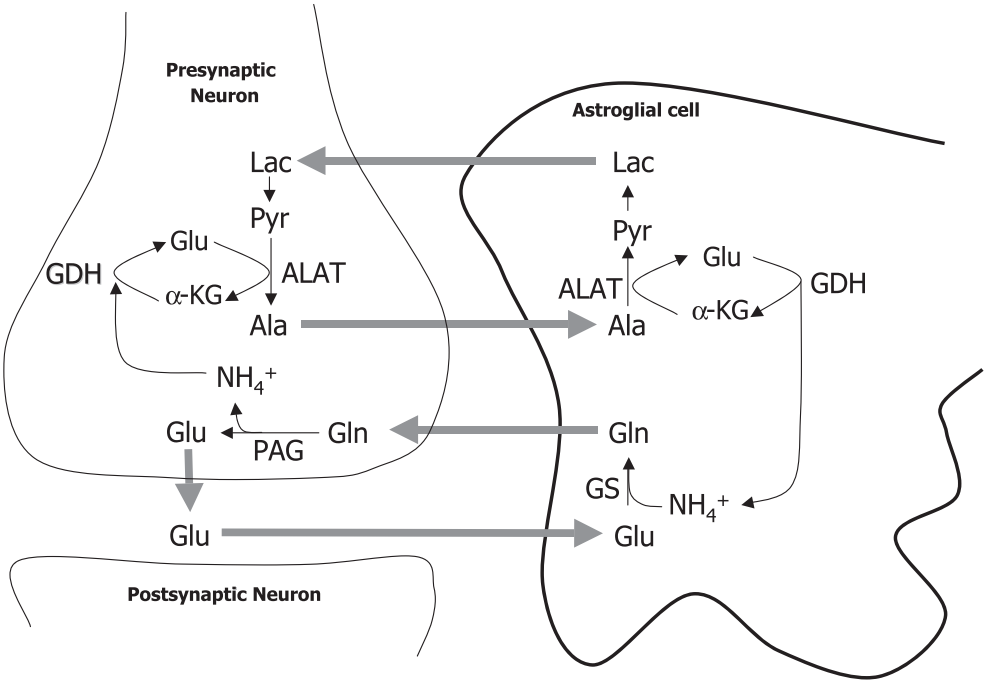

Figure 2. Illustration of the glutamate-glutamine cycle and of a proposed amino acid shuttle involved in the return of ammonia generated in neurons [modified from 311]. Abbreviations: Ace-CoA, acetyl-CoA; Ala, alanine; ALAT, alanine aminotransferase; α-KG, α-ketoglutarate; GDH, glutamate dehydrogenase; Gln, glutamine; Glu, glutamate; GS, glutamine synthetase; Lac, lactate; PAG, phosphate-activated glutaminase; Pyr, pyruvate.

fect glutamate conversion and could lead to glutamate toxicity [285]. The significance of reduced expression of *Glul* is also illustrated by data from **chapter 8**. A 50% *Glul* expression/activity reduction in haploinsufficient *Glul* knockout mice dramatically increased the susceptibility to FS. Amino acid composition was not significantly affected, although the data suggested a slightly increased level of alanine (Ala), which is involved in the lactate-alanine shuttle in the glutamate-glutamine cycle (figure 2). Recessive *Glul* enzyme activity obliteration mutations have been described in human [307], resulting in extensive brain malformations, seizures and multiorgan failure and death within a few days after birth. Both parents, heterozygote for the mutation, had reduced GS activity and low serum glutamine levels but were unaffected. Although unaffected, these families have not been investigated in detail for epilepsy symptoms (no MRI, EEG). It is possible that *Glul* mutation carriers, especially in the light of our results, are more susceptible to seizures and possibly predispose to epilepsy. Moreover, preliminary results from our lab [Bos, de Graan, van Nieuwenhuizen, unpublished] have shown reduced *GLUL* mRNA levels in leukocytes of newly diagnosed symptomatic epilepsy patients. These data suggest that *Glul* is a major susceptibility gene for FS and epilepsy. Association studies will be required to investigate whether gene variation in *GLUL* and other components of the glutamate-glutamine cycle are associated with epilepsy and FS.

CONCLUDING REMARKS

This thesis provides insight in the emerging role of the immune system in MTLE and identified genes and processes involved in

FS and epileptogenesis. In human MTLE we identified high expression of chemokines, which *in vitro* increased neuronal activity. Blocking chemokines could prove beneficial to MTLE patients and is of interest for future studies. FS were shown to induce a process of epileptogenesis possibly culminating in MTLE in which *Camk2a* plays a key role. The role of *Camk2a* is currently being investigated in more detail. Although FS predispose to MTLE, we showed that genes influencing FS and epileptogenesis susceptibility are distinct. *Glul* was shown to be a major FS susceptibility gene and FS susceptibility loci have been localized to chromosomes 1, 2, 10, 13 and X of the A/J strain. Fine-mapping and subsequent sequencing will be necessary to identify causative genes and will increase our understanding of the FS/MTLE mechanisms and relationships.

References

REFERENCES

1. Berkovic, S. F., Mulley, J. C., Scheffer, I. E., Petrou, S. (2006) Human epilepsies: interaction of genetic and acquired factors. *Trends Neurosci.* 29:391-7.
2. Sander, J. W. (2003) The epidemiology of epilepsy revisited. *Curr Opin Neurol.* 16:165-70.
3. ILAE (1993) Guidelines for epidemiologic studies on epilepsy. Commission on Epidemiology and Prognosis, International League Against Epilepsy. *Epilepsia.* 34:592-6.
4. Kjeldsen, M. J., Corey, L. A., Solaas, M. H., Friis, M. L., Harris, J. R., Kyvik, K. O., Christensen, K., Pellock, J. M. (2005) Genetic factors in seizures: a population-based study of 47,626 US, Norwegian and Danish twin pairs. *Twin Res Hum Genet.* 8:138-47.
5. Berkovic, S. F., Howell, R. A., Hay, D. A., Hopper, J. L. (1998) Epilepsies in twins: genetics of the major epilepsy syndromes. *Ann Neurol.* 43:435-45.
6. Lennox, W. G. (1951) The heredity of epilepsy as told by relatives and twins. *J Am Med Assoc.* 146:529-36.
7. Martin, M. S., Tang, B., Papale, L. A., Yu, F. H., Catterall, W. A., Escayg, A. (2007) The voltage-gated sodium channel Scn8a is a genetic modifier of severe myoclonic epilepsy of infancy. *Hum Mol Genet.* 16:2892-9.
8. Bergren, S. K., Chen, S., Galecki, A., Kearney, J. A. (2005) Genetic modifiers affecting severity of epilepsy caused by mutation of sodium channel Scn2a. *Mamm Genome.* 16:683-90.
9. Tan, N. C., Mulley, J. C., Scheffer, I. E. (2006) Genetic dissection of the common epilepsies. *Curr Opin Neurol.* 19:157-63.
10. Kjeldsen, M. J., Corey, L. A., Christensen, K., Friis, M. L. (2003) Epileptic seizures and syndromes in twins: the importance of genetic factors. *Epilepsy Res.* 55:137-46.
11. French, J. A., Williamson, P. D., Thadani, V. M., Darcey, T. M., Mattson, R. H., Spencer, S. S., Spencer, D. D. (1993) Characteristics of medial temporal lobe epilepsy: I. Results of history and physical examination. *Ann Neurol.* 34:774-80.
12. Steinlein, O. K., Mulley, J. C., Propping, P., Wallace, R. H., Phillips, H. A., Sutherland, G. R., Scheffer, I. E., Berkovic, S. F. (1995) A missense mutation in the neuronal nicotinic acetylcholine receptor alpha 4 subunit is associated with autosomal dominant nocturnal frontal lobe epilepsy. *Nat Genet.* 11:201-3.
13. De Fusco, M., Becchetti, A., Patrignani, A., Annesi, G., Gambardella, A., Quattrone, A., Ballabio, A., Wanke, E., Casari, G. (2000) The nicotinic receptor beta 2 subunit is mutant in nocturnal frontal lobe epilepsy. *Nat Genet.* 26:275-6.
14. Du, W., Bautista, J. F., Yang, H., Diez-Sampedro, A., You, S. A., Wang, L., Kotagal, P., Luders, H. O., Shi, J., Cui, J., Richerson, G. B., Wang, Q. K. (2005) Calcium-sensitive potassium channelopathy in human epilepsy and paroxysmal movement disorder. *Nat Genet.* 37:733-8.
15. Singh, N. A., Charlier, C., Stauffer, D., DuPont, B. R., Leach, R. J., Melis, R., Ronen, G. M., Bjerre, I., Quattlebaum, T., Murphy, J. V., McHarg, M. L., Gagnon, D., Rosales, T. O., Peiffer, A., Anderson, V. E., Leppert, M. (1998) A novel potassium channel gene, KCNQ2, is mutated in an inherited epilepsy of newborns. *Nat Genet.* 18:25-9.
16. Charlier, C., Singh, N. A., Ryan, S. G., Lewis, T. B., Reus, B. E., Leach, R. J., Leppert, M. (1998) A pore mutation in a novel KQT-like potassium channel gene in an idiopathic epilepsy family. *Nat Genet.* 18:53-5.
17. Mantegazza, M., Gambardella, A., Rusconi, R., Schiavon, E., Annesi, F., Cassulini, R. R., Labate, A., Carrideo, S., Chifari, R., Canevini, M. P., Canger, R., Franceschetti, S., Annesi, G., Wanke, E., Quattrone, A. (2005) Identification of an Nav1.1 sodium channel (SCN1A) loss-of-function

mutation associated with familial simple febrile seizures. *Proc Natl Acad Sci U S A.* 102:18177-82.

18. Escayg, A., MacDonald, B. T., Meisler, M. H., Baulac, S., Huberfeld, G., An-Gourfinkel, I., Brice, A., LeGuern, E., Moulard, B., Chaigne, D., Buresi, C., Malafosse, A. (2000) Mutations of SCN1A, encoding a neuronal sodium channel, in two families with GEFS+2. *Nat Genet.* 24:343-5.
19. Fujiwara, T., Sugawara, T., Mazaki-Miyazaki, E., Takahashi, Y., Fukushima, K., Watanabe, M., Hara, K., Morikawa, T., Yagi, K., Yamakawa, K., Inoue, Y. (2003) Mutations of sodium channel alpha subunit type 1 (SCN1A) in intractable childhood epilepsies with frequent generalized tonic-clonic seizures. *Brain.* 126:531-46.
20. Wallace, R. H., Wang, D. W., Singh, R., Scheffer, I. E., George, A. L., Jr., Phillips, H. A., Saar, K., Reis, A., Johnson, E. W., Sutherland, G. R., Berkovic, S. F., Mulley, J. C. (1998) Febrile seizures and generalized epilepsy associated with a mutation in the Na+-channel beta1 subunit gene SCN1B. *Nat Genet.* 19:366-70.
21. Scheffer, I. E., Harkin, L. A., Grinton, B. E., Dibbens, L. M., Turner, S. J., Zielinski, M. A., Xu, R., Jackson, G., Adams, J., Connellan, M., Petrou, S., Wellard, R. M., Briellmann, R. S., Wallace, R. H., Mulley, J. C., Berkovic, S. F. (2007) Temporal lobe epilepsy and GEFS+ phenotypes associated with SCN1B mutations. *Brain.* 130:100-9.
22. Sugawara, T., Tsurubuchi, Y., Agarwala, K. L., Ito, M., Fukuma, G., Mazaki-Miyazaki, E., Nagafuji, H., Noda, M., Imoto, K., Wada, K., Mitsudome, A., Kaneko, S., Montal, M., Nagata, K., Hirose, S., Yamakawa, K. (2001) A missense mutation of the Na+ channel alpha II subunit gene Na(v)1.2 in a patient with febrile and afebrile seizures causes channel dysfunction. *Proc Natl Acad Sci U S A.* 98:6384-9.
23. Berkovic, S. F., Heron, S. E., Giordano, L., Marini, C., Guerrini, R., Kaplan, R. E., Gambardella, A., Steinlein, O. K., Grinton, B. E., Dean, J. T., Bordo, L., Hodgson, B. L., Yamamoto, T., Mulley, J. C., Zara, F., Scheffer, I. E. (2004) Benign familial neonatal-infantile seizures: characterization of a new sodium channelopathy. *Ann Neurol.* 55:550-7.
24. Cossette, P., Liu, L., Brisebois, K., Dong, H., Lortie, A., Vanasse, M., Saint-Hilaire, J. M., Carmant, L., Verner, A., Lu, W. Y., Wang, Y. T., Rouleau, G. A. (2002) Mutation of GABRA1 in an autosomal dominant form of juvenile myoclonic epilepsy. *Nat Genet.* 31:184-9.
25. Maljevic, S., Krampfl, K., Cobilanschi, J., Tilgen, N., Beyer, S., Weber, Y. G., Schlesinger, F., Ursu, D., Melzer, W., Cossette, P., Bufler, J., Lerche, H., Heils, A. (2006) A mutation in the GABA(A) receptor alpha(1)-subunit is associated with absence epilepsy. *Ann Neurol.* 59:983-7.
26. Dibbens, L. M., Feng, H. J., Richards, M. C., Harkin, L. A., Hodgson, B. L., Scott, D., Jenkins, M., Petrou, S., Sutherland, G. R., Scheffer, I. E., Berkovic, S. F., Macdonald, R. L., Mulley, J. C. (2004) GABRD encoding a protein for extra- or peri-synaptic GABAA receptors is a susceptibility locus for generalized epilepsies. *Hum Mol Genet.* 13:1315-9.
27. Baulac, S., Huberfeld, G., Gourfinkel-An, I., Mitropoulou, G., Beranger, A., Prud'homme, J. F., Baulac, M., Brice, A., Bruzzone, R., LeGuern, E. (2001) First genetic evidence of GABA(A) receptor dysfunction in epilepsy: a mutation in the gamma2-subunit gene. *Nat Genet.* 28:46-8.
28. Harkin, L. A., Bowser, D. N., Dibbens, L. M., Singh, R., Phillips, F., Wallace, R. H., Richards, M. C., Williams, D. A., Mulley, J. C., Berkovic, S. F., Scheffer, I. E., Petrou, S. (2002) Truncation of the GABA(A)-receptor gamma2 subunit in a family with generalized epilepsy with febrile seizures plus. *Am J Hum Genet.* 70:530-6.
29. Kananura, C., Haug, K., Sander, T., Runge, U., Gu, W., Hallmann, K., Rebstock, J., Heils, A., Steinlein, O. K. (2002) A splice-site mutation in GABRG2 associated with childhood absence epilepsy and febrile convulsions. *Arch Neurol.* 59:1137-41.

30. Audenaert, D., Schwartz, E., Claeys, K. G., Claes, L., Deprez, L., Suls, A., Van Dyck, T., Lagae, L., Van Broeckhoven, C., Macdonald, R. L., De Jonghe, P. (2006) A novel GABRG2 mutation associated with febrile seizures. *Neurology.* 67:687-90.
31. Marini, C., King, M. A., Archer, J. S., Newton, M. R., Berkovic, S. F. (2003) Idiopathic generalised epilepsy of adult onset: clinical syndromes and genetics. *J Neurol Neurosurg Psychiatry.* 74:192-6.
32. Chioza, B., Wilkie, H., Nashef, L., Blower, J., McCormick, D., Sham, P., Asherson, P., Makoff, A. J. (2001) Association between the alpha(1a) calcium channel gene CACNA1A and idiopathic generalized epilepsy. *Neurology.* 56:1245-6.
33. Chen, Y., Lu, J., Pan, H., Zhang, Y., Wu, H., Xu, K., Liu, X., Jiang, Y., Bao, X., Yao, Z., Ding, K., Lo, W. H., Qiang, B., Chan, P., Shen, Y., Wu, X. (2003) Association between genetic variation of CACNA1H and childhood absence epilepsy. *Ann Neurol.* 54:239-43.
34. Sarah E. Heron, H. K., Diego Varela, Chris Bladen, Tristiana C. Williams, Michelle R. Newman, Ingrid E. Scheffer, Samuel F. Berkovic, John C. Mulley, Gerald W. Zamponi, (2007) Extended spectrum of idiopathic generalized epilepsies associated with CACNA1H functional variants. *Annals of Neurology.* 62:560-568.
35. Haug, K., Warnstedt, M., Alekov, A. K., Sander, T., Ramirez, A., Poser, B., Maljevic, S., Hebeisen, S., Kubisch, C., Rebstock, J., Horvath, S., Hallmann, K., Dullinger, J. S., Rau, B., Haverkamp, F., Beyenburg, S., Schulz, H., Janz, D., Giese, B., Muller-Newen, G., Propping, P., Elger, C. E., Fahlke, C., Lerche, H., Heils, A. (2003) Mutations in CLCN2 encoding a voltage-gated chloride channel are associated with idiopathic generalized epilepsies. *Nat Genet.* 33:527-32.
36. Moore, T., Hecquet, S., McLellann, A., Ville, D., Grid, D., Picard, F., Moulard, B., Asherson, P., Makoff, A. J., McCormick, D., Nashef, L., Froguel, P., Arzimanoglou, A., LeGuern, E., Bailleul, B. (2001) Polymorphism analysis of JRK/JH8, the human homologue of mouse jerky, and description of a rare mutation in a case of CAE evolving to JME. *Epilepsy Res.* 46:157-67.
37. Nakayama, J., Fu, Y. H., Clark, A. M., Nakahara, S., Hamano, K., Iwasaki, N., Matsui, A., Arinami, T., Ptacek, L. J. (2002) A nonsense mutation of the MASS1 gene in a family with febrile and afebrile seizures. *Ann Neurol.* 52:654-7.
38. Kalachikov, S., Evgrafov, O., Ross, B., Winawer, M., Barker-Cummings, C., Martinelli Boneschi, F., Choi, C., Morozov, P., Das, K., Teplitskaya, E., Yu, A., Cayanis, E., Penchaszadeh, G., Kottmann, A. H., Pedley, T. A., Hauser, W. A., Ottman, R., Gilliam, T. C. (2002) Mutations in LGI1 cause autosomal-dominant partial epilepsy with auditory features. *Nat Genet.* 30:335-41.
39. Suzuki, T., Delgado-Escueta, A. V., Aguan, K., Alonso, M. E., Shi, J., Hara, Y., Nishida, M., Numata, T., Medina, M. T., Takeuchi, T., Morita, R., Bai, D., Ganesh, S., Sugimoto, Y., Inazawa, J., Bailey, J. N., Ochoa, A., Jara-Prado, A., Rasmussen, A., Ramos-Peek, J., Cordova, S., Rubio-Donnadieu, F., Inoue, Y., Osawa, M., Kaneko, S., Oguni, H., Mori, Y., Yamakawa, K. (2004) Mutations in EFHC1 cause juvenile myoclonic epilepsy. *Nat Genet.* 36:842-9.
40. Combi, R., Dalpra, L., Ferini-Strambi, L., Tenchini, M. L. (2005) Frontal lobe epilepsy and mutations of the corticotropin-releasing hormone gene. *Ann Neurol.* 58:899-904.
41. Pennacchio, L. A., Lehesjoki, A. E., Stone, N. E., Willour, V. L., Virtaneva, K., Miao, J., D'Amato, E., Ramirez, L., Faham, M., Koskiniemi, M., Warrington, J. A., Norio, R., de la Chapelle, A., Cox, D. R., Myers, R. M. (1996) Mutations in the gene encoding cystatin B in progressive myoclonus epilepsy (EPM1). *Science.* 271:1731-4.
42. Ranta, S., Zhang, Y., Ross, B., Lonka, L., Takkunen, E., Messer, A., Sharp, J., Wheeler, R., Kusumi, K., Mole, S., Liu, W., Soares, M. B., Bonaldo, M. F., Hirvasniemi, A., de la Chapelle, A., Gilliam, T. C., Lehesjoki, A. E. (1999) The neuronal ceroid lipofuscinoses in human EPMR and mnd

mutant mice are associated with mutations in CLN8. *Nat Genet.* 23:233-6.

43. Minassian, B. A., Lee, J. R., Herbrick, J. A., Huizenga, J., Soder, S., Mungall, A. J., Dunham, I., Gardner, R., Fong, C. Y., Carpenter, S., Jardim, L., Satishchandra, P., Andermann, E., Snead, O. C., 3rd, Lopes-Cendes, I., Tsui, L. C., Delgado-Escueta, A. V., Rouleau, G. A., Scherer, S. W. (1998) Mutations in a gene encoding a novel protein tyrosine phosphatase cause progressive myoclonus epilepsy. *Nat Genet.* 20:171-4.
44. Chan, E. M., Young, E. J., Ianzano, L., Munteanu, I., Zhao, X., Christopoulos, C. C., Avanzini, G., Elia, M., Ackerley, C. A., Jovic, N. J., Bohlega, S., Andermann, E., Rouleau, G. A., Delgado-Escueta, A. V., Minassian, B. A., Scherer, S. W. (2003) Mutations in NHLRC1 cause progressive myoclonus epilepsy. *Nat Genet.* 35:125-7.
45. Mills, P. B., Struys, E., Jakobs, C., Plecko, B., Baxter, P., Baumgartner, M., Willemsen, M. A., Omran, H., Tacke, U., Uhlenberg, B., Weschke, B., Clayton, P. T. (2006) Mutations in antiquitin in individuals with pyridoxine-dependent seizures. *Nat Med.* 12:307-9.
46. Wyler, A. R., Dohan, F. C., Schweitzer, J. B., Berry, A. D. (1992) A Grading System for Mesial Temporal Pathology (Hippocampal Sclerosis) from Anterior Temporal Lobectomy. *Journal of Epilepsy.* 5:220-225.
47. Houser, C. R. (1990) Granule cell dispersion in the dentate gyrus of humans with temporal lobe epilepsy. *Brain Res.* 535:195-204.
48. Heinrich, C., Nitta, N., Flubacher, A., Muller, M., Fahrner, A., Kirsch, M., Freiman, T., Suzuki, F., Depaulis, A., Frotscher, M., Haas, C. A. (2006) Reelin deficiency and displacement of mature neurons, but not neurogenesis, underlie the formation of granule cell dispersion in the epileptic hippocampus. *J Neurosci.* 26:4701-13.
49. Houser, C. R., Miyashiro, J. E., Swartz, B. E., Walsh, G. O., Rich, J. R., Delgado-Escueta, A. V. (1990) Altered patterns of dynorphin immunoreactivity suggest mossy fiber reorganization in human hippocampal epilepsy. *J Neurosci.* 10:267-82.
50. Mathern, G. W., Adelson, P. D., Cahan, L. D., Leite, J. P. (2002) Hippocampal neuron damage in human epilepsy: Meyer's hypothesis revisited. *Prog Brain Res.* 135:237-51.
51. Kalviainen, R., Salmenpera, T. (2002) Do recurrent seizures cause neuronal damage? A series of studies with MRI volumetry in adults with partial epilepsy. *Prog Brain Res.* 135:279-95.
52. Kauffman, M. A., Moron, D. G., Consalvo, D., Bello, R., Kochen, S. (2008) Association study between interleukin 1 beta gene and epileptic disorders: a HuGe review and meta-analysis. *Genet Med.* 10:83-8.
53. Kanemoto, K., Kawasaki, J., Miyamoto, T., Obayashi, H., Nishimura, M. (2000) Interleukin (IL)1beta, IL-1alpha, and IL-1 receptor antagonist gene polymorphisms in patients with temporal lobe epilepsy. *Ann Neurol.* 47:571-4.
54. Kanemoto, K., Kawasaki, J., Yuasa, S., Kumaki, T., Tomohiro, O., Kaji, R., Nishimura, M. (2003) Increased frequency of interleukin-1beta-511T allele in patients with temporal lobe epilepsy, hippocampal sclerosis, and prolonged febrile convulsion. *Epilepsia.* 44:796-9.
55. Haspolat, S., Baysal, Y., Duman, O., Coskun, M., Tosun, O., Yegin, O. (2005) Interleukin-1alpha, interleukin-1beta, and interleukin-1Ra polymorphisms in febrile seizures. *J Child Neurol.* 20:565-8.
56. Buono, R. J., Ferraro, T. N., O'Connor, M. J., Sperling, M. R., Ryan, S. G., Scattergood, T., Mulholland, N., Gilmore, J., Lohoff, F. W., Berrettini, W. H. (2001) Lack of association between an interleukin 1 beta (IL-1beta) gene variation and refractory temporal lobe epilepsy. *Epilepsia.* 42:782-4.
57. Jin, L., Jia, Y., Zhang, B., Xu, Q., Fan, Y., Wu, L., Shen, Y. (2003) Association analysis of a polymorphism of interleukin 1 beta (IL-1 beta) gene with temporal lobe epilepsy in a Chinese population.

Epilepsia. 44:1306-9.

58. Ozkara, C., Uzan, M., Tanriverdi, T., Baykara, O., Ekinci, B., Yeni, N., Kafadar, A., Buyru, N. (2006) Lack of association between IL-1beta/alpha gene polymorphisms and temporal lobe epilepsy with hippocampal sclerosis. *Seizure.* 15:288-91.
59. Heils, A., Haug, K., Kunz, W. S., Fernandez, G., Horvath, S., Rebstock, J., Propping, P., Elger, C. E. (2000) Interleukin-1beta gene polymorphism and susceptibility to temporal lobe epilepsy with hippocampal sclerosis. *Ann Neurol.* 48:948-50.
60. Cavalleri, G. L., Lynch, J. M., Depondt, C., Burley, M.-W., Wood, N. W., Sisodiya, S. M., Goldstein, D. B. (2005) Failure to replicate previously reported genetic associations with sporadic temporal lobe epilepsy: Where to from here? *Brain.* 128:1832-1840.
61. Stogmann, E., Zimprich, A., Baumgartner, C., Aull-Watschinger, S., Hollt, V., Zimprich, F. (2002) A functional polymorphism in the prodynorphin gene promotor is associated with temporal lobe epilepsy. *Ann Neurol.* 51:260-3.
62. Kauffman, M. A., Consalvo, D., Gonzalez, M. D., Kochen, S. (2008) Transcriptionally less active prodynorphin promoter alleles are associated with Temporal Lobe Epilepsy: A case-control study and meta-analysis. *Dis Markers.* 24:135-40.
63. Gambardella, A., Manna, I., Labate, A., Chifari, R., Serra, P., La Russa, A., LePiane, E., Cittadella, R., Andreoli, V., Sasanelli, F., Zappia, M., Aguglia, U., Quattrone, A. (2003) Prodynorphin gene promoter polymorphism and temporal lobe epilepsy. *Epilepsia.* 44:1255-6.
64. Tilgen, N., Rebstock, J., Horvath, S., Propping, P., Elger, C. E., Heils, A. (2003) Prodynorphin gene promoter polymorphism and temporal lobe epilepsy. *Ann Neurol.* 53:280-1; author reply 281-2.
65. Kanemoto, K., Kawasaki, J., Tarao, Y., Kumaki, T., Oshima, T., Kaji, R., Nishimura, M. (2003) Association of partial epilepsy with brain-derived neurotrophic factor (BDNF) gene polymorphisms. *Epilepsy Res.* 53:255-8.
66. Lohoff, F. W., Ferraro, T. N., Dahl, J. P., Hildebrandt, M. A., Scattergood, T. M., O'Connor, M. J., Sperling, M. R., Dlugos, D. J., Berrettini, W. H., Buono, R. J. (2005) Lack of association between variations in the brain-derived neurotrophic factor (BDNF) gene and temporal lobe epilepsy. *Epilepsy Res.* 66:59-62.
67. Gambardella, A., Manna, I., Labate, A., Chifari, R., La Russa, A., Serra, P., Cittadella, R., Bonavita, S., Andreoli, V., LePiane, E., Sasanelli, F., Di Costanzo, A., Zappia, M., Tedeschi, G., Aguglia, U., Quattrone, A. (2003) GABA(B) receptor 1 polymorphism (G1465A) is associated with temporal lobe epilepsy. *Neurology.* 60:560-563.
68. Kauffman, M. A., Levy, E. M., Consalvo, D., Mordoh, J., Kochen, S. (2008) GABABR1 (G1465A) gene variation and temporal lobe epilepsy controversy: New evidence. *Seizure.*
69. Ma, S., Abou-Khalil, B., Sutcliffe, J. S., Haines, J. L., Hedera, P. (2005) The GABBR1 locus and the G1465A variant is not associated with temporal lobe epilepsy preceded by febrile seizures. *BMC Med Genet.* 6:13.
70. Tan, N. C., Heron, S. E., Scheffer, I. E., Berkovic, S. F., Mulley, J. C. (2005) Is variation in the GABA(B) receptor 1 gene associated with temporal lobe epilepsy? *Epilepsia.* 46:778-80.
71. Salzmann, A., Moulard, B., Crespel, A., Baldy-Moulinier, M., Buresi, C., Malafosse, A. (2005) GABA receptor 1 polymorphism (G1465A) and temporal lobe epilepsy. *Epilepsia.* 46:931-3.
72. Stogmann, E., Zimprich, A., Baumgartner, C., Gleiss, A., Zimprich, F. (2006) Lack of association between a GABA receptor 1 gene polymorphism and temporal lobe epilepsy. *Epilepsia.* 47:437-9.
73. Ren, L., Jin, L., Zhang, B., Jia, Y., Wu, L., Shen, Y. (2005) Lack of GABABR1 gene variation (G1465A)

in a Chinese population with temporal lobe epilepsy. *Seizure.* 14:611-613.
74. Labate, A., Manna, I., Gambardella, A., Le Piane, E., La Russa, A., Condino, F., Cittadella, R., Aguglia, U., Quattrone, A. (2007) Association between the M129V variant allele of PRNP gene and mild temporal lobe epilepsy in women. *Neurosci Lett.* 421:1-4.
75. Walz, R., Castro, R. M. R. P. S., Velasco, T. R., Alexandre, V., Jr., Lopes, M. H., Leite, J. P., Santos, A. C., Assirati, J. A., Jr., Wichert-Ana, L., Terra-Bustamante, V. C., Bianchin, M. M., Maciag, P. C., Ribeiro, K. B., Guarnieri, R., Araujo, D., Cabalero, O., Moura, R., Salim, A. C. M., Kindlmann, K., Landemberger, M. C., Marques, W., Jr., Fernandes, R. M. F., Serafini, L. N., Machado, H. R., Carlotti, C. G., Jr., Brentani, R. R., Sakamoto, A. C., Martins, V. R. (2003) Surgical outcome in mesial temporal sclerosis correlates with prion protein gene variant. *Neurology.* 61:1204-1210.
76. Manna, I., Labate, A., Gambardella, A., Forabosco, P., La Russa, A., Le Piane, E., Aguglia, U., Quattrone, A. (2007) Serotonin transporter gene (5-Htt): association analysis with temporal lobe epilepsy. *Neurosci Lett.* 421:52-6.
77. Chou, I. C., Peng, C. T., Huang, C. C., Tsai, J. J., Tsai, F. J., Tsai, C. H. (2003) Association analysis of gamma 2 subunit of gamma- aminobutyric acid type A receptor polymorphisms with febrile seizures. *Pediatr Res.* 54:26-9.
78. Xiumin, W., Meichun, X., Lizhong, D. (2007) Association analysis of gamma2 subunit of gamma-aminobutyric acid (GABA) type A receptor and voltage-gated sodium channel type II alpha-polypeptide gene mutation in southern Chinese children with febrile seizures. *J Child Neurol.* 22:714-9.
79. Chou, I. C., Lee, C. C., Huang, C. C., Wu, J. Y., Tsai, J. J., Tsai, C. H., Tsai, F. J. (2003) Association of the neuronal nicotinic acetylcholine receptor subunit alpha4 polymorphisms with febrile convulsions. *Epilepsia.* 44:1089-93.
80. Mulley, J., Heron, S., Scheffer, I., Berkovic, S. (2004) Febrile convulsions and genetic susceptibility: role of the neuronal nicotinic acetylcholine receptor alpha 4 subunit. *Epilepsia.* 45:561; author reply 561-2.
81. Yinan, M., Yu, Q., Zhiyue, C., Jianjun, L., Lie, H., Liping, Z., Jianhui, Z., Fang, S., Dingfang, B., Qing, L., Xiru, W. (2004) Polymorphisms of casein kinase I gamma 2 gene associated with simple febrile seizures in Chinese Han population. *Neurosci Lett.* 368:2-6.
82. Nakayama, J., Yamamoto, N., Hamano, K., Iwasaki, N., Ohta, M., Nakahara, S., Matsui, A., Noguchi, E., Arinami, T. (2004) Linkage and association of febrile seizures to the IMPA2 gene on human chromosome 18. *Neurology.* 63:1803-7.
83. Virta, M., Hurme, M., Helminen, M. (2002) Increased frequency of interleukin-1beta (-511) allele 2 in febrile seizures. *Pediatr Neurol.* 26:192-5.
84. Tilgen, N., Pfeiffer, H., Cobilanschi, J., Rau, B., Horvath, S., Elger, C. E., Propping, P., Heils, A. (2002) Association analysis between the human interleukin 1beta (-511) gene polymorphism and susceptibility to febrile convulsions. *Neurosci Lett.* 334:68-70.
85. Hauser, W. A. (1994) The prevalence and incidence of convulsive disorders in children. *Epilepsia.* 35 Suppl 2:S1-6.
86. Tsuboi, T. (1984) Epidemiology of febrile and afebrile convulsions in children in Japan. *Neurology.* 34:175-81.
87. Waruiru, C., Appleton, R. (2004) Febrile seizures: an update. *Arch Dis Child.* 89:751-6.
88. Dulac, O., Nabbout, R., Plouin, P., Chiron, C., Scheffer, I. E. (2007) Early seizures: causal events or predisposition to adult epilepsy? *Lancet Neurol.* 6:643-51.
89. Depondt, C., Van Paesschen, W., Matthijs, G., Legius, E., Martens, K., Demaerel, P., Wilms, G. (2002)

Familial temporal lobe epilepsy with febrile seizures. *Neurology.* 58:1429-33.

90. Claes, L., Audenaert, D., Deprez, L., Van Paesschen, W., Depondt, C., Goossens, D., Del-Favero, J., Van Broeckhoven, C., De Jonghe, P. (2004) Novel locus on chromosome 12q22-q23.3 responsible for familial temporal lobe epilepsy associated with febrile seizures. *J Med Genet.* 41:710-4.
91. Gurnett, C. A., Dobbs, M. B., Keppel, C. R., Pincus, E. R., Jansen, L. A., Bowcock, A. M. (2007) Additional evidence of a locus for complex febrile and afebrile seizures on chromosome 12q22-23.3. *Neurogenetics.* 8:61-3.
92. Hedera, P., Blair, M. A., Andermann, E., Andermann, F., D'Agostino, D., Taylor, K. A., Chahine, L., Pandolfo, M., Bradford, Y., Haines, J. L., Abou-Khalil, B. (2007) Familial mesial temporal lobe epilepsy maps to chromosome 4q13.2-q21.3. *Neurology.* 68:2107-12.
93. Deprez, L., Peeters, K., Van Paesschen, W., Claeys, K. G., Claes, L. R., Suls, A., Audenaert, D., Van Dyck, T., Goossens, D., Del-Favero, J., De Jonghe, P. (2007) Familial occipitotemporal lobe epilepsy and migraine with visual aura: linkage to chromosome 9q. *Neurology.* 68:1995-2002.
94. Wallace, R. H., Berkovic, S. F., Howell, R. A., Sutherland, G. R., Mulley, J. C. (1996) Suggestion of a major gene for familial febrile convulsions mapping to 8q13-21. *J Med Genet.* 33:308-12.
95. Johnson, E., Dubovsky, J., Rich, S., O'Donovan, C., Orr, H., Anderson, V., Gil-Nagel, A., Ahmann, P., Dokken, C., Schneider, D., Weber, J. (1998) Evidence for a novel gene for familial febrile convulsions, FEB2, linked to chromosome 19p in an extended family from the Midwest. *Hum. Mol. Genet.* 7:63-67.
96. Kugler, S. L., Stenroos, E. S., Mandelbaum, D. E., Lehner, T., McKoy, V. V., Prossick, T., Sasvari, J., Swannick, K., Katz, J., Johnson, W. G. (1998) Hereditary febrile seizures: phenotype and evidence for a chromosome 19p locus. *Am J Med Genet.* 79:354-61.
97. Peiffer, A., Thompson, J., Charlier, C., Otterud, B., Varvil, T., Pappas, C., Barnitz, C., Gruenthal, K., Kuhn, R., Leppert, M. (1999) A locus for febrile seizures (FEB3) maps to chromosome 2q23-24. *Ann Neurol.* 46:671-8.
98. Nakayama, J., Hamano, K., Iwasaki, N., Nakahara, S., Horigome, Y., Saitoh, H., Aoki, T., Maki, T., Kikuchi, M., Migita, T., Ohto, T., Yokouchi, Y., Tanaka, R., Hasegawa, M., Matsui, A., Hamaguchi, H., Arinami, T. (2000) Significant evidence for linkage of febrile seizures to chromosome 5q14-q15. *Hum. Mol. Genet.* 9:87-91.
99. Nabbout, R., Prud'homme, J. F., Herman, A., Feingold, J., Brice, A., Dulac, O., LeGuern, E. (2002) A locus for simple pure febrile seizures maps to chromosome 6q22-q24. *Brain.* 125:2668-80.
100. Nabbout, R., Baulac, S., Desguerre, I., Bahi-Buisson, N., Chiron, C., Ruberg, M., Dulac, O., LeGuern, E. (2007) New locus for febrile seizures with absence epilepsy on 3p and a possible modifier gene on 18p. *Neurology.* 68:1374-81.
101. Hedera, P., Ma, S., Blair, M. A., Taylor, K. A., Hamati, A., Bradford, Y., Abou-Khalil, B., Haines, J. L. (2006) Identification of a novel locus for febrile seizures and epilepsy on chromosome 21q22. *Epilepsia.* 47:1622-8.
102. Wallace, R. H., Marini, C., Petrou, S., Harkin, L. A., Bowser, D. N., Panchal, R. G., Williams, D. A., Sutherland, G. R., Mulley, J. C., Scheffer, I. E., Berkovic, S. F. (2001) Mutant GABA(A) receptor gamma2-subunit in childhood absence epilepsy and febrile seizures. *Nat Genet.* 28:49-52.
103. Vestergaard, M., Basso, O., Henriksen, T. B., Ostergaard, J. R., Olsen, J. (2002) Risk factors for febrile convulsions. *Epidemiology.* 13:282-7.
104. Kjeldsen, M. J., Kyvik, K. O., Friis, M. L., Christensen, K. (2002) Genetic and environmental factors in febrile seizures: a Danish population-based twin study. *Epilepsy Res.* 51:167-77.
105. Hirose, S., Mohney, R. P., Okada, M., Kaneko, S., Mitsudome, A. (2003) The genetics of febrile

seizures and related epilepsy syndromes. *Brain Dev.* 25:304-12.
106. Tan, N. C., Mulley, J. C., Berkovic, S. F. (2004) Genetic association studies in epilepsy: “the truth is out there”. *Epilepsia.* 45:1429-42.
107. Holtzman, D., Obana, K., Olson, J. (1981) Hyperthermia-induced seizures in the rat pup: a model for febrile convulsions in children. *Science.* 213:1034-6.
108. Baram, T. Z., Gerth, A., Schultz, L. (1997) Febrile seizures: an appropriate-aged model suitable for long-term studies. *Brain Res.Dev.Brain Res.* 98:265-270.
109. Schuchmann, S., Schmitz, D., Rivera, C., Vanhatalo, S., Salmen, B., Mackie, K., Sipila, S. T., Voipio, J., Kaila, K. (2006) Experimental febrile seizures are precipitated by a hyperthermia-induced respiratory alkalosis. *Nat Med.* 12:817-23.
110. Dube, C. M., Brewster, A. L., Richichi, C., Zha, Q., Baram, T. Z. (2007) Fever, febrile seizures and epilepsy. *Trends Neurosci.* 30:490-6.
111. Dube, C., Richichi, C., Bender, R. A., Chung, G., Litt, B., Baram, T. Z. (2006) Temporal lobe epilepsy after experimental prolonged febrile seizures: prospective analysis. *Brain.* 129:911-22.
112. Toth, Z., Yan, X. X., Haftoglou, S., Ribak, C. E., Baram, T. Z. (1998) Seizure-induced neuronal injury: vulnerability to febrile seizures in an immature rat model. *J Neurosci.* 18:4285-94.
113. Bender, R. A., Dube, C., Gonzalez-Vega, R., Mina, E. W., Baram, T. Z. (2003) Mossy fiber plasticity and enhanced hippocampal excitability, without hippocampal cell loss or altered neurogenesis, in an animal model of prolonged febrile seizures. *Hippocampus.* 13:399-412.
114. Jiang, W., Duong, T. M., de Lanerolle, N. C. (1999) The neuropathology of hyperthermic seizures in the rat. *Epilepsia.* 40:5-19.
115. Dube, C., Yu, H., Nalcioglu, O., Baram, T. Z. (2004) Serial MRI after experimental febrile seizures: altered T2 signal without neuronal death. *Ann Neurol.* 56:709-14.
116. Dube, C., Vezzani, A., Behrens, M., Bartfai, T., Baram, T. Z. (2005) Interleukin-1beta contributes to the generation of experimental febrile seizures. *Ann Neurol.* 57:152-5.
117. Brewster, A., Bender, R. A., Chen, Y., Dube, C., Eghbal-Ahmadi, M., Baram, T. Z. (2002) Developmental febrile seizures modulate hippocampal gene expression of hyperpolarization-activated channels in an isoform- and cell-specific manner. *J Neurosci.* 22:4591-9.
118. Chen, K., Ratzliff, A., Hilgenberg, L., Gulyas, A., Freund, T. F., Smith, M., Dinh, T. P., Piomelli, D., Mackie, K., Soltesz, I. (2003) Long-term plasticity of endocannabinoid signaling induced by developmental febrile seizures. *Neuron.* 39:599-611.
119. Hatalski, C. G., Brunson, K. L., Tantayanubutr, B., Chen, Y., Baram, T. Z. (2000) Neuronal activity and stress differentially regulate hippocampal and hypothalamic corticotropin-releasing hormone expression in the immature rat. *Neuroscience.* 101:571-80.
120. Chen, K., Aradi, I., Thon, N., Eghbal-Ahmadi, M., Baram, T. Z., Soltesz, I. (2001) Persistently modified h-channels after complex febrile seizures convert the seizure-induced enhancement of inhibition to hyperexcitability. *Nat Med.* 7:331-7.
121. Chen, K., Baram, T. Z., Soltesz, I. (1999) Febrile seizures in the developing brain result in persistent modification of neuronal excitability in limbic circuits. *Nat Med.* 5:888-94.
122. Dube, C., Chen, K., Eghbal-Ahmadi, M., Brunson, K., Soltesz, I., Baram, T. Z. (2000) Prolonged febrile seizures in the immature rat model enhance hippocampal excitability long term. *Ann. Neurol.* 47:336-344.
123. Chen, K., Neu, A., Howard, A. L., Foldy, C., Echegoyen, J., Hilgenberg, L., Smith, M., Mackie, K., Soltesz, I. (2007) Prevention of plasticity of endocannabinoid signaling inhibits persistent limbic hyperexcitability caused by developmental seizures. *J Neurosci.* 27:46-58.
124. Skradski, S. L., Clark, A. M., Jiang, H., White, H. S., Fu, Y. H., Ptacek, L. J. (2001) A novel gene

causing a mendelian audiogenic mouse epilepsy. *Neuron.* 31:537-44.

125. Rudolf, G., Therese Bihoreau, M., R, F. G., S, P. W., R, D. C., Lathrop, M., Marescaux, C., Gauguier, D. (2004) Polygenic control of idiopathic generalized epilepsy phenotypes in the genetic absence rats from Strasbourg (GAERS). *Epilepsia.* 45:301-8.
126. Todorova, M. T., Mantis, J. G., Le, M., Kim, C. Y., Seyfried, T. N. (2006) Genetic and environmental interactions determine seizure susceptibility in epileptic EL mice. *Genes Brain Behav.* 5:518-27.
127. Ferraro, T. N., Golden, G. T., Smith, G. G., Longman, R. L., Snyder, R. L., DeMuth, D., Szpilzak, I., Mulholland, N., Eng, E., Lohoff, F. W., Buono, R. J., Berrettini, W. H. (2001) Quantitative genetic study of maximal electroshock seizure threshold in mice: evidence for a major seizure susceptibility locus on distal chromosome 1. *Genomics.* 75:35-42.
128. Kosobud, A. E., Crabbe, J. C. (1990) Genetic correlations among inbred strain sensitivities to convulsions induced by 9 convulsant drugs. *Brain Res.* 526:8-16.
129. Loscher, W. (2002) Animal models of epilepsy for the development of antiepileptogenic and disease-modifying drugs. A comparison of the pharmacology of kindling and post-status epilepticus models of temporal lobe epilepsy. *Epilepsy Res.* 50:105-23.
130. Morimoto, K., Fahnestock, M., Racine, R. J. (2004) Kindling and status epilepticus models of epilepsy: rewiring the brain. *Prog Neurobiol.* 73:1-60.
131. Sankar, R., Shin, D. H., Liu, H., Mazarati, A., Pereira de Vasconcelos, A., Wasterlain, C. G. (1998) Patterns of status epilepticus-induced neuronal injury during development and long-term consequences. *J Neurosci.* 18:8382-93.
132. Pitkanen, A., Kharatishvili, I., Karhunen, H., Lukasiuk, K., Immonen, R., Nairismagi, J., Grohn, O., Nissinen, J. (2007) Epileptogenesis in Experimental Models. *Epilepsia.* 48:13-20.
133. McNamara, J. O., Huang, Y. Z., Leonard, A. S. (2006) Molecular signaling mechanisms underlying epileptogenesis. *Sci STKE.* 2006:re12.
134. Croucher, M. J., Bradford, H. F. (1990) 7-Chlorokynurenic acid, a strychnine-insensitive glycine receptor antagonist, inhibits limbic seizure kindling. *Neurosci Lett.* 118:29-32.
135. Holmes, K. H., Bilkey, D. K., Laverty, R., Goddard, G. V. (1990) The N-methyl-D-aspartate antagonists aminophosphonovalerate and carboxypiperazinephosphonate retard the development and expression of kindled seizures. *Brain Res.* 506:227-35.
136. McNamara, J. O., Russell, R. D., Rigsbee, L., Bonhaus, D. W. (1988) Anticonvulsant and antiepileptogenic actions of MK-801 in the kindling and electroshock models. *Neuropharmacology.* 27:563-8.
137. Sprengel, R., Suchanek, B., Amico, C., Brusa, R., Burnashev, N., Rozov, A., Hvalby, O., Jensen, V., Paulsen, O., Andersen, P., Kim, J. J., Thompson, R. F., Sun, W., Webster, L. C., Grant, S. G., Eilers, J., Konnerth, A., Li, J., McNamara, J. O., Seeburg, P. H. (1998) Importance of the intracellular domain of NR2 subunits for NMDA receptor function in vivo. *Cell.* 92:279-89.
138. Ghosh, A., Greenberg, M. E. (1995) Calcium signaling in neurons: molecular mechanisms and cellular consequences. *Science.* 268:239-47.
139. Hanson, P. I., Schulman, H. (1992) Neuronal Ca2+/calmodulin-dependent protein kinases. *Annu Rev Biochem.* 61:559-601.
140. Butler, L. S., Silva, A. J., Abeliovich, A., Watanabe, Y., Tonegawa, S., McNamara, J. O. (1995) Limbic epilepsy in transgenic mice carrying a Ca2+/calmodulin-dependent kinase II alpha-subunit mutation. *Proc Natl Acad Sci U S A.* 92:6852-5.
141. Churn, S. B., Sombati, S., Jakoi, E. R., Severt, L., DeLorenzo, R. J. (2000) Inhibition of calcium/calmodulin kinase II alpha subunit expression results in epileptiform activity in cultured

hippocampal neurons. *Proc Natl Acad Sci U S A.* 97:5604-9.
142. Churn, S. B., Kochan, L. D., DeLorenzo, R. J. (2000) Chronic inhibition of Ca(2+)/calmodulin kinase II activity in the pilocarpine model of epilepsy. *Brain Res.* 875:66-77.
143. Singleton, M. W., Holbert, W. H., 2nd, Lee, A. T., Bracey, J. M., Churn, S. B. (2005) Modulation of CaM kinase II activity is coincident with induction of status epilepticus in the rat pilocarpine model. *Epilepsia.* 46:1389-400.
144. Gorter, J. A., van Vliet, E. A., Aronica, E., Breit, T., Rauwerda, H., Lopes da Silva, F. H., Wadman, W. J. (2006) Potential new antiepileptogenic targets indicated by microarray analysis in a rat model for temporal lobe epilepsy. *J Neurosci.* 26:11083-110.
145. Sola, C., Tusell, J. M., Serratosa, J. (1998) Decreased expression of calmodulin kinase II and calcineurin messenger RNAs in the mouse hippocampus after kainic acid-induced seizures. *J Neurochem.* 70:1600-8.
146. Yamagata, Y., Imoto, K., Obata, K. (2006) A mechanism for the inactivation of Ca2+/calmodulin-dependent protein kinase II during prolonged seizure activity and its consequence after the recovery from seizure activity in rats in vivo. *Neuroscience.* 140:981-92.
147. Wasterlain, C. G., Farber, D. B. (1984) Kindling alters the calcium/calmodulin-dependent phosphorylation of synaptic plasma membrane proteins in rat hippocampus. *Proc Natl Acad Sci U S A.* 81:1253-7.
148. Dong, Y., Rosenberg, H. C. (2004) Prolonged changes in Ca2+/calmodulin-dependent protein kinase II after a brief pentylenetetrazol seizure; potential role in kindling. *Epilepsy Res.* 58:107-17.
149. Yamagata, Y., Obata, K. (2004) Ca2+/calmodulin-dependent protein kinase II is reversibly autophosphorylated, inactivated and made sedimentable by acute neuronal excitation in rats in vivo. *J Neurochem.* 91:745-54.
150. Yechikhov, S., Morenkov, E., Chulanova, T., Godukhin, O., Shchipakina, T. (2001) Involvement of cAMP- and Ca(2+)/calmodulin-dependent neuronal protein phosphorylation in mechanisms underlying genetic predisposition to audiogenic seizures in rats. *Epilepsy Res.* 46:15-25.
151. Battaglia, G., Pagliardini, S., Ferrario, A., Gardoni, F., Tassi, L., Setola, V., Garbelli, R., LoRusso, G., Spreafico, R., Di Luca, M., Avanzini, G. (2002) AlphaCaMKII and NMDA-receptor subunit expression in epileptogenic cortex from human periventricular nodular heterotopia. *Epilepsia.* 43 Suppl 5:209-16.
152. Murray, K. D., Isackson, P. J., Eskin, T. A., King, M. A., Montesinos, S. P., Abraham, L. A., Roper, S. N. (2000) Altered mRNA expression for brain-derived neurotrophic factor and type II calcium/calmodulin-dependent protein kinase in the hippocampus of patients with intractable temporal lobe epilepsy. *J Comp Neurol.* 418:411-22.
153. Lie, A. A., Sommersberg, B., Elger, C. E. (2005) Analysis of pThr286-CaMKII and CaMKII immunohistochemistry in the hippocampus of patients with temporal lobe epilepsy. *Epilepsy Res.* 67:13-23.
154. Merrill, M. A., Chen, Y., Strack, S., Hell, J. W. (2005) Activity-driven postsynaptic translocation of CaMKII. *Trends Pharmacol Sci.* 26:645-53.
155. Billiau, A. D., Wouters, C. H., Lagae, L. G. (2005) Epilepsy and the immune system: is there a link? *Eur J Paediatr Neurol.* 9:29-42.
156. Lukasiuk, K., Dabrowski, M., Adach, A., Pitkanen, A. (2006) Chapter 11 Epileptogenesis-related genes revisited. *Prog Brain Res.* 158:223-41.
157. Maghazachi, A. A. (2000) Intracellular signaling events at the leading edge of migrating cells. *Int J Biochem Cell Biol.* 32:931-43.
158. Biber, K., de Jong, E. K., van Weering, H. R., Boddeke, H. W. (2006) Chemokines and their receptors

in central nervous system disease. *Curr Drug Targets.* 7:29-46.

159. Lahrtz, F., Piali, L., Spanaus, K. S., Seebach, J., Fontana, A. (1998) Chemokines and chemotaxis of leukocytes in infectious meningitis. *J Neuroimmunol.* 85:33-43.
160. Tran, P. B., Miller, R. J. (2003) Chemokine receptors: signposts to brain development and disease. *Nat Rev Neurosci.* 4:444-55.
161. Bruno, V., Copani, A., Besong, G., Scoto, G., Nicoletti, F. (2000) Neuroprotective activity of chemokines against N-methyl-D-aspartate or beta-amyloid-induced toxicity in culture. *Eur J Pharmacol.* 399:117-21.
162. Bajetto, A., Bonavia, R., Barbero, S., Schettini, G. (2002) Characterization of chemokines and their receptors in the central nervous system: physiopathological implications. *J Neurochem.* 82:1311-29.
163. Dalby, N. O., Mody, I. (2001) The process of epileptogenesis: a pathophysiological approach. *Curr Opin Neurol.* 14:187-92.
164. Bender, R. A., Dube, C., Baram, T. Z. (2004) Febrile seizures and mechanisms of epileptogenesis: insights from an animal model. *Adv Exp Med Biol.* 548:213-25.
165. Scimemi, A., Schorge, S., Kullmann, D. M., Walker, M. C. (2006) Epileptogenesis is associated with enhanced glutamatergic transmission in the perforant path. *J Neurophysiol.* 95:1213-20.
166. Vezzani, A., Granata, T. (2005) Brain inflammation in epilepsy: experimental and clinical evidence. *Epilepsia.* 46:1724-43.
167. Nakayama, J., Arinami, T. (2006) Molecular genetics of febrile seizures. *Epilepsy Res.* 70 Suppl 1: S190-8.
168. Jamali, S., Bartolomei, F., Robaglia-Schlupp, A., Massacrier, A., Peragut, J. C., Regis, J., Dufour, H., Ravid, R., Roll, P., Pereira, S., Royer, B., Roeckel-Trevisiol, N., Fontaine, M., Guye, M., Boucraut, J., Chauvel, P., Cau, P., Szepetowski, P. (2006) Large-scale expression study of human mesial temporal lobe epilepsy: evidence for dysregulation of the neurotransmission and complement systems in the entorhinal cortex. *Brain.* 129:625-41.
169. Becker, A. J., Chen, J., Paus, S., Normann, S., Beck, H., Elger, C. E., Wiestler, O. D., Blumcke, I. (2002) Transcriptional profiling in human epilepsy: expression array and single cell real-time qRT-PCR analysis reveal distinct cellular gene regulation. *Neuroreport.* 13:1327-33.
170. Becker, A. J., Chen, J., Zien, A., Sochivko, D., Normann, S., Schramm, J., Elger, C. E., Wiestler, O. D., Blumcke, I. (2003) Correlated stage- and subfield-associated hippocampal gene expression patterns in experimental and human temporal lobe epilepsy. *Eur J Neurosci.* 18:2792-802.
171. Ozbas-Gerceker, F., Redeker, S., Boer, K., Ozguc, M., Saygi, S., Dalkara, T., Soylemezoglu, F., Akalan, N., Baayen, J. C., Gorter, J. A., Aronica, E. (2006) Serial analysis of gene expression in the hippocampus of patients with mesial temporal lobe epilepsy. *Neuroscience.* 138:457-74.
172. Proper, E. A., Oestreicher, A. B., Jansen, G. H., Veelen, C. W., van Rijen, P. C., Gispen, W. H., de Graan, P. N. (2000) Immunohistochemical characterization of mossy fibre sprouting in the hippocampus of patients with pharmaco-resistant temporal lobe epilepsy. *Brain.* 123 (Pt 1):19-30.
173. Debets, R. M., van Veelen, C. W., van Huffelen, A. V., van Emde Boas, W. (1991) Presurgical evaluation of patients with intractable partial epilepsy: the Dutch epilepsy surgery program. *Acta Neurol Belg.* 91:125-40.
174. Roepman, P., Wessels, L. F., Kettelarij, N., Kemmeren, P., Miles, A. J., Lijnzaad, P., Tilanus, M. G., Koole, R., Hordijk, G. J., van der Vliet, P. C., Reinders, M. J., Slootweg, P. J., Holstege, F. C. (2005) An expression profile for diagnosis of lymph node metastases from primary head and neck squamous cell carcinomas. *Nat Genet.* 37:182-6.

175. Yang, Y. H., Dudoit, S., Luu, P., Lin, D. M., Peng, V., Ngai, J., Speed, T. P. (2002) Normalization for cDNA microarray data: a robust composite method addressing single and multiple slide systematic variation. *Nucleic Acids Res.* 30:e15.
176. Thomas, P. D., Campbell, M. J., Kejariwal, A., Mi, H., Karlak, B., Daverman, R., Diemer, K., Muruganujan, A., Narechania, A. (2003) PANTHER: a library of protein families and subfamilies indexed by function. *Genome Res.* 13:2129-41.
177. Zhang, B., Kirov, S., Snoddy, J. (2005) WebGestalt: an integrated system for exploring gene sets in various biological contexts. *Nucleic Acids Res.* 33:W741-8.
178. Ashburner, M., Ball, C. A., Blake, J. A., Botstein, D., Butler, H., Cherry, J. M., Davis, A. P., Dolinski, K., Dwight, S. S., Eppig, J. T., Harris, M. A., Hill, D. P., Issel-Tarver, L., Kasarskis, A., Lewis, S., Matese, J. C., Richardson, J. E., Ringwald, M., Rubin, G. M., Sherlock, G. (2000) Gene ontology: tool for the unification of biology. The Gene Ontology Consortium. *Nat Genet.* 25:25-9.
179. Millenaar, F. F., Okyere, J., May, S. T., van Zanten, M., Voesenek, L. A., Peeters, A. J. (2006) How to decide? Different methods of calculating gene expression from short oligonucleotide array data will give different results. *BMC Bioinformatics.* 7:137.
180. Whitaker, W. R., Faull, R. L., Dragunow, M., Mee, E. W., Emson, P. C., Clare, J. J. (2001) Changes in the mRNAs encoding voltage-gated sodium channel types II and III in human epileptic hippocampus. *Neuroscience.* 106:275-85.
181. van Zeijl, J. H., Mullaart, R. A., Galama, J. M. (2002) The pathogenesis of febrile seizures: is there a role for specific infections? *Rev Med Virol.* 12:93-106.
182. Yamashita, N., Morishima, T. (2005) HHV-6 and seizures. *Herpes.* 12:46-9.
183. Millichap, J. G., Millichap, J. J. (2006) Role of Viral Infections in the Etiology of Febrile Seizures. *Pediatr Neurol.* 35:165-172.
184. Dunzendorfer, S., Schratzberger, P., Reinisch, N., Kahler, C. M., Wiedermann, C. J. (1998) Secretoneurin, a novel neuropeptide, is a potent chemoattractant for human eosinophils. *Blood.* 91:1527-32.
185. Brogden, K. A., Guthmiller, J. M., Salzet, M., Zasloff, M. (2005) The nervous system and innate immunity: the neuropeptide connection. *Nat Immunol.* 6:558-64.
186. Bossy-Wetzel, E., Schwarzenbacher, R., Lipton, S. A. (2004) Molecular pathways to neurodegeneration. *Nat Med.* 10 Suppl:S2-9.
187. Kalwy, S. A., Akbar, M. T., Coffin, R. S., de Belleroche, J., Latchman, D. S. (2003) Heat shock protein 27 delivered via a herpes simplex virus vector can protect neurons of the hippocampus against kainic-acid-induced cell loss. *Brain Res Mol Brain Res.* 111:91-103.
188. Wells, T. N., Power, C. A., Shaw, J. P., Proudfoot, A. E. (2006) Chemokine blockers--therapeutics in the making? *Trends Pharmacol Sci.* 27:41-7.
189. Meisler, M. H., Kearney, J. A. (2005) Sodium channel mutations in epilepsy and other neurological disorders. *J Clin Invest.* 115:2010-7.
190. Wood, J. N., Baker, M. (2001) Voltage-gated sodium channels. *Curr Opin Pharmacol.* 1:17-21.
191. Klein, J. P., Khera, D. S., Nersesyan, H., Kimchi, E. Y., Waxman, S. G., Blumenfeld, H. (2004) Dysregulation of sodium channel expression in cortical neurons in a rodent model of absence epilepsy. *Brain Res.* 1000:102-9.
192. Aronica, E., Troost, D., Rozemuller, A. J., Yankaya, B., Jansen, G. H., Isom, L. L., Gorter, J. A. (2003) Expression and regulation of voltage-gated sodium channel beta1 subunit protein in human gliosis-associated pathologies. *Acta Neuropathol (Berl).* 105:515-23.
193. Gastaldi, M., Robaglia-Schlupp, A., Massacrier, A., Planells, R., Cau, P. (1998) mRNA coding for

voltage-gated sodium channel beta2 subunit in rat central nervous system: cellular distribution and changes following kainate-induced seizures. *Neurosci Lett.* 249:53-6.

194. Bartolomei, F., Gastaldi, M., Massacrier, A., Planells, R., Nicolas, S., Cau, P. (1997) Changes in the mRNAs encoding subtypes I, II and III sodium channel alpha subunits following kainate-induced seizures in rat brain. *J Neurocytol.* 26:667-78.
195. van Gassen, K. L. I., de Wit, M., Koerkamp, M. J. A. G., Rensen, M. G. A., van Rijen, P. C., Holstege, F. C. P., Lindhout, D., de Graan, P. N. E. (2007) Possible role of the innate immunity in temporal lobe epilepsy. *Epilepsia*.doi:10.1111/j.1528-1167.2007.01470.x.
196. Notenboom, R. G., Hampson, D. R., Jansen, G. H., van Rijen, P. C., van Veelen, C. W., van Nieuwenhuizen, O., de Graan, P. N. (2006) Up-regulation of hippocampal metabotropic glutamate receptor 5 in temporal lobe epilepsy patients. *Brain.* 129:96-107.
197. Morgan, K., Stevens, E. B., Shah, B., Cox, P. J., Dixon, A. K., Lee, K., Pinnock, R. D., Hughes, J., Richardson, P. J., Mizuguchi, K., Jackson, A. P. (2000) beta 3: an additional auxiliary subunit of the voltage-sensitive sodium channel that modulates channel gating with distinct kinetics. *Proc Natl Acad Sci U S A.* 97:2308-13.
198. Wong, H. K., Sakurai, T., Oyama, F., Kaneko, K., Wada, K., Miyazaki, H., Kurosawa, M., De Strooper, B., Saftig, P., Nukina, N. (2005) beta Subunits of voltage-gated sodium channels are novel substrates of beta-site amyloid precursor protein-cleaving enzyme (BACE1) and gamma-secretase. *J Biol Chem.* 280:23009-17.
199. Wells, T. N., Power, C. A., Proudfoot, A. E. (1998) Definition, function and pathophysiological significance of chemokine receptors. *Trends Pharmacol Sci.* 19:376-80.
200. Adler, M. W., Rogers, T. J. (2005) Are chemokines the third major system in the brain? *J.Leukoc. Biol.* 78:1204-1209.
201. Biber, K., de Jong, E. K., van Weering, H. R., Boddeke, H. W. (2006) Chemokines and their receptors in central nervous system disease. *Curr.Drug Targets.* 7:29-46.
202. Biber, K., Zuurman, M. W., Dijkstra, I. M., Boddeke, H. W. (2002) Chemokines in the brain: neuroimmunology and beyond. *Curr Opin Pharmacol.* 2:63-8.
203. Cartier, L., Hartley, O., Dubois-Dauphin, M., Krause, K. H. (2005) Chemokine receptors in the central nervous system: role in brain inflammation and neurodegenerative diseases. *Brain Res Brain Res Rev.* 48:16-42.
204. Meucci, O., Fatatis, A., Simen, A. A., Bushell, T. J., Gray, P. W., Miller, R. J. (1998) Chemokines regulate hippocampal neuronal signaling and gp120 neurotoxicity. *Proc.Natl.Acad.Sci.U.S.A.* 95:14500-14505.
205. Cowell, R. M., Xu, H., Galasso, J. M., Silverstein, F. S. (2002) Hypoxic-ischemic injury induces macrophage inflammatory protein-1alpha expression in immature rat brain. *Stroke.* 33:795-801.
206. Perrin, F. E., Lacroix, S., Aviles-Trigueros, M., David, S. (2005) Involvement of monocyte chemoattractant protein-1, macrophage inflammatory protein-1alpha and interleukin-1beta in Wallerian degeneration. *Brain.* 128:854-66.
207. Rempel, J. D., Murray, S. J., Meisner, J., Buchmeier, M. J. (2004) Differential regulation of innate and adaptive immune responses in viral encephalitis. *Virology.* 318:381-92.
208. Lee, T. S., Mane, S., Eid, T., Zhao, H., Lin, A., Guan, Z., Kim, J. H., Schweitzer, J., King-Stevens, D., Weber, P., Spencer, S. S., Spencer, D. D., de Lanerolle, N. C. (2007) Gene expression in temporal lobe epilepsy is consistent with increased release of glutamate by astrocytes. *Mol Med.* 13:1-13.
209. Vereyken, E. J., Bajova, H., Chow, S., de Graan, P. N., Gruol, D. L. (2007) Chronic interleukin-6

alters the level of synaptic proteins in hippocampus in culture and in vivo. *Eur J Neurosci.* 25:3605-16.

210. Loetscher, P., Seitz, M., Clark-Lewis, I., Baggiolini, M., Moser, B. (1994) Monocyte chemotactic proteins MCP-1, MCP-2, and MCP-3 are major attractants for human CD4+ and CD8+ T lymphocytes. *Faseb J.* 8:1055-60.
211. Ankarcrona, M., Dypbukt, J. M., Bonfoco, E., Zhivotovsky, B., Orrenius, S., Lipton, S. A., Nicotera, P. (1995) Glutamate-induced neuronal death: a succession of necrosis or apoptosis depending on mitochondrial function. *Neuron.* 15:961-73.
212. Conroy, S. M., Nguyen, V., Quina, L. A., Blakely-Gonzales, P., Ur, C., Netzeband, J. G., Prieto, A. L., Gruol, D. L. (2004) Interleukin-6 produces neuronal loss in developing cerebellar granule neuron cultures. *J Neuroimmunol.* 155:43-54.
213. Grynkiewicz, G., Poenie, M., Tsien, R. Y. (1985) A new generation of Ca2+ indicators with greatly improved fluorescence properties. *J Biol Chem.* 260:3440-50.
214. Gruol, D. L., Netzeband, J. G., Parsons, K. L. (1996) Ca2+ signaling pathways linked to glutamate receptor activation in the somatic and dendritic regions of cultured cerebellar purkinje neurons. *J Neurophysiol.* 76:3325-40.
215. van Gassen, K. L., Netzeband, J. G., de Graan, P. N., Gruol, D. L. (2005) The chemokine CCL2 modulates Ca2+ dynamics and electrophysiological properties of cultured cerebellar Purkinje neurons. *Eur J Neurosci.* 21:2949-57.
216. Przewlocki, R., Parsons, K. L., Sweeney, D. D., Trotter, C., Netzeband, J. G., Siggins, G. R., Gruol, D. L. (1999) Opioid enhancement of calcium oscillations and burst events involving NMDA receptors and L-type calcium channels in cultured hippocampal neurons. *J Neurosci.* 19:9705-15.
217. Bacci, A., Verderio, C., Pravettoni, E., Matteoli, M. (1999) Synaptic and intrinsic mechanisms shape synchronous oscillations in hippocampal neurons in culture. *Eur J Neurosci.* 11:389-97.
218. Beach, T. G., Woodhurst, W. B., MacDonald, D. B., Jones, M. W. (1995) Reactive microglia in hippocampal sclerosis associated with human temporal lobe epilepsy. *Neurosci Lett.* 191:27-30.
219. Aronica, E., Gorter, J. A., Redeker, S., Ramkema, M., Spliet, W. G., van Rijen, P. C., Leenstra, S., Troost, D. (2005) Distribution, characterization and clinical significance of microglia in glioneuronal tumours from patients with chronic intractable epilepsy. *Neuropathol Appl Neurobiol.* 31:280-91.
220. Boer, K., Spliet, W. G., van Rijen, P. C., Redeker, S., Troost, D., Aronica, E. (2006) Evidence of activated microglia in focal cortical dysplasia. *J Neuroimmunol.* 173:188-95.
221. Singhrao, S. K., Neal, J. W., Newman, G. R. (1993) Corpora amylacea could be an indicator of neurodegeneration. *Neuropathol Appl Neurobiol.* 19:269-76.
222. Van Paesschen, W., Revesz, T., Duncan, J. S. (1997) Corpora amylacea in hippocampal sclerosis. *J Neurol Neurosurg Psychiatry.* 63:513-5.
223. Rigby, M., Le Bourdelles, B., Heavens, R. P., Kelly, S., Smith, D., Butler, A., Hammans, R., Hills, R., Xuereb, J. H., Hill, R. G., Whiting, P. J., Sirinathsinghji, D. J. (1996) The messenger RNAs for the N-methyl-D-aspartate receptor subunits show region-specific expression of different subunit composition in the human brain. *Neuroscience.* 73:429-47.
224. Goebel, D. J., Poosch, M. S. (1999) NMDA receptor subunit gene expression in the rat brain: a quantitative analysis of endogenous mRNA levels of NR1Com, NR2A, NR2B, NR2C, NR2D and NR3A. *Brain Res Mol Brain Res.* 69:164-70.
225. Mathern, G. W., Pretorius, J. K., Leite, J. P., Kornblum, H. I., Mendoza, D., Lozada, A., Bertram, E.

H., 3rd (1998) Hippocampal AMPA and NMDA mRNA levels and subunit immunoreactivity in human temporal lobe epilepsy patients and a rodent model of chronic mesial limbic epilepsy. *Epilepsy Res.* 32:154-71.

226. Mathern, G. W., Pretorius, J. K., Mendoza, D., Leite, J. P., Chimelli, L., Born, D. E., Fried, I., Assirati, J. A., Ojemann, G. A., Adelson, P. D., Cahan, L. D., Kornblum, H. I. (1999) Hippocampal N-methyl-D-aspartate receptor subunit mRNA levels in temporal lobe epilepsy patients. *Ann Neurol.* 46:343-58.
227. Mathern, G. W., Pretorius, J. K., Mendoza, D., Lozada, A., Leite, J. P., Chimelli, L., Fried, I., Sakamoto, A. C., Assirati, J. A., Adelson, P. D. (1998) Increased hippocampal AMPA and NMDA receptor subunit immunoreactivity in temporal lobe epilepsy patients. *J Neuropathol Exp Neurol.* 57:615-34.
228. McNamara, J. O., Russell, R. D., Rigsbee, L., Bonhaus, D. W. (1988) Anticonvulsant and antiepileptogenic actions of MK-801 in the kindling and electroshock models. *Neuropharmacology.* 27:563-568.
229. Croucher, M. J., Cotterell, K. L., Bradford, H. F. (1995) Amygdaloid kindling by repeated focal N-methyl-D-aspartate administration: comparison with electrical kindling. *Eur J Pharmacol.* 286:265-71.
230. DeLorenzo, R. J., Pal, S., Sombati, S. (1998) Prolonged activation of the N-methyl-D-aspartate receptor-Ca2+ transduction pathway causes spontaneous recurrent epileptiform discharges in hippocampal neurons in culture. *Proc Natl Acad Sci U S A.* 95:14482-7.
231. Rice, A. C., DeLorenzo, R. J. (1998) NMDA receptor activation during status epilepticus is required for the development of epilepsy. *Brain Res.* 782:240-7.
232. Sun, D. A., Sombati, S., Blair, R. E., DeLorenzo, R. J. (2002) Calcium-dependent epileptogenesis in an in vitro model of stroke-induced “epilepsy”. *Epilepsia.* 43:1296-305.
233. Neder, L., Valente, V., Carlotti, C. G., Jr., Leite, J. P., Assirati, J. A., Paco-Larson, M. L., Moreira, J. E. (2002) Glutamate NMDA receptor subunit R1 and GAD mRNA expression in human temporal lobe epilepsy. *Cell Mol Neurobiol.* 22:689-98.
234. Brines, M. L., Sundaresan, S., Spencer, D. D., de Lanerolle, N. C. (1997) Quantitative autoradiographic analysis of ionotropic glutamate receptor subtypes in human temporal lobe epilepsy: up-regulation in reorganized epileptogenic hippocampus. *Eur J Neurosci.* 9:2035-44.
235. During, M. J., Symes, C. W., Lawlor, P. A., Lin, J., Dunning, J., Fitzsimons, H. L., Poulsen, D., Leone, P., Xu, R., Dicker, B. L., Lipski, J., Young, D. (2000) An oral vaccine against NMDAR1 with efficacy in experimental stroke and epilepsy. *Science.* 287:1453-60.
236. Allen, S. J., Crown, S. E., Handel, T. M. (2007) Chemokine: receptor structure, interactions, and antagonism. *Annu Rev Immunol.* 25:787-820.
237. Ferraro, T. N., Golden, G. T., Smith, G. G., Berrettini, W. H. (1995) Differential susceptibility to seizures induced by systemic kainic acid treatment in mature DBA/2J and C57BL/6J mice. *Epilepsia.* 36:301-307.
238. Martin, B., Clement, Y., Venault, P., Chapouthier, G. (1995) Mouse chromosomes 4 and 13 are involved in beta-carboline-induced seizures. *J.Hered.* 86:274-279.
239. Clement, Y., Martin, B., Venault, P., Chapouthier, G. (1996) Mouse chromosome 9 involvement in beta-CCM-induced seizures. *Neuroreport.* 7:2226-2230.
240. Hain, H. S., Crabbe, J. C., Bergeson, S. E., Belknap, J. K. (2000) Cocaine-induced seizure thresholds: quantitative trait loci detection and mapping in two populations derived from the C57BL/6 and DBA/2 mouse strains. *J.Pharmacol.Exp.Ther.* 293:180-187.
241. Nadeau, J. H., Singer, J. B., Matin, A., Lander, E. S. (2000) Analysing complex genetic traits with

chromosome substitution strains. *Nat.Genet.* 24:221-225.
242. Singer, J. B., Hill, A. E., Burrage, L. C., Olszens, K. R., Song, J., Justice, M., O'Brien, W. E., Conti, D. V., Witte, J. S., Lander, E. S., Nadeau, J. H. (2004) Genetic dissection of complex traits with chromosome substitution strains of mice. *Science.* 304:445-448.
243. Kamal, A., Notenboom, R. G., de Graan, P. N., Ramakers, G. M. (2006) Persistent changes in action potential broadening and the slow afterhyperpolarization in rat CA1 pyramidal cells after febrile seizures. *Eur J Neurosci.* 23:2230-4.
244. White, H. S. (1998) In *Neuropharmacology Methods in Epilepsy Research*(Eds, Peterson, S. L. and Alberstson, T. E.) CRC Press, Boca Raton, pp. 24-40.
245. Kosobud, A. E., Cross, S. J., Crabbe, J. C. (1992) Neural sensitivity to pentylenetetrazol convulsions in inbred and selectively bred mice. *Brain Res.* 592:122-8.
246. Dobbing, J., Sands, J. (1973) Quantitative growth and development of human brain. *Arch Dis Child.* 48:757-67.
247. Clancy, B., Darlington, R. B., Finlay, B. L. (2001) Translating developmental time across mammalian species. *Neuroscience.* 105:7-17.
248. Bland, J. M., Altman, D. G. (1986) Statistical methods for assessing agreement between two methods of clinical measurement. *Lancet.* 1:307-10.
249. Lemmens, E. M., Lubbers, T., Schijns, O. E., Beuls, E. A., Hoogland, G. (2005) Gender differences in febrile seizure-induced proliferation and survival in the rat dentate gyrus. *Epilepsia.* 46:1603-12.
250. Gastaut, H., Aguglia, U., Tinuper, P. (1986) Benign versive or circling epilepsy with bilateral 3-cps spike-and-wave discharges in late childhood. *Ann Neurol.* 19:301-3.
251. Ponnio, T., Conneely, O. M. (2004) nor-1 regulates hippocampal axon guidance, pyramidal cell survival, and seizure susceptibility. *Mol Cell Biol.* 24:9070-8.
252. Petkov, P. M., Ding, Y., Cassell, M. A., Zhang, W., Wagner, G., Sargent, E. E., Asquith, S., Crew, V., Johnson, K. A., Robinson, P., Scott, V. E., Wiles, M. V. (2004) An efficient SNP system for mouse genome scanning and elucidating strain relationships. *Genome Res.* 14:1806-11.
253. Ferraro, T. N., Golden, G. T., Smith, G. G., DeMuth, D., Buono, R. J., Berrettini, W. H. (2002) Mouse strain variation in maximal electroshock seizure threshold. *Brain Res.* 936:82-86.
254. van Gassen, K. L., Hessel, E. V., Ramakers, G. M., Notenboom, R. G., Wolterink-Donselaar, I. G., Brakkee, J. H., Godschalk, T. C., Qiao, X., Spruijt, B. M., van Nieuwenhuizen, O., de Graan, P. N. (2008) Characterization of febrile seizures and febrile seizure susceptibility in mouse inbred strains. *Genes Brain Behav.*
255. Bender, R. A., Soleymani, S. V., Brewster, A. L., Nguyen, S. T., Beck, H., Mathern, G. W., Baram, T. Z. (2003) Enhanced expression of a specific hyperpolarization-activated cyclic nucleotide-gated cation channel (HCN) in surviving dentate gyrus granule cells of human and experimental epileptic hippocampus. *J Neurosci.* 23:6826-36.
256. Chang, J. T., Nevins, J. R. (2006) GATHER: a systems approach to interpreting genomic signatures. *Bioinformatics.* 22:2926-33.
257. Krueger-Naug, A. M., Hopkins, D. A., Armstrong, J. N., Plumier, J. C., Currie, R. W. (2000) Hyperthermic induction of the 27-kDa heat shock protein (Hsp27) in neuroglia and neurons of the rat central nervous system. *J Comp Neurol.* 428:495-510.
258. Franklin, T. B., Krueger-Naug, A. M., Clarke, D. B., Arrigo, A. P., Currie, R. W. (2005) The role of heat shock proteins Hsp70 and Hsp27 in cellular protection of the central nervous system. *Int J Hyperthermia.* 21:379-92.
259. Bidmon, H. J., Gorg, B., Palomero-Gallagher, N., Behne, F., Lahl, R., Pannek, H. W., Speckmann, E.

J., Zilles, K. (2004) Heat shock protein-27 is upregulated in the temporal cortex of patients with epilepsy. *Epilepsia.* 45:1549-59.

260. Kedmi, M., Orr-Urtreger, A. (2007) Expression changes in mouse brains following nicotine-induced seizures: the modulation of transcription factor networks. *Physiol Genomics.* 30:242-52.
261. Flood, W. D., Moyer, R. W., Tsykin, A., Sutherland, G. R., Koblar, S. A. (2004) Nxf and Fbxo33: novel seizure-responsive genes in mice. *Eur J Neurosci.* 20:1819-26.
262. Chang, L., Karin, M. (2001) Mammalian MAP kinase signalling cascades. *Nature.* 410:37-40.
263. Pearson, G., Robinson, F., Beers Gibson, T., Xu, B. E., Karandikar, M., Berman, K., Cobb, M. H. (2001) Mitogen-activated protein (MAP) kinase pathways: regulation and physiological functions. *Endocr Rev.* 22:153-83.
264. Maroni, P., Bendinelli, P., Tiberio, L., Rovetta, F., Piccoletti, R., Schiaffonati, L. (2003) In vivo heat-shock response in the brain: signalling pathway and transcription factor activation. *Brain Res Mol Brain Res.* 119:90-9.
265. Mielke, K., Brecht, S., Dorst, A., Herdegen, T. (1999) Activity and expression of JNK1, p38 and ERK kinases, c-Jun N-terminal phosphorylation, and c-jun promoter binding in the adult rat brain following kainate-induced seizures. *Neuroscience.* 91:471-83.
266. Xi, Z. Q., Wang, X. F., He, R. Q., Li, M. W., Liu, X. Z., Wang, L. Y., Zhu, X., Xiao, F., Sun, J. J., Li, J. M., Gong, Y., Guan, L. F. (2007) Extracellular signal-regulated protein kinase in human intractable epilepsy. *Eur J Neurol.* 14:865-72.
267. Nateri, A. S., Raivich, G., Gebhardt, C., Da Costa, C., Naumann, H., Vreugdenhil, M., Makwana, M., Brandner, S., Adams, R. H., Jefferys, J. G., Kann, O., Behrens, A. (2007) ERK activation causes epilepsy by stimulating NMDA receptor activity. *Embo J.* 26:4891-901.
268. Liu, F. Y., Wang, X. F., Li, M. W., Li, J. M., Xi, Z. Q., Luan, G. M., Zhang, J. G., Wang, Y. P., Sun, J. J., Li, Y. L. (2007) Upregulated expression of postsynaptic density-93 and N-methyl-D-aspartate receptors subunits 2B mRNA in temporal lobe tissue of epilepsy. *Biochem Biophys Res Commun.* 358:825-30.
269. Heck, N., Garwood, J., Loeffler, J. P., Larmet, Y., Faissner, A. (2004) Differential upregulation of extracellular matrix molecules associated with the appearance of granule cell dispersion and mossy fiber sprouting during epileptogenesis in a murine model of temporal lobe epilepsy. *Neuroscience.* 129:309-24.
270. Eng, L. F., Ghirnikar, R. S. (1994) GFAP and Astrogliosis. *Brain Pathology.* 4:229-237.
271. van der Hel, W. S., Notenboom, R. G., Bos, I. W., van Rijen, P. C., van Veelen, C. W., de Graan, P. N. (2005) Reduced glutamine synthetase in hippocampal areas with neuron loss in temporal lobe epilepsy. *Neurology.* 64:326-33.
272. Mohajeri, M. H., Madani, R., Saini, K., Lipp, H. P., Nitsch, R. M., Wolfer, D. P. (2004) The impact of genetic background on neurodegeneration and behavior in seizured mice. *Genes Brain Behav.* 3:228-39.
273. Lisman, J., Schulman, H., Cline, H. (2002) The molecular basis of CaMKII function in synaptic and behavioural memory. *Nat Rev Neurosci.* 3:175-90.
274. Chang, Y. C., Kuo, Y. M., Huang, A. M., Huang, C. C. (2005) Repetitive febrile seizures in rat pups cause long-lasting deficits in synaptic plasticity and NR2A tyrosine phosphorylation. *Neurobiol Dis.* 18:466-75.
275. Liang, X., Wu, L., Hand, T., Andreasson, K. (2005) Prostaglandin D2 mediates neuronal protection via the DP1 receptor. *J Neurochem.* 92:477-86.
276. Wu, L., Wang, Q., Liang, X., Andreasson, K. (2007) Divergent effects of prostaglandin receptor signaling on neuronal survival. *Neurosci Lett.* 421:253-8.

277. Liang, X., Wu, L., Wang, Q., Hand, T., Bilak, M., McCullough, L., Andreasson, K. (2007) Function of COX-2 and prostaglandins in neurological disease. *J Mol Neurosci.* 33:94-9.
278. Bate, C., Kempster, S., Williams, A. (2006) Prostaglandin D2 mediates neuronal damage by amyloid-beta or prions which activates microglial cells. *Neuropharmacology.* 50:229-37.
279. Rantala, H., Tarkka, R., Uhari, M. (2001) Systematic review of the role of prostaglandins and their synthetase inhibitors with respect to febrile seizures. *Epilepsy Research.* 46:251-257.
280. Bianchi, M. E., Manfredi, A. A. (2007) High-mobility group box 1 (HMGB1) protein at the crossroads between innate and adaptive immunity. *Immunol Rev.* 220:35-46.
281. Hara, H., Wada, T., Bakal, C., Kozieradzki, I., Suzuki, S., Suzuki, N., Nghiem, M., Griffiths, E. K., Krawczyk, C., Bauer, B., D'Acquisto, F., Ghosh, S., Yeh, W. C., Baier, G., Rottapel, R., Penninger, J. M. (2003) The MAGUK family protein CARD11 is essential for lymphocyte activation. *Immunity.* 18:763-75.
282. Babic, A. M., Kireeva, M. L., Kolesnikova, T. V., Lau, L. F. (1998) CYR61, a product of a growth factor-inducible immediate early gene, promotes angiogenesis and tumor growth. *Proc Natl Acad Sci U S A.* 95:6355-60.
283. Kim, K. H., Min, Y. K., Baik, J. H., Lau, L. F., Chaqour, B., Chung, K. C. (2003) Expression of angiogenic factor Cyr61 during neuronal cell death via the activation of c-Jun N-terminal kinase and serum response factor. *J Biol Chem.* 278:13847-54.
284. Rigau, V., Morin, M., Rousset, M. C., de Bock, F., Lebrun, A., Coubes, P., Picot, M. C., Baldy-Moulinier, M., Bockaert, J., Crespel, A., Lerner-Natoli, M. (2007) Angiogenesis is associated with blood-brain barrier permeability in temporal lobe epilepsy. *Brain.* 130:1942-56.
285. Choi, D. W., Maulucci-Gedde, M., Kriegstein, A. R. (1987) Glutamate neurotoxicity in cortical cell culture. *J Neurosci.* 7:357-68.
286. Eid, T., Thomas, M. J., Spencer, D. D., Runden-Pran, E., Lai, J. C., Malthankar, G. V., Kim, J. H., Danbolt, N. C., Ottersen, O. P., de Lanerolle, N. C. (2004) Loss of glutamine synthetase in the human epileptogenic hippocampus: possible mechanism for raised extracellular glutamate in mesial temporal lobe epilepsy. *Lancet.* 363:28-37.
287. Petroff, O. A., Errante, L. D., Rothman, D. L., Kim, J. H., Spencer, D. D. (2002) Glutamate-glutamine cycling in the epileptic human hippocampus. *Epilepsia.* 43:703-10.
288. Winawer, M. R., Kuperman, R., Niethammer, M., Sherman, S., Rabinowitz, D., Guell, I. P., Ponder, C. A., Palmer, A. A. (2007) Use of chromosome substitution strains to identify seizure susceptibility loci in mice. *Mamm Genome.* 18:23-31.
289. Nairismagi, J., Grohn, O. H., Kettunen, M. I., Nissinen, J., Kauppinen, R. A., Pitkanen, A. (2004) Progression of brain damage after status epilepticus and its association with epileptogenesis: a quantitative MRI study in a rat model of temporal lobe epilepsy. *Epilepsia.* 45:1024-34.
290. Belknap, J. K. (2003) Chromosome substitution strains: some quantitative considerations for genome scans and fine mapping. *Mamm.Genome.* 14:723-732.
291. Scheffer, I. E., Turner, S. J., Dibbens, L. M., Bayly, M. A., Friend, K., Hodgson, B., Burrows, L., Shaw, M., Wei, C., Ullmann, R., Ropers, H. H., Szepetowski, P., Haan, E., Mazarib, A., Afawi, Z., Neufeld, M. Y., Andrews, P. I., Wallace, G., Kivity, S., Lev, D., Lerman-Sagie, T., Derry, C. P., Korczyn, A. D., Gecz, J., Mulley, J. C., Berkovic, S. F. (2008) Epilepsy and mental retardation limited to females: an under-recognized disorder. *Brain.* 131:918-27.
292. Gershenfeld, H. K., Neumann, P. E., Li, X., St Jean, P. L., Paul, S. M. (1999) Mapping quantitative trait loci for seizure response to a GABAA receptor inverse agonist in mice. *J.Neurosci.* 19:3731-3738.
293. Frankel, W. N., Valenzuela, A., Lutz, C. M., Johnson, E. W., Dietrich, W. F., Coffin, J. M. (1995) New

seizure frequency QTL and the complex genetics of epilepsy in EL mice. *Mamm Genome.* 6:830-8.

294. Eid, T., Hammer, J., Runden-Pran, E., Roberg, B., Thomas, M. J., Osen, K., Davanger, S., Laake, P., Torgner, I. A., Lee, T. S., Kim, J. H., Spencer, D. D., Ottersen, O. P., de Lanerolle, N. C. (2007) Increased expression of phosphate-activated glutaminase in hippocampal neurons in human mesial temporal lobe epilepsy. *Acta Neuropathol.* 113:137-52.
295. Bjornsen, L. P., Eid, T., Holmseth, S., Danbolt, N. C., Spencer, D. D., de Lanerolle, N. C. (2007) Changes in glial glutamate transporters in human epileptogenic hippocampus: inadequate explanation for high extracellular glutamate during seizures. *Neurobiol Dis.* 25:319-30.
296. Proper, E. A., Hoogland, G., Kappen, S. M., Jansen, G. H., Rensen, M. G., Schrama, L. H., van Veelen, C. W., van Rijen, P. C., van Nieuwenhuizen, O., Gispen, W. H., de Graan, P. N. (2002) Distribution of glutamate transporters in the hippocampus of patients with pharmaco-resistant temporal lobe epilepsy. *Brain.* 125:32-43.
297. Dutuit, M., Didier-Bazes, M., Vergnes, M., Mutin, M., Conjard, A., Akaoka, H., Belin, M. F., Touret, M. (2000) Specific alteration in the expression of glial fibrillary acidic protein, glutamate dehydrogenase, and glutamine synthetase in rats with genetic absence epilepsy. *Glia.* 32:15-24.
298. Laming, P. R., Cosby, S. L., O'Neill, J. K. (1989) Seizures in the Mongolian gerbil are related to a deficiency in cerebral glutamine synthetase. *Comp Biochem Physiol C.* 94:399-404.
299. Letwin, N. E., Kafkafi, N., Benjamini, Y., Mayo, C., Frank, B. C., Luu, T., Lee, N. H., Elmer, G. I. (2006) Combined application of behavior genetics and microarray analysis to identify regional expression themes and gene-behavior associations. *J Neurosci.* 26:5277-87.
300. Rowe, W. B., Meister, A. (1970) Identification of L-methionine-S-sulfoximine as the convulsant isomer of methionine sulfoximine. *Proc Natl Acad Sci U S A.* 66:500-6.
301. Morimoto, T., Nagao, H., Yoshimatsu, M., Yoshida, K., Matsuda, H. (1993) Pathogenic role of glutamate in hyperthermia-induced seizures. *Epilepsia.* 34:447-52.
302. Morimoto, T., Kida, K., Nagao, H., Yoshida, K., Fukuda, M., Takashima, S. (1995) The pathogenic role of the NMDA receptor in hyperthermia-induced seizures in developing rats. *Brain Res Dev Brain Res.* 84:204-7.
303. He, Y., Hakvoort, T. B., Vermeulen, J. L., Lamers, W. H., Van Roon, M. A. (2007) Glutamine synthetase is essential in early mouse embryogenesis. *Dev Dyn.* 236:1865-75.
304. Pierce, J. P., Punsoni, M., McCloskey, D. P., Scharfman, H. E. (2007) Mossy cell axon synaptic contacts on ectopic granule cells that are born following pilocarpine-induced seizures. *Neurosci Lett.* 422:136-40.
305. Tanaka, K., Watase, K., Manabe, T., Yamada, K., Watanabe, M., Takahashi, K., Iwama, H., Nishikawa, T., Ichihara, N., Kikuchi, T., Okuyama, S., Kawashima, N., Hori, S., Takimoto, M., Wada, K. (1997) Epilepsy and Exacerbation of Brain Injury in Mice Lacking the Glutamate Transporter GLT-1. *Science.* 276:1699-1702.
306. Rise, M. L., Frankel, W. N., Coffin, J. M., Seyfried, T. N. (1991) Genes for epilepsy mapped in the mouse. *Science.* 253:669-73.
307. Haberle, J., Gorg, B., Rutsch, F., Schmidt, E., Toutain, A., Benoist, J. F., Gelot, A., Suc, A. L., Hohne, W., Schliess, F., Haussinger, D., Koch, H. G. (2005) Congenital glutamine deficiency with glutamine synthetase mutations. *N Engl J Med.* 353:1926-33.
308. Griffiths, M., Neal, J. W., Gasque, P. (2007) Innate immunity and protective neuroinflammation: new emphasis on the role of neuroimmune regulatory proteins. *Int Rev Neurobiol.* 82:29-55.
309. Sternberg, E. M. (2006) Neural regulation of innate immunity: a coordinated nonspecific host

response to pathogens. *Nat Rev Immunol.* 6:318-28.
310. Adler, M. W., Rogers, T. J. (2005) Are chemokines the third major system in the brain? *J Leukoc Biol.* 78:1204-9.
311. Bak, L. K., Schousboe, A., Waagepetersen, H. S. (2006) The glutamate/GABA-glutamine cycle: aspects of transport, neurotransmitter homeostasis and ammonia transfer. *J Neurochem.* 98:641-53.

Samenvatting

SAMENVATTING

Epilepsie is een chronische neurologische ziekte die gekarakteriseerd wordt door spontane, herhaalde aanvallen of stuiptrekkingen. Epilepsie kan erfelijk zijn, kan ontstaan na specifieke neurologische gebeurtenissen gedurende het leven, of kan ontstaan door een combinatie van deze twee oorzaken. Een van de meest voorkomende vorm van epilepsie is temporaalkwab epilepsie (TLE). Bij deze vorm van epilepsie beginnen de aanvallen in de temporale hersenkwab (slaapkwab). TLE wordt gezien als een ziekte die in belangrijke mate beïnvloedt wordt door gebeurtenissen gedurende het leven (omgevingsfactoren), maar hiernaast ook beïnvloedt wordt door erfelijke factoren. TLE wordt daarom ook wel als multifactoriaal geclassificeerd. Het proces dat een gezond brein omvormt tot een epileptisch brein wordt epileptogenese genoemd. Een voorbeeld van een gebeurtenis die de kans groter maakt om TLE te ontwikkelen is koortsstuipen. Koortsstuipen zijn stuiptrekkingen die kunnen optreden bij hoge koorts in jonge kinderen. Meestal zijn deze stuiptrekkingen relatief onschadelijk, maar in sommige kinderen kunnen ze uiteindelijk leiden tot TLE. Het is echter niet duidelijk of koortsstuipen zelf de kans verhogen op TLE of dat er al een prenatale schade of genetische gevoeligheid bestaat waardoor deze kinderen koortsstuipen en TLE ontwikkelen. Dit proefschrift beschrijft onderzoek gericht tot het identificeren van sleutelgenen, -eiwitten en -processen die een rol spelen bij TLE, koortsstuipen en epileptogenese.

In **hoofdstuk 2** is weefsel onderzocht van TLE patiënten waarbij, als therapie, het hersengebied dat de epilepsie veroorzaakt is weggenomen. Dit hersenweefsel is vervolgens te gebruiken om de genexpressie te meten en te vergelijken met de genexpressie van gezond hersenweefsel. De resultaten lieten zien dat de “aangeboren” immuniteit een belangrijke rol speelt in TLE. Chemokinen spelen een belangrijke rol in deze immuniteit en kunnen ontstekingscellen naar de plek van ontsteking leiden. Twee chemokinen, *CCL3* en *CCL4*, kwamen zeer sterk tot expressie in het hersenweefsel van TLE patiënten. In **hoofdstuk 4** zijn de effecten van één van deze chemokinen onderzocht op de activiteit van gekweekte rattenneuronen. We hebben aangetoond dat CCL3 de activiteit en calciumdynamiek van neuronen kan moduleren en dat deze effecten grotendeels veroorzaakt werden door een verhoogde expressie van N-methyl D-aspartate (NMDA) receptoren. Deze resultaten suggereren een belangrijke rol voor chemokinen in TLE en epileptogenese. Het blokkeren van de functie van deze chemokinen zou een remmend effect kunnen hebben op de ontwikkeling van TLE.

De meeste genetische epilepsievormen worden veroorzaakt door mutaties in ionkanaalgenen (**hoofdstuk 1**) en worden ook wel “channelopathies” genoemd. Een voorbeeld hiervan is een ernstige genetische vorm van koortsstuipen en epilepsie die veroorzaakt wordt door mutaties in natriumkanalen (*SCN1A*, *SCN2A*, *SCN1B*). In multifactoriale epilepsie, zoals TLE, laten bovendien steeds meer studies zien dat de ontregeling van ionkanalen ook een rol speelt. In **hoofdstuk 2** hebben we naast immuungenen ook een relatief recent ontdekt natriumkanaalonderdeel geïdentificeerd (*SCN3B* of Navβ3) met veranderde expressie in epilepsiepatiënten. **Hoofdstuk 3** beschrijft een gedetailleerde expressie analyse van dit kanaalonderdeel. *SCN3B* mRNA expressie was 2-maal hoger in deze epilepsiepatiënten, terwijl de expressie van het corresponderende eiwit (Navβ3) 2- tot 3-maal lager was. Deze tegenstelling zou verklaard kunnen worden door een mutatie in het *SCN3B* gen. We hebben echter geen mutaties kunnen identificeren in dit gen. Het is mogelijk dat dit gen onder sterke translationele of post-translationele controle staat en

zodoende de eiwitexpressie remt. Post-translationele controle is in overeenstemming met een verhoogde expressie van ubiquitine en proteasomale degradatie processen in deze patiënten (**hoofdstuk 2**). De functionele consequenties van lagere Navβ3 expressie zijn nog onduidelijk, maar deze resultaten suggereren dat ontregeling van natriumkanalen een rol spelen in TLE.

Zoals eerder genoemd, zijn koortsstuipen een veel voorkomende omgevingsfactor in de ontwikkeling van TLE. We hebben onderzocht of koortsstuipen op zichzelf kunnen leiden tot epileptogenese. Hiervoor hebben we in muizen van 10 dagen oud met behulp van warme lucht, koorts en koortsstuipen opgewekt (**hoofdstuk 5**). We toonden aan dat deze koortsstuipen de epileptische aanvalsgevoeligheid in volwassen dieren verhoogde. Deze resultaten lieten zien dat koortsstuipen inderdaad kunnen leiden tot een epileptogenese proces. Om dit epileptogenese proces verder te onderzoeken, hebben we de genexpressie van muizen met koortsstuipen vergeleken met de genexpressie van muizen die geen koortsstuipen hebben gehad (**hoofdstuk 6**). Resultaten lieten zien dat koortsstuipen al na één uur een grote genexpressie respons gaven. We identificeerden vooral transcriptie en stress genen. Drie dagen en twee weken na de koortsstuipen werden voornamelijk genen gevonden die een rol spelen bij neuronaal herstel en herstructurering. Deze processen zijn waarschijnlijk een teken van het ontstaan van nieuwe connecties tussen neuronen (mossy fiber sprouting, zie **hoofdstuk 1**). Deze nieuwe connecties kunnen een soort kortsluiting in de hersenen veroorzaken, waardoor gesynchroniseerde en epileptische activiteit kan ontstaan. Na in totaal acht weken waren de meeste koortsstuipveranderingen genormaliseerd. Eén gen, *Camk2a*, kwam lager tot expressie. Lagere expressie van *Camk2a* is één van de meest gevonden effecten in epileptogenese en is ook aanwezig in humaan epilepsie weefsel (**hoofdstuk 2**). Studies hebben ook laten zien dat een lagere expressie van CAMK2A epileptische activiteit kan veroorzaken in een concentratie afhankelijke wijze. Deze resultaten suggereren dat koortsstuipen epileptogenese kunnen veroorzaken waarbij neuronale herstructurering en *Camk2a* een belangrijke rol spelen.

Om te onderzoeken of er een genetische gevoeligheid ten grondslag ligt aan koortsstuipen, hebben we de koortsstuipgevoeligheid bepaald van meerdere ingeteelde muizenstammen (**hoofdstuk 5**). Hiernaast hebben we met speciaal gekweekte muizenstammen chromosomen geïdentificeerd waar koortsstuipgevoeligheidsgenen op liggen (**hoofdstuk 7**). We hebben laten zien dat koortsstuipgevoeligheid in ingeteelde muizenstammen bepaald wordt door complexe genetica en dat de C57BL/6J muizenstam relatief gevoelig is terwijl de A/J muizenstam relatief ongevoelig is voor koortsstuipen (**hoofdstuk 5)**. Dit is in tegenstelling tot wat gevonden is met chemisch geïnduceerde epileptische aanvallen, waarbij de A/J muizenstam juist de meest gevoelige stam is. Dit laat zien dat koortsstuipgevoeligheidsgenen specifiek zijn. Vervolgens hebben we chromosomen geïdentificeerd waar deze koortstuipgevoeligheidsgenen liggen (**hoofdstuk 7**). Chromosomen 2 en X van de A/J stam verhogen de gevoeligheid voor koortsstuipen, terwijl de chromosomen 1, 10 en 13 de gevoeligheid voor koortsstuipen verlagen. Op de chromosomen 1, 2, 10 en 13 liggen eerder geïmpliceerde koortsstuipgenen, die gevonden zijn bij koortsstuipen in de mens. Door gebruik te maken van een muizenstam waar één van de kopieën van het gen *Glul* geïnactiveerd is, hebben we *Glul* kunnen identificeren als één van de gevoeligheidsgenen op chromosoom 1 (**hoofdstuk 8**). Verdere gedetailleerde kruisings-, locatie- en sequentiestudies blijven echter nodig om de koorts-

stuipgevoeligheidsgenen op te sporen.

Dit proefschrift verschaft inzicht in de opkomende rol van het immuunsysteem in TLE, en identificeert genen en processen die belangrijk zijn bij koortsstuipen en epileptogenese. In TLE hebben we hoge expressie geïdentificeerd van chemokinen, die in vitro de neuronale activiteit verhoogden. Het blokkeren van de effecten van chemokinen zou een remmend effect kunnen hebben op de ontwikkeling van TLE en is onderwerp van verdere studies. We hebben laten zien dat koortsstuipen het epileptogenese proces kunnen aanzetten, waarbij *Camk2a* een sleutelrol vervult. De rol van *Camk2a* in epileptogenese wordt momenteel onderzocht. Hoewel koortsstuipen TLE kunnen veroorzaken, hebben we aangetoond dat gevoeligheidsgenen voor koortsstuipen en epileptogenese apart zijn. We hebben *Glul* geïdentificeerd als belangrijk gen dat de koortsstuipgevoeligheid beïnvloed. De chromosomen 1, 2, 10, 13 en X bevatten ook genen die de koortsstuipgevoeligheid beïnvloeden. De identificatie van deze genen kan leiden tot een beter begrip van de mechanismen die een rol spelen bij koortsstuipen. Onze resultaten suggereren dat koortsstuipen direct kunnen bijdragen aan TLE en dat gevoeligheidsgenen voor koortsstuipen anders zijn dan gevoeligheidsgenen voor TLE.

Dankwoord

DANKWOORD

Als laatste het dankwoord. Het is nu 23 juli, één dag voordat het boekje naar de drukker gaat. Dit moment komt na een lange periode van 4 jaar en 8 maanden waarin het leven toch grotendeels bestond uit AIOen.

Het begon allemaal tijdens mijn eerste stage bij het RMI onder begeleiding van Robbert Notenboom en Pierre de Graan. Via Pierre kon ik hierna 7 maanden stage lopen in San Diego. Eenmaal terug in Nederland, werd ik al snel gevraagd voor het AIO project dat nu voor jullie ligt. Ik begin dan ook met het bedanken van Pierre, mijn mentor en begeleider vanaf het eerste uur. Bedankt voor het vertrouwen en de mogelijkheden. Bij Pierre was in overleg alles mogelijk. Bedankt ook voor de kritische blik en sturende koers wanneer mijn ideeën soms wat te ver gezocht waren. Gedurende de afronding liep er wel eens wat spaak, maar het resultaat heeft daar niet onder te geleden. Dan mijn promotoren, Peter Burbach en Dick Lindhout. Peter, al was je niet nauw betrokken bij het onderzoek, ik heb toch veel aan je gehad. Van het in de gaten houden van de voortgang tot het kritisch bekijken van mijn proefschrift, bedankt! De samenwerking met mijn andere promotor was iets groter. Dick, bedankt voor het waken over de klinische component en bedankt voor de mogelijkheid om tijdelijk in het genetisch diagnostisch lab te kunnen werken. Ook bedankt voor de kritische review van het proefschrift.

Zonder de hulp van de vele collega's was ik zeker niet zover gekomen. Een aantal wil ik apart noemen. Zonder overdrijven moet ik zeker beginnen bij Marina. Marina is niet zomaar een analist. Marina hoeft alleen verteld te worden wat je doel is. De opzet, uitwerking en rapportage doet Marina allemaal zelf en deze data vormt dan ook de basis van veel van mijn moleculaire hoofdstukken. Ik heb je dan ook niet voor niets gevraagd als paranimf. Met jouw bijna fotografisch geheugen over experimenten van soms 10 jaar geleden, kan ik geen betere aan mijn zijde hebben. Dan de derde rechterhand van Marina, Marije. Samen op het PCR apparaat onder mama. Bedankt voor je inzet en altijd goede humeur. Jan, de ultieme dieranalist, bedankt voor je harde werk bij het ontwikkelen van de nieuwe diermodellen en bij het aanpassen van het koortsstuipmodel voor muizen. Inge, bedankt voor alles aangaande de proefdieren. Marian, bedankt voor de hulp bij de analyse van de microarray data, en Frank, bedankt voor de kritische review van de papers en voor het goede advies betreffende de opzet van de microarray experimenten. Donna, thanks for a good start of my scientific career and thanks for accommodating Marijn. San Diego will always be in my hearth. Tony, thanks for the excellent discussions regarding the expression of our common interest protein.

Natuurlijk wil ik ook mijn mede promovendi bedanken. Saskia, het was altijd gezellig en je hebt een goed luisterend oor voor problemen. De echte samenwerking kwam pas in het laatste jaar, maar ik heb het als zeer prettig ervaren. Laten we af en toe die biertjes en wijntjes niet vergeten. Ellen, je nam het stokje over van onderzoek dat we in samenwerking met Martien Kas waren gestart. Al snel heb je er je eigen draai aan gegeven en het loopt dan ook als een trein. Laat die publicaties maar komen! Anne, jij staat nog aan het begin van een project met veel mogelijkheden, maak er het beste van en houdt de lol erin!

"Mijn studenten" moet ik ook niet vergeten. In chronologische volgorde; Thea, Xin, Gokhan, Sara en Marijn. Bedankt voor jullie inzet. Ik heb veel geleerd van jullie en ik heb er alle vertrouwen in dat jullie succesvolle wetenschappers zullen worden.

Kamergenootjes, Ineke, Koen H., Dianne, Marijke, Mirte en Rou-Afza, bedankt voor de gezelligheid, snoep en cake! Verder wil ik iedereen van de afdeling bedanken voor hun hulp en inbreng en voor de gezelligheid tijdens de lunch, borrels en feesten. Ik kom zeker nog eens langs voor een biertje. Lars, ik kom zeker af en toe nog eens luisteren naar je bandje.

Naast het werk was er natuurlijk ook tijd voor ontspanning. Pieter, Josse en Lude, bedankt voor alle spelletjesavonden die toch steeds minder spelletjes kenden. Lude, bedankt voor de gastvrijheid in Oxford. De tijd zal leren of El Gore het bij het rechte eind had. Eelke en Pieter, bedankt voor alle sportieve uitspattingen, van een snoeihard schot op doel tot afstappen in Simpelveld. USVF6, bedankt voor de gezellige wedstrijden en derde helften en Joost, ja nu is het proefschrift echt af! Bestuurtje, bedankt voor alle etentjes. Straks weer een leuk feestje! Oude buurtjes, Thijs en Esmeralda, tot snel!

Lieve familie, lieve mam, broer, zus, Ronan, Jurgen, kleine Veerle, oma en al de rest. Bedankt voor de interesse, al was het soms moeilijk uit te leggen waar ik zoveel tijd aan kon besteden. Ik hoop dat de Nederlandse samenvatting een hoop duidelijk maakt.

Liefste meisje van de wereld, lieve Maya. We leerden elkaar kennen toen ik net begonnen was met mijn promotieonderzoek. De wandelingetjes op het landgoed Rhijnauwen achter onze studentenflats is toch de basis van iets heel moois geworden. Sindsdien hebben we de hoogte- en dieptepunten in mijn onderzoek gedeeld. Bedankt voor het luisteren en relativeren wanneer ik mijn frustraties weer eens moest uiten. Binnenkort een nieuw avontuur in ons nieuwe huis. Eindelijk een stekkie echt van onszelf. Ik houd van je!

Publications and Curriculum Vitae

PUBLICATIONS

van Gassen, K. L., Netzeband, J. G., de Graan, P. N., Gruol, D. L. (2005) The chemokine CCL2 modulates Ca2+ dynamics and electrophysiological properties of cultured cerebellar Purkinje neurons. *Eur J Neurosci*. 21:2949-57.

van Gassen, K. L., de Wit, M., Koerkamp, M. J., Rensen, M. G., van Rijen, P. C., Holstege, F. C., Lindhout, D., de Graan, P. N. (2008) Possible role of the innate immunity in temporal lobe epilepsy. *Epilepsia*. 49:1055-65.

van Gassen, K. L., Hessel, E. V., Ramakers, G. M., Notenboom, R. G., Wolterink-Donselaar, I. G., Brakkee, J. H., Godschalk, T. C., Qiao, X., Spruijt, B. M., van Nieuwenhuizen, O., de Graan, P. N. (2008) Characterization of febrile seizures and febrile seizure susceptibility in mouse inbred strains. *Genes Brain Behav*. 7:578-586.

van Gassen, K. L., de Wit, M., van Kempen, M., van der Hel, W. S., van Rijen, P. C., Jackson, A. P., Lindhout, D., de Graan, P. N. (2008) Hippocampal Navβ3 expression in patients with temporal lobe epilepsy: An acquired channelopathy? *Epilepsia*. Revision under review.

van Gassen, K. L., de Wit, M., Groot Koerkamp, M. J., van Nieuwenhuizen, O., Holstege, F. C., de Graan, P. N. (2008) Expression profiling after prolonged experimental febrile seizures reveals the involvement of neuronal remodeling and *Camk2a*. *Experimental neurology*. Under review.

van Gassen, K. L., Hessel, E. V., Wolterink, I. G., Stienen, P. J., Fernandes, C., Brakkee, J. H., Kas, M. J., de Graan, P. N. (2008) Phenotyping mouse chromsome substitution strains reveal multiple QTLs for febrile seizure susceptibility. *Genes Brain Behav*. Under review.

van Gassen, K. L., van der Hel, W. S., Hakvoort, T. B., Lamers, W. H., de Graan, P. N. (2008) Haploinsufficiency of glutamine synthetase increases susceptibility to experimental febrile seizures. *Genes Brain Behav*. Under review.

Kas, M. J., de Mooij-van Malsen, A., de Krom, M., **van Gassen, K. L.**, van Lith, H. A., Olivier, B., Oppelaar, H., Hendriks, J., de Wit, M., Groot Koerkamp, M. J., Holstege, F. C., van Oost, B. A., de Graan, P. N. (2008) High resolution genetic mapping of mammalian motor activity levels in mice. *Genes Brain Behav*. Under review.

van der Hel, W. S., Verlinde, S. A., Meijer, D. H., de Wit, M., Rensen, M. G., **van Gassen, K. L.**, van Rijen, P. C., van Veelen, C. W., de Graan, P. N. (2008) Hippocampal distribution of Vesicular Glutamate Transporter 1 in temporal lobe epilepsy patients. *Epilepsia*. In revision.

CURRICULUM VITAE

Koen Lucien Irma van Gassen werd op 23 februari 1978 geboren in Sint-Niklaas, België. In 1996 behaalde hij zijn HAVO diploma aan de Jansenius scholengemeenschap in Hulst. Dit zelfde jaar ging hij de laboratoriumopleiding (HLO) volgen aan de Polytechnische faculteit in Etten-Leur. In 1997 haalde hij daar zijn propedeuse en ging dat zelfde jaar Medische Biologie studeren aan de Universiteit van Utrecht. Stages werden gevolgd bij het Rudolf Magnus Institute of Neuroscience in Utrecht onder begeleiding van dr. R.G.E. Notenboom en dr. P.N.E. de Graan en bij The Scripps Research Instituut, Department of Neuropharmacology onder begeleiding van D. Gruol, PhD. In december 2003 behaalde hij zijn doctoraal examen. In dezelfde maand trad hij als promovendus in dienst bij het Rudolf Magnus Institute of Neuroscience, om onder leiding van dr. P.N.E. de Graan en Prof. dr. J.P.H. Burbach aan het in dit proefschrift beschreven onderzoek te werken. In juni 2008 is hij begonnen als postdoc in de groep van Prof. dr. M. Verhage aan de Vrije Universiteit in Amsterdam.